The Interaction of Cellulose with Xyloglucan and Other Glucan-Binding Polymers

Sarah E.C. Whitney

Submitted for the Degree of PhD, Stirling University,
September 1996

Table of Contents

Table of Figures

Acknowledgements

I would like to acknowledge the following people for their technical support and advice throughout: Jennie Brigham, for her excellent microscopy skills, Tony Weaver, for his endless patience with the electron diffraction, Nigel Lindner and Anna Hill, who trained me to be a microbiologist, Arthur Darke and Dave Caswell, for their NMR expertise, Michelle Gothard, for her help with rheology and John Mitchell for his patience as I repeatedly broke the GC! I also extend thanks to my two supervisors: Grant Reid, at the University of Stirling for continual, though distant support and in particular, Mike Gidley, who bore the brunt of the supervision and who, as a result, had the dubious pleasure of proof-reading this thesis.

On a personal level, I thank all the members of the lab, Cookie, Alison, Martine, Sally, Sid, Hattie, Stuart etc, for help and support, and making this, by and large, a thoroughly enjoyable 3 years. I extend particular thanks to my husband Patrick, for his continual encouragement and support throughout.

Abstract

This thesis examines the interaction of xyloglucan, the major hemicellulosic component of type I primary plant cell walls, with cellulose. Initial attempts to form xyloglucan-cellulose complexes by *in vitro* association methods are described, which gave low levels of interaction, with features not similar to those found in primary wall networks. The majority of the work focusses on the use of the bacterium *Acetobacter aceti* ssp. *xylinum* (ATCC 53524), which synthesise highly pure, crystalline cellulose as an extracellular polysaccharide. Addition of xyloglucan to a cellulose-synthesising bacterial culture results in the formation of cellulose-xyloglucan networks with ultrastructural and molecular features similar to those of the networks of higher plants. Applicatioon of the bacterial fermentation system is extended to incorporate the polysaccharides glucomannan, galactomannan, xylan, mixed-linkage glucan, pectin and carboxymethylcellulose, all of which impart unique architectural and molecular effects on the composistes formed. Preliminary data on the mechanical properties of composite structures under large and small deformation conditions are also described.

Chapter 1: Introduction

1.1 Introduction

The wall surrounding plant cells was for many years regarded as a static structure, which encased living cells and imparted mechanical strength to plant tissues in the absence of an endo- or exo-skeleton. This concept is undergoing radical revision as it becomes clear that the cell wall is in fact a highly dynamic structure, capable of dramatic alterations in composition in response to stress factors (Iraki *et al*, 1989a 1989b, 1989c; McCann *et al*, 1994; Shedletzky *et al*, 1990, 1992; Wells *et al*, 1994) and undergoing major architectural rearrangements during growth (McCann *et al*, 1993). Rather than being a discrete component, the primary wall maintains a dynamic interaction with the cytoplasm as an extension of the living cell; for this reason some authors prefer the term extracellular matrix when referring to the primary cell wall (Roberts, 1989). Oligosaccharides derived from cell walls under pathogen attack can act as elicitors of plant defense responses (Northnagel *et al*, 1983) or as signalling molecules (York *et al*, 1984; Joseleau *et al*, 1994; McDougall & Fry, 1989a,b, 1991) termed oligosaccharins (Darvill *et al*, 1992; Aldington & Fry, 1993). In this review I shall focus on the primary cell wall, which surrounds cells during the processes of growth and differentiation and as such is the most dynamic, undergoing massive rearrangements with concomitant synthesis of new components. The major components of type I primary walls (the wall of most dicotyledons and non-graminaceous monocotyledons are discussed. In view of the subject of this thesis, particular attention is paid to the cellulose and xyloglucan components which are considered to comprise the major load-bearing network in these plants.

1.2 The Primary Cell Wall

The primary cell wall of plants is defined as that which is laid down during the process of growth and differentiation (Fry, 1988) Once the cell has fully developed, the wall may be 'locked' into position possibly by structural proteins (Carpita & Gibeaut, 1993) and may be further elaborated by the formation of a secondary wall, which may have a quite different composition and structure and usually functions to impart increased strength to tissues.

The primary cell wall comprises a cellulose framework in a matrix of non-cellulosic polysaccharides and proteins (Carpita & Gibeaut, 1993; Fry, 1988, McCann *et al,* 1990). Using chemical and enzymic techniques much information has been elucidated on the primary structure of individual components (eg York *et al,* 1985) and a number of models for the interaction of wall components have been proposed on the basis of such observations (eg Keegstra *et al,* 1973; Lamport, 1986). However recent technological advances in the development of high resolution microsopy (Heuser, 1981; Goodenough & Heuser, 1985, 1988: McCann *et al,* 1990, 1995), high resolution ^{13}C-NMR spectroscopy and Fourier Transform Infra-Red microspectroscopy, (McCann *et al,* 1992a) and their application to examination of plant cell walls has added an extra level of knowledge in that they all allow observation of components in association with each other rather than in isolation. The former two techniques have been used extensively in this thesis and will be discussed further in sections 1.8 and 1.9.

1.2.1 Models of the Primary Cell Wall

The primary cell wall is placed under considerable tensile stress as a result of the internal hydraulic pressure essential for cell expansion to occur (Cosgrove, 1993a; Passioura & Fry, 1992). During cell expansion, the cell may enlarge to as much as 100 times its original volume. This requires extensive architectural rearrangements of existing material coupled with synthesis of new material as both wall thickness and microfibril spacing are conserved (Carpita & Gibeaut, 1993). This situation is further

complicated in elongating cells since rearrangements and deposition must be directed to only the longitudinal and not the transverse walls (McCann *et al*, 1993). Any models of primary cell walls must therefore reconcile the apparently conflicting requirements of substantial tensile strength and the capacity for expansion. Moreover, it is clear that, apart from the common cellulose framework, the cell walls of the Gramineae have fundamental compositional differences to those of other flowering plants (Bacic *et al*, 1988; Carpita *et al*, 1987). Despite these differences, graminaceous cell walls show similar growth physics and respond in similar ways to the same classes of growth regulators (Cleland, 1981). Differences between, and alternative models for, these two types of plant cell walls are reviewed by Carpita and Gibeaut (1993).

Although a comprehensive review of all previous models for primary cell walls is beyond the scope of this thesis, it is worth looking at a couple of the more well known examples to demonstrate how thinking about the organisation of the cell wall has developed in line with technological developments.

The first model for dicotyledonous plant cell walls was proposed in 1973 by Albersheims group (Keegstra *et al*, 1973) based on enzymic analysis of isolated components from the cell walls of suspension-cultured sycamore (*Acer pseudoplantus*) cells. This model proposed that, apart from H-bonds between cellulose and the xyloglucan component (the major hemicellulose in type I primary walls), non-cellulosic polymers are associated via covalent bonds, with growth mediated by temporary dissociation of xyloglucan and cellulose at acid pH, allowing lateral slippage. Although this model dominated thinking for many years, it has largely been discredited, partly because the association between xyloglucan and cellulose is in fact strengthened at acid pH (Valent and Albersheim, 1974; this observation led to some revision of the early model), but mainly because no covalent linkages between cell wall polymers have ever been unequivocally identified (Monro *et al*, 1976; Darvill *et al*, 1980; Talbott & Ray, 1992a).

Lamport and Northcote (1960) identified an integral hydroxyproline-rich protein in primary walls, which was later named extensin and proposed to play a fundamental role in extension growth (Lamport, 1965). Isodityrosine, which has been identified in the cell wall, is proposed to cross-link an extensin precursor weft around a cellulose microfibrillar warp, thereby forming an extensin-cellulose network via peroxidase-catalysed formation of isodityrosyl bridges (Lamport, 1986). Although no evidence of intermolecular isodityrosine cross-linkages is available, there is some indirect evidence for a role for structural proteins in elongation growth from McCann *et al* (1993), who observed polarisation of polymers with respect to microfibrils in elongating carrot cells using polarised FTIR-microscopy. Recently, Qi *et al* (1995) presented some evidence for covalent linkages between the majority of the measured extensin component and the pectic fraction of cotton suspension cells.

1.2.2 The Multi-Domain Model of the Primary Cell Wall

More recent models of primary walls of dicotyledons and non-graminaceous monocotyledons propose a multi-domain structure. McCann *et al* (1990) used high-resolution microscopy techniques to examine the molecular architecture of isolated onion parenchyma cell walls, and the alteration of structure under mild extraction procedures which selectively removed cell wall components (Redgwell & Selvendran, 1986). On the basis of such studies, a revised model for primary cell wall architecture was proposed, in which the cellulose/xyloglucan network is embedded in a highly heterogeneous matrix of pectic polymers (McCann & Roberts, 1991). These two networks are envisaged as independent, although there are extensive interactions between them. It should be pointed out that onion parenchyma cells contain very little protein and hence this model does not incorporate a role for structural proteins. The model is extended by Carpita and Gibeaut (1993) to include proteins as a third domain. Talbott and Ray (1992a) proposed a similar multi-phase model based on studies of pea cell wall polysaccharides.

There is a substantial body of evidence to suggest that the cellulose/xyloglucan network and the pectin matrix are functionally independent. Removal of the pectin matrix by sodium carbonate extraction increases the porosity of the wall imparting an open fibrous appearence, but the integrity of the

cellulose/xyloglucan network is preserved (McCann *et al*, 1990). Cells of tomato (*Lycopersicon esculentum*), adapted to grow on the cellulose synthesis inhibitor 2,6-dichlorobenzonitrile (DCB) produce a functional wall comprising 99% pectin in which Ca^{2+}-linked pectins form the major load-bearing network although their 3-dimensional architecture is very different (Shedletzky *et al*, 1990, 1992; Wells *et al*, 1994). Regenerated walls of carrot protoplasts initially comprise a pectin shell prior to the formation of a cellulose/xyloglucan network (Shea *et al*, 1989). However, despite their independence, the two networks interact extensively and it is therefore pertinent at this point to briefly discuss the pectin matrix in the context of the cellulose/xyloglucan network.

1.3 The Pectin Matrix

Plant pectins comprise a highly heterogeneous and complex set of polymers and a detailed discussion of their structure and function is well beyond the remit of this review. Briefly, the two major constituents of pectins are polygalacturonic acid comprising contiguous α-(1→4)-linked D-galacturonic acid, and rhamnogalacturonans, polymers of repeating (1→2)- α-L-rhamnosyl-(1→4)-α-D galacturonic acid which are heavily substituted with arabinan and arabinogalactan side chains at O-4 of rhamnose.

Rees *et al* (1977) showed that gels of polygalacturonic acid (PGA) can be formed by cross-linking with calcium in regions of deesterification. This results in the formation of junction zones, later tentatively proposed to be between anti-parallel chains (Jarvis *et al*, 1984; Powell *et al*, 1982). On the other hand gels of highly methylesterified pectin can also be formed, probably this time between parallel chains (Morris *et al*, 1980) and this led to the proposal of an intermediate gel type, particularly at low pH, which incorporates both Ca^{2+}-mediated junction zones and ester-acid linkages in partially de-esterified PGA (Gidley *et al*, 1980). Certainly, regions of relatively esterified and relatively de-esterified pectins can be localised throughout the wall (Knox *et al*, 1990) although there is typically a preponderance of relatively de-esterified pectin, potentially cross-linked by Ca^{2+}, in the middle lamella.

It is generally percieved that, for cell expansion to occur, hydrolysis or dissociation of xyloglucan from cellulose microfibrils is a fundamental requirement (Cleland, 1981; Taiz, 1984), although the discovery of proteins such as xyloglucan endotransglycosylase or XET (Fry *et al*, 1991) and expansins (McQueen-Mason *et al*, 1992) suggest that more subtle rearrangements may be adequate for growth to proceed. Nevertheless, it is necessary for enzymes to access the cellulose/xyloglucan network; as this is surrounded by the pectin matrix the properties of this matrix are speculated to control this accessibility. For example, Baron-Eppel *et al*, (1988) showed that pore size is determined by the pectin matrix. Nari *et al* (1986) propose that localised action of pectin methyl esterase may control the charge environment in the vicinity of xyloglucan, thereby facilitating enzyme action. It has been shown that the properties of artificial gels are highly sensitve to changes in pH, ionic strength, electropotential, divalent cations and water potential (Tanaka *et al*, 1980, 1982) and subtle changes in the pectin matrix of plants conferred by enzyme action or electrochemical activities at the plasma-membrane may have profound effects on accessibility of the cellulose/xyloglucan matrix. Occasionally the opposite view is purported, ie that it is degradation of the xyloglucan component that facilitates access to pectin-degrading enzymes (Sakurai & Nevins, 1995). It should be remembered however that pectins do also play a major structural role in plant cell walls; in the absence of cellulose/xyloglucan they can form a functional wall (Shedletzky *et al*, 1990) and during elongation, pectic molecules can show strict orientation (McCann *et al*, 1993).

1.4 Cellulose

Cellulose is a major component of plant cell walls and represents the most abundant naturally occurring macromolecule on earth. Chemically, cellulose is defined as a β-(1→4)-D-glucan, ie it is a linear polymer comprising glucose residues with identical chemical linkages, with no modifications or side-chain substitutions. It will become apparent however, that this description, whilst accurate, is deceptively simple since there is no clear consensus as to the precise crystallographic structure of cellulose, or even the mechanism by which it is synthesised. What is clear however is that native

celluloses show great variation in crystallite size, degree of crystallinity and the ratio of the two crystalline allomorphs of cellulose I, Iα and Iβ. It is believed that the nature of cellulose synthases or terminal complexes may determine the variation described above; this has been particularly discussed with reference to algae whose terminal complexes are less labile than those of higher plants (Giddings *et al*, 1980; Itoh & Brown, 1988; Katsaros *et al*, 1996; Kuga & Brown, 1989; Mizuta & Brown, 1992; Okuda *et al*, 1994; Quadar, 1991; Sugiyama *et al*, 1994). Furthermore, in plant cell walls, xyloglucan is believed to interact with cellulose close to the site of synthesis (see section 1.6.1) and hence a brief overview of cellulose biosynthesis is useful. For a more comprehensive review, the reader is referred to recent articles on cellulose biosynthesis (Delmer, 1987; Delmer & Amor, 1995) and the role of terminal complexes and rosettes in microfibril assembly (Blanton & Haigler, 1995; Emons, 1991).

1.4.1 Cellulose Biosynthesis

Cellulose microfibril assembly is believed to occur at the site of terminal complexes (TCs) located on the plasma membrane (Emons, 1991). Using freeze-fracture techniques a number of different types of TCs have been identified. For example, the Gram -ve bacterium *Acetobacter xylinum* posesses a single row of terminal complexes along one of the long axes of the cell (Brown *et al*, 1976; Zaar, 1979) and hexagonally arranged TCs or 'rosettes' have been identified in zygnematalean green algae (Giddings et al, 1980) and in higher plants (Emons, 1985; Mueller & Brown, 1980; Herth, 1985; Herth & Weber, 1984). Isolation of rosettes from higher plants which retain cellulose-synthesising activity is technically difficult due to their instability (eg Herth & Weber, 1984) and such preparations usually revert to callose synthesis, leading to the assumption that callose synthase is in fact a deregulated form of cellulose synthase. Most progress on elucidating the mode of cellulose biosynthesis has been made using bacterial systems.

1.4.1.1 Cellulose Biosynthesis in Bacteria

Acetobacter xylinum synthesises cellulose I of exceptionally high purity as an extracellular polysaccharide. Up to 200,000 molecules per second may be polymerised into β-1,4 glucan chains by a single *Acetobacter xylinum* cell (Hestrin & Schramm, 1954). These chains are crystallised first into microfibrils and subsequently into a twisted ribbon structure, which elongates in direct association with the cell envelope, remaining attached during cell division (Brown *et al,* 1976; Ring, 1982; Zaar, 1979).

Membrane preparations from *A.xylinum* retain catalytically active cellulose synthase activities in the presence of GTP and a soluble protein factor (Aloni *et al,* 1982). Synthesis of cellulose by *A.xylinum* is a Mg^{2+}-dependent reaction, UDP-glucose is the substrate (Aloni *et al,* 1983) and GTP is in fact converted to cyclic diguanylic acid (c-di-GMP), the presence of which in micromolar concentrations stimulates *in vitro* synthesis to rates approximating those *in vivo (*Aloni *et al,* 1982; Ross *et al,* 1987; 1991). Wong *et al* (1990) cloned an operon of four *A.xylinum* genes (*bcsA-D*) which are involved in cellulose synthesis. The *bcsB* gene was believed to encode for the catalytic subunit (Wong *et al,* 1990); however the *bcsA* gene is homologous with another gene, *acsAB*, purported to encode the catalytic subunit cloned by Saxena *et al* (1990). A second gene downstream of the catalytic subunit gene encodes a 93kDa protein tightly associated with the catalytic subunit and this gene shows high homology with the *bcsB* gene described by Wong *et al* (1990) (Saxena *et al,* 1991). The *acsAB/bcsA* and *bcsB* genes were confirmed as having roles in the polymerisation step of cellulose production by sequence comparisons whcih showed polypeptide sequence homology with other β-glycosyl transferases (Saxena *et al,* 1994). Saxena & Brown (1995) have recently identified a second gene (*acsAII*) in *A.xylinum* mutants in which the *acsAB* gene was disrupted. These mutants produced no detectable cellulose, but had significant cellulose synthase activity *in vitro* which was ecncoded by the *acsAII* gene.

Agrobacterium tumefaciens is a pathogenic bacterium which synthesises cellulose fibrils that emerge at random from all sides of the cell surface (Matthysse *et al,* 1981), binding the bacterium tightly to the

surface of the host cell (Matthysse, 1983). *In vitro* cellulose synthesis is not activated by c-di-GMP (Mathysse *et al,* 1995a) and a gene homologous to the putative c-di-GMP product (Saxena *et al,* 1991) was not identified (Matthysse *et al,* 1995b). Only one gene (CelA) from the 5 identified ORFs arranged into 2 operons showed homolgy to cellulose synthase genes from *A.xylinum* (Matthysse *et al,* 1995b) although interestingly, this gene contains the conserved motif identified by Saxena *et al* (1994) existing among bacterial catalytic subunits and other enzymes catalysing polymerisation of β-glycosyl residues from either UDP-glucose or UDP-*N*-acetylglucosamine.

1.4.1.2 Cellulose Biosynthesis in Plants

In contrast to bacteria, cellulose-synthases of higher plants are extremely labile, usually reverting to callose-synthase activity during isolation procedures. Hence, callose-synthase is generally regarded as deregulated cellulose synthase (Delmer, 1987). Cellulose synthase is generally regarded as a multimeric enzyme complex and Gibeaut & Carpita (1994) suggest that there is a requirement for several glucosyl transferases in order to form the β-1,4-D-linkage, in which each glucose residue is rotated almost 180° with respect to its neighbour. Synthesis of β-1,3-D-glucan (callose) requires no such rotation of adjacent residue and hence is produced when glucosyl transferases become dissociated during preparation.

The lability of cellulose synthases has meant that much less progress has been made in elucidating the mechanism of cellulose biosynthesis in higher plants. Recent reports from Browns group (Okuda *et al,* 1993; Li & Brown, 1993; Li *et al,* 1993) of cellulose synthesis by plasma membrane- enriched fractions of cotton (*Gossypium hirsutum*) cells have been received with caution (Brown *et al,* 1994; Delmer *et al,* 1993). However, this process has been recently improved, yielding a greater amount of cellulose synthesis relative to callose, with the two products identified using EM (Kudlicka *et al,* 1995). Some progress has been made using mutants of *Arabidopsis thaliana* which show temperature-sensitive alterations in root morphology (Baskin *et al,* 1992). Mutants show radial root swelling at 31°C but not 21°C and this is correlated with an 80% reduction in cellulose synthesis (Williamson *et*

al, 1992). Mutations are mapped to 4 genetic loci of which 3 reduce incorporation of ^{14}C into cellulose and 1 which apparently affects general polysaccharide synthesis (Arioli *et al*, 1995). Interestingly, these mutants are shown using freeze-fracture techniques to be deficient in particle rosettes on the plasma membrane, providing further indirect evidence fior their role in cellulose biosynthesis (Arioli *et al*, 1995). Potikha & Delmer (1995) report another mutant of *Arabidopsis thaliana* which has impaired ability to synthesise the cellulosic secondary wall of stem and leaf trichomes, but not the primary wall.

A mjor step forward in elucidating the mechanism of cellulose biosynthesis has occurred with the discovery of a membrane-bound sucrose synthase (SuSy) in cotton fibres (Amor *et al*, 1995; Delmer *et al* 1995). SuSy is traditionally regarded as a soluble enzyme but by probing for proteins that bound glucose, this enzyme was found in substantial amounts in tight association with the plasma membrane. The enzyme catalyses the following reaction:

$$\text{Sucrose} \leftrightarrow \text{UDP-Glc} + \text{fructose}$$

and hence addition of sucrose should stimulate UDP-glucose production, generally considered to be the substrate for cellulose biosynthesis. Addition of sucrose to isolated membrane preparations failed to stimulate cellulose biosynthesis, but digitonin-permeabilised cotton fibres, which are semi-intact, could synthesise β-1,4-glucan under these conditions occasionally at levels comparable to those seen *in vivo*. Furthermore, SuSy was immunolocalised exactly paralleling cellulose deposition. Under the right conditions (UDP-Glc + Ca^{2+}/cellobiose) these fibres could be induced to synthesise callose, which correlates with the fact that isolated putative cellulose synthases complexes traditionally produce callose *in vitro*, and SuSy was also localised to the callose-rich cell plate of dividing cells (Delmer *et al*, 1995). Further work by this group has shown that SuSy interacts with calnexin, an ER membrane protein which has been shown in mammalian systems to act as a molecular chaperone (Kawagoe & Delmer, 1995). Based on these studies a model for the cellulose synthase complex in higher plants was proposed, in which SuSy is intimately associated with the catalytic cellulose synthase subunit, providing a source of UDP-Glc to the catalytic site, with calnexin assisting in the assembly of the

complex. Very recently, the purification of a cellulose synthase gene has been reported (Delmer, 1996).

Further progress towards determining the structure of cellulose synthase complex in higher plants has been reported with the identification of plasma membrane intrinsic proteins associated with callose synthase activity in red beet (*Beta vulgaris* L.) (Wasserman *et al*, 1995). These proteins co-purified with callose synthase activity and sequence data suggested trans-membrane helices. The proteins were proposed to serve a porin-like function, facilitating assembly and/or passage of elongating glucan chains through the plasma membrane, and to have the same function in callose- and cellulose-synthase complexes.

1.4.2 Microfibril Crystallisation

The process of glucan polymerisation is only the first step in cellulose biogenesis. The basic molecular structure of cellulose is conserved, with a few exceptions, throughout bacteria, algae and higher plants, all of which produce cellulose I. As previously mentioned, it is the nature of the cellulose-synthase which is believed to determine differences in crystallite size, Iα/Iβ ratios etc, with a number of common organisational characteristics which can be attributed to similar microfibril assembly mechanisms (Okuda *et al*, 1994).

In prokaryotes, such as *A.xylinum*, cellulose synthesis occurs at sites comprising fixed intra-membrane particles (Kuga & Brown 1989; Brown *et al,* 1983). In contrast, many eukaryotes, including higher plants, have synthetic sites which engage in lateral movement within the cytoplasmic membrane, channeled in appropriate directions under the control of the underlying tubular cytoskeleton (Gunning & Hardham, 1982; Robinson & Quadar, 1981). The orientation of these microtubules thus determines cellulose deposition patterns and hence cell shape. In helicoidal cell walls however, it should be noted

that work by Satiat-Jeunemaitre *et al* (1989) reveals no microtubular structures associated with shifts in microfibril orientation.

1.4.1.1 The Cell-Directed Self-Assembly Model

Most work on microfibril crystallisation has been performed on *A.xylinum.* Observations of a 200-400% increase in the rate of glucan chain polymerisation as the result of addition of fluorescent brighteners or Calcofluor White, which binds nascent glucan chains thereby preventing microfibril crystallisation (Benziman *et al*, 1980; Haigler, 1985) and a 30% increase in the presence of CMC (Ben-Hayim & Ohad, 1965) which prevents fasciation of microfibrils into ribbons, shows that glucan polymerisation, microfibril crystalliisation and, to a lesser extent, ribbon formation, are tightly coupled processes in cellulose biogenesis. This led to the cell-directed self-assembly model, as comprehensively reviewed by Haigler (1985). The process is cell-directed in that the orientation and association of glucan chains is mediated by the TC arrangement in the membrane.

In plant cell walls there is still debate as to whether microfibril orientation is mediated by the orientation of TCs in the plasma membrane or by the interaction of nascent cellulose with other polymers in the wall (Jarvis, 1992). Certainly there is evidence that xyloglucan interacts with cellulose produced by *A.xylinum* causing perturbation of ribbon assembly (Hayashi *et al*, 1987; Yamamoto & Horii, 1994). This implies that, in the wall, cellulose deposition may, at least in part, be controlled by the presence of other polymers, such as xyloglucan.

1.4.3 Crystalline Structure

Cellulose I is the predominantly occurring native cellulose in which the glucan chains are oriented parallel to one another with the same polarity (Kuga & Brown, 1988). This orientation is in fact thermodynamically unfavourable and formation of this conformation is probably dictated by the spatial

conditions within the cellulose-synthase complex producing many cellulose chains simultaneously (Jarvis, 1992). The thermodynamically favourable cellulose II, where chains are thought to be in anti-parallel alignment results from chemical treatments of cellulose I (Ranby, 1952; Stipanovic & Sarko, 1978). This form is also synthesised by a few organisms in nature (Roberts *et al*, 1989), notably a mutant of *A.xylinum*, in which there is evidence that cellulose II formation invovles specific chain folding events (Kuga *et al*, 1993). Isolated cellulose synthases from *A.xylinum* also produce cellulose II (see section 1.4.1.1), providing further evidence that it is the association of TCs with the membrane that allows cellulose I formation. Lee *et al* (1994) provide the first evidence of *in vitro* assembly of synthetic cellulose I as very thin microfibrils, only 1-2 glucan chains thick, by means of a cellulase-catalysed polymerisation of a β-cellobiosyl fluoride substrate monomer in acetonitrile/acetate buffer. The process of crystallisation has recently been studied using molecular mechanics (Cousins & Brown, 1995). When considered in the light of other experimental evidence, the results suggest the requirement for three sequential steps for native cellulose I crystallisation. The initial step, the formation of mini-sheets of glucan chains associated by van der Waals forces, is contrary to the widely-held view that H-bonding is responsible for association between chains, however these sheets are shown to be at a lower energy than H-bonded mini-sheets and are likely to be formed spontaneously in aqueous environments (formation of mini-sheets by H-bonding would be subject to competition by water molecules). These sheets are subsequently associated into mini-crystals by H-bonding and finally converge into microfibrils.

Recent studies using ^{13}C-NMR and electron diffraction have revealed that the cellulose I allomorph does in fact comprise 2 distinct crystalline allomorphs Iα and Iβ (Atalla & VanderHart, 1984; Sugiyama *et al*, 1991a,b; VanderHart & Atalla, 1984). Cael *et al* (1985) proposed that the ^{13}C-NMR spectra are linear combinations of two spectra, in which the C-1 region comprises a triplet and a doublet; however electron diffraction data supports the explanation of Atalla's group, which views this region as a combination of a singlet and a doublet. The crystalline nature of cellulose I is discussed in further detail in chapters 5 and 6.

1.5 Xyloglucan

Xyloglucan is the major hemicellulose component of type I primary walls (Carpita & Gibeaut, 1993), typically accounting for 20-25% of the growing cell wall in dicotyledons (McNeill *et al*, 1984; Fry, 1989; Hayashi, 1989). It forms a tightly associated macromolecular complex with cellulose in the wall, probably via hydrogen bonds (Bauer *et al*, 1973; Chambat *et al*, 1984; Hayashi & Maclachlan, 1984; Hayashi *et al*, 1987). The ability of a xyloglucan molecule to cross-link adjacent microfibrils (Baba *et al*, 1994; Hayashi *et al*, 1987; McCann *et al*, 1990) has led to proposals of a role for xyloglucan in maintaining spatial organisation of cellulose microfibrils and as the major load-bearing structure in type I primary walls (Hayashi, 1989; McCann *et al*, 1990). Promotors of primary cell wall elongation such as auxin and H^+ promote cleavage of xyloglucan (Hayashi & Maclachlan, 1984; Labavitch & Ray, 1974; Nishitani & Masuda, 1981,1982; Talbott & Ray, 1992b) and it is proposed that the rate of cell expansion is determined, at least in part, by the rate at which xyloglucan is metabolised.

1.5.1 Xyloglucan Chemical Structure

The backbone of xyloglucan consists of contiguous β-1,4-linked D-Glc*p* residues identical to that of cellulose, but differing from cellulose in that it is highly branched, with up to 75% of glucose residues being substituted at *O*-6 with α-D-xyl*p* residues (Hayashi, 1989; York *et al*, 1990). Further substitution with β-D-Gal*p* or α-L-Fuc*p*(1→2)-β-D-Gal*p* moieties at *O*-2 of the α-D-xyl*p* residues may occur and in some xyloglucans, the β-D-Gal*p* residue is acetylated, predominantly at *O*-6 (Kiefer *et al*, 1989; Pauly *et al*, 1995;York *et al*, 1988). Primary cell wall xyloglucan of dicotyledons and non-graminaceous monocotyledons is normally fucosylated and the presence of fucose may confer biological activity on oligosaccharides (see section 1.5.2). An exception is the xyloglucan from Solanaceae, an arabinoxyloglucan with substitution of some α-D-xyl*p* residues at O-2 with α-L-Ara*f* (Akiyama & Kato, 1982; Eda & Kato, 1978; Mori *et al*, 1979; Ring & Selvendran, 1981).

Species-specific differences occur in both the magnitude and nature of substitution of the cellulosic backbone. All xyloglucans can be hydrolysed into component oligosaccharides by the action of fungal endo-glucanases and the oligosaccharide units have been characterised in a number of species (eg poplar (*Populus alba*) cells, (Hayashi & Takeda, 1994); gobo (*Arctium lappa* L., Kato & Watanabe, 1993); pea (*Pisum sativum*, Hayashi & Maclachlan, 1984); *Allium* spp., (Ohsumi & Hayashi, 1994); cyclamen seeds (Braccini, *et al*, 1995) and apple (*Malus domesticus*, Renard *et al*, 1992). In particular the reader is referred to the exhaustive structural characterisation of xyloglucan oligosaccharides from a number of species, particularly sycamore (*Acer pseudoplatanus*) by Albersheims group (Hisamatsu *et al*, 1991,1992; York *et al*, 1990,1993,1995)

The basic repeating unit of the xyloglucan of most dicotyledons and non-graminaceous monocotyledons comprises 4 glucosyl residues, fungal endo-glucanases cleaving the backbone at every fourth residue. An exception is arabinoxyloglucan, in which the major oligosaccharide is XXG (Mori *et al,* 1979). For example, tamarind xyloglucan can be entirely cleaved into 4 component oligosaccharides: XXXG, XXLG, XLXG a,d XLLG (Fig. 3.4; York *et al,* 1990) and pea xyloglucan contains 2 basic oligosaccharide units XXXG and XXFG (Hayashi & Maclachlan, 1984), although there is recent evidence that pea xyloglucan is in fact much more complicated than this (Pauly *et al*, 1995). Some substitution patterns may confer resistance to hydrolysis (Hisamatsu *et al*, 1992) and it is possible that control of substitution may exert fine control over enzyme degradation and hence have important implications for growth.

1.5.2 Xyloglucan and Growth

Cosgrove (1993) proposes that the measured stress relaxation of walls in growing intact tissues is evidence that the wall relaxes as a consequence of chemical creepage of load-bearing linkages in the cell wall network structure. The observed metabolism of xyloglucan during elongation (Labavitch & Ray, 1974; Talbott & Ray, 1992a) and differential distribution in xyloglucan Mr on the upper and lower sides of gravitropically responding pea epicotyls (Talbott & Pickard, 1994) suggest that

xyloglucan is involved in major load-bearing networks. Elevated activity of *endo*-glucanase during elongation suggests that xyloglucan degradation during growth is essentially a hydrolytic process (Hayashi *et al*, 1984; Hayashi & Ohsumi, 1994; McDougall & Fry, 1990). However there is now evidence that xyloglucan Mr can increase and decrease during elongation (Talbott & Ray, 1992b) suggesting a more precise control than this, possibly via endotransglycosylases (Smith & Fry, 1991; Nishitani & Tominaga, 1991).

As well as being a component of the major load-bearing network in type I primary walls, xyloglucan oligosaccharides generated by enzyme action have been shown to have biological activity (Emmerling & Seitz, 1990; McDougall & Fry, 1988, 1989a, 1989b, 1990; York *et al*, 1984). As well as acting as a non-classical anti-auxin by inhibiting 2,4-D-induced growth non-competitively (Hoson & Masuda, 1991; York et al, 1984) xyloglucan oligosaccharides can also inhibit biberallin-induced growth (Warneck & Seitz, 1993). Furthermore, they can act as acceptors in endotransglycosylation reactions (Farkas *et al*, 1992; Lorences & Fry, 1993). XXFG has also been shown to directly affect the morphology of the primary wall at the ultrastructural level (Ruel & Joseleau, 1993; Ruel *et al*, 1995). Specific structural requirements are required for activity; the terminal fucose is essential for anti-auxin activity (McDougall & Fry, 1989b) and at least 2 α-D-Xylp residues are necessary for an oligosaccharide to act as an acceptor substrate for xyloglucan endotransglycosylase (XET) (Lorences & Fry, 1993). The identification of a plethora of enzymes which modify xyloglucan oligosaccharides, such as β-galactosidase (Edwards *et al*, 1988), a xyloglucan oligosaccharide-specific α-xylosidase (McNeill *et al*, 1989; Fanutti *et al*, 1991) and an α-fucosidase that inactivates the biologically active XXFG (Auger *et al*, 1993) suggests that xyloglucan is of vital importance in the wall, not just as a structural component, but as a major source of biological activity

1.5.3 Xyloglucan Biosynthesis

Xyloglucan is believed to interact with cellulose at the site of cellulose synthesis ie at the external face of the plasma membrane, but xyloglucan itself is in fact synthesised in the Golgi apparatus. The addition of both UDP-Glc and UDP-Xyl to a Golgi membrane preparation is required for significant xyloglucan synthesis (Hayashi & Matsuda, 1981; Ray, 1980). There is little experimental evidence on the nature of the coordination between the glucosyl-and xylosyltransferases, but Gibeaut & Carpita (1994) speculate that, due to restrictions imposed by synthesis of β-1,4-D-glucan chains (as with cellulose biosynthesis, section 1.4.1.2), a complex of 2 glucosyl- and xylosyltransferases is required. Addition of further residues such as galactose, arabinose and fucose apparently occurs independently (Camirand *et al*, 1987; Farkas & Maclachlan, 1998b; Feingold, 1982).

Transfer of xyloglucan to the plasma membrane is believed to occur in secretory vesicles. However, the size of these vesicles implies that only xyloglucan molecules approximately 100nm in length can be transported, yet there is experimental evidence that xyloglucan molecules can be extracted from the wall up to 700nm long (McCann *et al*, 1992). It is suggested that the action of XET may incorporate newly synthesised xyloglucan molecules in the wall and Thompson & Fry (1995) have recently presented the first experimental evidence for *in muro* elongation of xyloglucan molecules by transglycosylation in the walls of suspension-cultured rose cells.

1.6 Cellulose/Xyloglucan Interactions

1.6.1 Interactions in the Cell Wall

Cellulose and xyloglucan form a tightly associated network in the cell wall. An intramicrofibrillar association between the two components is implied by the requirement for strong alkali or chaotropic agents for effective dissociation of the two components (Chambat *et al*, 1984), which is sufficient to cause microfibril swelling (Edelmann & Fry, 1992). Xyloglucan is also localised on and between

microfibrils (Baba *et al*, 1994; Hayashi & Maclachlan, 1984; McCann *et al*, 1990) and removal of xyloglucan causes a collapse of the cellulose network, suggesting a role in maintaining intermicrofibrillar spacing (McCann *et al*, 1990).

The intimate interaction between cellulose and xyloglucan suggest that xyloglucan is present at or very close to the site of cellulose synthesis. However, in cells adapted to grow on DCB, which display much reduced cellulose synthesis, xyloglucan is not incorporated into the wall, but is secreted into the extracellular medium of cultured cells at comparable rates to that seen in control experiments (Shedletzky *et al*, 1990). Cellulose and xyloglucan synthesis are therefore probably not tightly coupled, but this work supports the theory that the major function of xyloglucan in the wall is in its association with cellulose. However, some workers have reported that newly synthesised xyloglucan can be tightly bound into the wall, even when cellulose synthesis is depressed by 80-85% (Edelmann & Fry, 1992c), although there was a concomitant reduction in xyloglucan synthesis in these experiments.

1.6.2 Elucidating the Nature of the Cellulose/Xyloglucan Interaction

The interaction of cellulose and xyloglucan remains poorly understood. Xyloglucan is believed to cross-link microfibrils (Fry, 1989) maintaining spatial organisation of the network (McCann *et al*, 1990), but what are the structural features, if any, of xyloglucan which enable it to effectively 'lift-off' a microfibril and become available to cross-link another? Cross-bridge lengths are highly conserved and extracted xyloglucan molecules show a periodicity of length of ca. 30nm (McCann *et al*, 1992), but the structural basis for this is not known. Hydrolysis of xyloglucan with *endo*-glucanases yields a wide range of oligosaccharides, some of which have biological activity and some patterns of substitution may confer resistance to hydrolysis, but what are the implications of such a highly heterogeneous structure in its interaction with cellulose? The preceeding discussion has highlighted the importance of the cellulose/xyloglucan network both structurally and as a source of biological activity, and therefore a greater understanding of the interaction between these components is desirable. Until

recently, attempts to elucidate the cellulose/xyloglucan association have proceeded along two main lines: firstly, looking at *in vitro* interactions and secondly using molecular modelling techniques.

1.6.2.1 In vitro *Interactions*

Cellulose and xyloglucan can be bound *in vitro* (Bauer *et al*, 1973; Hayashi & Maclachlan, 1984) in a highly specific interaction unaffected by the presence of a ten-fold excess of 1,2-β-glucan, 1,3-β-glucan, 1,6-β-glucan, 1,3-1,4-β-glucan, arabinogalactan and pectin (Hayashi *et al*, 1987). Valent and Albersheim (1974) examined the interaction of xyloglucan fragments generated by the action of endo-glucanase on sycamore extracellular polysaccharides with cellulose, but the work of Hayashi *et al* (1987) was the first to look at the association under physiological conditions. However, this group failed to achieve binding at comparable levels to those seen in vivo, and the association was weak, a finding confirmed by Baba *et al* (1994) and Acebes *et al* (1993). Furthermore, immunogold labelling failed to localise xyloglucan between microfibrils in reconstituted complexes in the cross-linkages proposed for the primary cell wall (Baba *et al*, 1994).

The heating of amorphous celluloses with xyloglucan in water to temperatures in excess of 160°C has produced complexes in ratios more comparable with cell wall levels (cellulose:xyloglucan = 1:0.19) (Hayashi *et al*, 1994a). X-ray diffraction indicated that, when heating was used, there was intramicrofibril association, and there was also a requirement for strong alkali to dissociate the complex. However, the non-physiological conditions required, combined with the fact that cellulose II rather than cellulose I is produced, argue against this system being an accurate representation of the situation *in muro*.

Addition of polymeric xyloglucan to cultures of *A.xylinum* during active cellulose synthesis has been shown to perturb ribbon assembly (Hayashi *et al*, 1987; Uhlin *et al*, 1995; Yamamoto & Horii, 1994) and to alter the molecular organisation of the cellulose component of the composite to become more like plant cellulose as judged by X-ray diffraction and ^{13}C NMR (Atalla *et al*, 1993; Hackney *et al*,

1994; Uhlin *et al*, 1995; Yamamoto & Horii, 1994). Since use of *Acetobacter* as a system for modelling cellulose/xyloglucan interactions forms the major part of this thesis, this work will be discussed in more detail in chapters 5 onwards.

Although attempts at reconstitution using polymeric xyloglucan under physiological conditions have proved largely unsuccessful in mimicing native complexes, some progress has been made recently using xyloglucan oligosaccharide fragments. Hayashi *et al* (1994b) prepared oligosaccharides of both xyloglucan and cellulose and investigated binding to amorphous and microcrystalline celluloses at temperatures of ca 120°C. The authors identified firstly that xyloglucan and cellulose oligosaccharides differed in their mode of binding and secondly that there was a minimum requirement of 5 consecutive glucosyl residues in the xyloglucan fragment to allow binding to occur, with an increase in the number of residues conferring a concomitant increase in the extent of binding (up to dp12). Vincken *et al* (1995) examined the absorption of tamarind xyloglucan fragments, comprising multiples of 4 contiguous glucosyl units [XG] to Avicel microcrystalline cellulose. In accordance with Hayashis work and that of Valent and Albersheim (1974), $[XG]_1$ failed to bind, $[XG]_2$ and $[XG]_3$ bound in increasing amounts and $[XG]_4$ absorbed quantitatively. Relative to polymeric xyloglucan, adsorption of $[XG]_4$ was high, indicating that the smaller molecules may more efficiently colonise small pores in cellulose, which may in fact account for a large percentage of total surface area (Stone & Scallan, 1968). There was an apparent selection against heavily substituted residues in binding to cellulose as although the population of $[XG]_4$ was enriched in galactose (substitution with galactose apparently conferring partial resistance to hydrolysis, Hisamatsu *et al*, 1992), proportionally more of XXXG and XXLG was bound to cellulose. On the basis of this work, the authors suggested a model of cellulose/xyloglucan binding, in which part of the molecule is adsorbed onto the cellulose surface (so-called 'trains') with the remainder sticking out into solution. At excess xyloglucan concentrations, binding of larger molecules is favoured due to the increased entropy gain, so that unbound 'loops' and 'tails' contribute more to the total amount of xyloglucan, even though coverage of cellulose remains the same.

1.6.2.2 Molecular Modelling Approaches

Levy *et al* (1991) used Metropolis Monte Carlo simulations to model energetically favourable conformations both in solution and in association with cellulose. Modelling predicts that the trisaccharide sidechain -Xyl-Gal-Fuc enables a xyloglucan oligosaccharide to adopt a molecular conformation favourable for cellulose binding via the backbone (ie a flattened 'cellulosic' backbone) with greater frequency than regions substituted with -Xyl-Gal or -Xyl. For polymeric xyloglucan, the region of the xyloglucan molecule containing this fucosylated sidechain is thus proposed to act as a nucleation site for binding; once bound, flattening along the backbone to facilitate binding to cellulose is propagated. This model has recently been supported by experimental data, in which fucosylated xyloglucan from pea bound to Avicel microcrystalline cellulose at a much higher rate than the non-fucosylated nasturtium xyloglucan (Levy, 1995). However, this model does not predict structural requirements for dissociation of the two components for cross-bridge formation.

In contrast to the work above, Finkenstadt *et al* (1995) predict that binding to cellulose via the xyloglucan backbone is in fact sterically restricted, with sidechains preventing direct edge-to-edge or face-to-face associations. They suggest that cellulose binding may be mediated by xylose residues without involving the backbone, if the 1→6 linkage is in a favourable conformation. The presence of Gal and Fuc residues may modulate binding and this model therefore does address the phenomonen of 'lift-off' the cellulose microfibril which results in the formation of cross-linkages.

1.7 Other Hemicellulose Polymers

Xyloglucan is the major hemicellulose polymer of primary walls of dicotyledonous and non-graminaceous monocotyledonous plants. In other cell wall types however, other hemicellulosic polysaccharides, very different in structure and function to xyloglucan, may predominate. Chapters 7 and 8 of this thesis look at the interactions of some other hemicelluloses and it is therefore pertinent to look at some of the major features of these polysaccharides here.

1.7.1 Xylan

Across the plant kingdom, xylans are quantitatively the most abundant hemicellulose, being the most common in the majority of angiosperms (Aspinall, 1980). Xylans comprise a backbone of (1→4)-linked D-xylopryranosyl residues substituted at *O*-2 and/or *O*-3 by side-chains of either α-D-glucuronic acid, 4-*O*-methyl-α-D-glucuronic acid or α-L-arabinofuranose.

In type II cell walls, as defined by Carpita & Gibeaut (1993) and unique to the Poaceae, glucuronoarabinoxylans, rather than xyloglucans, are believed to be the principal polymers interlocking microfibrils. Glucuronoarabinoxylan is synthesised as heavily substituted molecules, with selective cleavage of sidechains after incorporation into the wall to yield a highly heterogeneous population of molecules (Carpita, 1983; Gibeaut & Carpita, 1991). These post-incorporation modifications may affect interactions with other wall polymers and, in these pectin-poor walls, may alter the charge environment with implications for porosity and enzyme action in a role similar to that ascribed to pectins in type I walls (section 1.3).

Xylans substituted predominantly with glucuronic acid are found in the secondary walls of monocotyledons and also dicotyledons where they account for 20-30% of the dry weight of woody tissues. The role of glucuronoxylans in determining cell wall structure has been studied extensively by Vians group, where they have been shown to associate with cellulose microfibrils to spontaneously form a helicoidal pattern, typical of many cell walls, that is analagous to a cholesteric liquid crystal order (Reis *et al*, 1994; Vian *et al*, 1994). Xylans are also implicated in deterrmining secondary cell-wall assembly in tracheary elements as part of a self perpetuating cascade (Taylor *et al*, 1992; Taylor & Haigler, 1993). Parameters of absorption of xylans onto isolated cellulose fibres were reported by Mitikka *et al* (1995), suggesting that xylan alters its conformation upon association with cellulose.

1.7.2 Mixed-Linkage Glucan

These glucan homopolymers comprise a mixture of β-1,4-linkages, which are associated with linear chain segments, and β-1,3-linkages, which introduce 'kinks' into the molecule. Typically, these are arranged as blocks of ca. 50 residues (Huber & Nevins, 1981) of contiguous cellobiosyl- and cellotriosyl-(1→3)-β-D-glucose in a ratio of ca. 2:1 (Staudte *et al*, 1983). These are interspersed with oligomers of >4 contiguous β-1,4-D-glucosyl units, terminating with a β-1,3-D-glucosyl linkage (Kato & Nevins, 1986; Woodward *et al*, 1983). Mixed-linkage glucans are of particular interest as they appear only transiently in the type II cell wall during the period of cell expansion, disappearing once growth is completed. Although undoubtedly located in the wall at this time (Stone, 1984), their structural role is not fully determined. There is some evidence that β-1→3-linked residues may be spliced to give cellodextrin-rich regions imparting greater flexibility to the molecule (Buliga *et al*, 1986). Carpita & Gibeaut (1993) suggest that as a result, mixed-linkage glucans may act as a molecular thread during elongation, interlocking microfibrils in a manner analagous to xyloglucan in type I walls.

1.7.3 Mannan

The mannan family of polysaccharides are widely distributed throughout nature. Polymers of essentially pure β-1,4-linked mannose are found in the endosperm of a number of species, such as dates, ivory nuts (Meier & Reid, 1982; Meier, 1958) and coffee beans (Bradbury & Halliday, 1990) where they act as energy reserves. Galactomannans, where there is partial substitution at C-6 of the mannosyl backbone with α-D-galactose form major storage components in endosperms of all leguminous and some non-luguminous seeds (Meier & Reid, 1982). Glucomannans, in which some of the mannose residues in the backbone are replaced by (1→4)-linked -β-D-glucose form the major hemicellulose of secondary walls of gymnosperms as well as being a minor component of angiosperm secondary walls (Brett & Waldron, 1991). They are also found in a number of roots, tubers, bulbs and seeds (Meier & Reid, 1982). Commercially, purified galacto- and glucomannans are used extensively in the food industry as gelling and thickening agents (Dea and Morrison, 1975). Glucomannan and its interaction with cellulose will be discussed in more detail in chapter 7.

1.8 Deep-Etch, Freeze-Fracture Transmission Electron Microscopy

This technique confers several advantages over other microscopy technique in that no chemical fixatives or dehydrating conditions are required. Hence, macromolecular structures sustain little damage and images obtained are believed to closely represent native structures. Use of this technique for biological materials was first described by Heuser (1981). Rapid freezing of a thin layer of the sample minimises formation of ice crystals which may damage molecular structure. The sample is then warmed slightly to freeze-dry and water is etched away leaving minimally damaged non-aqueous components. A replica is then produced and these are visualised as negative images. The technique has been used to great effect in examining cell wall architecture in algae (Goodenough & Heuser, 1985, 1988; Fujini & Itoh, 1994) and plants (Itoh & Ogawa, 1993; McCann *et al*, 1990,1992).

1.9 ^{13}C-NMR Spectroscopy

As described elsewhere in this thesis (Chapter 5), high resolution solid state ^{13}C NMR has proved a vital tool in determining the molecular organisation of native cellulose (Atalla & VanderHart, 1984; VanderHart & Atalla, 1984; Newman & Hemmingson, 1995). ^{13}C CP/DD/MAS NMR (cross polarisation/dipolar decoupling/magic angle spinning) has been used to examine intact cell walls of specialised plant tissues capable of withstanding the tremendous centrifugal forces in the rotor (Jarvis & Apperly, 1990). However, most spectral information obtained is limited to the organisation of the cellulose component.

Application of various spectral aquisition techniques to ^{13}C NMR may facilitate resolution of molecules in terms of their relative mobility; this is described as 'mobility-resolved spectroscopy' (Gidley, 1992). This technique has been successfully applied to macromolecular systems such as

deoxyhemoglobin gels (Sutherland *et al*, 1979), eye proteins (Morgan *et al*, 1989) and plant polyesters (Garbow *et al*, 1989). Foster *et al* (1996) have made a detailed study of how varying parameters such as build-up of magnetisation (cross polarisation vs single pulse excitation) or its relaxation decay (eg contact time), together with use of dipolar decoupling eliminating strong dipole interactions and magic angle spinning to abolish chemical shift anisotropy, can make this a valuable technique for examining molecular features of isolated cell walls. These authors looked at isolated onion cell walls and the products after application of standard sequential chemical extraction techniques and found that information provided was complementary to that obtained by chemical (Redgwell & Selvendran, 1986) and high resolution microscopy (McCann *et al*, 1990, 1992) techniques. In particular, it was shown that, whilst it was difficult to observe cellulose/hemicellulose interactions in the presence of pectins due to chemical shift overlap, much information about the mobility of galactan and galacturonan segments was obtained. The technique was also applied to other plant species, which showed various common spectral features.

Chapter 2: General Materials and Methods

2.1 Phenol/Sulphuric Acid Assay for Carbohydrates

1. Add 200µl 5.0% phenol (w/v) to 200µl sample solution containing up to 40µg carbohydrate

2. Mix thoroughly and place in a water bath at 70°C for exactly 5 minutes

3. Remove, add 1ml concentrated H_2SO_4 and mix thoroughly

4. Cool to room temperature

5. Read absorbance at 492nm and determine carbohydrate concentration from a standard curve of 0-40µg glucose/200µl H_2O

(Dubois *et al*, 1956)

Note: This assay is strongly affected by alkali (Fig. 2.1). If the original sample is strongly alkaline (>0.5M), neutralise with acetic acid prior to assaying.

2.2 PAHBAH Assay for Reducing Sugars

<u>SOLUTION A</u>

Slurry 10g parahydroxybenzoic acid hydrazide in 60ml deionised H_2O. Add 10ml conc. HCl, mix, and make up to a total volume of 200ml with H_2O.

Figure 2.1 Effect of Acid/Alkali on the Phenol/Sulphuric Acid Assay

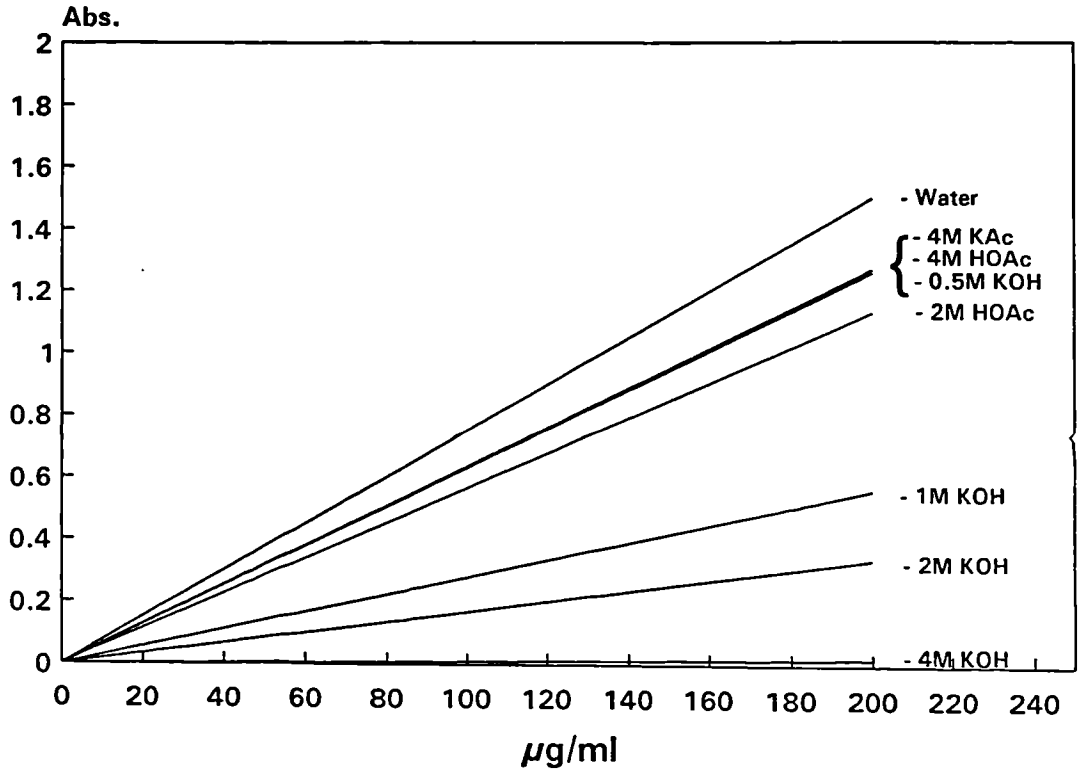

Standard curves of 0-40µg glucose in solutions of water (control) and a range of concentrations of KOH and acetic acid. Strong alkali drastically reduced the effectiveness of the assay and alkaline samples should thus be neutralised prior to analysis and carbohydrate concentration determined against a standard curve of glucose in 4M salt solution

SOLUTION B

Dissolve 29.4g trisodium citrate ($Na_3C_6H_5O_7$) (50mM) in ca. 500ml deionised H_2O. Add 2.2g $CaCl_2$ (anhydrous) (10mM) and mix thoroughly. Add 40.0g NaOH (0.5M) and make up to a total volume of 2l.

PAHBAH SOLUTION

Add 10 ml solution A to 90ml solution B and mix thoroughly. Store on ice during use.

ASSAY

1. Add 0.5ml freshly made PAHBAH solution to sample solution containing < 100µg/ml of reducing sugar
2. Mix thorougly and incubate in a boiling water bath for exactly 6 minutes
3. Cool to room temperature and measure absorbance immediately at 410nm.

(Lever, 1972)

The PAHBAH assay was used to determine the activity of *endo*-glucanase enzymes.

2.3 Iodine/Potassium Iodide Assay

1. To 1ml xyloglucan solution (0.05-0.3mg/ml) add 0.5ml I_2KI solution (0.5% I_2/1.0% KI in deionised H_2O and 5ml Na_2SO_4 solution (20% Na_2SO_4 in deionised H2O)
2. Mix thoroughly and incubate at RT for 60 minutes
3. Measure absorbance at 640nm

(Kooiman, 1960b)

Note: This assay shows alkali sensitivity (cf the phenol/sulphuric acid assay), so alkaline samples should be neutralised prior to analysis

2.4 Purification of Tamarind Xyloglucan from Glyloid 3S

1. Add 12.0g Glyloid 3S (Dainippon Pharmaceutical Co., Osaka, Japan) to 1000ml deionised H_2O containing 0.05% NaN_3.

2. Stir at room temperature overnight

3. Centrifuge at 13,000rpm (Sorvall RC5C centrifuge, GSA rotor) for 20 minutes at 4°C, followed by 20 minutes at 20,000rpm (SS-34 rotor) at 4°C.

4. Decant supernatant and dialyse extensively at 1°C against 12 changes of deionised water

5. Freeze-dry

(D.Cooke, Unilever Research, pers.comm)

2.5 Purification of Commercial Preparations of Cell Wall Enzymes

Commercial preparations of pectinase (Viscozyme 120L), cellobiohydrolase (Novozyme 188) and cellulase (Celluclast 1.5L) were supplied by Novo. These enzymes were supplied in crude form, containing large amounts of extraneous carbohydrate. To remove most of this carbohydrate, which would affect the monosaccharide analysis, these commercial preparations were subjected to a purification regime. Note that all steps were performed at 4°C.

1. Add $(NH_4)_2SO_4$ to commercial enzyme preparations to 80% saturation

2. Centrifuge at 13000g for 20 minutes and collect the pellet

3. Wash pellet with 80% saturated solution of $(NH_4)_2SO_4$ until the supernatant is clear

4. Resolubilise proteins in 50mM sodium acetate buffer (pH 4.5) (1ml/ml original preparation)

5. Dialyse at 4°C against ultrapure water to a conductivity of < 10 μSiemens.cm^{-1}, changing the dialysis tubing containing Novozym 188 and Celluclast 1.5L hourly to prevent hydrolysis

6. Dialyse further at 4°C against 2 changes on 50mM sodium acetate buffer pH 4.5

7. Determine protein concentration by Pierce Protein Assay and dilute with water to a final concentration of 1mg/ml (Viscozyme 120L), 2mg/ml (Novozyme 188) or 4mg/ml (Celluclast, 1.5L)

8. Store at -18°C

(Quemener & Thibault, 1990)

2.6 Monosaccharide Analysis: Methanolysis

1. Incubate ≈1mg polysaccharide + ≈ 500nm mannitol at 47°C for 16 hours with a standard enzyme solution:

for pectins :	20μl Viscozyme 120L (Novo) @ 1mg/ml
for celluloses/hemicelluloses :	20μl Novozyme 188 (Novo) @ 2mg/ml + 20μl Celluclast 1.5L (Novo) @ 4mg/ml
for cell walls:	20μl Viscozyme 120L + 20μl Vovozyme 188 + 20μl Celluclast 1.5L

These crude enzyme preparations were partially purified according to method 2.6 and protein concentration measured according to the Pierce BCA protein assay

2. Prepare 2 standards:

(a). ≈ 1000nmol monosaccharides and ≈500nmol mannitol to determine molar adjustment factors

(b). enzyme solutions + ≈ 500nmol mannitol to determine monosaccharide component

3. After incubation, freeze-dry

4. Dry in *vacuo* over P_2O_5 overnight

5. Add 1ml 2M HCl/MeOH solution and incubate at 85°C for 16 hours with occasional shaking

6. Cool to room temperature and neutralise with Ag_2CO_3

7. Add 2 drops acetic anhydride

8. Centrifuge at 2000g for 5 minutes, transfer liquid layer and extract silver salts twice with anhydrous MeOH

9. Combine MeOH layers and evaporate to dryness at 35°C

10. Dry under *vacuo* over P_2O_5 overnight

11. Silylate with 200µl freshly made silylation reagent (Pyridine : Hexamethyldisilazane : Trimethylchlorosilane, 5 : 1 :1, v/v/v) and leave for 30 minutes at RT

12. Inject 0.1µl onto GLC (Carlo Erba HRGC 5300) CpSil 5CB Chrompack capillary column (25m x 0.32mm id) at 130°C increasing at 4°C/min to 220°C held for 5 minutes detected using a flame ionisation detector

The methanolysis method for monosaccharide analysis has advantages over alditol acetate methods in that it will also detect uronic acids. However, even with the enzyme pre-hydrolysis step incorporated, full hydrolysis of crystalline cellulose was not achieved using this technique. For samples containg a large proportion of cellulose, alditol acetate derivatisation methods were prefered.

2.7 Monosaccharide Analysis: Alditol Acetates 1

1. Weigh accurately 0.1-1.0mg polysaccharide, add ≈ 200nmol inositol (internal standard) and freeze-dry

2. Hydrolyse with 0.1ml 12M H_2SO_4 for 1 hour at 35°C (for cellulose-containing samples) followed by 3 hours at 100°C in1M H_2SO_4

3. Neutralise with conc. NH_4OH

4. Add 200µl freshly made $NaBH_4$ solution (100mg/ml in 2M NH_4OH) and leave for 1 hour at room temperature

5. Quench with conc. HOAc (to pH < 6)

6. Add 3ml acetic anhydride + 0.45ml 1-methyl-imidazole and leave for 30 minutes at RT

7. Add 5ml ice-cold H_2O and shake thoroughly

8. Add 3ml CH_2Cl_2 and shake thoroughly

9. Remove H_2O layer, wash organic layer 6 times with ice-cold H_2O, transfer organic layer and evaporate to dryness at 40°C under nitrogen

10. Add 1ml acetone and evaporate to dryness

11. Dissolve in 0.5ml acetone (heat mildly if residue is crystalline)

12. Separate alditol acetates on a Carlo Erba HRGC 5300 with an SP-2330 fused silica capillary column (30m x 0.25mm id) held at 230°C for 40 minutes, detected using a flame ionisation detector

(Blakeney *et al*, 1983)

This method for derivatisation of alditol acetates was low yielding although the results were highly reproducible (accurate to within 5%). However, the low yields meant that any non-carbohydrate contamination in the samples, which was particularly problematic in cell wall fractions, had a

significant distorting effect on the results. Work by Englyst and Cummings (1984) suggested that, for efficient acetylation, the ratio of 1-methyl-imidazole/acetic anhydride to the hydrolysed sample volume is critical. Therefore, this method was subsequently modified.

2.8 Monosaccharide Analysis: Alditol Acetates 2

1. Steps 1-3 as described in section 2.8

4. Add 100µl $NaBH_4$ solution (200mg/ml in 2M NH_4OH) and incubate for 1 hour at 60°C

5. Add 0.1ml conc. HOAc to pH < 6 and evaporate under nitrogen at 40°C to a final volume of 400µl

6. Add 0.6ml 1-methyl-imidazole + 4ml acetic anhydride, mix and leave for 10 minutes at RT

7. Transfer into 10ml ice-cold deionised H_2O, mix and allow to cool

8. Add 2ml CH_2Cl_2, vortex and centrifuge at 2000 rpm for 5 minutes.

9. Remove aqueous layer and wash organic layer six times with ice-cold H_2O

10. Dry organic layer

11. Redissolve in 200µl CH_2Cl_2 and inject onto GC as in section 2.8, step 12. A revised temperature regime was used which improved separation: 50-200°C at 30°C/min, 200-235°C at 1°C/min followed by 5 minutes at 240°C

(Englyst & Cummings, 1984)

2.9 Monosaccharide Analysis: Alditol Acetates 3

1. Weigh accurately 0.1-1.0mg polysaccharide, add 600µl formic acid (90%) and incubate at 100°C for 1 hour

2. Evaporate at 40°C

3. Add 600µl 2M TFA and incubate for 1 hour at 120°C

4. Evaporate at 40°C to a residual oily layer

5. Add 1ml freshly made $NaBH_4$ solution (40mg/ml in 2M NH4OH) and incubate for 1 hour at 60°C

6. Quench by addition of 0.5ml acetone + 500nmol insoitol

7. Evaporate overnight at RT under nitrogen

8. Add 200µl CH_2Cl_2, stir, and 1ml ethyl acetate + 3ml acetic anhydride, stir

9. Add 200µl perchloric acid (70%), stir, leave for 5 minutes at RT and transfer into 10ml ice-cold H_2O

10. Add 200µl 1-methyl-imidazole, stir, leave for 5 minutes at RT, add 2ml CH_2Cl_2 and vortex

11. Centrifuge at 2000rpm for 5 minutes

12. Remove aqueous layer and wash organic layer six times with H_2O

13. Dry with Na_2SO_4 and evaporate at 40°C under nitrogen

14. Redissolve in 400µl CH_2Cl_2 and inject onto GC as described in section 2.9, step 11

(Kvernheim, 1987; Stevenson & Furneaux, 1991; Taylor & Conrad, 1972)

The hydrolysis step in this technique is not sufficient to hydrolyse crystalline cellulose, but is sufficiently mild to minimise acid degradation of monosaccharides. Hence this is the preferred method for monosaccharide analysis of non-cellulosic, neutral polysaccharides.

2.10 Tomato Cell Wall Extraction Protocol

2.10.1 Preparation of Cell Wall Material

1. Harvest mature green fruit, cut into quarters, and remove locular material and skin

2. Finely chop pericarp and plunge immediately into boiling absolute ethanol (514g/2l ethanol to give ca. 75% ethanol) and boil for a minimum of 10 minutes

3. Cool to room temperature

4. Wash with 75% ethanol on a sintered glass P4 funnel until the filtrate runs clear

5. Homogenise on ice in 75% EtOH using a Silverson coarse, followed by medium, cutter

6. Filter and wash as step 4

7. Filter to dryness and rehydrate with ice-cold deionised H_2O

8. Centrifuge at 27,100g (Sorvall RC5C centrifuge, SS-34 rotor) at 4°C and wash pellet twice with deionised H_2O

9. Collect pellet and store at -18°C

(Carrington *et al*, 1993)

2.10.2 Extraction of Pectins by Imidazole Buffer

1. Suspend cell wall material from 2.11.1 in 1.0M imidazole/HCl buffer, pH 7.0 containing 0.05% NaN_3 (500ml/50mg dry weight cell wall)

2. Stir at RT for 20 hours

3. Centrifuge at 27,100g (Sorvall RC5C, SS-034) and wash pellet three times with ice-cold deionised H_2O

4. Collect supernatants, filter through 10μm Millipore LCWP04700 filters prewetted with MeOH, concentrate by rotary evaporation at 40°C, dialyse extensively against deionised water at 1°C and freeze-dry

5. Resuspend pellet in imidazole/HCl buffer and repeat steps 1-4

Imidazole is preferred to CDTA or EDTA as it is easy to remove by dialysis (Mort *et al*, 1991). Rather than acting as a chelating agent, imidazole apparently acts as an ion exchange agent or a mild chaotrope (J.Mitchell, Unilever Research, pers.comm.)

2.10.3 Extraction of Further Pectins by Sodium Carbonate

1. Suspend pellet from 2.11.2 (step 5) in 50mM Na_2CO_3 containing 20mM $NaBH_4$ (500ml/50mg dry weight) saturated with nitrogen

2. Stir for 16 hours at 1°C

3. Separate solubilised and insoluble material as in 2.11.2 (steps 3 & 4)

4. Repeat steps 1 & 2 at 20°C for 3 hours

5. Repeat step 3

(Redgwell & Selvendran, 1986; Seymour *et al*, 1990)

2.10.4 Extraction of Hemicelluloses

1. Suspend pellet from 2.11.3 step 5 in 0.5M KOH containing 20mM NaBH4 (500ml/50mg dry weight) saturated with nitrogen at RT for 4 hours

2. Separate solubilised and insoluble material as previously described (2.11.2 steps 3 & 4)

3. Repeat extraction

4. Repeat steps 1-3 with 1.0M KOH and 6.0M KOH

(Kato & Matsuda, 1976; Redgwell & Selvendran, 1986; Seymour *et al*, 1990)

2.11 Pea Cell Wall Extraction Protocol

2.11.1 Preparation of Cell Wall Material

1. Dark-grown pea seedlings (*Pisum sativum* var. Alaska) were harvested at the third internode stage

2. 8mm portions of the third internode were removed 3mm below the apical hook and plunged immediately into liquid nitrogen.

3. Excised segments were boiled in absolute ethanol (to make 75% ethanol) for 10 minutes and washed in several changes of 75% ethanol

4. Segments were ground to a fine white powder using a pestle and mortar in liquid nitrogen

5. After grinding, the material was transferred to a glass-on-glass homogeniser and further ground in 75% EtOH on ice

6. Insoluble CWM was separated by centrifugation (27,100g, 4°C, 20 minutes) and the pellet rehydrated with several changes of ice-cold deionised H_2O

7. Pellet stored at -80°C to prevent browning observed at -18°C

2.11.2 Sequential Extraction

Cell wall material was extracted essentially according to the extraction protocol for tomato cell wall material described in sections 2.11.2-2.11.4. However, the final alkali extraction step was performed with 4M KOH in accordance with Talbott and Ray (1992a).

2.12 Production of Bacterial Cellulose

2.12.1 Revival of Bacterial Stock Cultures

Acetobacter aceti ssp. *xylinum* (ATCC 53524, US Patent 4,863,565) was supplied as a freeze-dried culture. This was revived onto glucose/yeast extract agar plates and incubated for 5 days at 30°C. These plates were used to inoculate sterile 1/4 strength Ringers solution (BDH), to a final cell concentration of 5 x 10^5 cells/ml, as determined by Total Viable Cell counts. 1ml of this suspension was inoculated onto Cryo-Bead bacterial Preserver (Technical Service Consultants Ltd, UK) and stored at -80°C. When fresh cultures were required, one bead was removed and inoculated onto glucose/yeast extract agar plates as above. Cultures were prepared for long-term storage at 4°C by inoculating glucose/yeast extract agar slopes with bacteria from the original plates.

2.12.2 Production of Seed Cultures

5ml of inoculated, sterile, 1/4 strength Ringers solution was used to inoculate 95ml Hestrin/Schramm medium (Hestrin & Schramm, 1954) in a 500ml sterile Roux bottle. After gentle agitation to ensure thorough mixing, the cultures were incubated at 30°C for 3 days until a thick pellicle of cellulose was formed. This pellicle was transferred aseptically into 50ml sterilised 0.02M phosphate buffer pH 6.0

and ground using a pre-sterilised Ultra-Turrax T25 (Janke & Kunkel). The cellulose was removed by vacuum filtration through sterile Miracloth (Calbiochem Corp., USA) and the bacterial suspension collected in a sterilised shake flask and stored at 4°C until further use (R.H. Atalla, pers.comm.).

2.12.3 Growth Media for Acetobacter aceti *ssp.* xylinum

2.12.3.1 Glucose/Yeast Extract Agar

Component	g/l
Glucose	20
Yeast Extract	10
Agar	30

2.12.3.2 Hestrin Schramm medium

Component	g/l
Glucose	20
Bacteriological Peptone	5
Yeast Extract	5
Na_2PO_4	2.7
citric acid.H_2O	1.15

(Hestrin & Schramm, 1954)

2.12.4 Production of Cellulose Composites

9ml sterile Ringers solution was inoculated with a sterile loop of *A.aceti* ssp. *xylinum* from refrigerated culture slopes to a bacterial concentration of 5 x 10^5. 0.5ml of suspension was inoculated into 9ml Hestrin/Schramm medium (Hestrin & Schramm, 1954) or an equivalent volume of medium containing 0.5% of modifying polymers, into 25cm^2 canted neck, vented tissue culture flasks with a 2μm hydrophobic membrane cap (Corning Inc., USA). Cultures were incubated at 30°C with orbital agitation at 50rpm for 48 or 72 hours. After incubation pellicles were removed aseptically from the culture flasks and washed thoroughly in several changes of sterilised deionised H_2O at RT, with a final wash in H_2O containing 0.05% NaN_3.

2.12.5 Deep-Etch, Freeze-Fracture, Transmission Electron Microscopy

Samples were cut from fresh, hydrated cellulosic pellicles using a 4mm cork borer and placed on filter paper attached to an aluminium disc. Metal mirror impact freezing was carried out on a KF80 Cryostation (Leica, UK) using an MM80 Impact Freezer Head. After impact, the sample was transferred to a CFE-50 Freeze-Fracture Unit (Cressington, UK). Fracturing was performed at -179°C. After etching for 8 min at -95°C, samples were rotary shadowed at an angle of 45° using 1.5nm tungsten/tantalum, followed by rotary carbon at 90° to a thickness of 8nm.

Replicas were floated off in distilled water and cleaned in chromic acid overnight. After rinsing, replicas were collected on a 450 mesh hexagonal copper grid and visualized on a Jeol 1200EXII Transmission Elevtron Microscope. Micrographs were produced using Kodak Reverse Contrast Paper. Images were analysed using a Quantimet 570 Image Analyser (Leica, UK).

2.13 ^{13}C NMR Spectroscopy

NMR spectra were acquired on a Bruker MSL 300 instrument operating at 75.46mhz for ^{13}C and at 303 K unless otherwise stated. Dipolar decoupling (67 kHz) was used in all experiments. Spin-locking

fields for cross-polarization and magic angle spinning (CP/MAS) were approximately 40 kHz with a contact time of 1msec. Magic angle spinning speeds were typically 3 kHz and experimental recycle times were 3-5 sec.

2.14 HPAEC Analysis of Xyloglucan

Xyloglucan oligomers were generated by the action of *Trichoderma viride endo*-1,4-β-glucanase (Megazyme Pty, Australia). Oligomers were analysed on a Dionex HPAEC system. Samples were injected onto an Analytical CarboPac PA100 (4x250mm) column + guard column and eluted with a linear gradient from 95% 0.1M NaOH/5% 0.1M NaOH/500mM NaOAc to 70% 0.1M NaOH/30% 0.1M NaOH/500mM NaOAc in 40 minutes followed by a 5 minute wash in 100% 0.1M NaOH/500mM NaOAc at a flow rate of 1.0ml/min at ambient temperature. Samples were detected using a PED 2 detector.

Chapter 3: The Interaction of Tamarind Xyloglucan with Cotton Linters Cellulose

3.1. INTRODUCTION

In the primary cell wall of most dicotyledonous and non-graminaceous monocotyledonous plants xyloglucan and cellulose are intimately associated in a tightly organised macromolecular complex (Hayashi & Maclachlan, 1984; Fry, 1989; Hayashi, 1989). Complete dissociation of the two components is achieved only by the use of strong alkaline or chaotropic agents (Hayashi & Maclachlan, 1984; Chambat *et al*, 1984) which are sufficient to cause microfibril swelling (Edelmann & Fry, 1992a). The length of xyloglucan molecules is many times greater than microfibril diameters or intermicrofibril distances and xyloglucan is propsed to cross-link adjacent cellulose microfibrils (McCann *et al*, 1990). Iodine staining, autoradiography, electron microscopy (Hayashi & Maclachlan, 1984) and immunogold labelling (Baba *et al*, 1994a) localise xyloglucan on and between microfibrils in native xyloglucan/cellulose complexes. The above observations indicate that, *in muro*, xyloglucan is located within microfibrils, as a monolayer on microfibril surfaces and cross-linking adjacent microfibrils to form a highly ordered network.

Attempts to reconstruct macromolecular complexes of xyloglucan and cellulose with properties similar to those of native networks have met with only limited success. Using xyloglucan fragments isolated from suspension cultured sycamore cells, Valent and Albersheim (1974) found evidence for *in vitro* association with cellulose mediated by hydrogen bonds. Hayashi *et al* (1987) report a highly specific interaction between pea xyloglucan and a number of different celluloses *in vitro*, with binding being unaffected by the presence of a 10-fold excess of 1,2-B-glucan, 1,3-B-glucan, 1,3- and 1,4-mixed linkage glucan, arabinogalactan or pectin. However, levels of binding achieved *in vitro* were several-

fold less than those seen *in vivo* and were directly correlated with the surface area of the cellulose, interpreted by the authors as indicative of surface binding only. Baba *et al* (1994a) showed that xyloglucan in reconstituted complexes was confined solely to microfibrils, with no evidence for inter-microfibril association. Moreover, reconstitued complexes are much less tightly organised than those isolated from cell walls, requiring only weak alkali to effect their dissociation (Hayashi & Maclachlan, 1984; Hayashi *et al*, 1987; Acebes *et al*, 1993). No experimental information is available on the structural features which mediate the specific interaction between cellulose and xyloglucan, although two computer simulations are reported (Finkenstadt *et al*, 1995; Levy *et al*, 1991).

At the time that the work in this chapter was performed only two major pieces of literature, that of Valent and Albersheim (1974) and Hayashi *et al* (1987) demonstrated *in vitro* association of cellulose and xyloglucan and, in the former example, binding was achieved under non-physiological conditions. Despite the failure in both cases to produce complexes which mimic native networks studies of interactions between these two polymers *in vitro* provides an opportunity for manipulation of starting materials and binding conditions not readily achieved *in planta*. The ability to 'fingerprint' xyloglucan structures by *endo*-1,4-β-glucanase digestion in principle allows the unit substructuring (Fig 3.3a) involved in binding to be assessed. Selective de-binding would also allow the strength on *in vitro* (presumably surface) binding to be characterised with respect to polymer sub-structure and molecular size. Scant literature coverage, combined with the fact that our laboratory had no previous experience in this area, prompted us to pursue this line of research, focusing on the binding of tamarind xyloglucan with cotton linters cellulose. Tamarind xyloglucan is found as a major storage polysaccharide in seeds of *Tamarindus indica* (Kooiman, 1960a; Meier & Reid, 1982). It differs from many primary cell wall xyloglucans in that it is non-fucosylated, but has the advantage of being available in large quantities and is fully characterised (Gidley *et al*, 1991a; Lang *et al*, 1992; York *et al*, 1990). Cotton linters cellulose can be purchased commercially in kilogram quantities.

3.2. MATERIALS AND METHODS

3.2.1. Characterisation of Starting Materials

3.2.1.1 Cellulose

Powdered cotton linters cellulose was obtained from Fluka Biochemika. Neutral sugar composition was analysed by alditol acetates Method 1 (Section 2.7). ^{13}C NMR spectra were obtained as descibed in Section 2.12.6

3.2.1.2 Tamarind Xyloglucan

Tamarind xyloglucan was purified from Glyloid 3S (Dainippon Pharmaceutical Co., Osaka, Japan) as described in General Materials and Methods (Section 2.4). The oligosaccharide composition was determined by digestion with *endo*-1,4-β-glucanase from *Trichoderma viride* (Megazyme Pty, Australia) for 16 hours at 40°C with constant shaking in 25mM acetate buffer pH 4.5 containing 0.05% NaN_3. Oligosaccharides were analysed on a Dionex HPAEC system using the conditions described in Section 2.12.7 Tamarind xyloglucan has been extensively characterised by other authors (Gidley *et al*, 1991; York *et al*, 1990).

3.2.2. Formation of the Cellulose/Xyloglucan Complex

Complexes were formed essentially according to the method of Hayashi *et al*, (1987). Approximately 100mg of tamarind xyloglucan was dissolved in 50ml 25mM sodium acetate buffer, pH 5.0 containing 0.01% sodium azide. This solution was added slowly to a suspension of 5.00g cotton linters cellulose in 150ml buffer with constant stirring. The mixture was incubated at 37° C for 40 hours with constant orbital shaking at 150 rpm.

3.2.3. Establishment of the Column

After mixing for 40 hours the suspension was poured into a Pharmacia C26/40 column. Unbound xyloglucan was washed off the column with two volumes of acetate buffer followed by two volumes sterile deionised water. After washing, a small amount of column material was removed and subsequently freeze-dried for neutral sugar composition analysis by alditol acetates Method 1 (Section 2.7). The column was equilibrated overnight by eluting with deionised water containing 0.01% sodium azide at a constant flow rate of 0.5ml/min. After equilibration, a vertical arrangement of mixing and limit buffer was set up as shown in Figure 3.1. The column was run for 20 hours at a flow rate of 0.5ml/min, with 5ml fractions collected using an LKB 700 Fraction Collector.

3.2.4. Fraction Analysis.

3.2.4.1 Total Carbohydrate Content.

100µl of each fraction was neutralised with 100µl 4M acetic acid and assayed using the Phenol/Sulphuric Acid Test (Section 2.1). Carbohydrate content is recorded as glucose equivalents against a standard curve of glucose in 4M sodium acetate.

3.2.4.2 Xyloglucan Content

0.5ml aliquots from each fraction were neutralised with 0.5ml 4M acetic acid and assayed for xyloglucan content using the Iodine/Potassium Iodide Test (Section 2.3).

3.2.5. Cleaning Up Cotton Linters Cellulose

A number of washing procedures were employed to remove alkali-soluble material from the commercial cellulose preparation:

(a) Shaking in 2M KOH for 2 hours

(b) 10 washes in 2M KOH alternated with deionised water for 2 hours

(c) Shaking in 6M KOH for 2 Hours

(d) Refluxed for 2 hours in 2.5M HCl according to the method of Sugiyama *et al* (1991) for generating microcrystalline cellulose

(e) Refluxed in 2.5M HCl for 2 hours followed by shaking for 2 hours in 2M KOH

Figure 3.1: Diagram of the Cellulose/Xyloglucan Column

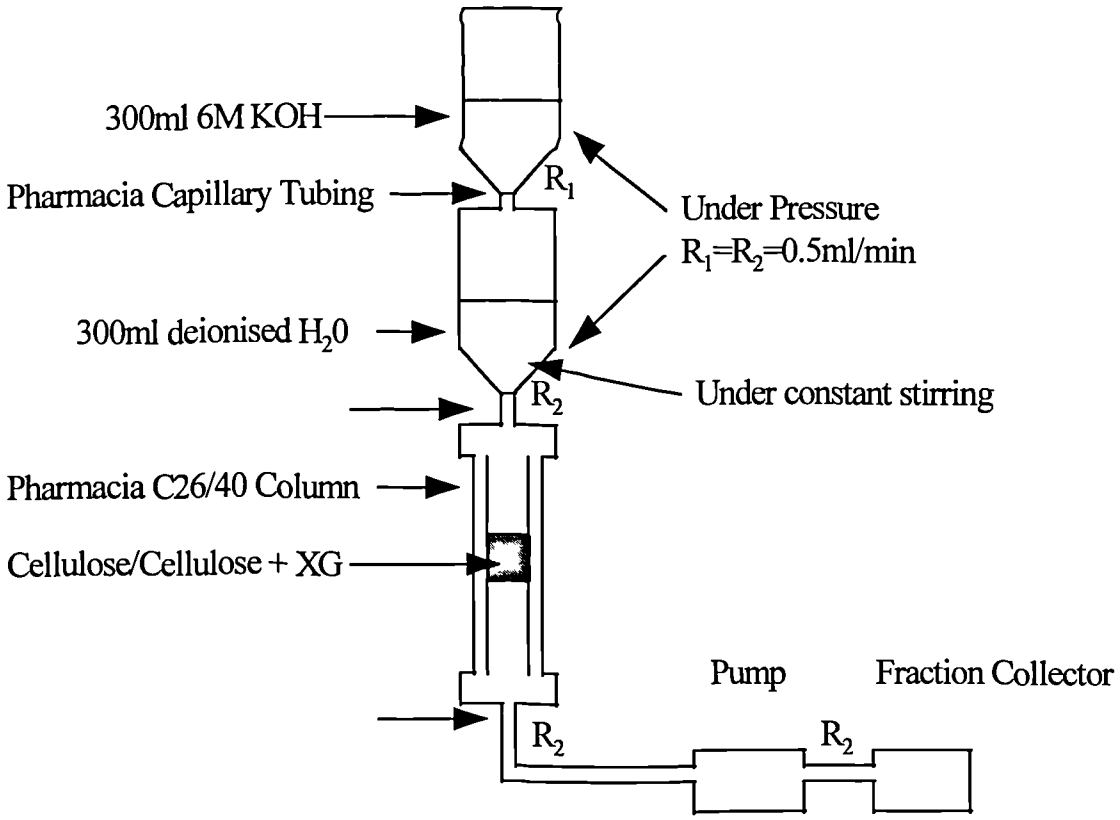

Showing the vertical mixing arrangement of limit (6.0M KOH) and mixing buffer (deionised H_2O) for eluting the cellulose/xyloglucan column

For all experiments, 10g of cellulose was washed in 200ml acid/alkali. After each washing regime, cellulose material was filtered on a P4 sintered glass filter, washed to neutrality using deionised water and subsequently freeze-dried. 5g of cleaned cellulose is suspended in 25mM sodium acetate buffer pH

5.0 containing 0.01% sodium azide, made into a column and eluted with an alkali gradient as described in section 3.2.3. Fractions were analysed for total carbohydrate content as described in section 3.2.4.1 Cellulose treated with 2.5M HCl formed a column in a 1:1 ratio of ceolite to prevent overpacking and impedance of eluent flow. Samples from washing regimes (c) and (d) were analysed by ^{13}C NMR as in 3.2.1.1.

3.2.6. Characterisation of Oligomers Generated by Alkali Treatment of Cotton Linters Cellulose.

2g of freeze-dried cellulose from 3.2.5(b) was shaken in 50ml 4M KOH for 2 hours. After washing to neutrality, the filtrate was collected and neutralised with acetic acid. The neutralised filtrate was passed through an Amicon Filter (YM2 mwt cut off < 1000 under a constant pressure of 50psi to remove salts. The desalted solution was freeze-dried and subsequently redissolved in 2M NaOH to a final concentration of 2mg/ml. Oligomers were compared with cellulose standards dp3-7 (provided by Mike Gidley, Unilever Research), D-+-glucose and D-+-cellobiose (Sigma) dissolved in 2M KOH to a concentration of 2mg/ml. Samples from fractions collected from elution of the cellulose/xyloglucan column were also compared.

Oligomers were analysed on a Dionex HPAEC system. 200µl of test samples and 10µl of standard solutions were injected onto an Analytical CarboPac PA100 (4x250mm) column + guard column and eluted with a linear gradient from 95% 0.15M NaOH/5% 0.15M NaOH/1000mM NaOAc to 60% 0.15M NaOH/40% 0.15M NaOH/1000mM NaOAc in 25 minutes followed by a 5 minute wash in 100% 0.15M NaOH/1000mM NaOAc at a flow rate of 1.0ml/min at ambient temperature. Samples were detected using a PED 2 detector.

3.3. RESULTS

3.3.1. Cellulose Characterisation

3.3.1.1 Sugar Composition

Neutral sugar analysis gave a sugar composition analysis for cotton linters cellulose of 96.35% glucose, 2.7% xylose and 0.95% mannose. The cellulose contained no detectable galactose and hence galactose can be used as an internal marker for the presence of xyloglucan in xyloglucan/cellulose composites

3.3.1.2 ^{13}C CP/MAS NMR

Under conditions of cross-polarisation, dipolar decoupling and magic angle spinning (CP/DD/MAS) relatively-rigid ('solid-like') segments are detected (Gidley 1992). A ^{13}C CP/DD/MAS spectrum of hydrated cotton linters cellulose is shown in Figure 3.2(a) with the same spectrum after application of resolution enhancement in Figure 3.2(b).

Signals at ca. 105, 88-91 and 84-86ppm correspond to C-1 and C-4 sites in crystalline and non-crystalline environments respectively (VanderHart & Atalla, 1984). Integration of signals at the latter two sites gives a crystalline content of ca. 60%, which is slightly lower than published estimates (e.g. 68%, Lennholm *et al*, 1994). Application of resolution enhancement allows the identification of the two crystalline allomorphs of cellulose I, Iα and Iβ as outlined by Atalla and VanderHart (Atalla & VanderHart, 1984; VanderHart & Atalla, 1984). In the resolution enhanced spectrum(Figure 3.2(b)) signals at 105.5, 90.1 and 89.3ppm corresponding to the Iα form, and 106.2, 104.4, 89.3 and 88.6ppm corresponding to the Iβ form, are shown (VanderHart & Atalla, 1984; Debzi *et al*, 1991; Yamamoto & Horii, 1993). Comparison of C-4 signals with published quantified signal patterns (Debzi *et al*, 1991; Yamamoto & Horii, 1993) gives Iα/Iβ ratios of 24/76, in close agreement with published estimates (Lennholm *et al*, 1994). The overall description for the molecular organisation of cotton linters cellulose is therefore 14% Iα, 46% Iβ and 36% non-crystalline.

Figure 3.2: ^{13}C CP/DD/MAS Spectrum of Cotton Linters Cellulose

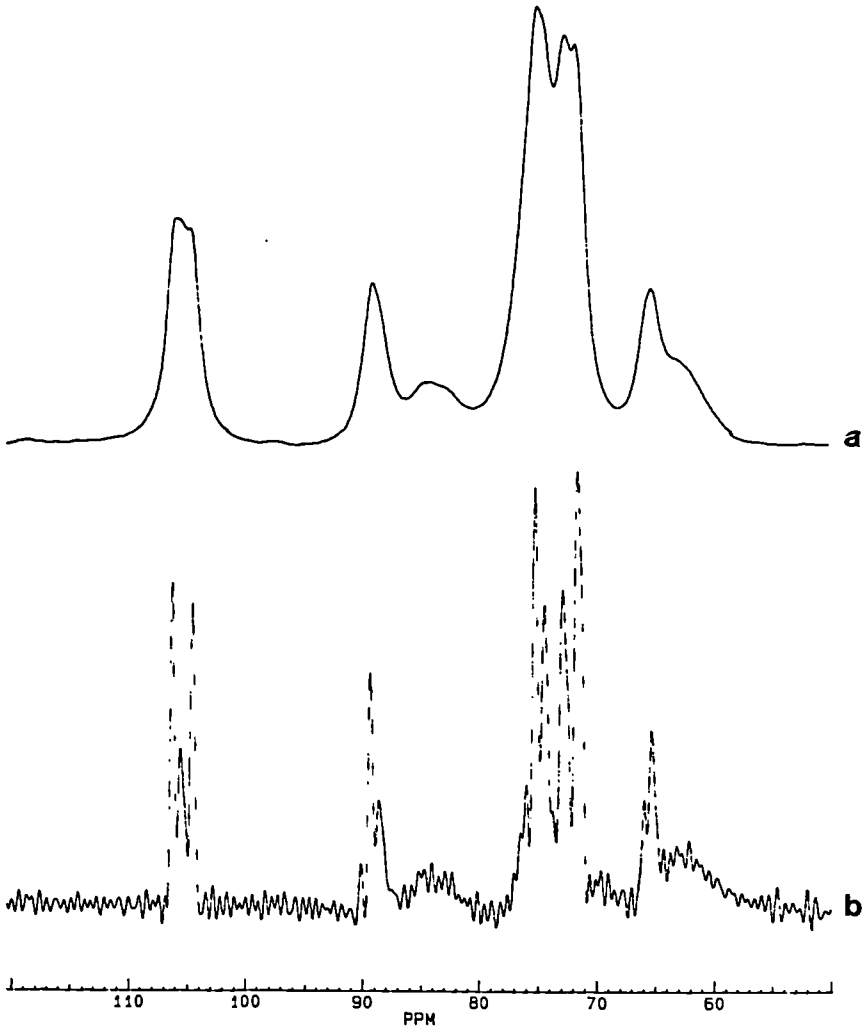

(a) Spectrum of hydrated cotton linters cellulose and (b) resolution enhancement (line broadening -70Hz, Gaussian multiplication 0.5) of spectrum (a).

3.3.2 Tamarind Xyloglucan Characterisation

Using the amount of enzyme calculated to digest tamarind xyloglucan over 16 hours complete digestion into four component oligosaccharides is achieved and the profile of these oligosaccharides after separation on the Dionex system is shown in Figure 3.4a. The oligosaccharides are assigned using the nomenclature for xyloglucan-derived oligosaccharides proposed by Fry *et al* (1993) and their structures are shown in Figure 3.3. The ratios of these oligosaccharides are (XXXG:XLXG:XXLG:XLLG = 1:0.4:1.9:2.7) in close agreement with that reported by Fanutti *et al* (1993). Controlled digestion using 1/3 of the enzyme used for complete digestion gives a slow degradation into the four oligosaccharides described above, with higher mwt oligomers eluting at approximately 29 minutes and approximately 40 minutes (Figure 3.4b). Further digestion yields a greater proportion of the four basic units with a concomitant reduction in the high mwt oligomers (Figure 3.4c). The ratios of the oligosaccharide components determined by integration are shown in Table 3.1. Under controlled digestion conditions all four basic oligosaccharide structural units are generated more slowly, which can be attributed to an enzyme quantity effect. However, the altered ratios of these four oligosaccharides under these conditions suggests that the more heavily substituted units, particularly XLLG are relatively more resistant to hydrolysis. Hisamatsu *et al* (1992) reported oligosaccharides comprising two basic units (ie 8 glucose residues) from suspension cultured sycamore cells which were generated by *endo*-1,4-β-glucanase action, but were either fully or partially resistant to further hydrolysis even when vast excesses of enzyme were used. This resistance to hydrolysis was correlated with substitution at C-2 of Glc^c or two adjacent fucosylated sidechains (please refer to Hisamatsu *et al,* 1992 for nomenclature protocols). Whilst in this case no fucose is present and tamarind can be degraded fully using stochiometric amounts of *endo*-1,4-β-glucanase, these results suggest that more heavily substituted regions of the tamarind seed polysaccharide confer a degree of steric hindrance at the catalytic site of the enzyme.

Figure 3.3: The Four Component Oligosaccharides of Tamarind Xyloglucan

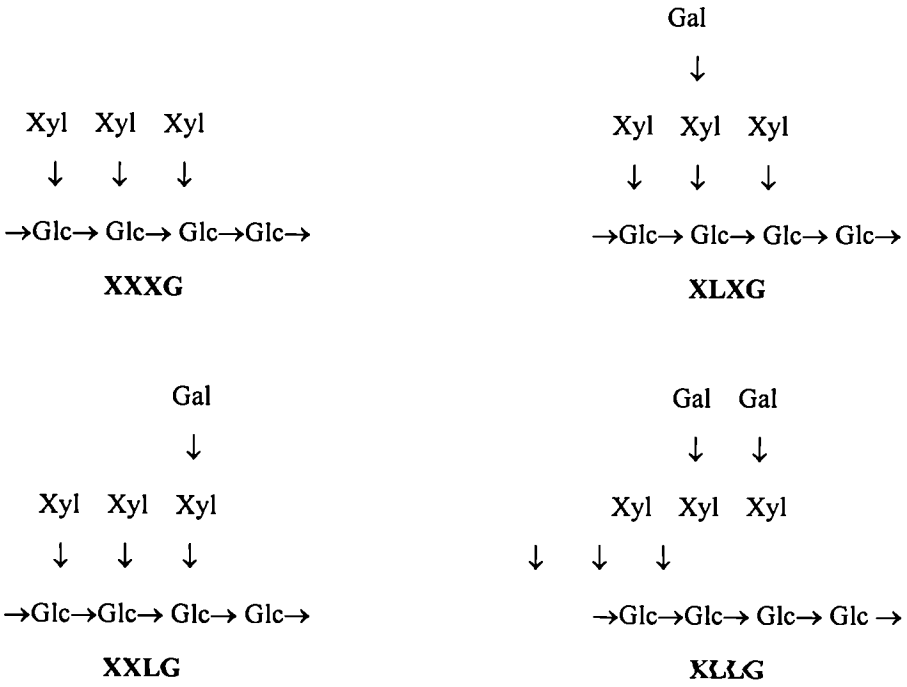

These oligosaccharides are the sole products of digestion of tamarind xyloglucan with *endo*-1,4-β-glucanase (York *et al*, 1990) showing that this polysaccharide is comprised entirely of a Glc_4,Xyl_3 repeating unit with various degrees of galactosyl substitution

3.3.3. Cellulose/Xyloglucan Complex

3.3.3.1 Sugar Composition

Analysis of the neutral sugar composition of the cellulose/xyloglucan complex after washing, using galactose as an internal marker (tamarind xyloglucan: Glc:Xyl:Gal = 2.8:2.25:1.0 (Gidley *et al*, 1991a) gives a cellulose/xyloglucan ratio of 1:0.03 if it is assumed that the bound xyloglucan has the same galactose content as the bulk material. This correlates closely with data reported by Hayashi *et al* (1987) reporting saturation of different celluloses with pea xyloglucan at between 1 and 5% (w/w), but is at least an order of magnitude lower than that seen *in muro* (e.g. 1:0.3 in onion bulbs, Redgwell & Selvendran, 1986).

Figure 3.4: Oligosaccharides Generated by the action of *endo*-Glucanase of Tamarind Xyloglucan

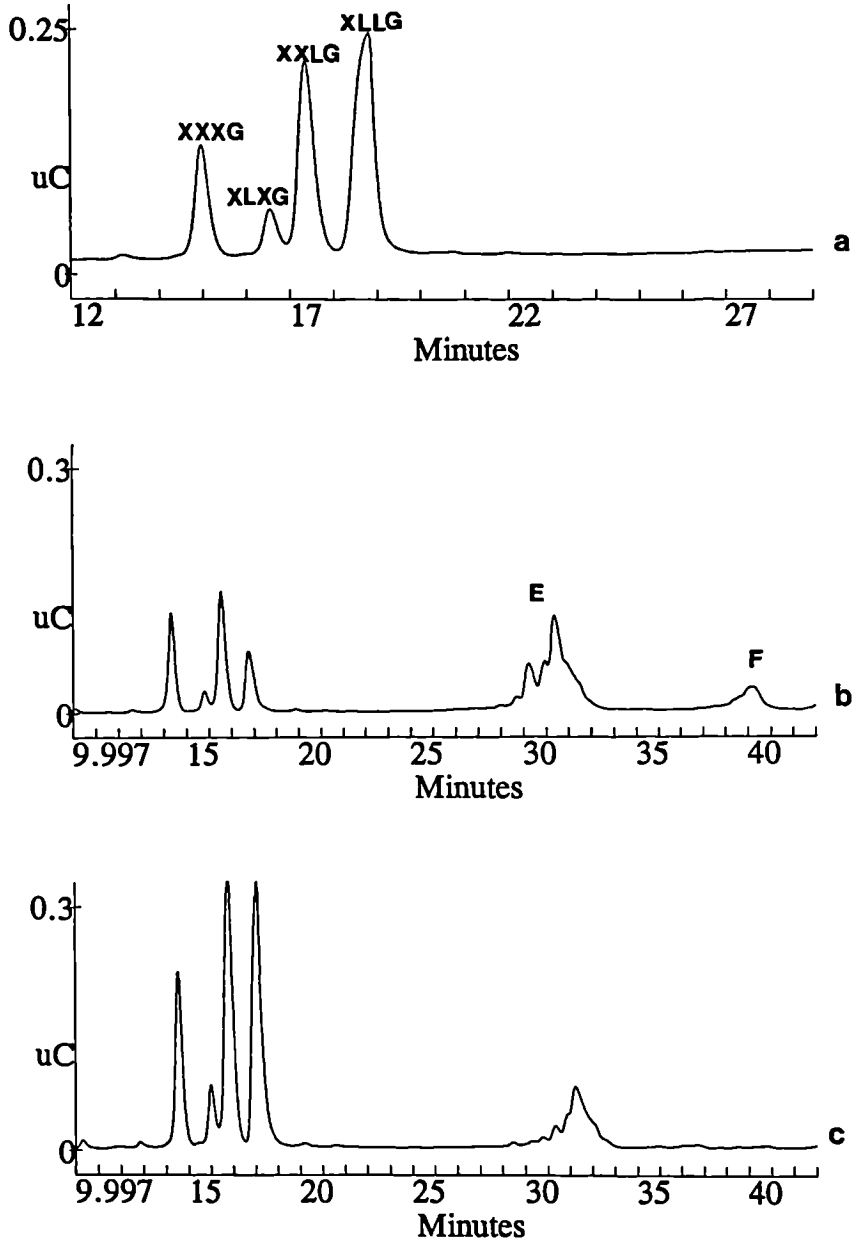

Profile of tamarind xyloglucan oligosaccharides separated using the Dionex HPAEC system (a) the four basic oligosaccharide units eluting between 14 and 18 minutes, (b) after partial digestion with 1/3 of enzyme required for full digestion showing the presence of higher mwt oligomers eluted at approximately 29 minutes (E) and approximately 40 minutes (f) and altered ratios of the four basic oligosaccharides, (c) after further digestion as (b) showing increase in four component oligosaccharides with concomitant decrease in higher mwt oligomers E and loss of oligomers F.

Table 3.1: Ratios of Oligosaccharides of Tamarind Xyloglucan Generated by *endo*-1,4-β-Glucanase Digestion

	XXXG	XLXG	XXLG	XLLG	Oligomers E	Oligomers F
Complete Digestion	1	0.4	1.9	2.7	-	-
Partial Digestion 1	1	0.21	1.36	0.82	3.75	0.6
Partial Digestion 2	1	0.33	1.82	1.99	1.14	-

3.3.3.2 ^{13}C NMR

A ^{13}C CP/DD/MAS spectrum of the cellulose/xyloglucan hydrate is shown in Figure 3.5(a) with the same spectrum after application of resolution enhancement in Figure 3.5(c). Xyloglucan C-1 chemical shifts in the absence of cellulose (Figure 3.5(b)) for galactose, glucose and xylose residues are 105.5, 103.6 and 99.8ppm respectively (Gidley *et al*, 1991a) and comparison of spectra (a) and (b) provides no evidence for the presence of xyloglucan. This is expected from the low level of incorporation into the complex as ^{13}C NMR is insufficiently sensitive to detect components comprising less than approximately 10% of the total material.

Calculation of crystalline/non-crystalline and Iα/Iβ ratios as described in section 3.3.1.2 gives an overall description for the cellulose component of 15.6% Iα, 49.4% Iβ and 35.0% non-crystalline. The appearance of a pair of signals at ca. 84.8 and 83.8ppm is in agreement with spectra of apple cell walls and Avicel microcrystalline cellulose showing fine structure of a band recently assigned to a pair of crystallographically non-equivalent structural units on the well-ordered surfaces of crystals (Newman *et al*, 1994). This band is more usually assigned to disordered cellulose (Horii *et al*, 1984) and resolution of fine structure is not seen in the spectrum of the starting material (Figure 3.2 (b)).

Figure 3.5: ^{13}C CP/DD/MAS Spectra of Cotton Linters Cellulose/Tamarind Xyloglucan Composites

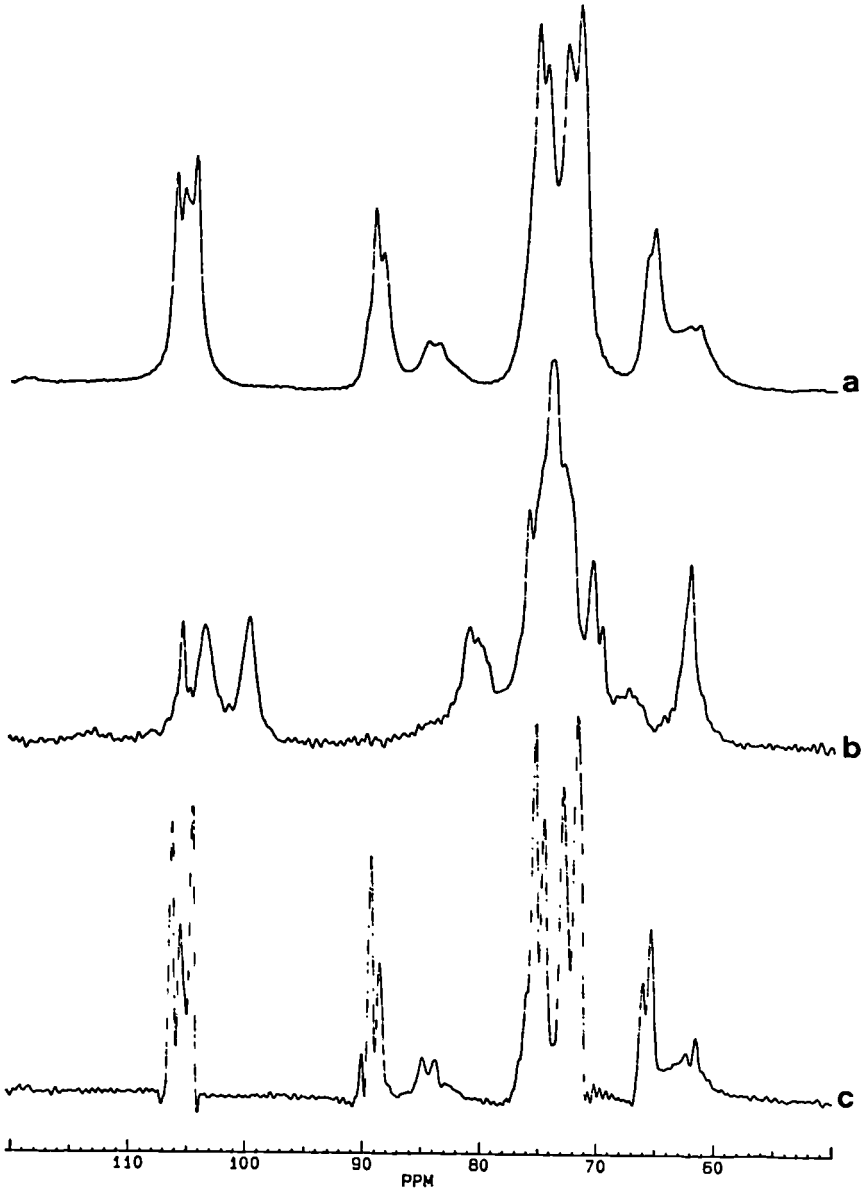

Spectra of (a) hydrated cellulose/xyloglucan composite, (b) 30% (w/v) hydrate of tamarind xyloglucan , (c) resolution enhancement (line broadening -70Hz, Guassian multiplication 0.5) of spectrum (a) illustrating fine structure of cellulose signals at C-1 and C-4 and particularly the fine structure of the band at ca.84-86ppm, and the absence of signals for xyloglucan at ca. 103.6 and 99.8ppm.

3.3.4 Deconstruction of the Cellulose/Xyloglucan Composite using an Alkali Gradient

Using a vertical mixing arrangement as illustrated in Figure 3.1, a convex gradient of KOH concentration can be calculated using the following equation:

$$C_1=C_0\,[1-e^{-tR1/Vo}] \qquad R_1=R_2$$

C_0 = concentration of limit buffer

C_1 = concentration of mixing buffer

V_0 = initial volume of limit buffer

t = time

The gradient of KOH concentration is shown in Figure 3.6.

Fractions eluted from the column were analysed for total carbohydrate and the results are shown in Figure 3.7(a). After fraction 9 (t = 90 minutes) a precipitate was formed upon neutralisation. Although the precipitate was dissolved after the addition of concentrated sulphuric acid (Section 2.1) measurements are likely to be an underestimate of total carbohydrate release. Integration of Figure 3.7 (a) gives approximately 158mg carbohydrate released by the alkali gradient, closely approximating the expected 145mg xyloglucan component as predicted by sugar analysis (cellulose:xyloglucan = 1:0.03) although the formation of a precipitate under neutralistion precludes accurate quantification. However, almost the same amount (ca. 134mg) of carbohydrate material is released in the control experiment suggesting that much of the material measured is cellulose rather than xyloglucan. The difference between traces (a) and (b) is less than the total amount of xyloglucan present. The elution profile for cellulose/xyloglucan complexes is almost identical to the control apart from between t=90 and t=200 and no xyloglucan remains on the column after application of the alkali gradient. Combined with the fact that this difference between traces (a) and (b) is reproducible, we speculate that most of the xyloglucan is eluted between t=90 and t=200 and the amount detected is less than predicted due to formation of cellulose/xyloglucan complexes when cellulose precipitates out of solution upon neutralisation, which renders the xyloglucan unavailable for analysis by the Phenol/Sulphuric acid test.

Sugar analysis of precipitated material revealed very small amounts of xyloglucan against a large excess of cellulosic material. Unfortunately the total amount of xyloglucan present in association with precipitated cellulose was not quantified so it is not possible to validate this hypothesis, but work by previous authors (Hayashi & Maclachlan, 1984; Hayashi *et al*, 1987; Acebes *et al*, 1993) supports dissociation from cellulose under relatively weak alkali conditions (in this case <1.0M KOH). It was not possible to use the iodine/potassium iodide assay to distinguish between xyloglucan and other carbohydrate components due to the large amounts of precipitate formed.

3.3.5 Effect of Washing Regimes on the Removal of Alkali Soluble Components from Cotton Linters Cellulose

Figure 3.7 (c-g) shows the effects of different pre-treatment washing regimes on solubilisation of cellulose under identical elution regimes to those in section 3.3.4. Washing in 2M KOH (c and d) reduced, but failed to eliminate, the leaching of cellulose components under an alkali gradient, with the major effect being a delay in the onset of significant solubilisation. Acid treatment actually increased the amount of material solubilised in an alkali gradient, implying partial degradation of the cellulose rendering it more susceptible to alkali leaching.

3.3.6 ^{13}C CP/DD/MAS NMR of Acid and Alkali Treated Cotton Linters Cellulose

Acid-treated cellulose (Figure 3.8 (a), (b)) exhibits an increase in crystallinity with negligible alteration in Iα/Iβ ratios compared with the starting material. Analysis of spectra (as in section 3.3.1 (b)) gives an overall description of acid-treated cotton linters cellulose of 17% Iα, 55% Iβ and 28% non-crystalline.

Figure 3.6: Gradient of KOH Concentration Using a Vertical Mixing Arrangement

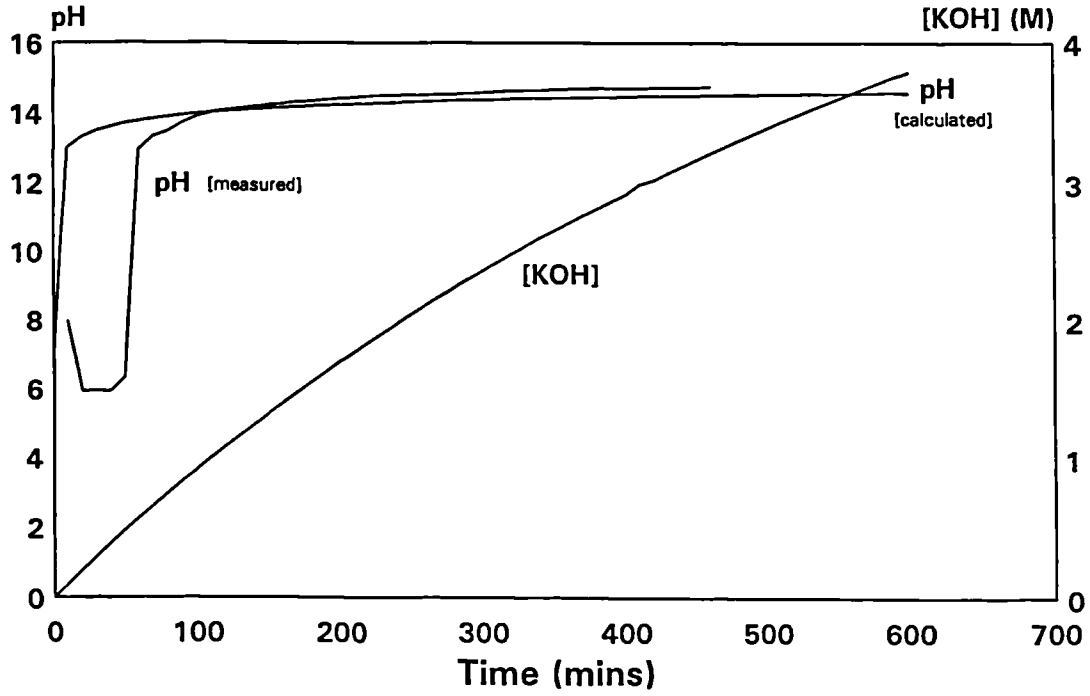

Limit Buffer = 6M KOH
R1 = R2 = 0.5ml/min

Gradient of KOH concentration with time using a vertical mixing arrangement shown against the increase in pH of the eluent calculated from pH = 14 + (log_{10}[OH-]) and measured from eluted fractions

Figure 3.7: Profile of Carbohydrate Released by Elution of Cellulose Columns with an Alkali Gradient (cf. Figure 3.4)

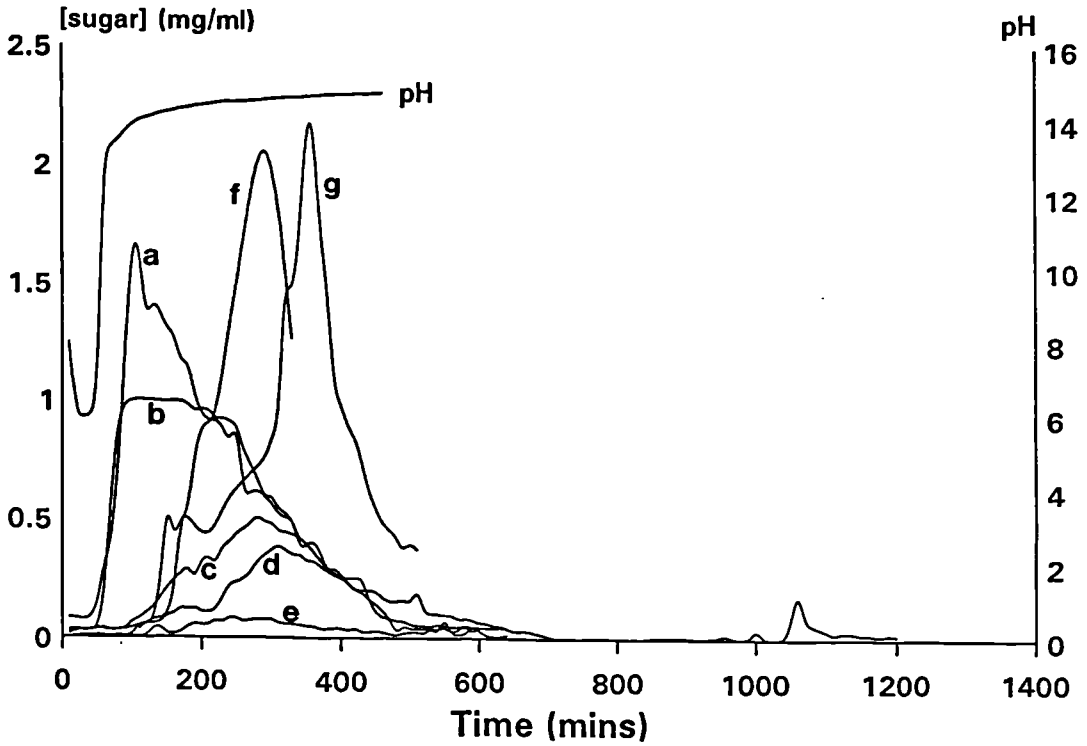

Glucose Standard
Limit Buffer = 6M KOH

Carbohydrate (mg/ml of 5ml fractions) released from (a) cellulose/xyloglucan column, (b) cellulose only, (c)cellulose washed once in 2M KOH, (d) cellulose washed 10 times in 2M KOH, (e) cellulose washed once in 6M KOH, (f) cellulose refluxed in 2.5M HCl, (g) cellulose refluxed in 2.5M HCl followed by washing in 2M KOH. All chromatography conditions are identical.

It is predicted that treatment with 6M KOH will effect a transformation from cellulose I to a mixture of cellulose II (Atalla *et al*, 1980) and non-crystalline cellulose I. Analysis of spectra (Figure 3.8 (c), (d)) gives a signal at C-1 of 107.9ppm, diagnostic of cellulose II. (Fyfe *et al*, 1983). The second chemical shift for cellulose II C-1 at 106.2 is not resolved. C-4 signals at 88.8, 89.6 and 85.3 are assigned to cellulose II, cellulose I (crystalline) and non-crystalline cellulose I respectively showing that 6M KOH has partially transformed cotton linters cellulose to the cellulose II polymorph, with a reduction in the crystallinity of residual cellulose I.

3.3.6 Analysis of Cellulose Oligomers using HPAEC

Filtration through an Amicon filter with mwt cut-off < 1000 should remove salts and also oligomeric material of dp < 4. However, analysis of oligomers released by alkali treatment of cellulose (Figure 3.9b) indicates the presence of oligomers < dp4 suggesting some degradation in the 2M KOH solvent. Comparison of oligomers obtained with those from fraction 47 (t = 470 minutes Figure 3.9a) shows essentially identical profiles. This indicates that treatment with 4M KOH effectively mimics column conditions. Comparison of profiles with those of standards (c-h) clearly identify low molecular weight oligomers in the test samples. Slight shifts in retention times are attributed to fluctuations in ambient temperature.

3.4 DISCUSSION

High molecular weight tamarind xyloglucan was successfully bound to cotton linters cellulose under physiological conditions to give a cellulose/xyloglucan ratio of 1:0.03. Whilst this ratio is much less than that seen *in muro*, which range typically from 1:0.3 (Redgewell & Selvendran, 1986) to 1:0.7 (Hayashi & Maclachlan, 1984), it is within the range of levels achieved *in vitro* by Hayashi *et al* (1987). Low levels of binding may be inferred to represent interaction of xyloglucan with the cellulose

Figure 3.8: ^{13}C CP/MAS NMR Spectra of Acid and Alkali-treated Cellulose

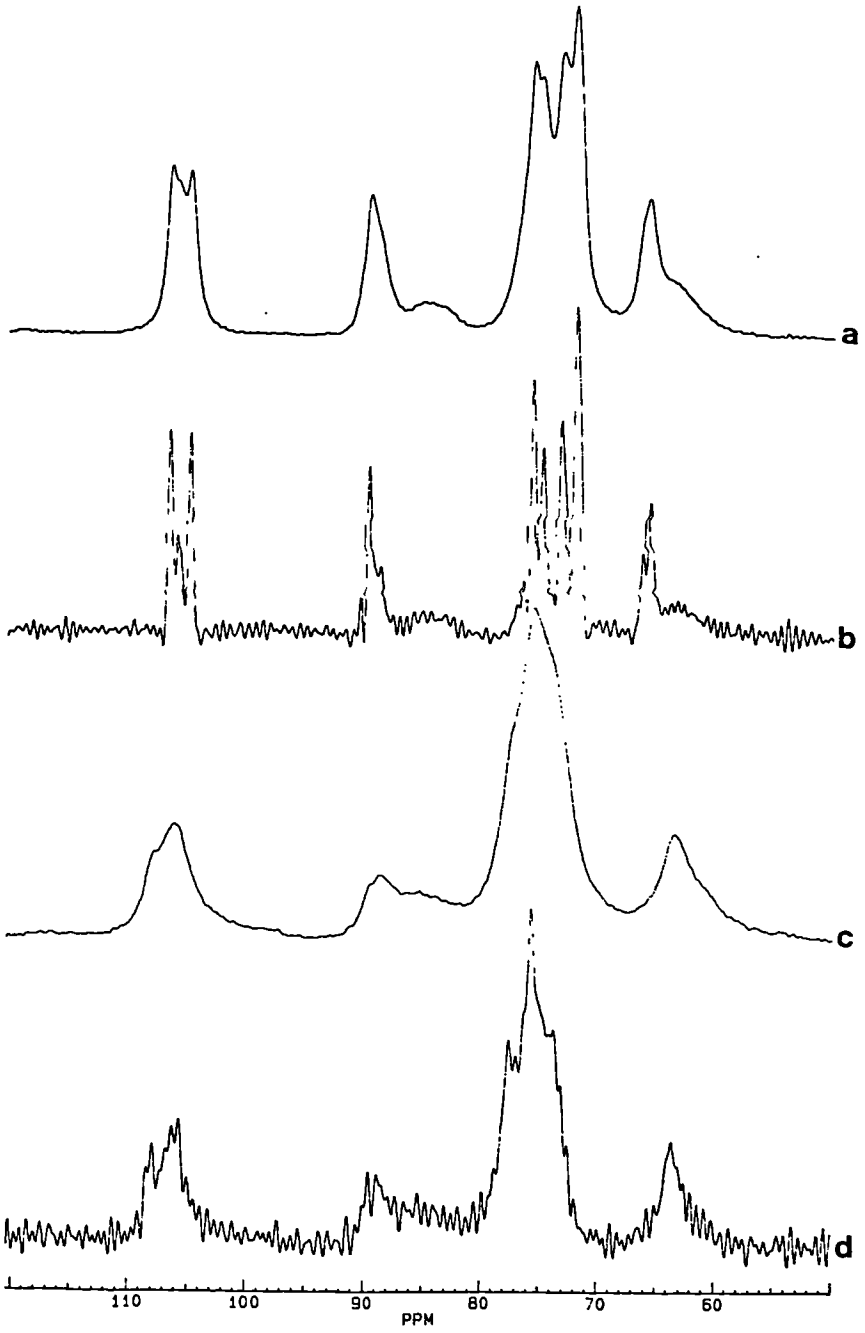

(a) spectrum of cellulose refluxed in 2.5M Hcl showing overall reduction in the non-crystalline component and (b) resolution enhancement (line broadening -70Hz, Gaussian multiplication 0.5) of (a) providing no evidence of alteration in Iα/Iβ ratios when compared to Figure 3.2, (c) after treatment with 6M KOH and (d) as (b) of spectrum (c) showing signals at ca. 107.9, 88.8 and 77.6 diagnostic of partial conversion to cellulose II.

Figure 3.9: HPAEC Profiles of Cellulose Oligomers

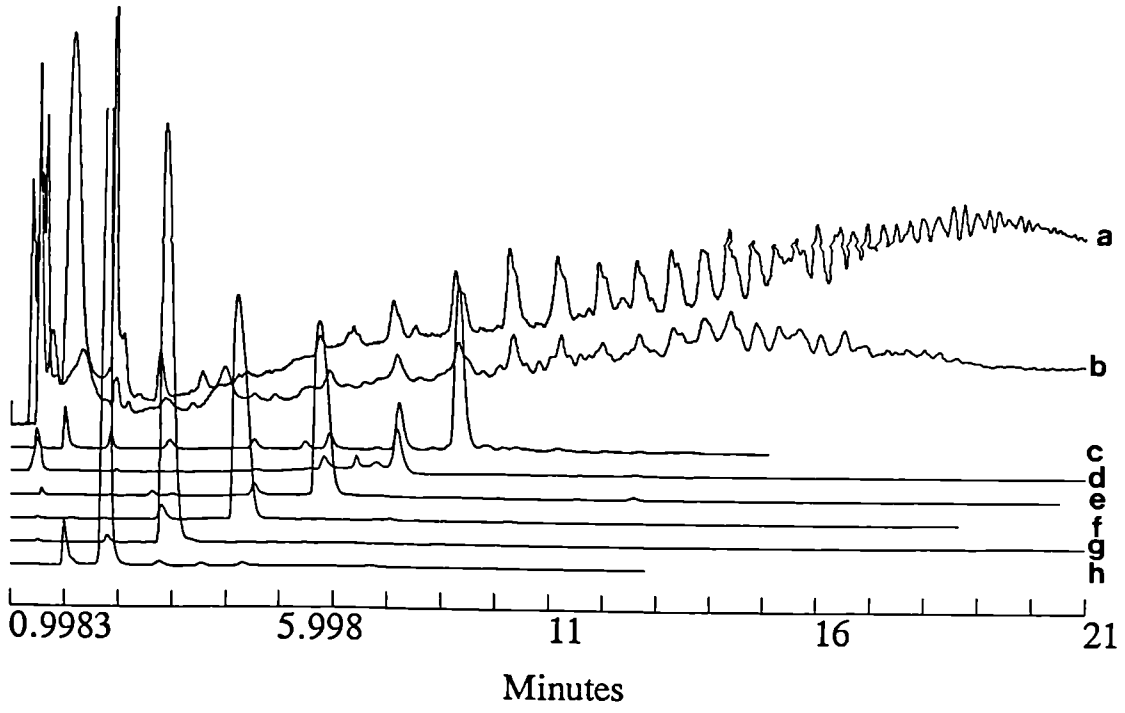

(a) fraction 47 collected from the control cellulose column (see Figure 3.6 (b)), (b) oligomers liberated by 4M KOH treatment of cellulose previously washed in 2M KOH, (c-h) cellulose oligomer standards of dp 7 - dp 2 respectively.

surface only (Hayashi *et al*, 1987). Apparent dissociation of the cellulose/xyloglucan complex at concentrations of alkali much less than that required to cause appreciable microfibil swelling (Edelmann & Fry, 1992a) concurs with the results of Hayashi *et al* (1987). This, combined with the absence of an effect of bound xyloglucan on cellulose molecular order as probed by ^{13}C NMR all argue against an intra-microfibril association between the two polymers in this system.

In addition to achieving only low levels of binding, cotton linters cellulose is clearly unsuitable as a substrate due to its susceptibility to alkaline degradation. Treatment with 6M KOH effected a drastic alteration in cellulose molecular order to give a cellulose not typical of that seen in plants (Foster *et al*, 1996). Plant-derived celluloses require treatment with 6M KOH for complete extraction of the hemicellulose component (Edelmann & Fry, 1992a); the inferred effect on molecular order by the extraction process questions the validity of using such celluloses in attempting to mimic the *in muro* interaction with xyolglucan.

Since this work was performed a number of publications have appeared which address the interaction of cellulose and xyloglucan *in vitro*. Complexes of the two polymers in ratios much more comparable to that seen in the cell wall have been formed by annealing tamarind xyloglucan to amorphous cellulose at temperatures in excess of 160°C (Hayashi *et al*, 1994a). Cellulose:xyloglucan ratios of 1:0.19 were reported and concentrated alkali was required for dissociation, implying intra-microfibril interactions. Although representing a significant improvement with respect to levels of incorporation, clearly such extreme reaction conditions are unrepresentative of cell wall processes.

Hayashi *et al* (1994b) report a minimum requirement of five consecutive glucosyl backbone units for binding of xyloglucan to cellulose, with an increase in association as degree of polymeristion is increased. Furthermore, use of smaller xyloglucan fragments, for example four contiguous oligosaccharide units where each oligosaccharide comprise 4 1,4-β-glucosyl residues, allows significantly greater colonisation of cellulose *in vitro* compared to polymeric xyloglucan (Vincken *et*

al, 1995). Xyloglucan is usually present in the cell wall as much larger molecules than this however (McCann *et al*, 1990, 1992b).

The low level of superficial binding achieved combined with the unsuitability of cotton linters cellulose and, by inference, other plant-derived celluloses, as mimics of cellulose in the wall, indicated that this system would not serve as a suitable model for the cellulose:xyloglucan network seen in plant primary cell walls. Moreover, literature published since this work was completed, whilst increasing our understanding of the relationship between the two polymers, still provides little insight into how to achieve greater physiological similarity between reconstituted and native complexes. In the light of these results subsequent work had two main aims. Firstly we looked at ways of incorporating a radiolabel onto xyloglucan to allow rapid, accurate quantification of binding levels in low yielding systems..Other work concentrated on the identification of alternative sources of cellulose which showed closer molecular correlation with native cell wall cellulose.

Chapter 4: Attempted Introduction of ^{3}H at Galactose C-6 of Tamarind Xyloglucan

4.1 INTRODUCTION

In chapter 3, the successful association of tamarind xyloglucan with cotton linters cellulose was described. Although the level of binding achieved (cellulose:xyloglucan = 1:0.03) was comparable to that reported by other authors for polymeric xyloglucan under physiological conditions (Hayashi *et al*, 1987; Acebes *et al*, 1993; Baba *et al*, 1994a), it is nevertheless an order of magnitude less than seen in the plant primary wall.

Prior to the recent publication of ways to increase *in vitro* association of the two polymers (Hayashi *et al*, 1994a; Vincken *et al*, 1995) and the development of a fermentation system using a cellulose-producing bacterium (Chapter 5, this thesis), it was expected that subsequent work would proceed in accordance with work outlined in chapter 3, providing a suitable cellulose substrate could be identified. The use of conventional sugar analysis techniques for quantifying binding is both time consuming and, due to the low levels achieved, operating at the limit of the accuracy of these methods. Using radiolabelled xyloglucan would facilitate rapid and accurate quantification of large numbers of samples.

Hayashi *et al* (1987) used ^{125}I labelled pea xyloglucan to monitor association with different celluloses. Fluorescein-derivatised xyloglucan (Glabe *et al*, 1983) was chemically radioiodinated with Iodo-beads (Markwell, 1982) to produce a molecule of high specific activity. Glabe *et al* (1983) report no detectable effect on polysaccharide structure or the interaction of ^{125}I-fluorescein-derivatised polysaccharides with lectins or with endothelial cell surfaces. However the introduction of ^{125}I-fluorescein moiety, which is relatively large in chemical terms, onto the xyloglucan sidechains may confer unknown effects on the binding properties of the xyloglucan molecule. This is particularly

relevant in the light of molecular simulation studies, which predict a role for xyloglucan sidechains in both mediating (Finkenstadt *et al*, 1995) and modulating (Levy *et al*, 1991; Finkenstadt *et al*, 1995) attachment to cellulose.

Incorporation of a ^3H label onto a xyloglucan molecule confers minimal chemical change. ^3H has previously been introduced into xyloglucan oligosaccharides where the hydrogen atom of position 1 of the reducing terminus is expected to exchange with $^3H_2$ (Smith & Fry, 1991). Alternatively, labelling of oligosaccharides can be effected using NaB^3H_4 (Fry, pers.comm.). Polymeric xyloglucan could feasibly be labelled at the reducing terminus using labelled oligosaccharides by the endotransglycosylation reaction of xylyglucan endotransglycosylase (XET). However, this will lead to a net reduction of polymer molecular weight (Farkas & Maclachlan, 1988) and the specific activity of the labelled xyloglucan will be low (each molecule labelled once only at the reducing terminus). Xyloglucan can also be labelled by the introduction of [^3H]-arabinose (Edelmann & Fry, 1992b) or [^3H]-fucose (McDougall & Fry, 1991) into actively growing suspension cultured cells. Use of such procedures, whilst providing labelled xyloglucan with a relatively high specific activity, requires additional preparation steps in the isolation of xyloglucan from the cell wall.

We propose an alternative method for introducing ^3H onto xyloglucan. The enzyme galactose oxidase (EC 1.1.3.9) oxides galactosyl C-6 hydroxymethyl groups to formyl groups (Avigad *et al*, 1962). Subsequent reduction of this aldehyde using NaB^3H_4 should introduce a ^3H label at each galactose residue of the molecule. Tamarind xyloglucan is heavily substituted with galactose (Glc:Xyl:Gal = 2.8:2.25:1, Gidley *et al*, 1991a). Furthermore, ca. 80% oxidation of the D-galactose residues of this xyloglucan using galactose oxidase have previously been reported (Lang *et al*, 1992). We predict therefore that, if successful, xyloglucan thus labelled will have a high specific activity.

Before using NaB^3H_4, initial experiments used NaB^2H_4 as the reducing agent. The extent of the reaction could be determined using mass spectrometry to calculate deuterated galactose as a percentage

of total galactose. Experiments using NaB^2H_4 were used to optimise reaction conditions prior to the use of radioactive material.

4.2 MATERIALS AND METHODS

4.2.1 Introduction of ^2H at Galactose C-6 of Tamarind Xyloglucan

4.2.1.1 Oxidation with D-Galactose Oxidase

Reaction conditions for the oxidation of galactose by galactose oxidase were based on methods developed for other polysaccharides (Rogers & Thompson, 1968; Hall & Yalpani, 1980; Dentini & Crescenzi, 1986) and for tamarind xyloglucan (Lang *et al*, 1992). All reaction quantities quoted are per 2mg polymer-bound galactose.

To a 0.1% solution of tamarind xyloglucan was added 0.7ml 0.1M phosphate buffer pH 6.0 and galactose oxidase (EC 1.1.3.9) and catalase (EC 1.11.1.6), both supplied by Boehringer Mannheim. Catalase is required to prevent inhibition of galactose oxidase by H_2O_2 (Hamilton *et al*, 1978).

Sample	*Units Galactose Oxidase (Batch 13248523.04)*	*Units Catalase (Batch 13738822.28)*
1	5.0	2600
2	5.0	2600
3	50.0	26000
4	50.0	26000
5	250	130000
6	50.0 (heat killed)	26000(heat killed)

The reaction mixture was incubated at 27°C for 40 hours.

4.2.1.2 Reduction with NaB^2H_4

A 20-fold molar excess of NaB^2H_4 with respect to galactose (ca. 250μM) was added in 1ml M NH_4OH after oxidation, mixed thoroughly and subsequently incubated at room temperature. After 12 hours the reaction mixture was rapidly cooled in an ice bath and 5M acetic acid slowly added to give a final pH of 4.9. Borate was removed as trimethyl borate by coevaporation with methanol under reduced pressure at 40°C (Albersheim *et al*, 1967). Remaining material was redissolved in 3ml deionised H_2O and heated in a boiling water bath to denature residual proteins, which were removed by passing through a Pasteur pipette containing Bio-Gel P-2. The filtrate was extensively dialysed to remove salts, and freeze-dried.

4.2.1.3 Analysis of Deuterated Polysaccharide by Mass Spectrometry

Deuterated samples were converted to alditol acetates using Alditol Acetates Method 1 (Section 2.8). 2μl of each sample was injected with a CE split/splitless injector operating at 220°C in splitless mode (SSL off for 1 minute) onto a SupelCo SP2330 fused silica capillary column (30m x i.d. 0.32mm, film thickness 0.2μm). Using a Carlo Erba 8035 oven the column temperature was held at 200°C for 1 minute increasing to 240°C at 2°C/minute and held for 5 minutes at 240°C.

Mass Spectrometry was performed using an Analytical Autospec Ultima E mass spectrometer running with a Vax 4000-60 data system operating in electron impact (EI), scanning (SCN) mode with 1000 resolution and 95% transmission, photon multiplier 200V at 220°C and an electron energy of 70eV at a trap current of 500μA.

4.2.2 Radiolabelling of Tamarind Xyloglucan

4.2.2.1 Oxidation with D-Galactose Oxidase

Reaction conditions are identical to those previously described, using the optimised enzyme quantities of 50U galactose oxidase and 26000U catalase.

4.2.2.2 Reduction with NaB^3H_4

Reduction using NaB^3H_4 was performed essentially as described in section 4.2.1.2 for NaB^2H_4, with certain modifications as highly radioactive material was being used. 25mCi NaB^3H_4 was supplied by Amersham International at a specific activity of 600mCi/mol, giving a total amount of 0.042mmols. To ensure a 20-fold molar excess of NaB^3H_4 with respect to galactose 2.1μmols of galactose are required, which is equivalent to 2.06mg tamarind xyloglucan. After oxidation, an aliquot containing 2.06mg xyloglucan was removed from the reaction mixture. To this aliquot was added all the NaB^3H_4 dissolved in 200μl NH_4OH. After incubation for 24 hours at room temperature, excess NaB^3H_4 was decomposed with 2 x 100μl 5M acetic acid and left open to the atmosphere overnight at room temperature in an fume cupboard approved for radioactive use. Polymeric material was precipitated with 3 volumes of methanol and collected by centrifugation. After washing three times by dissolving the precipitate in 1ml hot deionised water and reprecipitating in 3 volumes of methanol. the material was redissolved in 1 ml deionised water and a 10μl aliquot removed for scintillation counting. The remaining material was freeze-dried. 10μl aliquots of the supernatants were also assayed for radioactivity. Swab tests were performed on all equipment to monitor contamination.

4.2.2.3 Analysis of Oligomers of Radiolabelled Xyloglucan

Labelled material was dissolved in 1ml 50mM sodium acetate buffer pH 4.5 and incubated with 0.05U *endo*-1,4-β-glucanase from *Trichoderma viride* (Megazyme Pty, Australia) for 24 hours prior to analysis on the Dionex system (Section 2.14). Oligomers (XXXG, XXLG, XLXG and XLLG) were

collected as discrete fractions. Higher molecular weight oligomers were also collected as a single fraction. 1ml aliquots of each fraction were assayed for radioactivity.

4.2.3 Assaying for endo-β-*Glucanase Side-Activity in Commercial Preparations of D-Galactose Oxidase*

endo-β-glucanase side activity of D-galactose oxidase preparations was measured by viscometry using tamarind xyloglucan as a substrate (Edwards *et al*, 1985). A 100μl aliquot containing 25U of galactose oxidase dissolved in 0.1M phosphate buffer was added to 2ml 1% tamarind xyloglucan (in 0.1M phosphate buffer, pH 6.0) and incubated at 40°C. Readings were taken at 5 minute intervals using a graduated 1ml pipette. Initial flow times were approximately 30 seconds. Xyloglucan solutions were equilibrated at 40°C for 10 minutes prior to the addition of enzyme.

4.2.4 Assay for Galactose Oxidase Activity

Galactose oxidase activity is assayed according to a method supplied by Boehringer Mannheim. To a cuvette is added 1.0ml galactose solution (1.000g in 5ml deionised water left standing for 2 hours to ensure full mutorotation), 2.20ml ABTS™ (55mg in 50ml 0.1M phosphate buffer pH6.0, saturated with air prior to use) and 0.01ml horseradish peroxidase (0.1U). After equilibration at 25°C 0.05ml galactose oxidase (2.5U/ml) was added. The reaction was measured as the change in absorbance at a wavelength of 405nm (pathlength 1.0cm). Activity was calculated as:

$$\text{U/ml galactose oxidase} = \frac{\text{total reaction volume}}{\varepsilon_{405} \cdot \text{enzyme volume} \cdot \text{pathlength}} \cdot \Delta\text{Abs/min}$$

$$= \frac{3.26}{36.8 \cdot 0.05 \cdot 1} \cdot \Delta\text{Abs/min}$$

ΔAbs was measured in the linear region. Activity units can be converted to standard units by multiplying by a factor of 2.8 (Boehringer Mannheim).

4.2.5 Purification of Galactose Oxidase

0.5ml of a suspension of Whatman microgranular cellulose was added to a small Eppendorf tube which had previously had a hole cut in the base covered with a layer of small glass beads. This tube was placed in a larger Eppendorf tube and the cellulose was washed twice with 2 volumes of 0.01M phosphate buffer pH 6.0 by centrifugation at 13,000 rpm. 25U galactose oxidase in 100µl buffer was pipetted gently onto the cellulose surface. The column was spun at 13000 rpm and the filtrate collected in the second eppendorf. All experimentation was performed at 4°C.

4.3 RESULTS

4.3.1 Incorporation of ^2H at C-6 of D-Galactose in Tamarind Xyloglucan

After oxidation with D-galactose oxidase and subsequent reduction with NaB^2H_4 high molecular weight material was recovered from each sample, with an average yield recovery of 83%. The sugar composition of each sample as analysed by alditol acetates was identical to that of the starting material (Glc:Xyl:Gal = 2.8:2.25:1).

A typical GC trace showing separation of the alditol acetates is shown in Figure 4.1 and the mass spectrum for galactitol acetate derived from of sample 5 (250U galactose oxidase) compared with that of sample 6 (undeuterated control) in Figure 4.2. Possible degradation products of a galactitol acetate are shown below:

Doublet patterns of essentially equal intensity are ahown in Figure 4.2 for ions of *m/z* 361/362, 289/290, 259/260 and 187/188. As there is an equal probability of peaks being produced by sequential degradation from either the C-1 or C-6 end of the alditol acetate (see below) , equal intensity within

doublets is indicative of complete deuteration. Therefore use of a large excess of D-galactose oxidase can effect almost 100% oxidation and hence deuteration under these conditions.

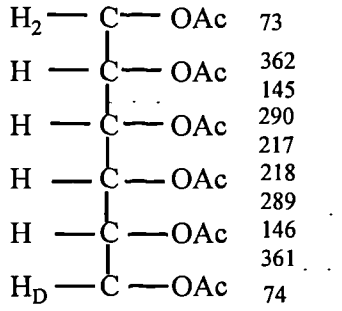

The percentage deuteration of D-galactose for each sample was calculated by integration of the doublet at *m/z* 361-362. To separate contributions from ^{13}C and ^{2}H, the intensity of *m/z* 362 as a percentage of *m/z* 361 for sample 6 (control) is a correction factor which needs to be applied to all peaks at *m/z* 362. This correction factor is calculated as 0.1525.

Table 4.1 Conversion of Tamarind Xyloglucan Galactose to [^{2}H]-Galactose

Sample	m/z 361	m/z 362	corrected m/z 362	percentage deuteration
1	2.026E5	9.248E4	7.83768E4	55.8
2	1.528E5	6.862E4	5.815545E4	55.1
3	1.285E5	1.392E5	1.17972E5	95.7
4	1.500E5	1.721E5	1.4585475E5	98.6
5	2.809E5	3.182E5	2.696745E5	98.0
6	1.245E5	1.899E4	-	-

These results suggest that the use of 25U galactose oxidase per mg polymer-bound galactose give optimal reaction conditions, which is approximately a factor of 10 more than that used by Lang *et al*, 1992). As the $NaB^{2}H_4$ used in this study is only 98% pure we can infer essentially 100% oxidation of polymeric galactose under these conditions, hence increasing enzyme amounts (sample 5) confers no

Figure 4.1: GC Chromatogram of Alditol Acetates for Tamarind Xyloglucan

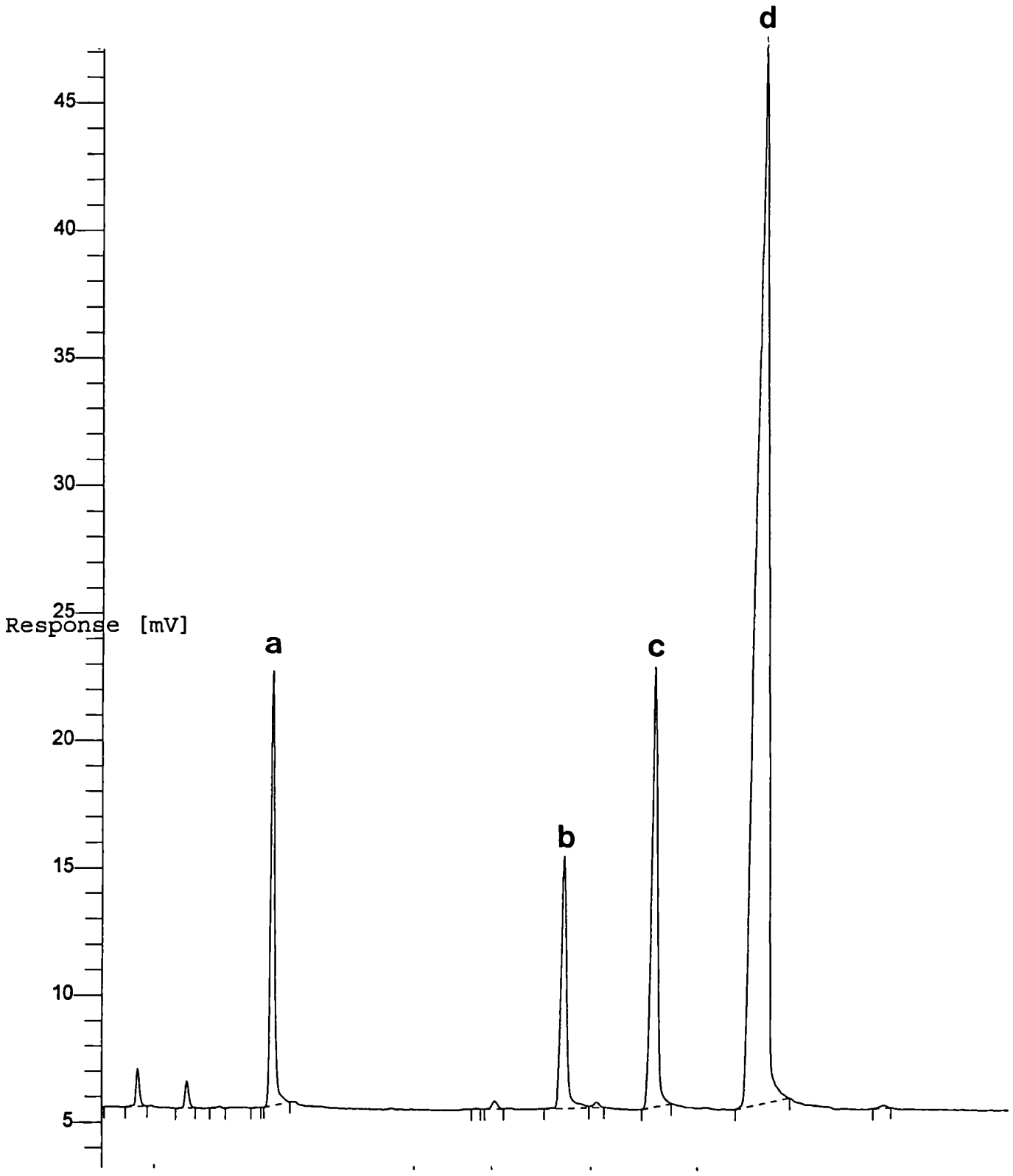

Alditol acetates derived from (a) xylose, (b) galactose and (c) glucose of tamarind xyloglucan and (d) inositol (internal marker)

Figure 4.2: Mass Spectra of Deuterated and Undeuterated Galactose

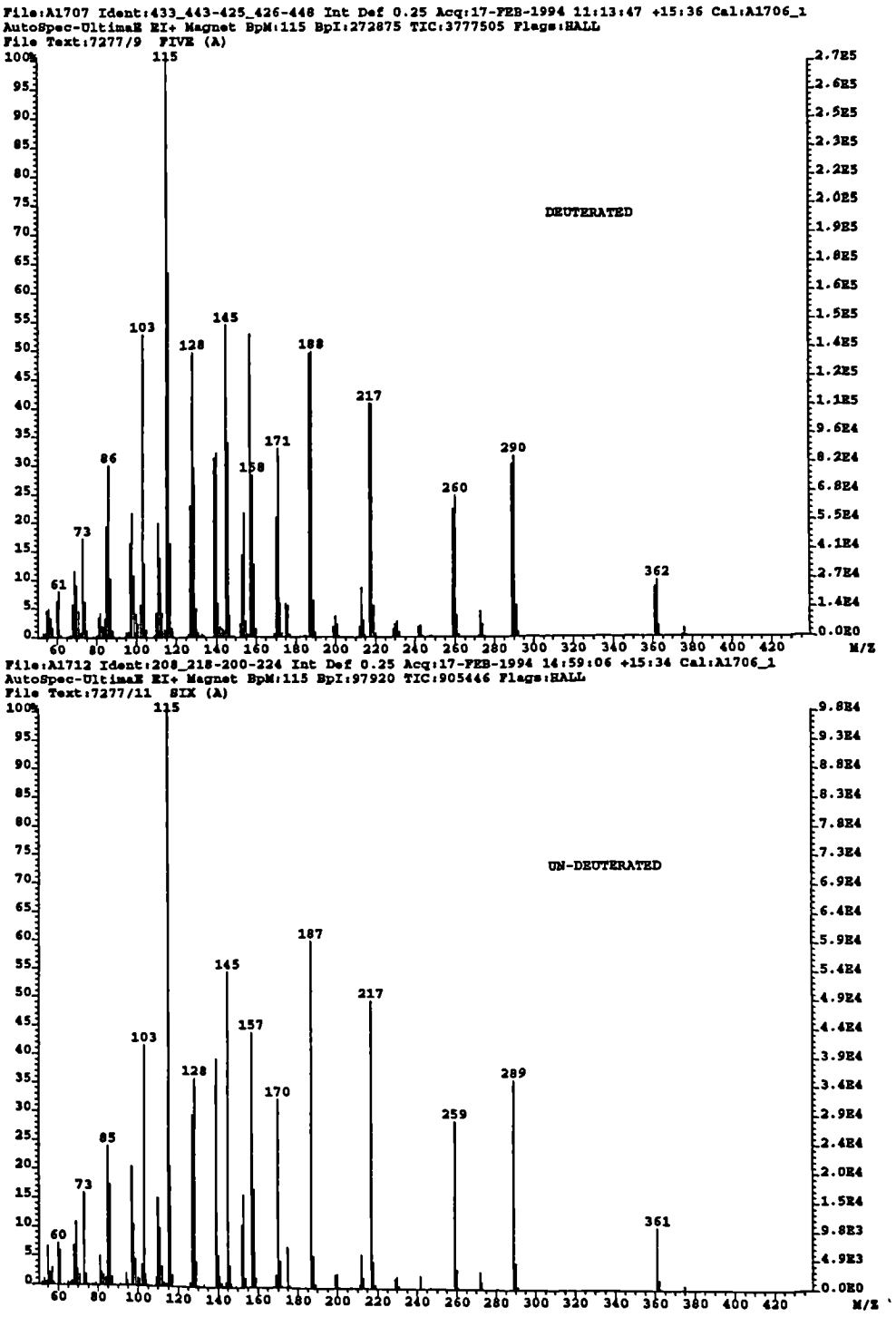

Mass spectra of galactitol acetates derived from the galactose residue of tamarind xyloglucan after reduction with NaB^2H_4 of samples oxidised with (a) an excess of galactose oxidase and (b) heat-killed galactose oxidase (control). Ions of *m/z* 362, 260, 218 and 188 are diagnostic of deuteration .

advantage. This level of oxidation by galactose oxidase is greater than that reported by Lang *et al*, (1992).

Analysis of the molecular weight of each sample compared to the starting material by viscometric assay indicated a reduction in viscosity of approximately 65% implying some degradation under these reaction conditions. A similar reduction in intrinsic viscosity of 57-61% was observed in previous studies (Lang *et al*, 1992). However, the loss in molecular weight was insufficient to allow the material to pass through dialysis membrane (mwt cut off = 12-14000) and on freeze-drying, the material had a felty appearance indicative of polymeric material.

4.3.2 Attempted Introduction of ^{3}H at Galactose C-6 of Tamarind Xyloglucan

Using the galactose oxidase and reduction conditions which resulted in an essentially complete reaction with $NaB^{2}H_4$ were initially unsuccessful when using $NaB^{3}H_4$. Xyloglucan underwent a dramatic loss in molecular weight such that the majority was lost in the precipitation step. The material recovered was of visibly low molecular weight (fluffy rather than felty after freeze-drying), had a viscosity only slightly greater than that of H_2O and a specific activity of 2μCi. Subsequent investigation of the purity of the enzyme preparations used (section 4.3.3) indicated the presence of *endo*-β-glucanase side activity in the batch of galactose oxidase (Batch 13839320.05, Boehringer Mannheim) used in this particular study.

Subsequent experiments used a galactose oxidase preparation obtained from Sigma (Batch 122H68271) which was shown to have negligable *endo*-glucanase activity (section 4.3.3). Following $NaB^{3}H_4$ reduction of galactose oxidase-treated tamarind xyloglucan and during the purification procedure (ie dissolving in 1ml hot deionised water and reprecipitation of polymeric material with 3 volumes of methanol) 1ml aliquots of the supernatant after centrifugation were assayed for radioactivity. Even after repeated washings it proved impossible to obtain a supernatant with negligible

radioactivity. After wash 5 a 10μl aliquot of the polymeric material was assayed for radioactivity and the remaining material freeze-dried. Material was recovered with a yield of 81.15%. Furthermore, the material recovered had a visibly polymeric appearence (cf. section 4.3.1). These results suggest that the xyloglucan had passed through the reaction procedure without significant degradation. It was calculated that, of the original 25mCi used, only 0.13μCi remained in the polymeric material. 227μCi was recovered in the supernatants and the vial in which the radioactive material was supplied had a residual radioactivity of 0.25mCi. 24.52mCi was therefore lost to the atmosphere during the reduction process.

Oligomers generated by *endo*-1,4-β-glucanase action had negligible radioactivity. The vast majority of the radioactivity (0.11μCi) was collected in the eluent (Figure 4.3).

4.3.3 endo-*1,4*-β-*glucanase Activity as a Contaminant of Galactose Oxidase Preparations*

The galactose oxidase preparation used in the initial radiolabelling experiment showed significant *endo*-1,4-β-glucanase acitivity, reducing the viscosity of a 1% tamarind xyloglucan solution by almost 50% within 1 hour (Figure 4.3 (b)). In contrast, the batch of galactose oxidase used in the ^{2}H-labelling experiment showed some activity, but to a much lesser extent (Figure 4.3 (d)). These results explain why the initial ^{3}H-labelling experiment resulted in a very low yield of low molecular weight material and the lesser reduction in molecular weight (as measured viscometrically) observed in the ^{2}H-labelling experiment. Purification of the galactose oxidase batch 13839320.05 by passing through cellulose spin columns (Figure 4.3 (f,g)) reduced *endo*-1,4-β-glucanase activity significantly, but there was a concomitant reduction in galactose oxidase activity of 62%. A galactose oxidase preparation obtained from Sigma (Figure 4.3 (h)) showed negligible *endo*-1,4-β-glucanase activity with viscosity only reduced by 65% after 48 hours and was subsequently used in radiolabelling experiments. Insignificant

Figure 4.3 Profile of Oligomers Generated by *endo*-1,4-β-glucanase Action on ^{3}H-Labelled Tamarind Xyloglucan

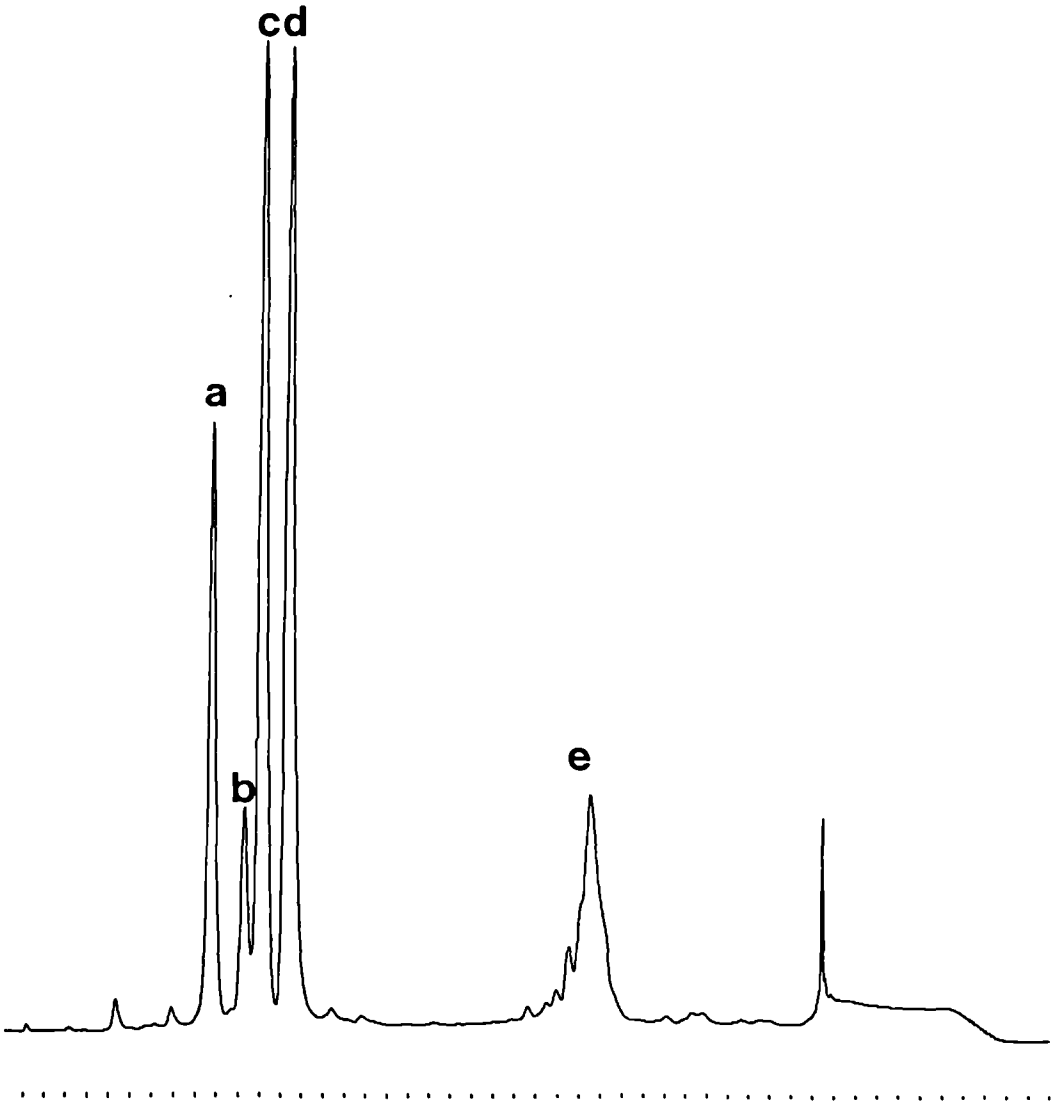

(a) XXXG; (b), XLXG; (c), XXLG; (d), XLLG; (e), higher molecular weight oligomers partially resistant to *endo*-1,4-β-glucanase digestion

endo-1,4-β-glucanase was detected in the catalase preparation obtained from Boehringer Mannheim (Figure 4.3 (h)).

Figure 4.4 *endo*-1,4-β-Glucanase Side Activity in Commercial Preparations of D-Galactose Oxidase

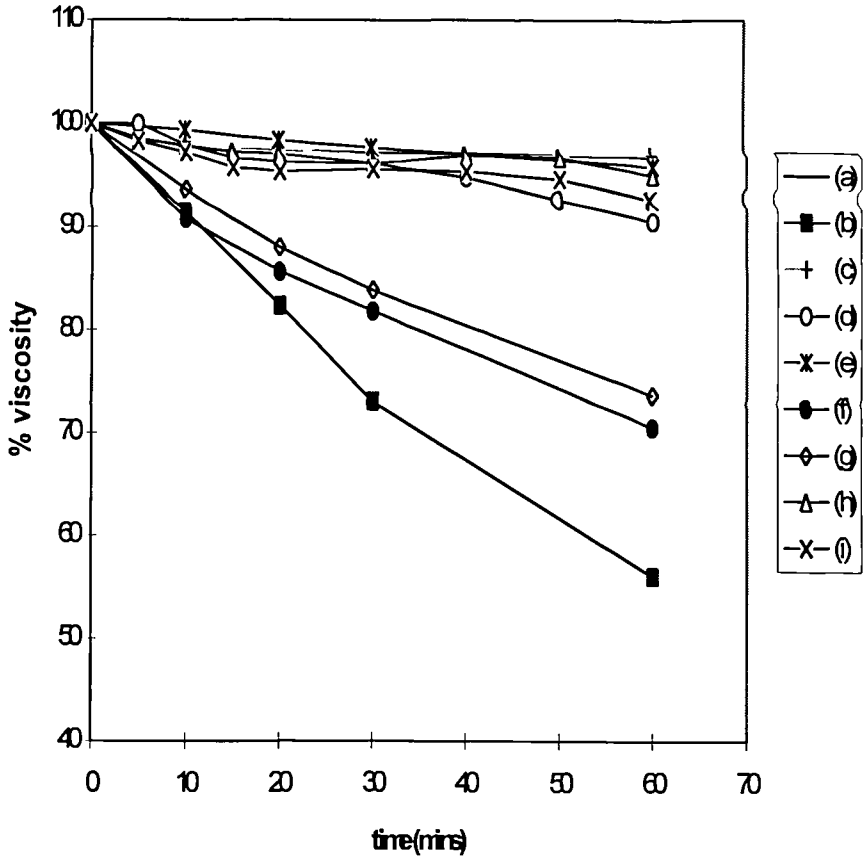

(a) 1% tamarind xyloglucan; (b)+ Galactose Oxidase Batch 13839320.05 (Boehringer Mannheim); (c) as (b), enzyme treated at 100°C for 5 minutes; (d) + Galactose Oxidase Batch 13248523.04 (Boehringer Mannheim); (e) as (d), enzyme treated as (c); (f) + enzyme as (b), passed through cellulose spin column once; (g), as (f), passed through column twice; (h) + Galactose Oxidase Batch 122H68271 (Sigma); (I), + Catalase Batch 13738822.28 (Boehringer Mannheim).

4.4 DISCUSSION

Oxidation of polymeric galactosyl C-6 hydroxymethyl groups to formyl groups and reduction using NaB^2H_4 results in approximately 98% conversion of galactosyl to [^{2}H]-galactosyl under optimised

enzyme conditions. We conclude that this is indicative of essentially 100% oxidation by galactose oxidase as the reducing agent comprises 98% NaB^2H_4 and 2% $NaBH_4$. The stoichiometry of the reaction suggests no competition between H^- and $^2H^-$ in the reduction process ie an insignificant kinetic isotope effect. A slight reduction in molecular weight, attributed to contaminating *endo*-1,4-β-glucanase activity in the galactose oxidase preparation is observed. Use of an enzyme preparation supplied from Sigma should reduce degradation, although Lang *et al* (1992) report some reduction in intrinsic viscosity of the carboxylated polysaccharide when using galactose oxidase from this source. However these authors suggest that this may have been attributable to an increased stiffness of the xyloglucan chain upon derivatisation rather than degradation.

The initial experiment using NaB^3H_4 gave only a low yield (ca. 10%) of low molecular weight material. This was attributed to the presence of a contaminating *endo*-1,4-β-glucanase in the galactose oxidase preparation used. However, radioactivity was apparently incorporated stably into the recovered material as no radioactivity was detected in the supernatant after three washes. Furthermore, the specific activity was far higher than that achieved in subsequent labelling experiments. As later experiments failed to reveal any incorporation of ^3H onto C-6 of polymeric galactose, the high specific activity recorded in this sample is attributed to tritiation of reducing ends generated by the action of *endo*-1,4-β-glucanase. In retrospect, this explanation could have been proved by acid hydrolysis of the labelled material followed by identification of 'hot' component monosaccharides.

When a galactose oxidase preparation from Sigma was used, high molecular weight material was recovered in a very high yield. During the washing process however, radioactive material was continually washed from the sample. Even after 5 washes, the supernatant contained significant amounts of radioactive material, with a concomitant reduction if radioactivity of the precipitate. Although washing was stopped at this pont and the precipitate freeze-dried, these results suggest that continued washing would have resulted in gradual depletion of the radioactivity in the sample. Therefore, unlike the first sample, it appears that the vast majority of the radiolabel has not been

chemically incorporated onto polymeric xyloglucan. Tritiation of reducing ends is expected, however in the absence of *endo*-1,4-β-glucanase activity these will be present in relatively low amounts.

Oligomeric fractions generated by *endo*-1,4-β-glucanase action were analysed for radioactivity. There was no significant difference between the level of radioactivity in oligomer XXXG and that in XXLG, XLXG and XLLG indicating that no ^{3}H has been incorporated onto C-6 of galactose. The majority of radioactivity is detected in eluent, not collected as discrete fractions ie. is not stably incorporated into the xyloglucan.

^{3}H is apparently stably incorporated into tamarind xyloglucan when reducing ends are generated by endo-1,4-β-glucanase action and this reduction of reducing ends with $NaB^{3}H_4$ is well established (Redgwell & Fry, 1993). However, we need to understand why, under similar reaction conditions, ^{2}H is incorporated at the galactose C-6 but ^{3}H is not. A likely possibility is the previously reported isotope effect in the borohydride reduction of ketones (Pasto and Lepestra 1976).

Pasto and Lepestra (1976) report a strong $H/^{3}H$ effect, quoting values for k_H/k_{3H} of approximately 5. Given equimolar concentrations of $NaBH_4$ and $NaB^{3}H_4$ the former would therefore react 5 times faster. Assuming first-order kinetics the actual rate of reaction would be $[NaBH_4] \times k_H$ and $[NaB^{3}H_4] \times k_{3H}$ respectively. Preparations of sodium borotritiide contain only a small amount of tritiide in a large amount of borohydride; under these conditions it is predicted that there will be a large differential between the rates of H^- and $^{3}H^-$ incorporation. This effect is exacerbated by the nature of $NaB^{3}H_4$. Even at the highest available specific activity, the borotritiide component is probably $NaBH_3{}^{3}H$, giving an $H^-/^{3}H^-$ of 3. A much less significant isotope effect with ^{2}H is reported by Pasto and Lepestra (1976) with k_H/k_{2H} of 0.8-1.5. This predicts that no significant discrimination in favour of H^- will be revealed in $NaBH_4/NaB^{2}H_4$ competition experiments and is supported by our results showing stoichiometry for the $NaB^{2}H_4$ reduction reaction.

Clearly, in our radiolabelling experiments $^3H^-$ was outcompeted by H^- in the reduction of the C-6 of the galactosyl residues. This can be explained at least partly by isotope effects and the discrepancy between the value for k_H/k_{3H} and k_H/k_{2H} indicates why $NaBH_4/NaB^2H_4$ competition experiments are not in fact good models for the reaction of NaB^3H_4. However, the apparently stable incorporation of ^3H into a sample containing a large number of reducing ends and the routine use of NaB^3H_4 to label the reducing ends of oligosaccharides (Redgwell and Fry (1993) indicates that this isotope effect is much less relevant in competition for reduction of reducing ends. This infers a different molecular environment at C-6 of galactose which causes the isotope effect to predominate although it is difficult to reconcile subtle environmental differences with such a dramatic chemical effect.

The success of labelling with ^2H means that ^2H-labelled tamarind xyloglucan could conceivably be used as a marker in xyloglucan/cellulose binding experiments, although it would still be necessary to perform sugar analyses. Hence, the benefit of this system over conventional analysis as used in Chapter 3 is questionable. However, we believe that this is the first report of ^2H-labelled xyloglucan. Attempts to incorporate ^3H onto the galactosyl residue have failed completely and it seems unlikely that, even using sodium borotritiide of a much higher specific activity, this method will work effectively.

Chapter 5: Production of Cellulose by Cultures of *Acetobacter aceti* ssp. *xylinum*

5.1 INTRODUCTION

Cotton linters cellulose, which is commercially available in large quantities, was shown in Chapter 3 to be unsuitable as a substrate for examining the interactions of xyloglucan and cellulose *in vitro*. For efficient extraction of hemicelluloses from native cellulose/hemicellulose composites, concentrated alkali, which causes microfibril swelling, is required (Edelmann & Fry, 1992a). The radical alteration of cellulose molecular order effected by such treatment was highlighted in Chapter 3, with a conversion of cellulose I to a mixture of cellulose II and non-crystalline cellulose, as predicted by Atalla *et al* (1980). These results suggest that use of plant-derived celluloses may be inappropriate for developing xyloglucan/cellulose composites *in vitro* that are representative of those derived from the cell wall, and prompted us to examine an alternative cellulose source.

The Gram -ve bacterium *Acetobacter xylinum* synthesises highly crystalline cellulose I extruded as a twisting ribbon parallel to the cell surface (Brown *et al*, 1976). Cellulose ribbon biogenesis occurs by a hierarchical, cell-directed self-assembly process (Haigler *et al*, 1980; Benziman *et al*, 1980: Haigler & Brown, 1981; Haigler & Benziman, 1982; Haigler *et al*, 1982) and is susceptible to perturbation by fluorescent brighteners (Haigler *et al*, 1980; Kai *et al*, 1994), cellulose derivatives such as CMC (Ben-Hayim & Ohad, 1965; Haigler *et al*, 1982) and xyloglucan (Hayashi *et al*, 1987; Atalla *et al*, 1993; Hackney *et al*, 1994; Yamamoto & Horii, 1994). As well as providing a source of relatively pure cellulose I for *in vitro* association studies, *Acetobacter xylinum* may also prove a useful system in which to examine interactions when xyloglucan (and other glucan-binding polymers) are added at the point of cellulose synthesis (Chapter 6).

Cellulose production by *Acetobacter* has been the subject of intense study for over 40 years. In 1947 Hestrin *et al* demonstrated cellulose synthesis in the presence of glucose and oxygen by non-proliferating cells. In static cultures *Acetobacter* produces a thick pellicle at the air/medium interface (Hestrin & Schramm, 1954). As an obligate aerobe, *Acetobacter* grows only at this interface and the pellicle comprises a thick mass of continually layered cellulose fibres supporting a growing population of cells at the surface of the culture medium.

For large-scale production of cellulose use of agitated cultures is desirable. Furthermore, if modifying agents are to be added to cellulose-synthesing cultures agitation is essential as the concentration of modifying agents is depleted at the aerobic interface early in pellicle growth, with the process of diffusion being inadequate to maintain a uniform concentration throughout the medium (Atalla *et al*, 1993). Traditionally, production of cellulose in agitated cultures of *Acetobacter* has been extremely problematic and is attributed to strain instability, in which spontaneous mutations to non-cellulose-producing (Cel^-) strains arise. Competition experiments using chemically induced Cel^- strains have shown that, in agitated cultures, the non-producing strain rapidly predominates (Valla & Kjosbakken, 1982). This is proposed to be due to the selective aggregation of cellulose-producing cells, resulting in mass-transfer limitations with respect to oxygen.

Use of the chemical mutagen ethyl methane sulfonate (EMS) has produced a number of strains which are stable under agitated culture conditions (Johnson *et al*, 1988, US Patent 4,863,565). These strains produce large quantites of cellulose in agitated culture and also exhibit reduced levels of gluconic acid and ketogluconic acid production, which inhibit cellulose synthesis both as the result of the drop in pH and by using glucose from the medium which would otherwise be use for cellulose production. Notable among these mutant strains is strain 1306-21, which was deposited at the American Type Culture Collection in 1986 and designated the accession number ATCC 53524. This strain has become the variant of choice for the routine production of large quantities of sample (Atalla *et al*, 1993) and is the strain used for all future work in this thesis.

Using high resolution ^{13}C NMR spectroscopy Atalla and VanderHart proposed the existence of two crystalline allomorphs of cellulose, designated Iα and Iβ, based on the observation of multiplicities of signals at each carbon atom (Atalla & VanderHart, 1984; VanderHart & Atalla, 1984). Studies of a range of celluloses showed that all native celluloses can be classified into two groups (Horii *et al*, 1987). Cellulose synthesised by *Acetobacter xylinum* is rich in the Iα component and therefore belongs to the bacterial-*Valonia* family. The cotton-ramie family, which is Iβ rich, comprises most higher plant cellulose. Tunicin, cellulose isolated from pelagic tunicates, is the only example of a native cellulose composed solely of the Iβ allomorph (Belton *et al,* 1989); to date no pure Iα celluloses have been identified.

Sugiyama *et al (*1990) used electron diffraction to confirm the existence of the Iα and Iβ components. Iβ cellulose is assigned to a 2-chain monoclinic cell defined by Gardner and Balckwell (1974) as the Meyer-Misch type. The Iα allomorph is not unambiguously assigned, being either a 2-chain triclinic (as defined by Sarko *et al*, 1974) or a 1-chain triclinic (Sugiyama *et al*, 1991b) unit cell. Using cellulose from the cell wall of the alga *Microdictyon tenuius*, Sugiyama *et al* (1991) were able to identify both monoclinic (Iβ) and triclinic (Iα) patterns during sequential examination of a single particle of microcrystalline cellulose. Domains giving pure monoclinic, triclinic or monoclinic/triclinic patterns were identified at intervals of ca. 50nm.

A feature of the Iα/Iβ dimorphism is that the Iα form is metastable and treatment of Iα-rich celluloses by annealing at high temperatures with saturated steam (Horii *et al*, 1987) or in aqueous alkaline solutions (Yamamoto *et al*, 1989; Sugiyama *et al*, 1990, 1991b) effects almost total conversion to the Iβ phase. Furthermore, culturing of *Acetobacter* at low temperatures (36-10°C) can increase the proportion of Iα cellulose produced (Yamamoto & Horii, 1994) implying that Iα has the lowest activation energy barrier for formation ie it is the kinetic product.

This chapter looks at the production of cellulose by *Acetobacter aceti* ssp. *xylinum* (ATCC 53524).. In the light of observations that alkali treatments can effect conversion of Iα to Iβ, less stringent washing procedures are employed to try and maximise the percentage of the Iα component of the native cellulose. The use of high resolution microscopy to examine cellulose pellicles formed undergentle agitation conditions is discussed.

5.2 Materials and Methods

5.2.1 Cellulose Production

Bacterial inoculum was obtained from previously cellulose-synthesising cultures as described in General Materials and Methods (2.12.2). 5ml inoculum was inoculated into 95ml Hestrin Schramm medium (Hestrin & Schramm, 1954) and incubated for 72 hours at 30°C either in Roux bottles with orbital agitation at 0 or 50rpm, or in 500ml shake flasks agitated at 125rpm.

After 72 hours, cellulosic material was removed aseptically, ground with an Ultra-Turrax T25 (Janke and Kunkel) and washed extensively with sterile deionised H_2O. Alternatively, pellicles from 0 and 50rpm incubations were harvested and washed intact. Material synthesised at 125rpm was highly compact, precluding grinding by the Ultra-Turrax, and was ground further using an Atomix blender. For comparison with methods previously described for purification of bacterial cellulose, intact pellicles were washed in either 0.5% NaOH at RT for 6 days (cf Debzi *et al*, 1991) or in 1% NaOH at 100°C for 6 hours (cf Atalla *et al*, 1993; Hackney *et al*, 1994). After alkali treatment samples were washed to neutrality with deionised H_2O and freeze-dried.

5.2.2 Monosaccharide Analysis

The monosaccharide composition of bacterial cellulose was determined using Alditol Acetates Method 1 (Section 2.7).

5.2.3 X-Ray Diffraction

Powder X-ray diffraction patterns were obtained using a Phillips powder diffractometer (PCW 1050/1390) mounted on a PW 1730/10 sealed-tube X-ray generator operating at the Cu-K_α wavelength (1.542Å), with diffraction intensity measured over the angular range 5-30° 2θ.

5.2.4 Birefringence

Ground, freeze-dried cellulose samples were mounted in a drop of deionised H_2O and viewed with a Leitz Ortholux II light microscope with x 16 objective, fitted with a variable magnification phototube set to 10x and a Polaroid camera attachment. Birefringence was observed using crossed polarised light. Photographs were printed on Kodak photographic film.

5.2.5 ^{13}C NMR Spectroscopy

^{13}C CP/MAS spectra were obtained as described in General Materials and Methods (Section 2.13). Material from incubations at 0 and 125rpm were analysed as freeze-dried samples, whereas that from incubation at 50rpm was examined as a native hydrate, for direct comparison with work in Chapter 6, which uses native, hydrated, cellulose/xyloglucan composites. Spectra for alkali-treated cellulose were obtained using 30% hydrates to improve resolution.

5.2.6 Low Temperature Scanning Electron Microscopy (LT-SEM)

Intact pellicles from incubations performed at 50rpm were harvested and washed extensively in deionised H_2O. A full thickness, 2mm x 10mm strip was cut from the pellicle and mounted onto an SEM stub using OCT compound (vryo-glue, Tissue-Tek®). The sample was rapidly cooled by plunging into N_2 slush, fractured at -98°C and etched for 5 mins. After cooling to -110°C the etched sample was coated using Ag/Pd (2×10^{-1} mBar, dry argon, 6mA, 40s) and transferred at high vacuum to a JEOL JSM 820 Scanning Electron Microscope for examination at -150°C.

5.2.7 Deep-Etch Freeze-Fracture TEM

Intact pellicles from cultures incubated at 50 rpm were extensively washed in sterile deionised H_2O and examined according to that described in General Materials and Methods (Section 2.12.5).

5.2.8 Cellulose Synthesis on EM grids

Intact pellicles from stationary cultures were aseptically removed and ground in 0.02M phosphate buffer, pH 6.0 using an Ultra-Turrax T25. After passing through sterilised Miracloth (Calbiochem, USA) to remove cellulose debris, the bacterial suspension was collected and stored on ice. Alternatively, suspensions were made by inoculating sterile Ringers solution direct from glucose/yeast extract agar plates.

Suspensions were concentrated by centrifugation in a Centaur Micro-Centrifuge at 2000rpm for 5 mins. Cells were introduced to carbon coated copper EM grids (GILDER 200 mesh) according to the method of Haigler *et al* (1982) by simply touching the surface of the grid to the bacterial cell suspension. Grids with attached cells were floated specimen side down in a watch glass containing a 1% glucose solution in 0.05M phosphate buffer pH 6.0 for 10 minutes or 1 hour. After incubation,

grids were washed with deionised water, stained with 1% uranyl acetate and examined using a JEOL 1200 EX MkII Transmission Electron Microscope.

5.2.9 Electron Diffraction

Cellulose material was obtained from stationary cultures, ground using an Ultra-Turrax T25 and freeze-dried after washing. Microcrystalline cellulose was prepared by refluxing this material in 2.5N HCl for 4 hours. Native or microcrystalline cellulose was suspended in deionised water and a drop of this suspension dried down onto carbon films supported by copper mesh grids. High resolution (micro-micro) electron diffraction was performed using an electron beam generated by a LaB6 filament operated at 120 kV. The smallest condenser aperture (20μm D) and the medium spot size setting on the ASID 10 scanning attachment were employed, using a camera length of 340mm. Exposure times of 8 or 11 seconds were used to record the patterns on Kodak 4489 photographic film. Diffraction patterns were visualised on a TV monitor using a GATAN 673CCD camera attached to the 35mm port of the TEM.

5.3 Results

5.3.1 Pellicle Morphology at Differnt Agitation Speeds

Stationary cultures synthesised an intact, thick cellulose pellicle which was easily broken down using the Ultra-Turrax T25. After extensive washing in deionised H_2O the sample was pure white in colour, even after freeze-drying. Application of these mild washing procedures to an intact pellicle also appeared sufficient to remove colour (believed to be indicative of the presence of fermentation media). Similarly, cellulose synthesised at 50 rpm formed pellicles at the media surface. However, synthesis was apparently initiated at several sites independently, forming small discrete pellicles which aggregated within 24 hours and continued to grow as a single pellicle after this time. Purification of

cellulose from these gently agitated cultures was possible using the mild extraction techniques, although a slight brown colour was apparent in freeze-dried intact pellicles, suggesting that some fermentation medium had become trapped within the pellicle. In contrast, cellulose synthesised by cultures agitated at 125rpm produced many discret balls of cellulose which were highly compact and resistant to breakdown even using the Atomix blender. It was impossible to clean cellulose produced in these cultures by mild extraction protocols, with the material remaining dark-brown in colour even after extensive grinding and washing.

5.3.2 Monosaccharide Analysis

Bacterial cellulose purified from cultures agitated at 0 or 50 rpm had a monosaccharide composition of >99% glucose. This is much purer than cotton linters cellulose, which was reported in chapter 3 to comprise 96.35% glucose.

5.3.3 X-Ray Diffraction

Figure 5.1 shows X-ray diffractograms obtained from the commercially available Avicel RC-581 (a) and cotton linters (b) cellulose, compared with bacterial cellulose purified from cultures grown at 0 or 125 rpm (c and d respectively). The diffractogram obtained from bacterial cellulose incubated at 0 rpm is identical to that reported by Atalla *et al* (1993) and Toyosaki *et al* (1995) and, by comparison with diffractograms for commercial celluloses, has a much higher degree of crystallinity. Identical, but weaker signals are seen in the diffractogram for bacterial cellulose synthesised at 125 rpm, suggesting that crystalline cellulose is synthesised in these cultures, but represents a much lower proportion of the sample. This is confirmed by birefringence studies (Fig 5.2) which show that both have a significant level of organisation. The diffractogram obtained for Avicel RC-581 microcrystalline cellulose is very similar to that reported by Hulleman *et al* (1994). Comparison of diffractograms (a) and (b) suggests that cotton linters cellulose is significantly more crystalline. However, integration of C-4 signals in ^{13}C-NMR spectra (Fig. 5.4) gives approximately equal crystalline contents, with ca. 55% for Avicel

Figure 5.1: Wide Angle X-Ray Scattering (WAXS) of Bacterial and Commercial Celluloses

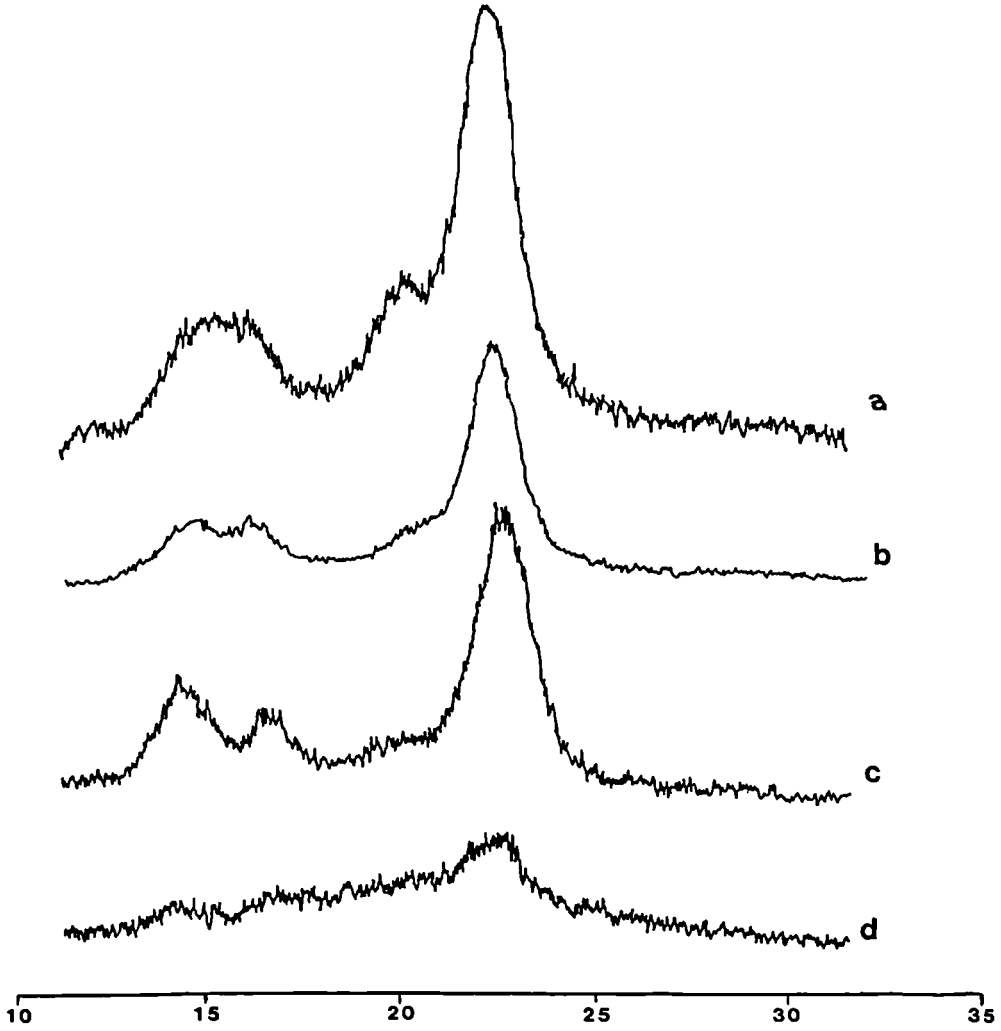

Diffractograms of Avicel RC-581 microcrystalline cellulose (a) and cotton linters cellulose (b) compared with cellulose ex. *Acetobacter aceti* ssp. *xylinum* from fermentations at 0 (c) and 125 (d) rpm

Figure 5.2 Micrographs of Bacterial Cellulose showing Birefringence

Birefringence of cellulose ex. *A.aceti* ssp. *xylinum* from fermentations at 0 (a) and 125 (b) rpm

cellulose (d) and ca. 60% for cotton linters cellulose of ca. 60% (c). Since NMR probes molecular organisation at a much shorter distance scale, this observation is evidence that molecular organisation as revealed by NMR should not necessarily be interpreted as indicative of crystallinity.

5.3.4 ^{13}C NMR Spectroscopy

^{13}C NMR spectroscopy under conditions of cross-polarisation, dipolar decoupling and magic angle spinning (CP/MAS) detects relatively rigid ('solid-like') segments and hence all cellulose is detected in this spectrum, with none in the SP/MAS (relatively mobile) spectrum (data not shown). The ^{13}C CP/MAS NMR spectra of cellulose synthesised at 0, 50 and 125rpm are shown in Fig 5.3 (a-c respectively). Signals at ca. 105, 88-91 and 84-86 ppm, corresponding to C-1 sites and C-4 sites in crystalline and non-crystalline sites respectively (VanderHart & Atalla, 1984), are detected in all 3 spectra. Integration of the latter 2 signals gives a crystalline content of ca. 75% in spectrum (a) and 80-85% in spectrum (b). Due to the large amount of extraneous material underneath the cellulose signals, such integration was not possible for spectrum (c). The slight discrepancy between crystalline contents for (a) and (b) may be due to the slight broadening of signals in spectrum (a) as this was recorded on a freeze-dried sample and may make integration less accurate. The results of X-ray diffraction and birefringence studies are confirmed, namely that the molecular organisation of cellulose is not greatly affected by agitation at these speeds. At higher agitation speeds (600-1200 rpm) a reduction in crystallinity and the synthesis of small amounts of cellulose II has been reported for a number of different *Acetobacter* strains (Johnson & Neogi, US Patent 4,863,565).

^{13}C CP/MAS spectra of cellulose synthesisied by *Acetobacter* cultures incubated at 50 rpm is compared with spectra obtained from cotton linters, acid-washed cotton linters and Avicel microcrystalline cellulose in Fig 5.4 (a-d) respectively. Integration of C-4 signals as above gives a crystalline content of ca. 50% for spectrum (b); ca. 60% for spectrum (c) and ca. 55 % for spectrum (d) compared with the value of 80-85% obtained for bacterial cellulose. The increase in crystallinity (c) over (b) is a

Figure 5.3: ^{13}C CP/DD/MAS Spectra of Cellulose Produced by *A.aceti* ssp. *xylinum* in Agitated Cultures

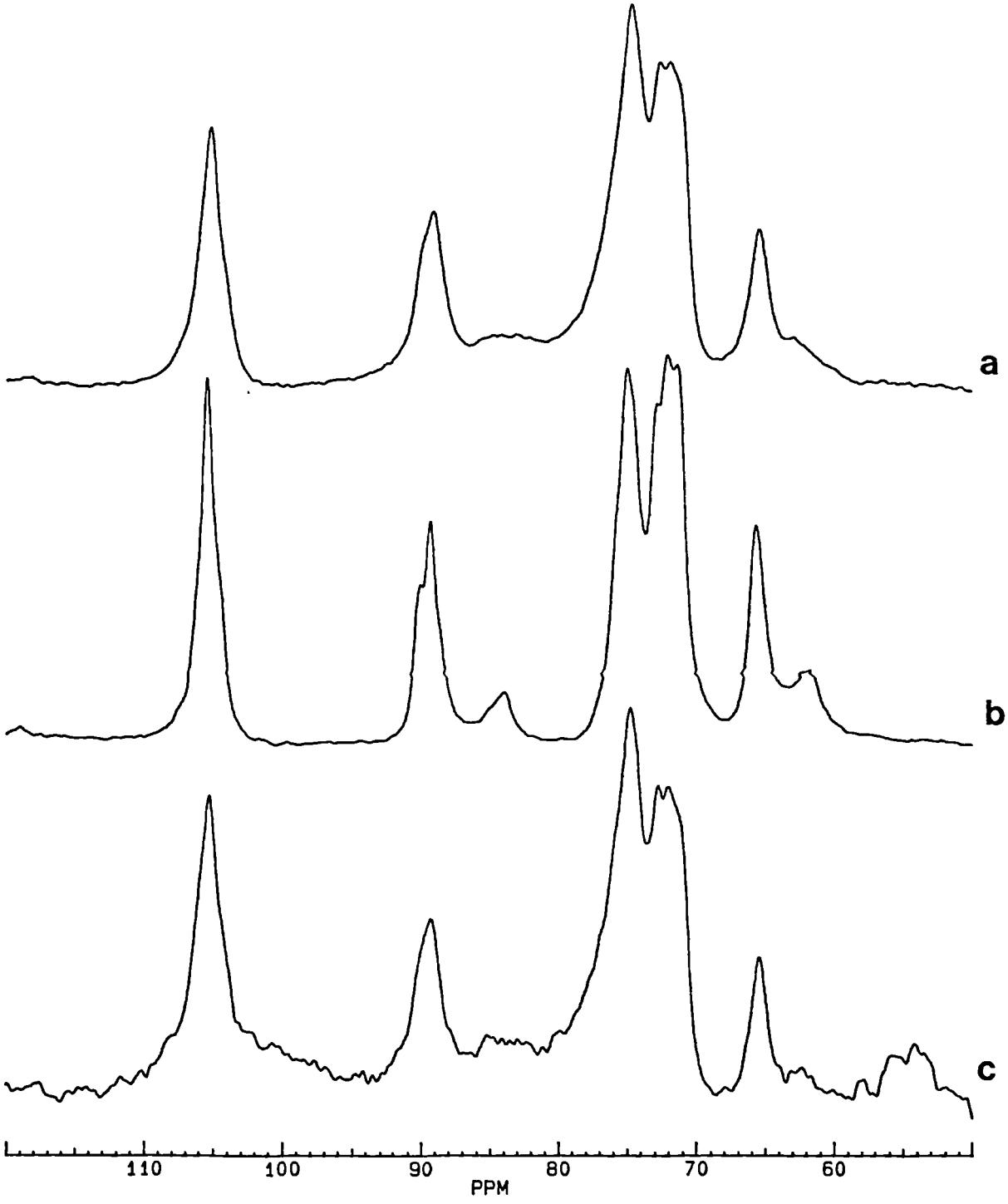

Spectra of cellulose ex. *A.aceti* spp. *xylinum* under magic angle spinning and dipolar decoupling conditions from fermentations at 0 (a), 50 (b) and 125 (c) rpm showing that molecular organisation is minimally affected by agitation speed

Figure 5.4: ^{13}C CP/DD/MAS Spectra of Bacterial and Commercial Celluloses

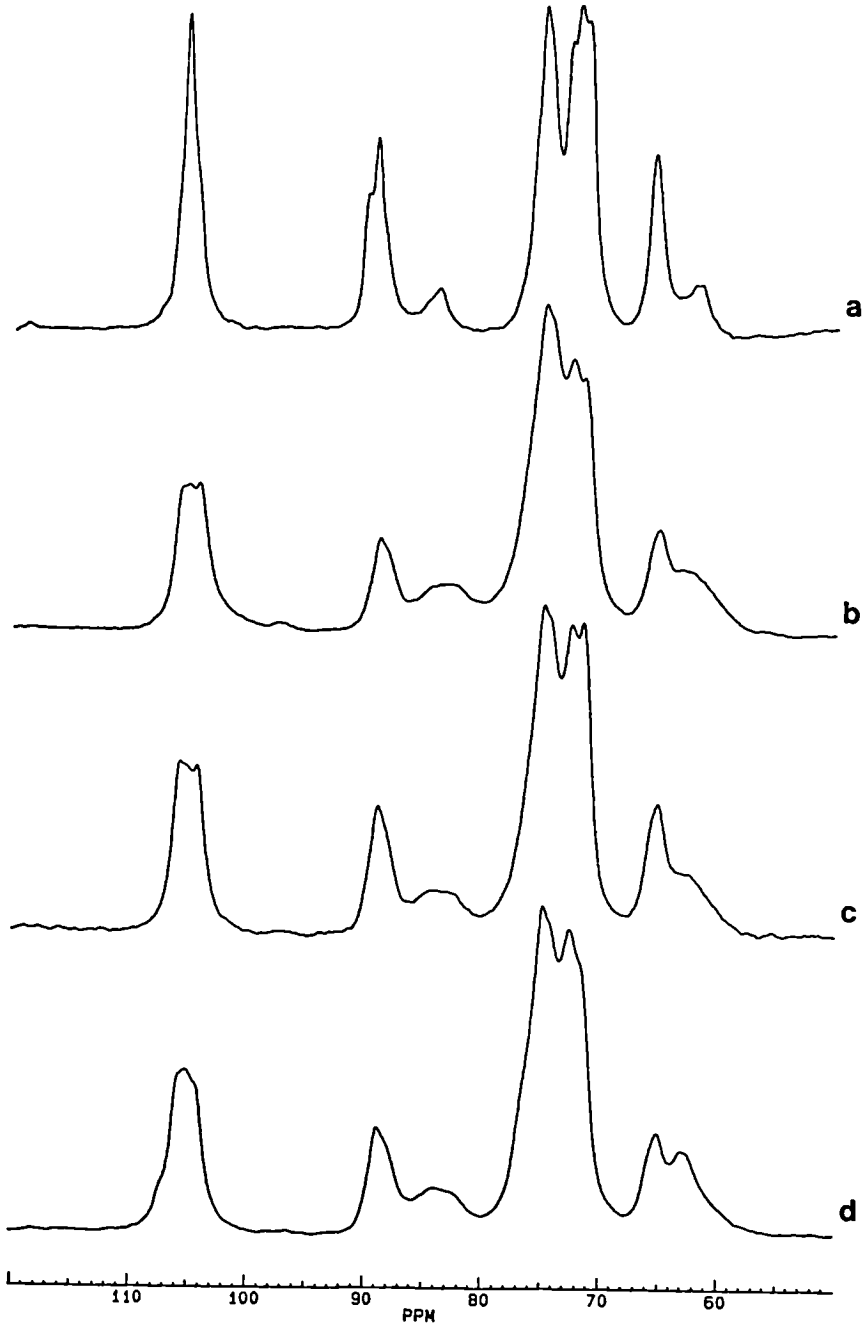

Spectra of cellulose ex. *A.aceti* ssp. *xylinum* (cf Fig 5.3 (b)) (a), cotton linters (b), cotton linters commercially acid treated (c) and Avicel RC-581 microcrystalline cellulose (d) showing overall higher crystallinity and lack of evidence for the presence of a C-1 triplet, which is indicative of a high proportion of Iα in spectrum (a) compared with spectra (b-d) which show lower crystallinty and splitting of the C-1 signal

reflection of commercial acid pretreatment. The spectral splitting of the C-1 signal in spectra (b-d) is indicative of lower Iα/Iβ ratios in these samples compared to bacterial cellulose (a). Application of resolution enhancement to spectrum (a) of Figure 5.4 (Fig 5.5 (a)) shows signals at 105.5, 90.2 and 89.3 ppm corresponding to the Iα crystalline allomorph and at 106.2, 104.4, 89.3 and 88.5 ppm corresponding to the Iβ form (Debzi *et al*, 1991; VanderHart & Atalla, 1984; Yamamoto & Horii, 1993). Figure 5.5 (b) and (c) show the resolution enhanced spectra of bacterial cellulose as (a) but purified by the methods of Debzi *et al* (1991) and Atalla *et al* (1993) respectively, both of which use alkali (see section 5.2.1). Comparison of C-4 signals with published, quantified signal patterns (Debzi *et al*, 1991; Yamamoto & Horii, 1993) gives Iα/Iβ ratios of approximately 70/30 for spectrum (a), 58/42 for spectrum (b) and 51/49 for spectrum (c). Bacterial cellulose purified by washing in deionised H_2O at RT therefore has a higher proportion of the Iα component than any previously reported (eg Debzi *et al*, 1991; Yamamoto & Horii, 1993) for cellulose synthesised at approximately 30°C (Yamamoto & Horii, 1994). Collation of data from Figures 5.3 (a) and 5.5 (b) leads to an overall molecular description for cellulose synthesised by *Acetobacter aceti* ssp. *xylinum* at 30°C in cultures agitated at 50 rpm and purified by washing in deionised H_2O at RT of 57% Iα, 25% Iβ and 18% non-crystalline.

5.3.5 Low Temperature Scanning Electron Microscopy

This technique allows examination of the cellulose pellicle formed by gently agitated (50 rpm) cultures of *A.aceti* ssp. xylinum. Figure 5.6 (a) shows a population of bacteria at the upper surface of the pellicle ie at the liquid/air interface. Towards the base of the pellicle ie the first-formed cellulose, the pellicle has a striated appearance, with successive layers apparently having altered directionality (Fig. 5.6 (b-d)). However, more recently formed cellulose, towards the upper surface, shows no evidence of layering (Fig. 5.6 (e)), suggesting that striation may be attributable to compressive effects of the pellicle rather than altered synthetic processes in the bacteria. Alternatively, there is a possibility that the layering is artefactual, caused by the preparative technique (M. Kirkland, Unilever Research, pers.comm.).

Figure 5.5: ^{13}C CP/DD/MAS Spectra of Bacterial Cellulose after Different Purification Protocols

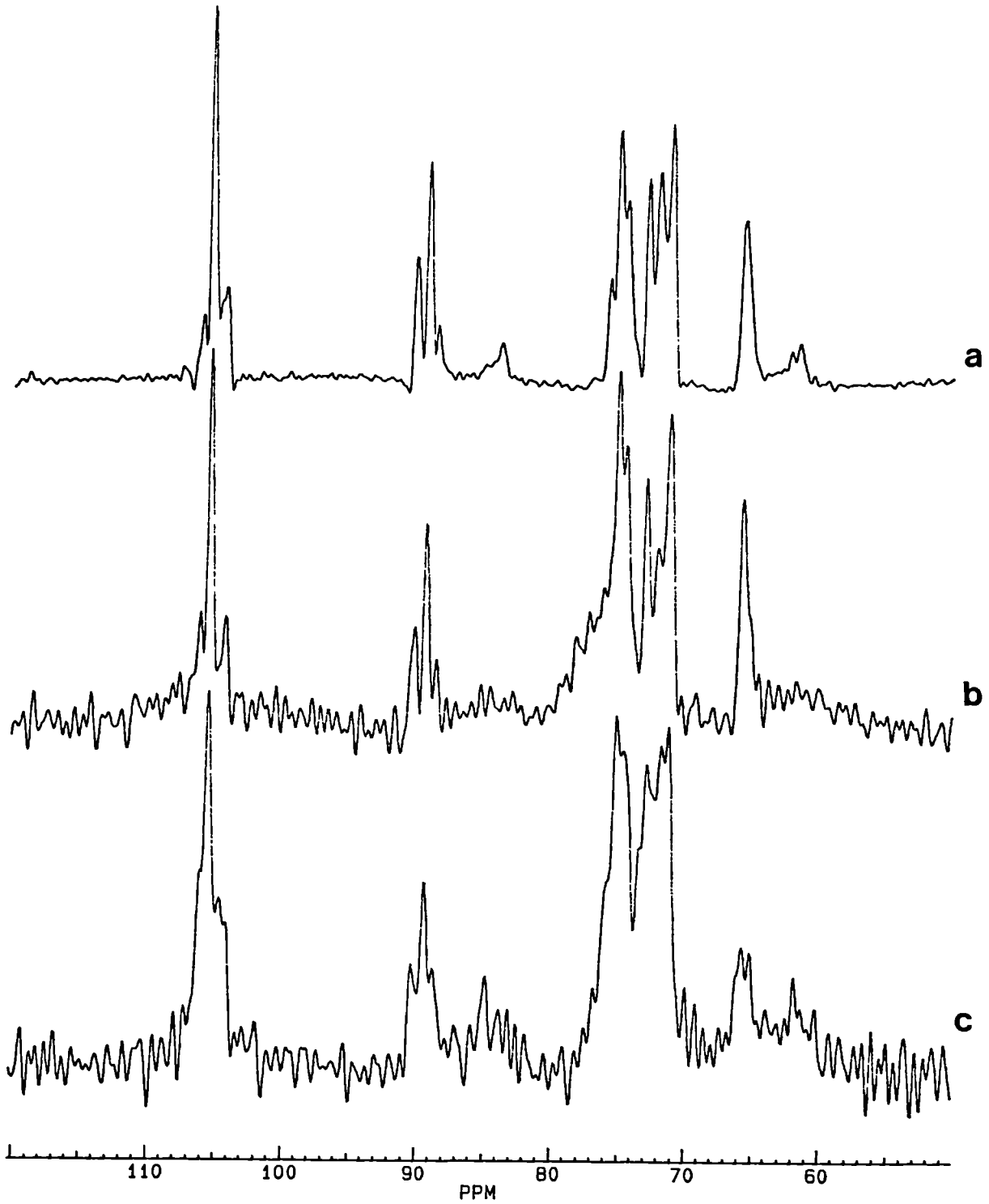

Spectra of cellulose ex. *A.aceti* ssp. *xylinum* from fermentations at 50 rpm after purification with deionised H_2O (a), 0.5% NaOH, 6 days, RT (b) and 1.0% NaOH, 6 hours, 100°C (c) after application of resolution enhancement (line broadening -70Hz, Guassian multiplication 0.5) illustrating fine structure on C-1 (ca. 105 ppm) and C-4 (88-92 ppm) cellulose signals (a) and altered fine structure on these signals following alkali purification protocols (b,c)

Figure 5.6: LT-SEM Micrographs of a Cross-Section through a Bacterial Cellulose Pellicle

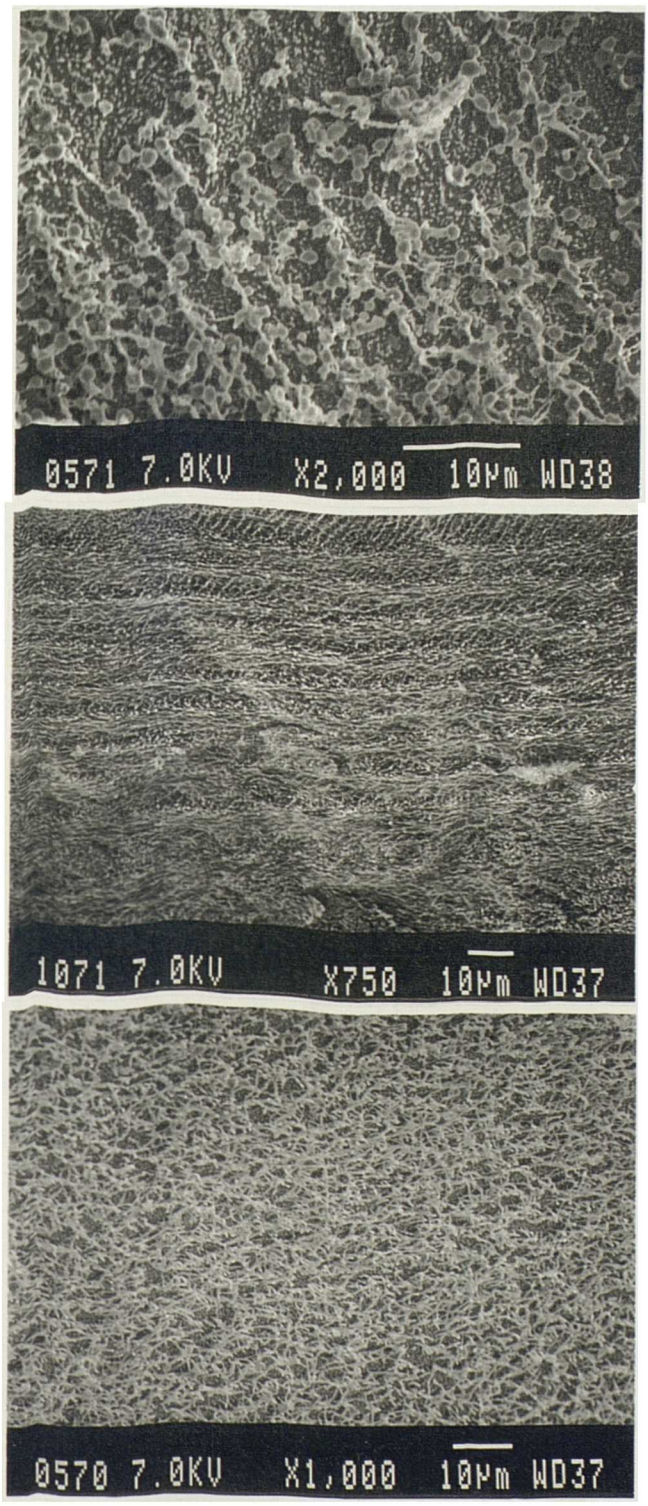

Section through a cellulose pellicle ex. *A.aceti* ssp. *xylinum* from fermentations at 50 rpm showing the upper surface colonised by the obligately aerobic bacteria residing at the liquid/air interface (a), the lower region of the pellicle showing an apparently layered structure (b) and the upper/middle region, showing no layering effect (c)

5.3.6 Deep-Etch Freeze-Fracture Transmission Electron Microscopy

Micrographs obtained from cellulose pellicles formed at 50 rpm reveal a densely packed network of apparently randomly oriented cellulose fibres (Fig. 5.7 (a,b)). Similar network architecture was seen at both the upper and lower regions of the pellicle, suggesting that the altered morphology between upper and lower sections as revealed by LT-SEM (section 5.3.5) is not reflected by differences in microstructure. Widths of cellulose fibres were measured according to the method outlined in Chapter 6 (section 6.3.1.1), giving an average ribbon width of 36nm ±6.7nm, in close agreement with Brown *et al* (1976) who quoted ribbon widths of 40-60nm.

5.3.7 Cellulose Synthesis in situ *by Bacteria Attached to EM grids*

Although bacteria could be visualised on EM grids and twisting ribbon-like material, confirmed as cellulose by the use of gold-labelled cellulase (supplied by Colin Smith, Unilever Research), was seen, it was not possible to assign individual ribbons to particular cells, as was achieved by Haigler *et al*, (1982). We concluded that, under these conditions, this strain of bacteria failed to synthesise cellulose *in situ*, and that the cellulose present was a contaminant from the preparation procedure. This failure may be due to strain-specific differences, as Haiglers group used the strain ATCC 23769.

5.3.8 Electron Diffraction

Native ground bacterial cellulose failed to give an electron diffraction pattern. However, when this cellulose was refluxed in 2.5N HCl for 4 hours according to the method of Sugiyama *et al*, (1991b) good diffraction patterns were obtained (Fig. 5.8 c,d). Integration of C-4 signals at 88-90 and 84-86 ppm, as in section 5.3.2, for ^{13}C NMR spectra of acid treated cellulose indicates that acid refluxing does not affect percentage crystallinity or alter Iα/Iβ ratios (data not shown). This correlates with data presented for *Microdictyon* cellulose by Sugiyama *et al* (1991b) where acid hydrolysis generates microcrystalline elements or 'cellulose microcrystals' which improve diffraction, but have identical FT-IR spectra to the controls.

Figure 5.7: DEFF-TEM Micrographs of a Bacterial Cellulose Pellicle

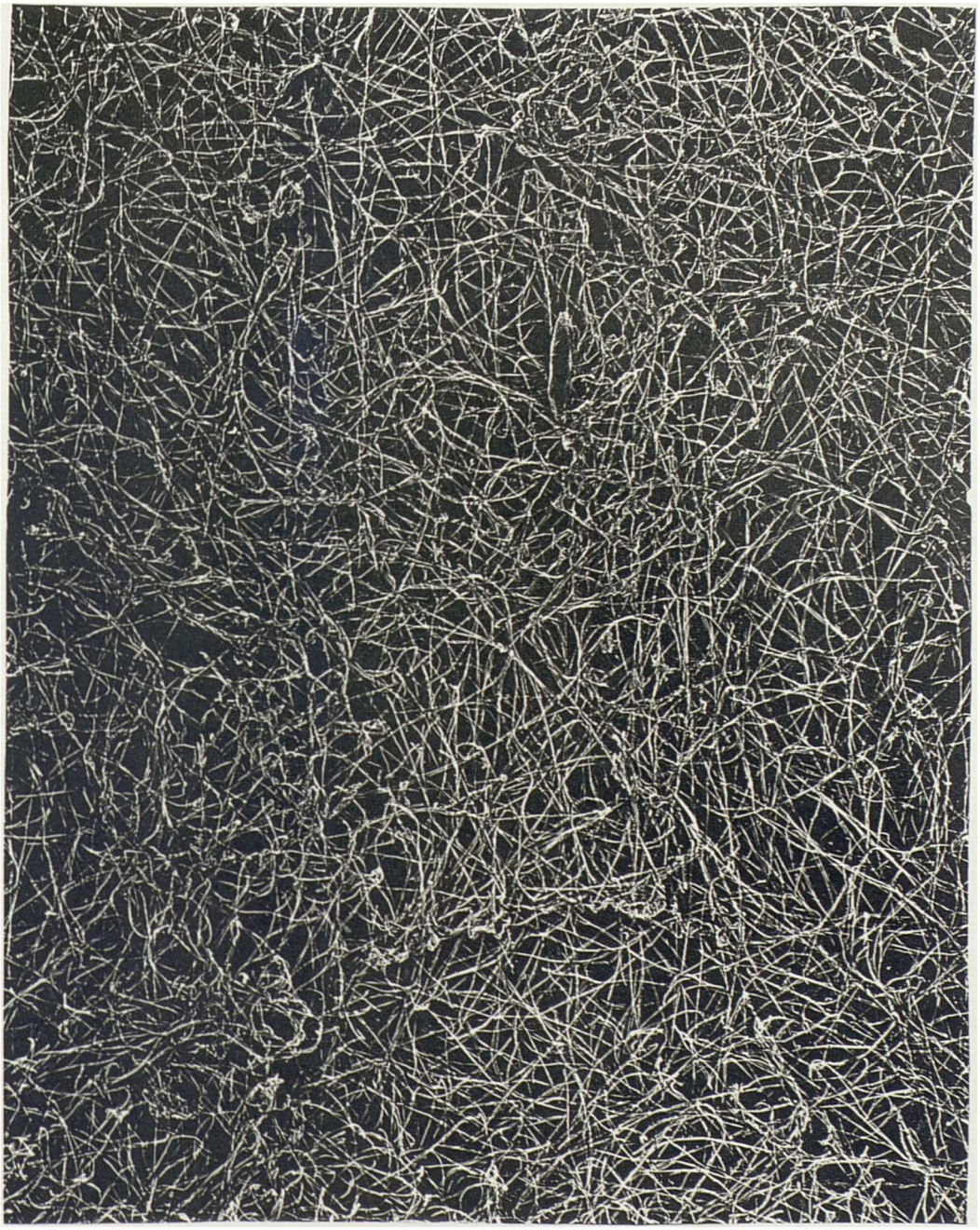

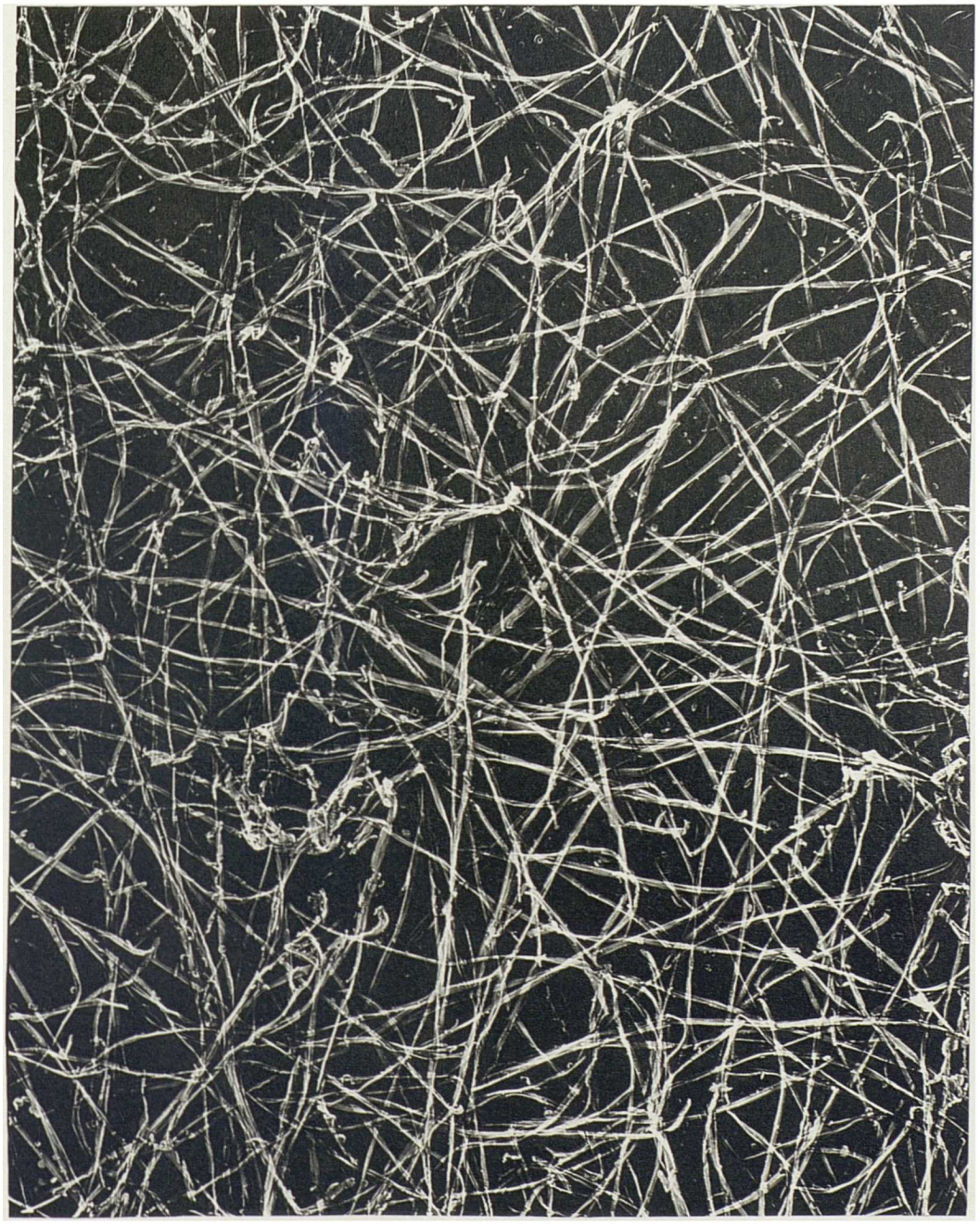

Micrographs of tungsten.tantalum/carbon replicas (printed in reverse contrast) of cellulose ribbons produced by *A.aceti* ssp. *xylinum*, at two different magnifications (a,b), illustrating an apparently random orientation of persistent strands

Standard methods of illumination were adequate to obtain diffraction patterns for the calibration standard graphite (Fig. 5.8 (a)), but proved problematical for cellulose samples as damage caused by the beam caused rapid fading of patterns, precluding photography. High resolution, or micro-micro diffraction was therefore used, with a scanning attachment, which had a narrower beam and minimised sample degradation (Fig. 5.8 (b-d)). Adequate dispersion of microcrystalline cellulose such that individual microcrystals could be unambiguously identified was not possible, but well defined diffraction spots are observed, suggesting unidirectionality of chain axis.

5.3.8.1 Graphite Calibration Standard

To establish that the diffraction pattern of Figure 5.8 (b) is graphite, the following Bragg equation was used

$$n\lambda = 2d\sin\theta$$

where: n = order

λ = wavelength at 120 kV

θ = angle of incidence

d = lattice spacing

For a diffraction pattern, distances and angles of the crystal lattice can be related by (from the above equation)

$$\frac{D/2}{L} = \tan 2\theta$$

where : D = diameter of diffraction ring

L = effective camera length

Eliminating θ from this equation using the Bragg relationship and assuming θ to be so small that :

$$\tan 2\theta \approx 2\sin\theta \approx 2\theta$$

then

$$D = 2L.2\theta$$

$$= 4L.\ \lambda/2d \quad \text{when } n=1$$

or:

$$\mathbf{D.}d\mathbf{/2 = L}\lambda\mathbf{ = Camera\ constant}$$

Using this equation, with the following parameters:

D = 6.8mm (distance between first layer diffraction spots on negative of Fig. 3.8 (b))

$\lambda = 0.003349 \times 10^{-9}$ (wavelength at 120 kV)

L = 340mm

then d = 0.3349nm, which is in close correlation with the predicted lattice spacing for graphite of 0.338nm.

5.3.8.2 Triclinic and Monoclinic Diffraction Patterns in Microcrystalline Cellulose

Identification of triclinic (Iα) and monoclinic (Iβ) diffraction patterns was done by comparison with published diffraction diagrams (Sugiyama *et al*, 1991b). Figure 5.8 (c) shows a triclinc diffraction pattern, equivalent to that of Figure 3b(1) from Sugiyama *et al* (1991b). Using the following equation:

$$d_{(exp)} = D_{(gra)} / D_{(exp)} \cdot d_{(gra)}$$

d-spacings were calculated as 0.420nm (110), 0.420nm (002), 0.428nm (-1-1 2) and 0.234nm (-1-1 4) which shows some correlation with published *d*-spacings of 0.396nm, 0.432nm, 0.439nm and 0.259nm respectively. Although many diffraction patterns were taken, this example gave the closest *d*-spacing correlation.

Figure 5.8 (d) shows a diffraction pattern which apparently correlates with the monclinic pattern illustrated in Figure 4b(2) of Sugiyama *et al* (1991b).. However, we were unable to correlate *d*-spacings with those published.

Figure 5.8:Spot Electron Diffractograms of Graphite and *Acetobacter* Cellulose Microcrystals

a

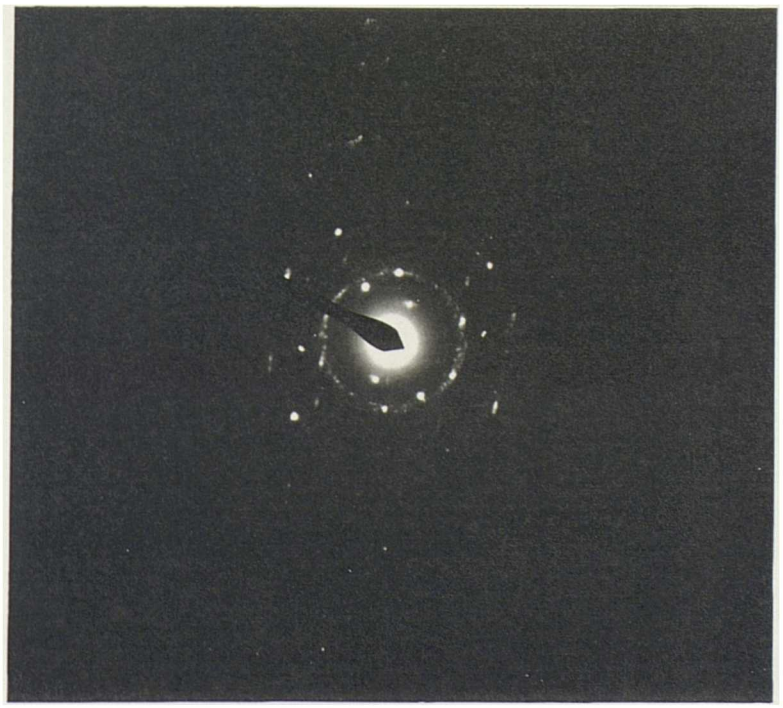

b

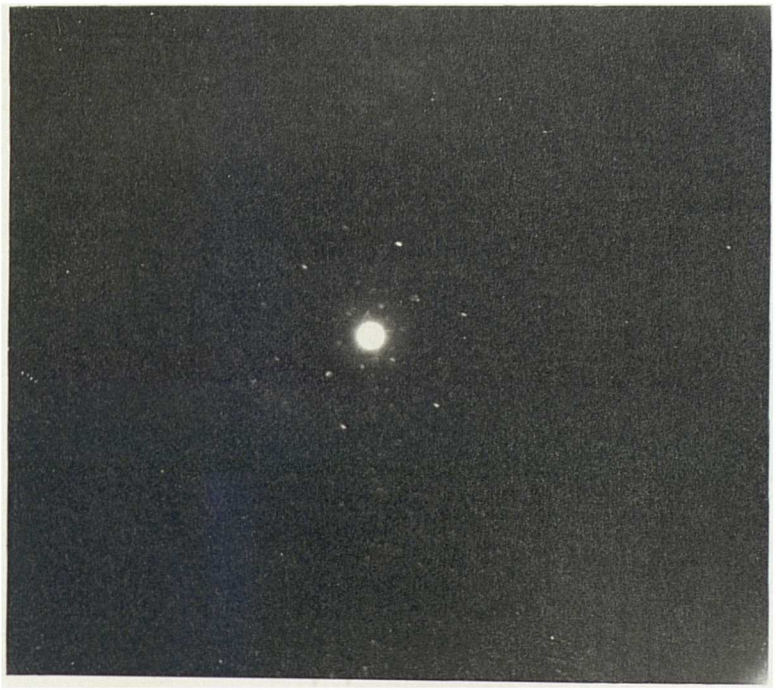

c

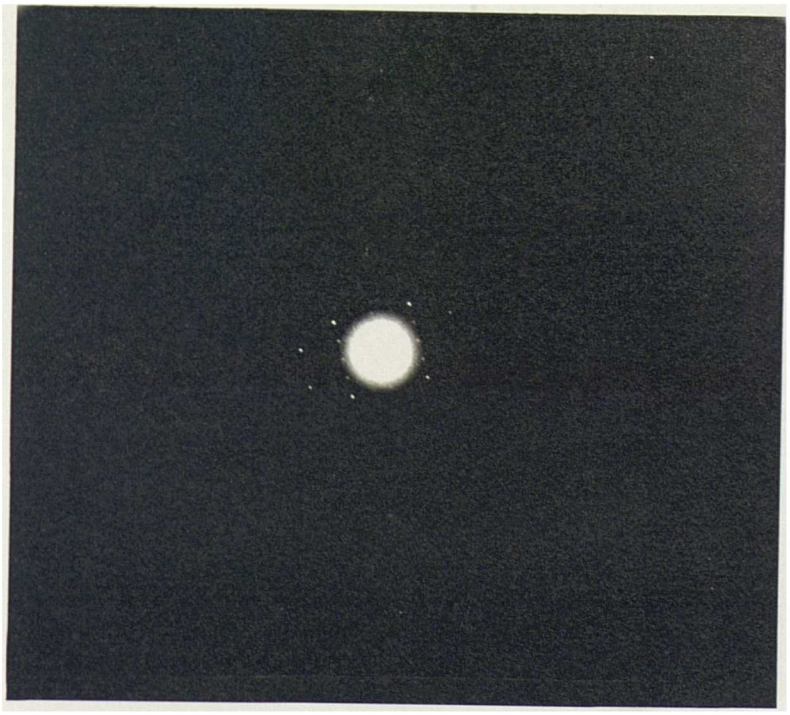

d

Electron diffractograms of the calibration standard graphite recorded using standard illumination (a) and micro-micro diffraction (b) techniques compared with microcrystals of cellulose ex. *A.aceti* ssp. *xylinum* presenting triclinic (c) and monoclinic (d) features

5.4 Discussion

Acetobacter aceti ssp. *xylinum* (ATCC 53524) routinely produced large quantities of essentially pure cellulose under gentle agitation conditions. At an agitation speed of 50 rpm, an intact pellicle was produced, which was adequately cleaned using very mild purification protocols. When modifying polymers are added to the incubation medium (Chapters 6-8) agitation of the culture is essential to ensure mixing (Atalla *et al*, 1993) but the production of intact pellicles is desirable for microscopic and mechanical testing (Chapter 10) techniques. Therefore, these incubation conditions are apparently ideal for this system.

Observations of the metastability of the Iα form under heating and aqueous alkaline conditions (eg Debzi *et al*, 1991; Yamamoto *et al*, 1989), coupled with the fact that cellulose/hemicellulose composites will be investigated (Chapters 6-8), but hemicelluloses are dissociated from cellulose using alkali (eg Chambat *et al*, 1984) prompted us to investigate mild, non-alkaline purification conditions. Using deionised H_2O at RT, Iα/Iβ ratios of ca. 70/30 were obtained for cellulose produced by *A.aceti* ssp. *xylinum* at 50 rpm. This is higher than previously reported (eg Debzi *et al*, 1993; Yamamoto & Horii, 1993) for bacterial cellulose produced at 30°C (Yamamoto & Horii, 1994) and we conclude that more rigorous purification protocols employed by other authors may have resulted in an inaccurate estimate of native bacterial cellulose crystalline character.

LT-SEM allowed visualisation of the cellulose pellicle in cross-section, clearly showing differences between newly formed and older cellulose layers. With the addition of polymers to the medium which might be expected to alter pellicle construction (Chapters 6-8), this technique may be valuable for identifying alterations in structure at the μm distance scale. DEFF-TEM probes network architecture at the nm distance scale, and these pellicles proved to be excellent material for what can be a difficult technique. Application of this technique has proved a major advance in understanding plant cell wall

architecture (McCann *et al*, 1990; Satiat-Jeunemaitre, 1992) and these results indicate that it may be an equally effective tool in examining network architecture in this system.

Haigler *et al* (1982) reported synthesis of cellulose by isolated *Acetobacter* cells on EM grids and perturbation of ribbon formation by additives such as CMC. Recent publications (eg Sugiyama *et al*, 1991b) have shown that it is possible to 'walk along' a cellulose microcrystal, identifying discrete Iα and Iβ domains. In light of evidence that additives such as xyloglucan and fluorescent brighteners may effect alteration of Iα/Iβ ratios of bacterial cellulose synthesised (Hackney *et al*, 1994; Kai *et al*, 1994; Yamamoto & Horii, 1994), we had hoped to use a combination of TEM and electron diffraction to visualise areas of ribbon perturbation by the addition of hemicelluloses and to record electron diffraction as a measure of IαIβ ratios at these defined points. This would have enabled us to identify specific areas of altered crystallinity, rather than an overall effect on the bulk sample as recorded by NMR spectroscopy. However, we were unable to develop this technique further than described in the results section (5.3.8) because no electron diffraction could be obtained on non-acid treated, native, bacterial cellulose, precluding diffraction on cellulose synthesised *in situ* (section 5.3.7).

The ultrastructure and molecular organisation of bacterial cellulose pellicles produced at 50 rpm and purified by washing in deionised H_2O can be probed using a combination of ^{13}C-NMR spectroscopy and specialised forms of both scanning and transmission EM. Based on these results it is predicted that alterations induced by the addition of modifying polymers to the fermentation medium can also be determined with these analytical techniques. We propose therefore that this cellulose-synthesising system may be valuable in investigations of cellulose/hemicellulose interactions.

Chapter 6: *In Vitro* Construction of Cellulose/Xyloglucan Networks

6.1 Introduction

The production of cellulose by the Gram -ve bacterium *Acetobacter aceti* ssp. *xylinum* was reported in Chapter 5. Under gentle agitation conditions (50rpm) an intact pellicle was formed at the surface of the medium which was easily cleaned by extensive washing in deionised water. The deep-etch, freeze-fracture technique showed a densely packed network of apparently randomly oriented fibres (Figure5.7). ^{13}C NMR spectroscopy revealed that the ratio of the two cellulose I crystalline allomorphs Iα and Iβ was higher (70:30) than had previously been reported (eg Debzi *et al*, 1991; Yamamoto & Horii, 1993) for bacterial cellulose produced at approximately 30°C (Yamamoto & Horii, 1994), probably reflecting the lack of alkali pre-treatment in this work (Uhlin *et al*, 1995; Whitney *et al*, 1995).

Acetobacter xylinum has a linear array of synthetic sites or pores arranged along one of the long axes of the cell (Brown *et al*, 1976). Glucan chains are synthesised at these sites and sub-elementary fibrils comprising 16 glucan chains are secreted through the pores (Zaar, 1979) where they aggregate to form microfibrils 3-4nm wide. Microfibrils further self-associate to form the characteristic twisting ribbon of cellulose I 40-60nm wide which is extruded parallel to the long axis of the cell (Brown *et al*, 1976). A schematic representation of ribbon assembly is shown in Figure 6.1. This process can be disrupted by fluorescent brighteners, which perturb microfibril crystallisation (Haigler *et al*, 1980; Kai *et al*, 1994) and CMC which prevents fasciation of microfibrils into ribbons (Haigler *et al*, 1982; Haigler & Brown, 1981).

Figure 6.1: Schematic Representation of Cellulose Ribbon Assembly by *Acetobacter xylinum*

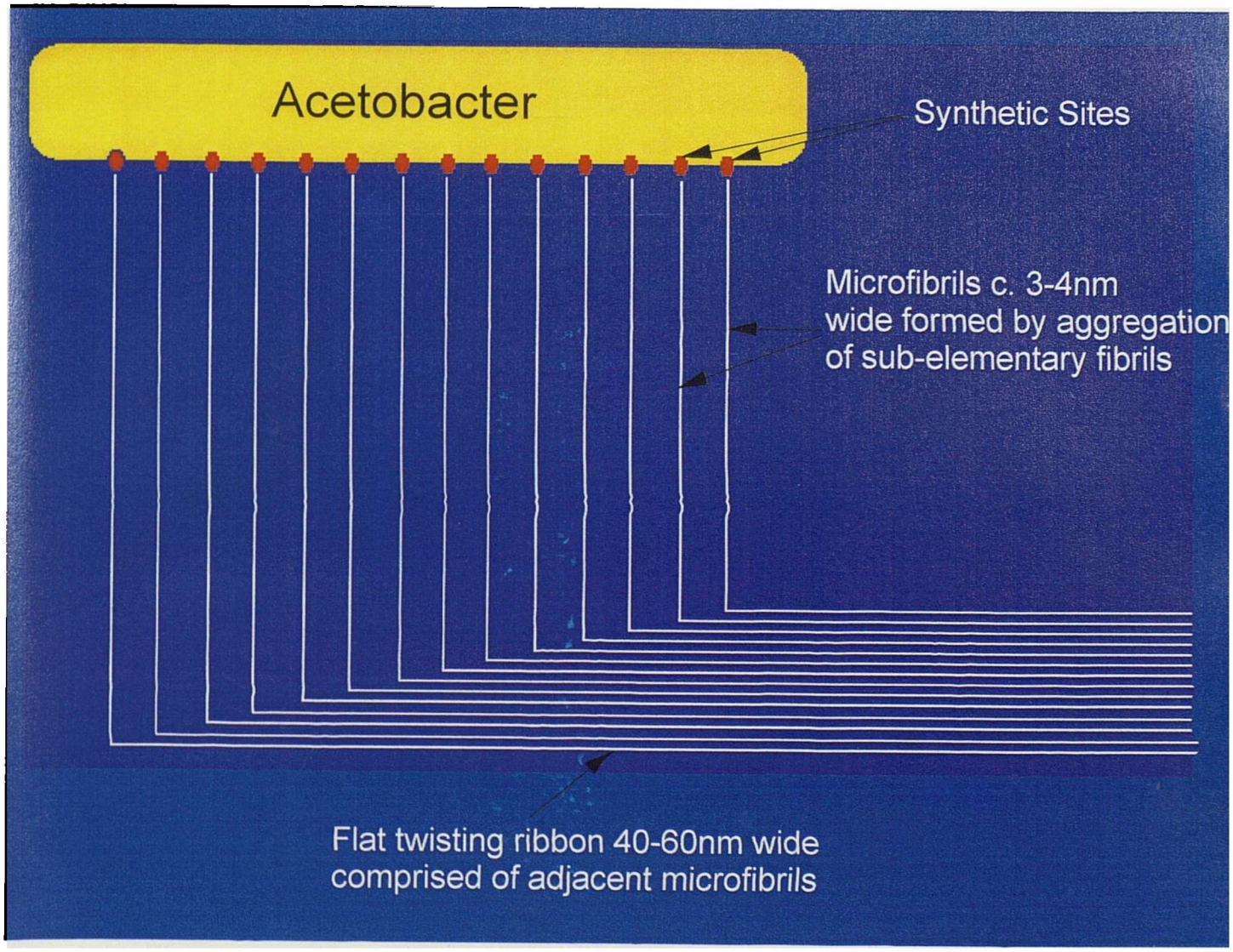

Sub-elementary fibrils comprising 16 glucan chains are synthesised within the pores located on the long axis of one side of the cell. This aggregate at or very close to the point of synthesis into microfibrils 3-4nm wide. These further associate at some distance away from the cell into a flat twisting ribbon 40-60nm wide, which is characteristic of *Acetobacter xylinum* cellulose (Brown *et al*, 1976; Zaar, 1979) Note: Not to Scale

As described in the introductory chapter (1.6), the Type I (Carpita & Gibeaut, 1993) primary cell wall in most dicotyledonous and non-graminaceous monocotyledonous plants is believed to comprise a tightly associated network of cellulose and xyloglucan, which is embedded in a pectic matrix (Carpita & Gibeaut, 1993; McCann & Roberts, 1991; Talbott & Ray, 1992a). Reconstruction of a cellulose/xyloglucan network *in vitro* with properties similar to those in plants has met with limited success (see 1.6.2 and Chapter 3 for discussion). Use of the *Acetobacter* system may provide an opportunity to associate the two components under physiological conditions. In a fermentation medium containing xyloglucan, it can be envisaged that the polymer will occupy all space around the bacterium (Figure 6.1) and hence xyloglucan will be present at or very close to the point of cellulose synthesis. In the cell wall, after synthesis in the Golgi, xyloglucan is secreted to extracellular sites in secretory vesicles, possibly with the concomitant activation of cellulose synthase (terminal complex) allowing association of xyloglucan with newly synthesised cellulose at the cell surface (Hayashi, 1989). This system may therefore mimic, at least partly, events occuring during deposition of the native cellulose/xyloglucan network.

Xyloglucan has previously been shown to interact with cellulose synthesised by *Acetobacter xylinum*, causing a reduction in ribbon dimensions (Hayashi *et al,* 1987; Uhlin *et al*, 1995; Yamamoto & Horii, 1994) and an alteration in the molecular organisation of the cellulose component to become more like that seen in higher plants (Atalla *et al,* 1993; Hackney *et al*, 1994; Uhlin *et al*, 1995; Yamamoto & Horii, 1994). In this chapter we report the construction and characterisation of cellulose/xyloglucan networks using the *Acetobacter* system. Networks are examined using deep-etch freeze-fracture TEM to establish network architecture and ^{13}C NMR spectroscopy to probe molecular organisation of the composite structure. The tightness of the association is probed by standard chemical sequential deconstruction protocols and the effect of xyloglucan molecular weight on ultrastructural and molecular features of composites is investigated.

6.2 Materials and Methods

6.2.1 Bacterial Cultures

Bacterial inoculum was obtained from previously cellulose-synthesing cultures as described in General Materials and Methods (2.12.2). Incubations were performed in Hestrin-Schramm medium pH 6.2 (Hestrin & Schramm, 1954) containing 2% glucose and 0.5% high mwt tamarind xyloglucan purified from Glyloid 3S (Dainippon Pharmaceutical Co., Osaka, Japan), or 0.5% or 2.0% low mwt tamarind xyloglucan (kindly provided by Tim Foster, Unilever Research) at 30°C and 50rpm. After 48 hours incubation, material was removed aseptically and washed extensively in sterilised deionised water at room temperature.

6.2.2 Binding of Bacterial Cellulose and Xyloglucan in vitro

Cellulose pellicles from control incubations (5.2.1, 50rpm cultures) were harvested after 7 days. After grinding with an Ultra-Turrax T-25 (Janke and Kunkel), samples were washed thoroughly and freeze-dried. The cellulose was ground further to a fine white powder with a mortar and pestle under liquid nitrogen.

Binding of bacterial cellulose and xyloglucan was carried out essentially according to the method of Hayashi *et al* (1987). 100 mg of finely ground cellulose were shaken in 50ml of a 25mM sodium phosphate buffer solution pH 5.0 (0.02% NaN_3) containing 30mg of high or low mwt tamarind xyloglucan. After 72 hours, samples were collected by centrifugation and washed thoroughly, first with buffer and then with deionised water.

6.2.3 Sequential Deconstruction Protocol

Cellulose/xyloglucan composites were deconstructed with increasing concentrations of alkali essentially according to the method of Selvendran (1983).

6.2.3.1 Intact pellicles

Intact control or high mwt xyloglucan-modified pellicles were extracted for 2 hours with orbital agitation at room temperature with 2 x 0.5M KOH, 2 x 1.0M KOH, 1 x 4.0M KOH and 2 x 4.0M KOH. All solutions were nitrogen presaturated and contained 20mM $NaBH_4$. After each extraction, pellicles were washed extensively with deionised water. Extracts were pooled, neutralised, dialysed extensively against deionised water at 1°C and freeze dried.

6.2.3.2 Ground Pellicles

High mwt xyloglucan-modified pellicles were gound using an Ultra-Turrax T-25 as a preliminary deconstruction step. Ground material was sequentially extracted as described in 6.2.3.1. Extracted material was collected by centrifugation at 27,100g at 4°C for 20 minutes and washed extensively with deionised water between each extraction step. Extracts were collected as described in 6.3.2.1.

6.2.3.3 Cellulose/Xyloglucan Composites Bound in vitro

In vitro associated composites of high and low mwt xyloglucan were sequentially extracted as in 6.3.2.2. The 4M KOH extraction step was omitted.

For all samples, oligomeric composition of extracted material was determined by digestion with *endo*-1,4-β-glucanase from *Trichoderma viride* (Megazyme Pty, Austarlia) and injection onto the Dionex system (see General Materials and Methods 2.14). Residual material was analysed for monosaccharide composition and by high resolution microscopy.

6.2.4 Enzymic Deconstruction of Cellulose/Xyloglucan Composites

Approximately 2mg (dry weight) of native or ground (cf 6.2.3.2) cellulose/xyloglucan composites was accurateley weighed into an Eppendorf tube. Buffer solution (25mM sodium acetate pH 4.5 containing

0.05% NaN3) was added to give a total volume of 1.0ml. Samples were incubated with 0.005U *endo*-1,4-β-glucanase from *Trichoderma viride* (Megazyme Pty, Australia) for 24 hours at 40°C with constant agitation. After incubation the enzyme was denatured in a boiling water bath for 5 minutes. The pellet was collected using a Microfuge (Centaur) at 13,00 rpm and freeze dried for sugar analysis. The supernatant was collected and aliquots injected onto the Dionex system using the gradient described in General Materials and Methods (2.14).

6.2.5 Monosaccharide Analysis

The monosaccharide composition of cellulose/xyloglucan composites was determined using Alditol Acetates Method 2 (section 2.8). The composition of low mwt tamarind xyloglucan was determined using Alditol Acetates Method 3 (section 2.9).

6.2.6 Deep-Etch Freeze-Fracture TEM

All microscopy was performed as described in General Materials and Methods (2.12.5).

6.2.7 ^{13}C NMR Spectroscopy

All spectroscopy was performed as described in General Materials and Methods (2.13).

6.2.8 Molecular Weight Analysis using High Performance Size Exclusion Chromatography with Multi-Angle Laser Light Scattering (HPSEC-MALLS)

Xyloglucan samples (0.3%) were prepared by dispersing in 0.2M sodium nitrate and, after swelling, heating to 100°C in a microwave oven. After filtration (hot) through a 0.45μm filter (PVRF, Whatman), 200μl of the reheated sample was applied to the SEC-MALLS-RI system.

Anagel-TSK PW_{XL} G4000, G5000 and G6000 columns in series (7.8 x 300mm, Anachem) in combination with a TSK PW_{XL} guard column (6.0 x 40mm) were used for chromatography, operating with a Gilson pump (model 305). Columns were eluted at 0.5ml/min with degassed 0.2M sodium nitrate filtered under vacuum through a 0.02μm membrane (Anodisc, Whatman). Light scattering was detected with a DAWN-F MALLS photometer equipped with an F2 flow cell (n=61655) and a high temperature read head. The photometer light source was a He-Ne laser, 633nm, 5mW (Wyatt Technology, Santa Barbara, USA). A Waters 410 differential refractometer with a measuring wavelength at 633nm was used. Columns, MALLS detector and differential refractometer were operated at 40°C. Data processing was performed using Astra for Windows v4.0 (Wyatt Technology).

The refractive index increment for xyloglucan in 0.2M sodium nitrate was calculated as 0.15. Prior to measurements, the DAWN-F MALLS photometer was calibrated and normalised giving the calibration constant required to convert instrument-dependent measurements into absolute excess Rayleigh ratios. The instrument is calibrated by determining the scattering (at the 90° detector) of a pure solvent (toluene) with known Rayleigh ratio. All other detectors are normalised to the calibrated detector by measuring the scattering from a sample for which the angular dependence of scattering is known (a P20 pullulan standard).

6.3 Results

6.3.1 Microstrure of Networks Formed in the Presence of Xyloglucan

6.3.1.1 High Mwt Xyloglucan

When cellulose is synthesised in the presence of high mwt tamarind xyloglucan, a thick pellicle is formed on the surface of the medium, similar to that seen in control incubations (section 5.3.1). After two days incubation, the viscosity of the medium is reduced to that of a control medium, implying that all xyloglucan had been incorporated into the composite. Occasionally cultures failed to incorporate all

xyloglucan after two days, due in part to different inoculum levels, and these cultures were incubated for a further period of time until viscosity had reduced to that of the controls. The rate of cellulose synthesis in cultures containing xyloglucan was increased by a factor of 2.2 (assuming a cellulose:xyloglucan ratio of 1:0.38) relative to the controls. This is in general agreement with results presented by Ben-Hayim & Ohad (1965) for increased cellulose synthesis in the presence of CMC, although the magnitude of the increase reported by these authors (30%) was less marked.

The association of xyloglucan with cellulose has imparted a level of lateral order absent in the controls (Figure 6.2). Thin strands of what are presumed to be xyloglucan can be distinguished as forming cross-linkages between cellulose fibres. Xyloglucan is apparently acting as a molecular tether, aligning adjacent fibres in a role consistent with that proposed for it in models of the primary cell wall (Carpita & Gibeaut, 1993; McCann & Roberts, 1991; Talbott & Ray, 1992a). Although there is considerable heterogeneity of microstructure throughout the pellicle, the highly ordered, cross-linked structure always forms a significant proportion of the structure. This experiemental variation may be due to the non-optimised conditions (see Discussion).

The length of cross-bridges between fibres in parallel alignment (indicated by small arrows in Figure 6.2b) was determined by image analysis to range from 20-70nm, with the majority between 30 and 50nm in length (Figure 6.3). This shows close correlation with the data of McCann *et al* (1990), who reported highly conserved putative xyloglucan cross-bridge lengths of between 20 and 40nm for depectinated onion cell walls. A small number of possible cross-linkages longer than 70nm are also apparent (Figure 6.2, large arrows). These appear thicker than the shorter linkages connecting ribbons (Figure 6.2, small arrows) and are predominantly found where ribbons diverge. It is possible that these are isolated cellulose microfibrils dissociated from the main ribbon and consequently they have not been included in the image analysis (Figure 6.3). Average ribbon widths for xyloglucan-modified composites (Figure 6.2) were determined by image analysis to be 36 ± 5nm compared with 36 ± 7nm in the controls (section 5.3.4 and Figure 5.7). This contrasts with previous reports where fibre widths

Figure 6.2: Bacterial Cellulose Composites Formed in the Presence of High Mwt Tamarind Xyloglucan

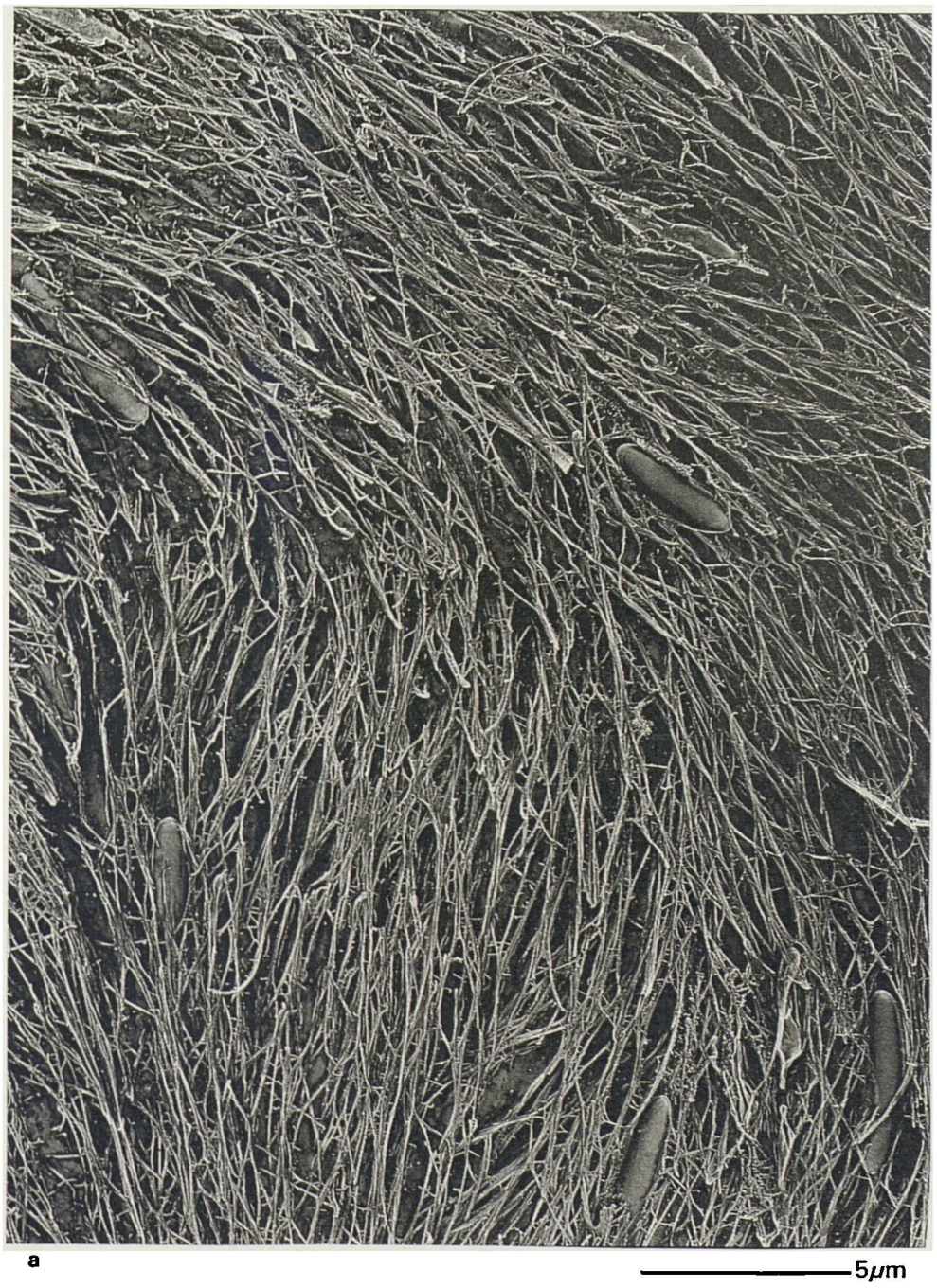

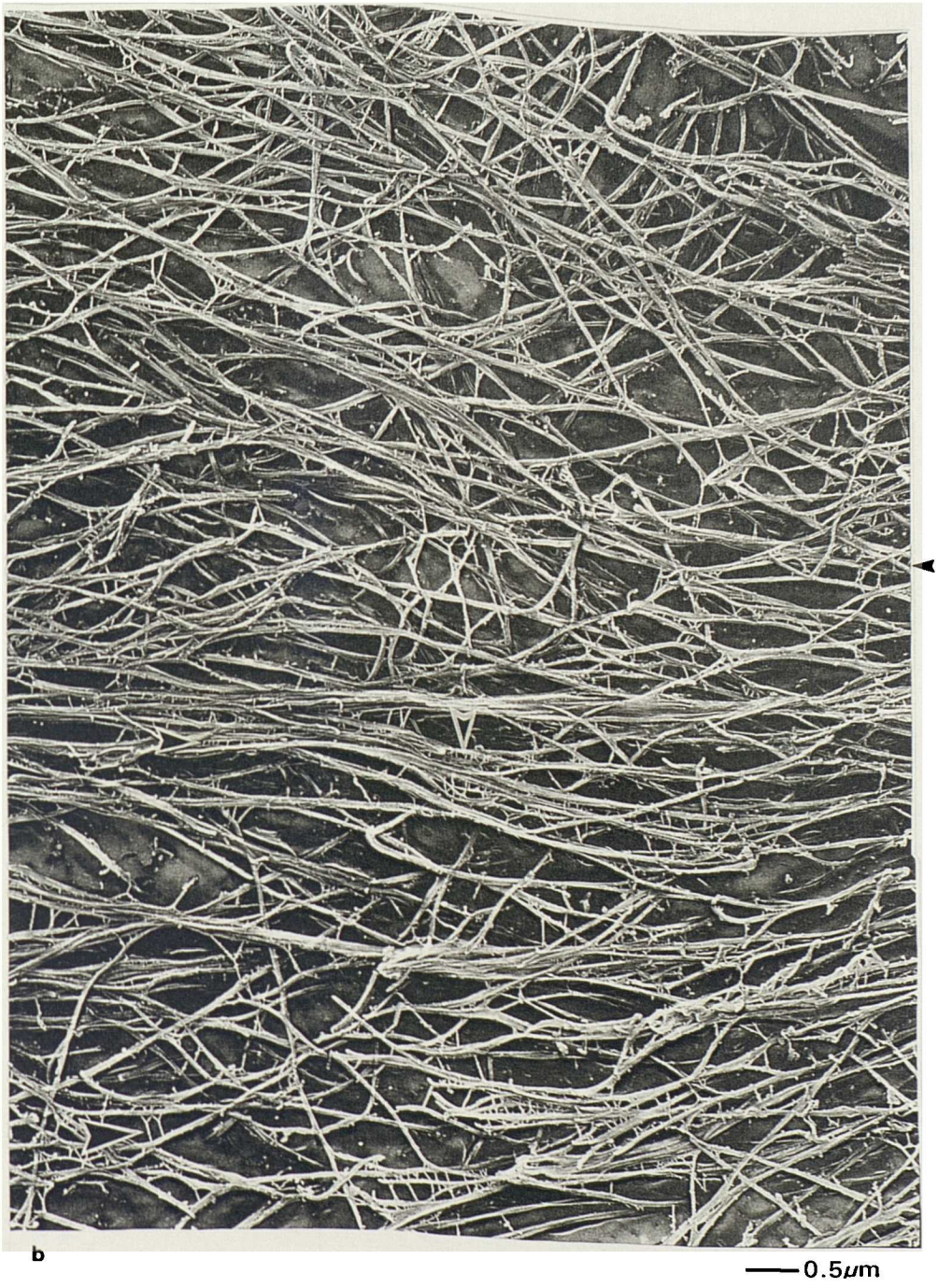

Micrographs of tungsten/tantalum/carbon replicas of composites produced by fermentation of *A.aceti* ssp. *xylinum* (ATCC 53524) in the presence of high mwt tamarind xyloglucan, illustrating abundant cross-bridges and an overall alignment of cellulose robbons. Small arrows (in black outside micrograph and black on white within the micrograph) illustrate cross-bridges measured by image analysis (see Figure 6.3). Large arrows illustrate apparent cross-linkages which are not obviously involved in alignment of ribbons or which appear thicker than expected for a single polysaccharide chain. Linkages of this type were not measured by image analysis.

were reduced to between 4 and 8 nm when cellulose was synthesised by *Acetobacter xylinum* (ATCC 23769) as isolated fibres (rather than as a network) in the presence of pea (Hayashi *et al*, 1987) and tamarind (Yamamoto & Horii, 1994; Uhlin *et al*, 1995) xyloglucan.

6.3.1.2 Low Mwt Xyloglucan

In the presence of low mwt tamarind xyloglucan, the characteristic thick cellulosic pellicle is synthesised on the medium surface (similar to control and high mwt xyloglucan incubations). The network architecture of pellicles synthesised in the presence of 0.5% and 2.0% low mwt xyloglucan is shown in Figures 6.4 and 6.5 respectively. Although close examination of the micrographs in Figure 6.4 does indicate the presence of a second polymer, no lateral organisation of cellulose fibres is seen with 0.5% low mwt xyloglucan, despite the high level of xyloglucan incorporation (6.3.3). At increased magnification (Figure 6.4b) some putative xyloglucan cross- linkages can be visualised. Clearly however, the dramatic alterations in network architecture into highly organised cross-linked structures seen with high mwt xyloglucan is not seen with xyloglucan of lower mwt. Raising the initial concentration of low mwt xyloglucan to 2% has no significant effect on the architecture (Figure 6.5).

6.3.2 Xyloglucan/Cellulose Interactions in an Abiotic System

When cellulose is extracted from the control incubations, freeze-dried, ground into a fine powder and rehydrated, electron microscopy reveales an aggregated structure in which few discrete fibres can be distinguished (Figure 6.6). When the powder is shaken in a solution of high mwt tamarind xyloglucan, association between the two polymers is evident (Figure 6.7a). Xyloglucan apparently acts in a similar way to that seen in the actively growing system (Figure 6.2), tethering adjacent fibres together and, as a result, imparting lateral organisation absent in the controls. Image analysis indicates cross-bridge lengths similar to those found for the high mwt xyloglucan-containing fermentation system. The impression from the micrographs is of xyloglucan cross-linking at the surface of particles and between exposed fibrils with a presumed inability to penetrate within particles.

Figure 6.3: Lengths of Xyloglucan Cross-Bridges in the Cellulose/Xyloglucan Composite

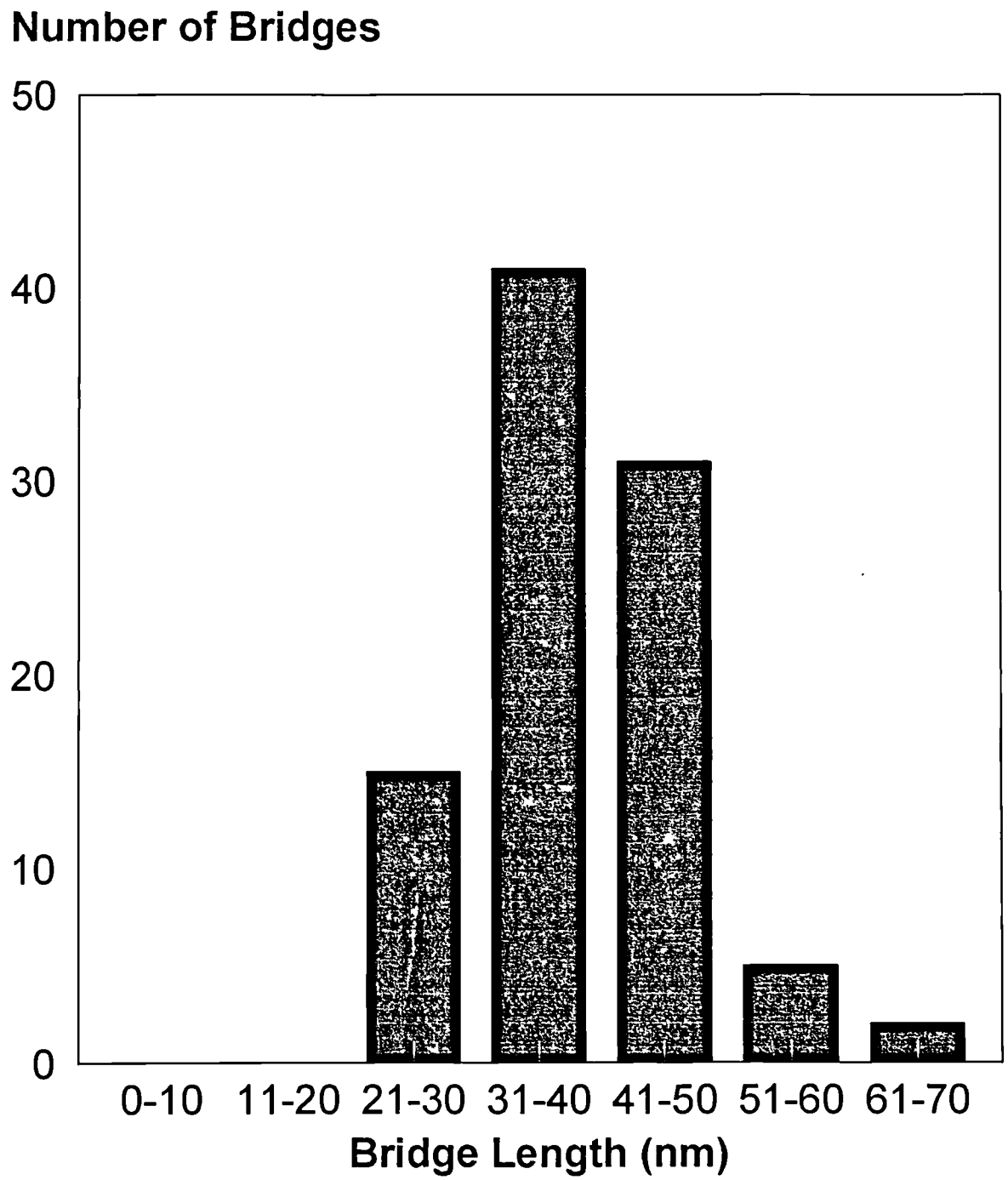

Lengths of cross-bridges involved in cellulose ribbon alignment measured from several preparations of cellulose/high mwt xyloglucan composites by analysis of images such as Figure 6.2

Figure 6.4: Micrographs of Cellulose Composites Formed in the Presence of 0.5% Low Mwt Tamarind Xyloglucan

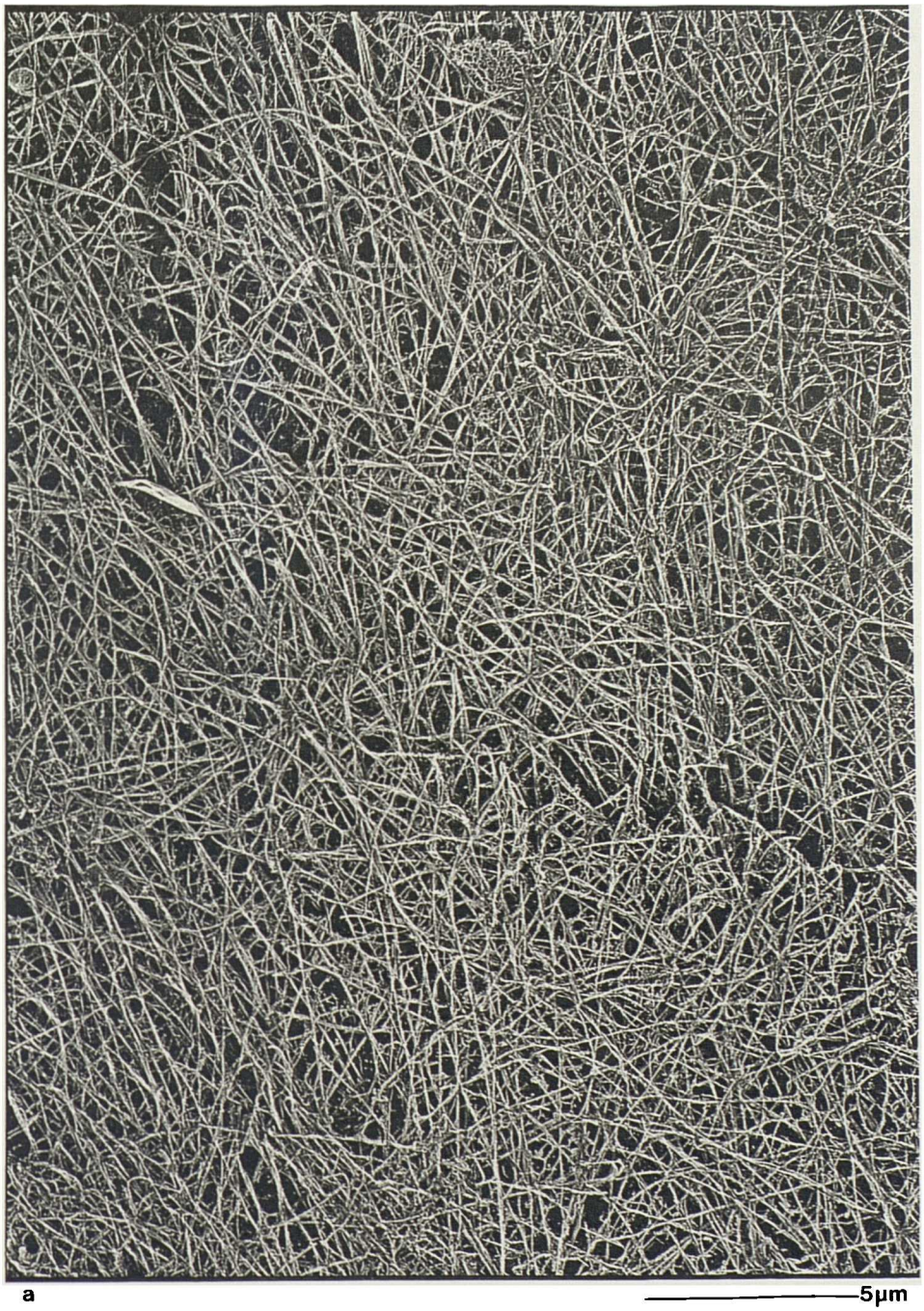

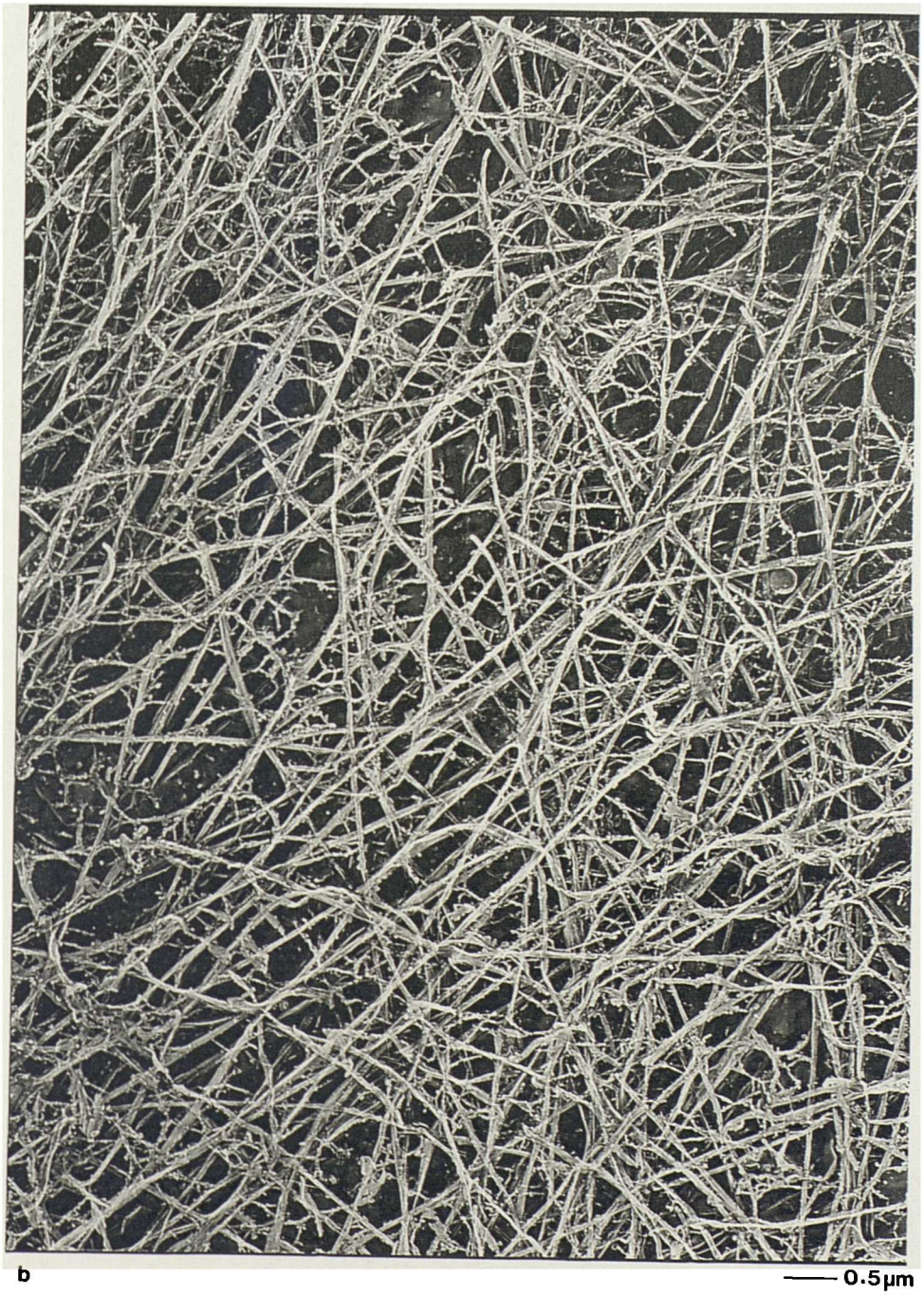

Micrographs of tungsten/tantalum/carbon replicas of composites produced by fermentation of *A.aceti* ssp. *xylinum* (ATCC 53524) in the presence of 0.5% low mwt tamarind xyloglucan illustrating no evidence for overall fibre alignment or conclusive evidence for cross-bridge formation (contrast Figure 6.2)

Figure 6.5 Micrographs of Cellulose Composites Formed in the Presence of 2% Low Mwt Tamarind Xyloglucan

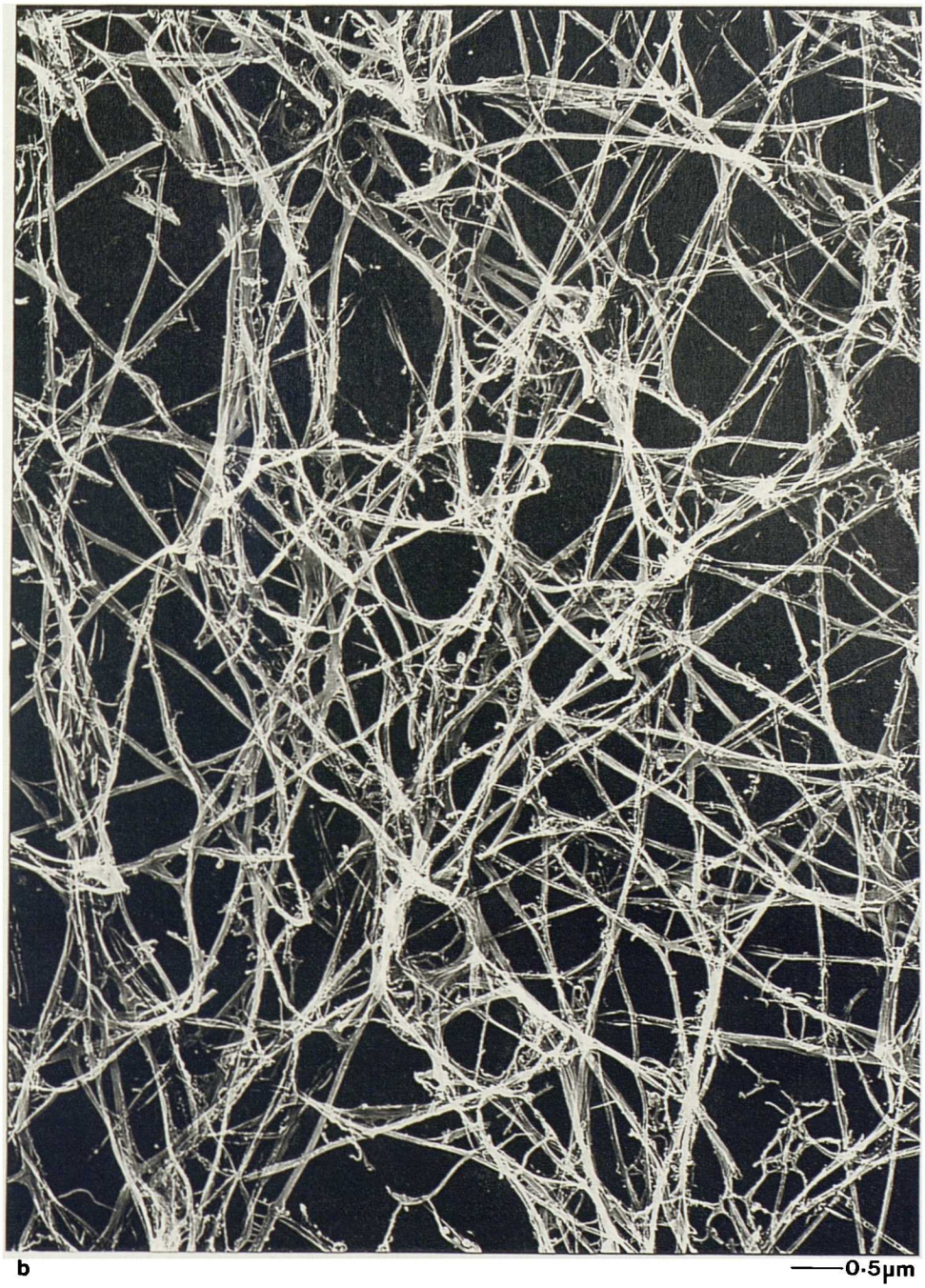

Micrographs of tungsten/tantalum/carbon replicas of composites produced by fermentation of *A.aceti* ssp. *xylinum* (ATCC 53524) in the presence of 2% low mwt tamarind xyloglucan illustrating interpolymer interaction but little evidence for cellulose fibre alignment or cross-bridge formation (cf Figure 6.4 and contrast Figure 6.2)

Figure 6.6: Micrograph of Finely Ground Bacterial Cellulose

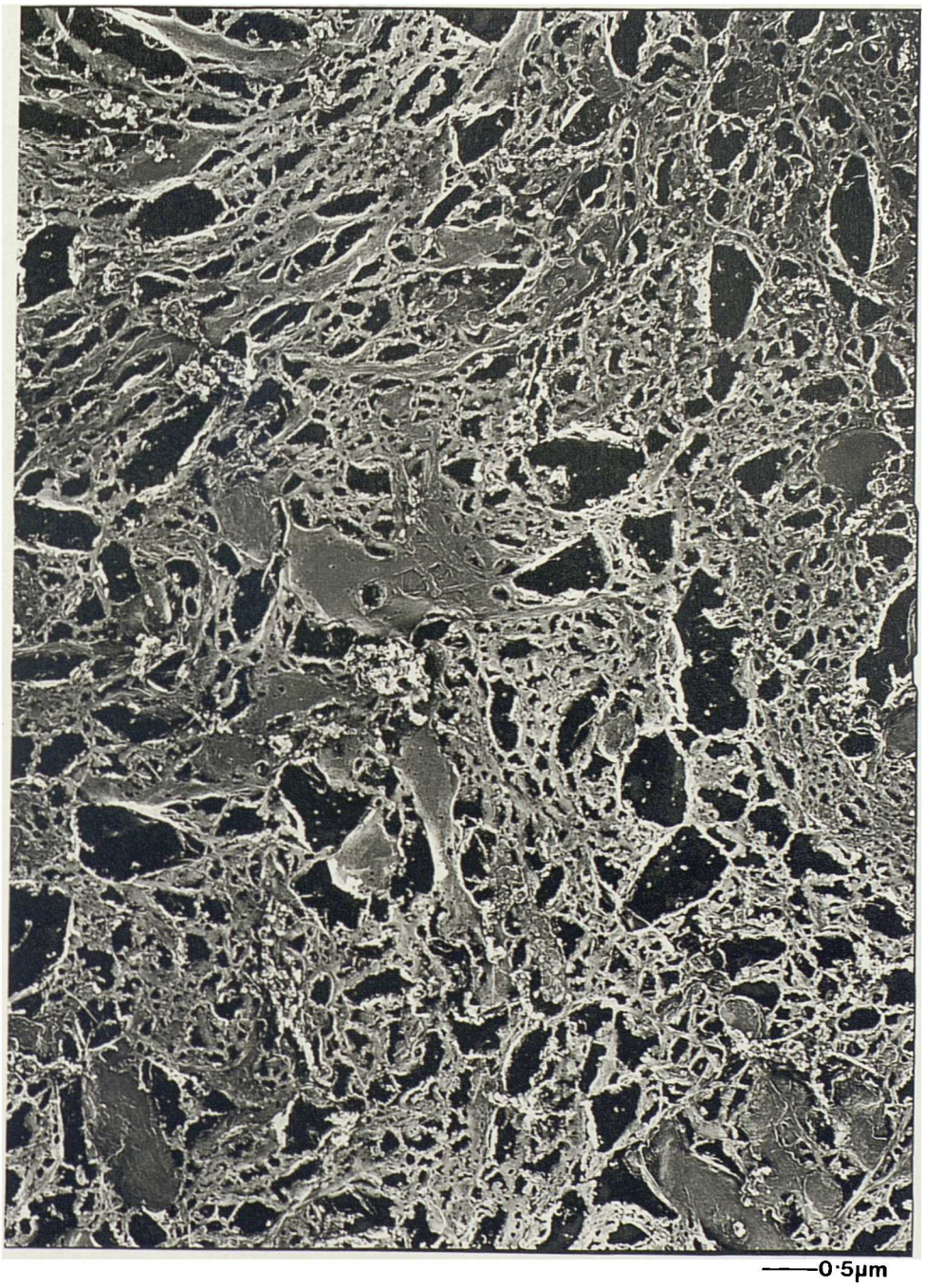

Micrograph of tungsten/tantalum/carbon replica of finely ground cellulose ex. *A.aceti* ssp. *xylinum* (ATCC 53524)

Figure 6.7: Micrographs of Composites of Cellulose and Xyloglucan Formed *in vitro*

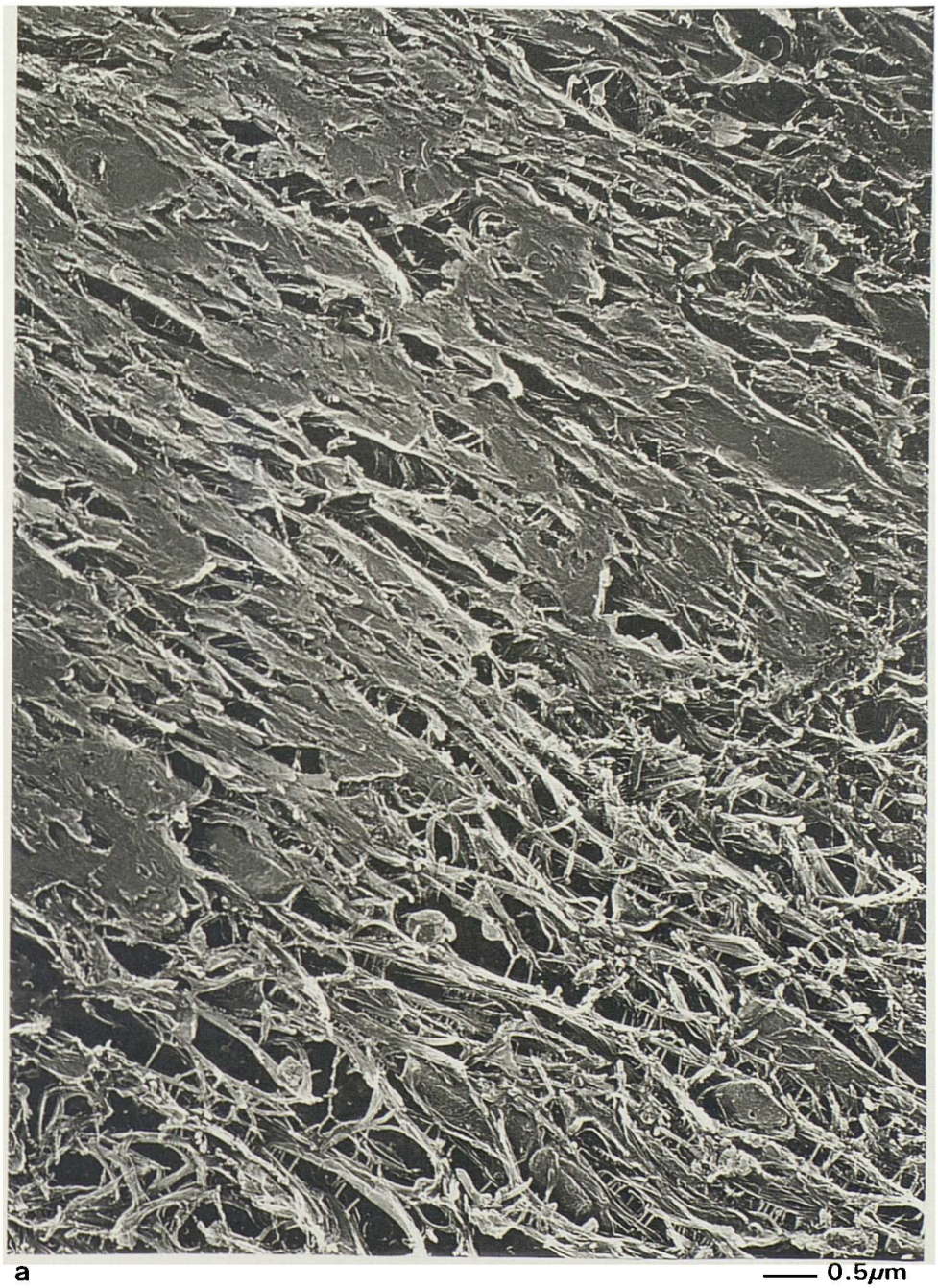

Micrographs of tungsten/tantalum/carbon replicas of finely ground cellulose ex. *A.aceti* ssp. *xylinum* (ATCC 53524) associated *in vitro* with (a) high mwt and (b) low mwt tamarind xyloglucan. Abundant cross-bridges and overall fibre alignment are apparent in (a) but not in (b) as inferred from results from the fermentation system (Figure 6.2, 6.4 and 6.5).

As observed in the fermentation system, the presence of lower mwt xyloglucan has much less effect on the organisation of cellulose fibres (Figure 6.7b). There is no evidence for fibre alignment or cross-bridge formation in this abiotic system. The longer cellulose fibres seen in this micrograph indicate that the cellulose component was less finely ground than the cellulose used with high mwt xyloglucan, but it is unlikely that this would have affected association significantly.

6.3.3 Levels of Xyloglucan Incorporation

The level of incorporation when celluose is synthesised in the presence of high mwt xyloglucan (Glc:Xyl:Gal = 2.8:2.25:1, Gidley *et al*, 1991a) is high, monosaccharide analysis giving a cellulose: xyloglucan ratio of 1:0.38 using xylose as an internal marker for xyloglucan. This data is in close agreement with the cellulose:xyloglucan ratio of 1:0.43 reported by Hackney *et al*, (1994) for a similar system and within the range of ratios found in plant cell walls (eg 1:0.7 in pea stem primary walls, Hayashi & Maclachlan, 1984 and 1:0.3 in onion bulbs, Redgwell & Selvendran, 1986). After 72hrs the ratio is slightly reduced (1:0.3 using xylose as an internal marker) suggesting either that all available xyloglucan is incorporated after 48 hours (see 6.3.1) or that the pellicle represents a barrier to diffusion after this time. Comparison of the measured cellulose:xyloglucan ratio with the observed level of cross bridges (Figure 6.2) suggests that only a small fraction of the xyloglucan is involved in bridges with the majority presumably aligned with cellulose.

For composites produced using low mwt tamarind xyloglucan (Glc:Xyl:Gal = 2.88:2.19:1) levels of incorporation are calculated as 1:0.2 ±0.02 and 1:0.24 ± 0.04 (using xylose as an internal marker) for cultures containing initial xyloglucan concentrations of 0.5% and 2% respectively.

For both high and low mwt xyloglucan, the level of association with cellulose is much reduced under abiotic conditions. Cellulose:xyloglucan ratios are calculated as 1:0.035 and 1:0.049 for high and low mwt xyloglucans at 0.5% initial concentrations respectively. This correlates closely with the results of

Hayashi *et al* (1987) who found between 1 and 5% (w/w) binding of pea xyloglucan on to different celluloses under the same conditions, interpreting this as indicative of surface binding only.

6.3.4 Molecular Weight Analysis of Tamarind Xyloglucans

The molecular weight profiles of high and low mwt xyloglucans are shown in Figure 6.8 and Table 6.1. The data shows significant polydispersity for both xyloglucans and considerable overlap of the two molecular weight distributions. This suggests that the different ultrastructural effects, ie cross-linking adjacent cellulose fibres with high but not low mwt xyloglucan are attributable primarily to the greater amount of high mwt material. The ability to form cross-linkages may therefore be partly a function of molecular weight. Some aggregation of low mwt tamarind xyloglucan was seen, as evidenced by the appearance of very high mwt material in this sample (higher than for high mwt xyloglucan). Figures in brackets in Table 6.1 give the mwt data of low mwt xyloglucan if the distorting effect of aggregated material is not corrected for.

Table 6.1: Molecular Weight Data of High and Low Mwt Xyloglucan Obtained using HPSEC-MALLS

	High Mwt Xyloglucan	Low Mwt Xyloglucan
Mn	294,000	150,000 (151,000)
Mw	413,000	234,000 (333,000)
Mz	541,000	740,000 (3,730,000)
Peak Mwt	450,000	153,000 (156,000)
Polydispersity (Mw/Mn)	1.405	1.558 (2.197)

Figure 6.8: Molecular Weight Profile of High and Low Mwt Xyloglucans

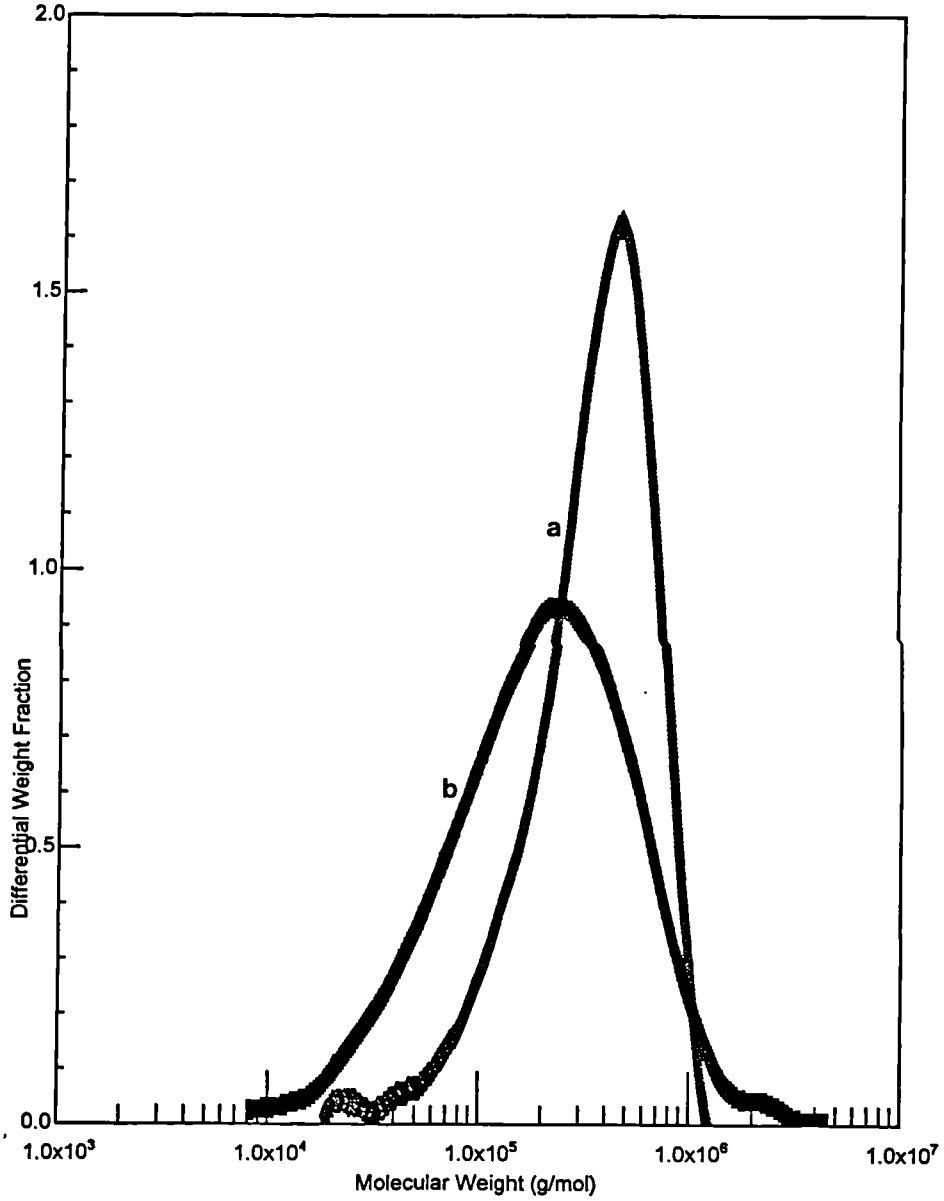

Molecular weight profiles of high (a) and low (b) molecular weight tamarind xyloglucans, showing considerable polydispersity in both materials and overlap between the two profiles. The very high mwt material present in (b) is attributed to aggregation in this solvent.

6.3.5 ^{13}C NMR Spectroscopy

6.3.5.1 High Mwt Xyloglucan

Bacterial cellulose grown in the presence of high mwt tamarind xyloglucan has the hydrate ^{13}C CP/MAS NMR spectrum shown in Figure 6.9b compared with that for native bacterial cellulose (Figure 6.9 a and see section 5.3.3). Signals at 99-100 ppm and ca. 80ppm are additional to those seen for cellulose alone, but are found in the spectrum of hydrated tamarind xyloglucan (Figure 6.9 c). The signal at 99-100 ppm is assigned to C-1 of xyloglucan xylosyl residues (Gidley *et al*, 1991a); corresponding signals for xyloglucan glucosyl and galactosyl residues are presumably coincident with the cellulose C-1 signal. From integration of the xylosyl C-1 signal in comparison with the composite cellulose and xyloglucan glucosyl.galactosyl signal (105ppm), and taking into account the sugar composition of the xyloglucan, the ratio of the cellulose to xyloglucan signals was found to be 1.00:0.33 ± 0.03. This suggests that the vast majority (80-90%) of the xyloglucan is detected in the CP/MAS spectrum, as chemical analysis gave a ratio of 1.00:0.38.

The presence of xyloglucan causes a marked decrease in the crystalline cellulose content from 80-85% (Figure 6.9 a) to 50-55% (Figure 6.9 b) as estimated from integration of signals at 88-91 and 84-86 ppm. This effect was not inferred by Hackney *et al* (1994) following boiling of the sample for 6h in 0.25M sodium hydroxide. Repetition of such alkali pretreatment in this study led to a similar spectrum (data not shown) to that obtained by Hackney *et al* (1994), but resulted in the extraction of xyloglucan to give a residual cellulose:xyloglucan ratio of 1.00:0.175.

The presence of xyloglucan in the composite also caused an increase in the relative abundance of the Iβ crystalline form of cellulose (see section 5.1), confirming results of Hackney *et al* (1994) and Yamamoto & Horii (1994). Resolution-enhanced spectra (Figure 6.9 d,e) show signals at 105.5, 90.2 and 89.3 ppm corresponding to the Iα form and at 106.2, 104.4, 89.3 and 88.5 ppm corresponding to

Figure 6.9: ^{13}C CP/MAS Spectra of Bacterial Cellulose/High Mwt Xyloglucan Composites

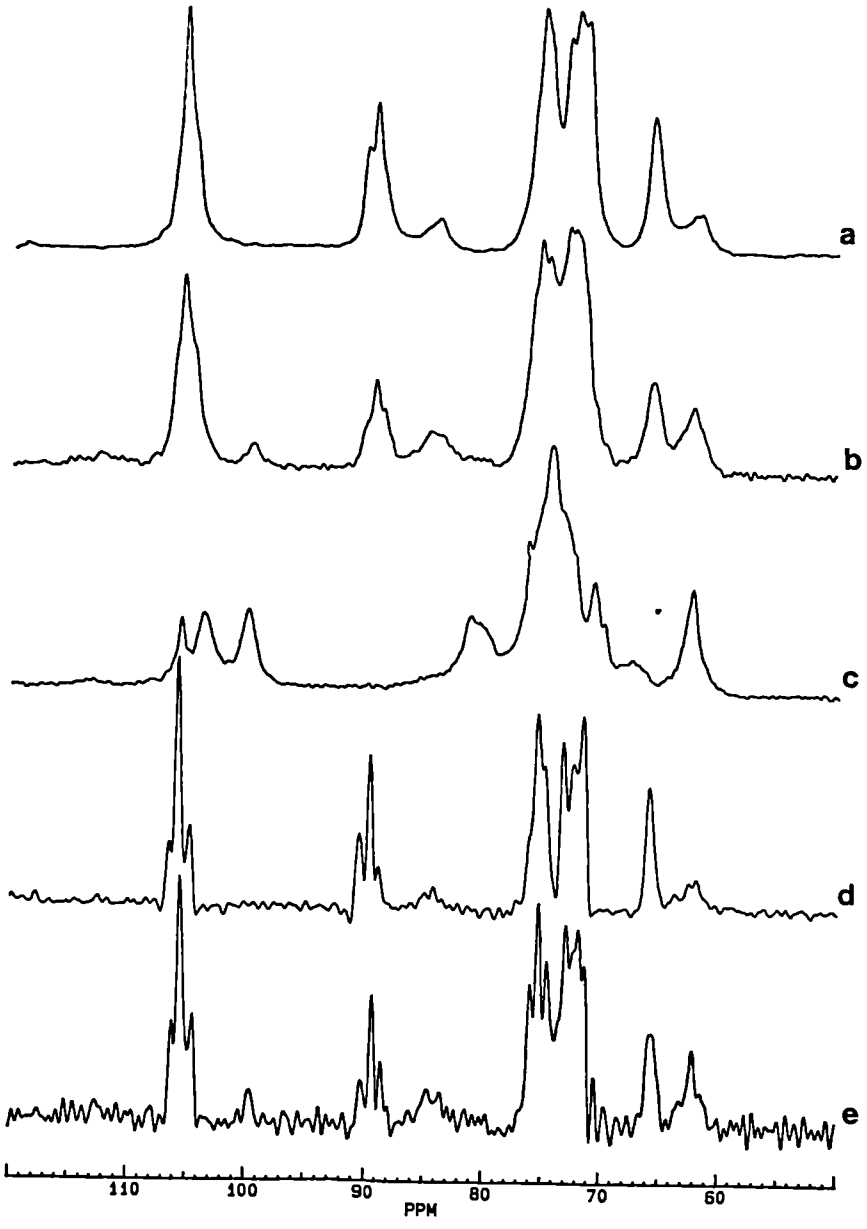

(a) Hydrated cellulose ex. *A.aceti* spp. *xylinum*; (b) hydrated cellulose/high mwt xyloglucan composite ex. *A.aceti* ssp. *xylinum* (cf Figure 6.2); (c) 30% w/w hydrate of tamarind xyloglucan, (d) resolution enhancement (line broadening -70 Hz, Gaussian multiplication 0.5) of spectrum (a) illustrating fine structure on C-1 (ca. 105 ppm) and C-4 (88-92 ppm) cellulose signals; (e) resolution enhancement as (d) of (b) illustrating altered fine structure on cellulose signals and the lack of a signal at 103.5 ppm as observed for hydrated xyloglucan (spectrum c)

the Iβ form (Debzi *et al*, 1991; VanderHart & Atalla, 1984; Yamamoto & Horii, 1993). Comparison of C-4 signals with published quantified signal patterns (Debzi *et al*, 1991; Yamamoto & Horii, 1993) gives a Iα/Iβ ratio of approximately 40/60 for xyloglucan-modified composites (Figure 6.9e) compared with ca. 70/30 for controls (Figure 6.9d and section 5.3.3).

Collating quantitative analyses for crystalline/non-crystalline and Iα/Iβ ratios gives an overall molecular description for cellulose as 21% Iα, 32% Iβ and 47% non-crystalline in the presence of xyloglucan compared with 57% Iα, 25% Iβ and 18% non-crystalline in controls (see section 5.3.3). Xyloglucan clearly has a profound effect on the molecular organisation of the cellulose component in the fermentation system; this effect was not seen under abiotic conditions where no effect on the molecular characteristics of cellulose in the composite was detected (data not shown).

Figure 6.9 also provides evidence for a change in chemical shift for xyloglucan glucosyl residues in the presence of cellulose. For hydrated xyloglucan (Figure 6.9c), C-1 chemical shifts for xyloglucan galactose, glucose and xylose residues are 105.5, 103.6 and 99.8 ppm respectively (Gidley *et al*, 1991a). In the presence of cellulose (Figure 6.9e), resolution enhancement identifies a peak at 99.5 ppm assigned to xylose, and the expected chemical shift of galactose is coincident with a cellulosic peak at 105.5 ppm. No signal is resolved at 103.6 ppm. Comparison with published spectra (eg Figure 6e in Debzi *et al*, 1991) would lead to an expectation of comparable C-1 peak heights at 106.2, 105.5 1nd 104.4 ppm. The height of the peak at 105.5 ppm in Figure 6.9e is taken as evidence that this is the chemical shift for the glucosyl as well as the galactosyl residues of xyloglucan in the presence of cellulose. We therefore infer a significant downfield chemical shift of ca. 2ppm for glucosyl C-1 with much smaller changes in chemical shift (<0.5 ppm) for xylosyl and galactosyl C-1 residues of 'rigid' xyloglucan in the presence of cellulose.

In contrast, more mobile segments of xyloglucan in the presence of cellulose show no significant chemical shift differences from the solution state. Single pulse excitation with dipolar decoupling,

magic angle spinning (SP/MAS) and a recycle time of 5 sec effectively discriminates against rigid segments, as evidenced from the lack of detectable signal from hydrated *A.aceti* spp. *xylinum* cellulose (data not shown). For cellulose grown in the presence of xyloglucan, the spectra shown in Figure 6.10a and b are observed. C-1 chemical shifts (105.2, 103.4 and 99.8 ppm) mirror those found by the same technique for hydrated tamarind xyloglucan (Figure 6.10c) at 105.5, 103.4 and 99.8 ppm respectively, and for dilute solutions (Gidley *et al*, 1991a). The relatively weak signals in Figure 6.10a and b reflect the expectation from analysis of CP/MAS spectra that 80-85% of the xyloglucan in the presence of cellulose would be too rigid to be detectable in the SP/MAS experiment. For comparison, Figure 6.10d shows the spectrum of a solution of cellotetraose. The major C-1 chemical shift at 103.3 ppm is essentially identical to that seen for related glucosyl residues in solutions and hydrates (Figures 6.9c and 6.10c) of xyloglucan and to that of the most mobile fraction of xyloglucan in the presence of cellulose.

As previously noted, micrographs (Figure 6.2) suggest that only a small percentage of the xyloglucan within the cellulose composite is present as cross-bridges. We assign CP/MAS-detected xyloglucan to cellulose-associated segments and SP/MAS-detected xyloglucan to cross-bridges.

6.3.5.2 Low Mwt Xyloglucan

The ^{13}C CP/MAS spectra of hydrated bacterial cellulose grown in the presence of 0.5% and 2.0% low mwt tamarind xyloglucan are shown in Figure 6.11a and c and after the application of resolution enhancement in b and d respectively. Spectra are almost identical to those obtained using high mwt xyloglucan (Figure 6.9b and e). Signals are identified at 99-100 ppm and ca. 80 ppm which are absent in the cellulose control (Figure 6.9a), but present in the CP/MAS spectrum of hydrated tamarind xyloglucan (Figure 6.9a) and the cellulose/high mwt xyloglucan composite (Figure 6.9b). As with the high mwt xyloglucan composite (section 6.3.5.1), the signal at ca. 99-100 ppm is assigned to C-1 of xylosyl residues (Gidley *et al*, 1991a), with signals for glucosyl and galactosyl residues presumably coincident with the cellulose C-1 signal.

Figure 6.10 ^{13}C SP/MAS Spectra of Bacterial Cellulose/High Mwt Xyloglucan Composites

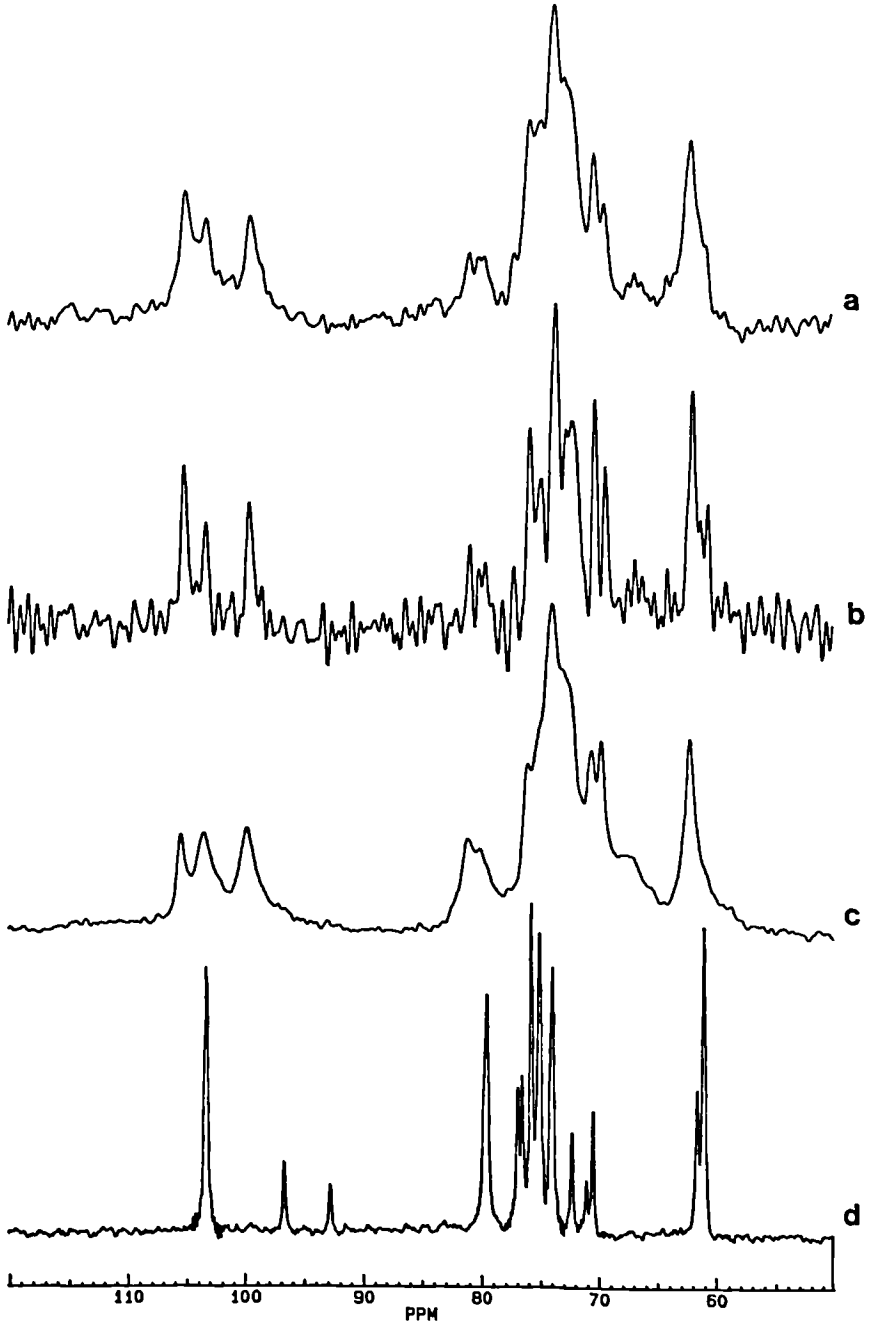

(a) Hydrated cellulose/xyloglucan composite ex. *A.aceti* spp. *xylinum* (cf Figures 6.2 and 6.9b) under magic angle spinning and dipolar decoupling conditions, (b) as (a), with resolution enhancement (line broadening -40Hz, Gaussian multiplication 0.5); (c) 30% w/w hydrate of tamarind xyloglucan under magic angle spinning and dipolar decoupling conditions illustrating essentially identical chemical shifts to (b) and Figure 6.9c; (d) 5% w/v solution of cellotetraose at 333K under scalar decoupling conditions illustrating a similarity in C-1 chemical shift (103-104 ppm) with peaks assigned to glucosyl residues in (a) - (c)

The molecular organisation of the cellulose component has been altered by the presence of low mwt xyloglucan; comparison of C-4 signals with published quantified signal patterns (Debzi *et al,* 1991; Yamamoto & Horii, 1993) to determine Iα/Iβ ratios and integration of signals at 88-91 and 84-86 ppm to calculate crystalline content gives an overall molecular description of 22% Iα, 32% Iβ and 44% non-crystalline and 20% Iα, 29% Iβ and 51% non-crystalline for cellulose grown in the presence of 0.5% and 2.0% low mwt xyloglucan respectively compared with 21% Iα, 32% Iβ and 47% non-crystalline for cellulose grown in the presence of high mwt xyloglucan. Despite differences in network architecture (Figures 6.3 and 6.4) and cellulose:xyloglucan ratios (section 6.3.2), the effect of low mwt xyloglucan on the molecular properties of the cellulose component is essentially identical to that seen with high mwt xyloglucan, and, apart from a slight increase in the non-crystalline component, this result is not affected by increasing the initial xyloglucan concentration.

As was seen with high mwt xyloglucan, there is an apparent conformational transition of the low mwt xyloglucan backbone in the CP/MAS spectrum. The C-1 glucosyl signal is not resolved at 103.6 ppm(Figure 6.11a) and, by comparison with Debzi *et al* (Figure 6e, 1991), the C-1 peak at 105.5 ppm is believed to be coincident with that for the xyloglucan glucosyl C-1 as well as the cellulose glucosyl C-1 and the xyloglucan galactosyl C-1 (see section 6.3.5.1 for explanation). For both high and low mwt xyloglucans therefore there is an apparent ca. 2 ppm downfield chemical shift of glucosyl C-1 on alignment with cellulose.

Figure 6.12 shows the ^{13}C SP/MAS spectra of cellulose/low mwt xyloglucan composites. The signal:noise ratio is low, a reflection of the low amount of xyloglucan which is not visible in the CP/MAS spectra and, by inference, not associated with the cellulose component. Again, these spectra are essentially identical with those obtained for high mwt xyloglucan composites, with a consistency of C-1 chemical shifts for xyloglucan in the composite and for xyloglucan as a hydrate (Figure 6.9c) and in dilute solutions (Gidley *et al*, 1991a).

Figure 6.11: ^{13}C CP/MAS Spectra of Bacterial Cellulose Composites formed in the Presence of 0.5% and 2.0% Low Mwt Tamarind Xyloglucan

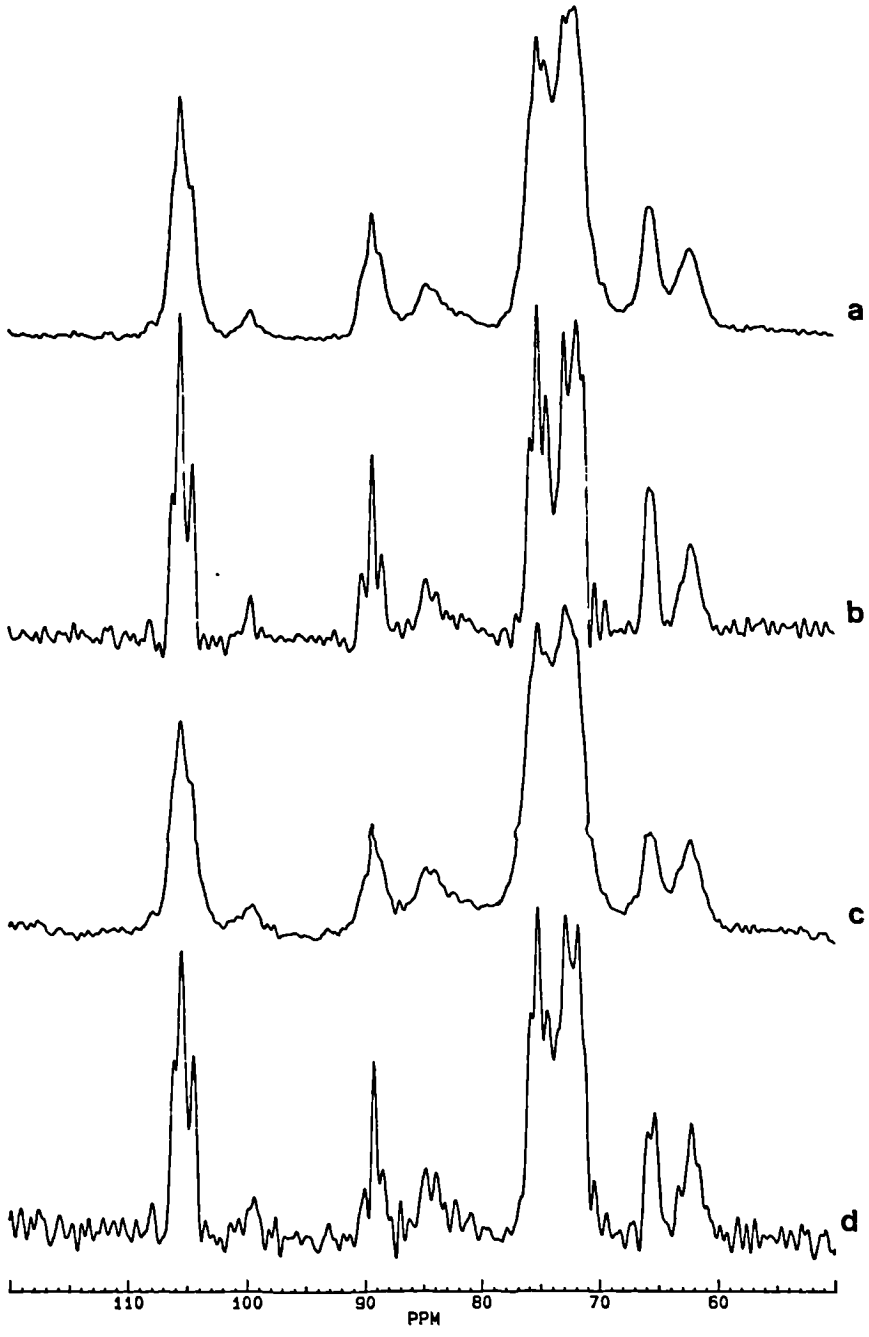

(a) Hydrated cellulose/xyloglucan composite from 0.5% low mwt xyloglucan starting concentration ex. *A.aceti* ssp. *xylinum* (cf Figure 6.3); (b) resolution enhancement (line broadening -70Hz, Gaussian multiplication, 0.5) of spectrum (a) illustrating altered fine structure on C-1) (ca. 105 ppm) and C-4 (88-92 ppm) compared with Figure 6.9a, similar to that seen with high mwt xyloglucan (Figure 6.9e); (c) as (a) but grown in the presence of 2.0% low mwt tamnarind xyloglucan; (d) resolution enhancement (as b) of (c) showing similar fine structure as (b) and Figure 6.9e

6.3.6 Sequential Deconstruction of Cellulose/High Mwt Xyloglucan Composites

6.3.6.1 Intact Pellicles

Application of standard alkali deconstruction protocols (Selvendran 1983) to intact cellulose/xyloglucan pellicles progressively reduced the xyloglucan content as determined by sugar analysis (Table 6.2). Galactose was used as an internal marker as there appeared to be some acid degradation of the xylose component. This should not affect comparison with earlier results as, if these are recalculated using galactose as the internal marker, the results are identical within the error range of the experiment. Interestingly, ca. 50% of the xyloglucan is removed by relatively mild (0.5M KOH) alkali treatment, but only 30-40% of this is believed to be involved in cross-linking cellulose (see section 6.3.5.1). This suggests that a significant proportion of the xyloglucan which is believed to be aligned with cellulose from NMR calculations is relatively loosely associated with the cellulose component.

Table 6.2: Effect of Increasing Alkali Concentrations on the Cellulose:Xyloglucan Ratio of the Composites

Alkali Treatment	Cellulose:Xyloglucan Ratio
2 x 0.5M KOH	1:0.175 ± 0.02
2 x 1.0M KOH	1:0.146 ± 0.03
1 x 4.0M KOH	1: 0.070 ± 0.00
2 x 4.0M KOH	1:0.022 ± 0.006

The requirement for 4M KOH, sufficient to cause microfibril swelling (Edelmann & Fry, 1992a), to dissociate the majority of the xyloglucan component from the composite is similar to that seen for the cellulose/xyloglucan network of cell walls (Chambat *et al,* 1984) and is consistent with intrafibril association. These results correlate with microscopy data on the composites (Figure 6.2) which suggest

Figure 6.12 ^{13}C SP/MAS Spectra of Bacterial Cellulose Composites Formed in the Presence of 0.5% and 2.0% Low Mwt Tamarind Xyloglucan

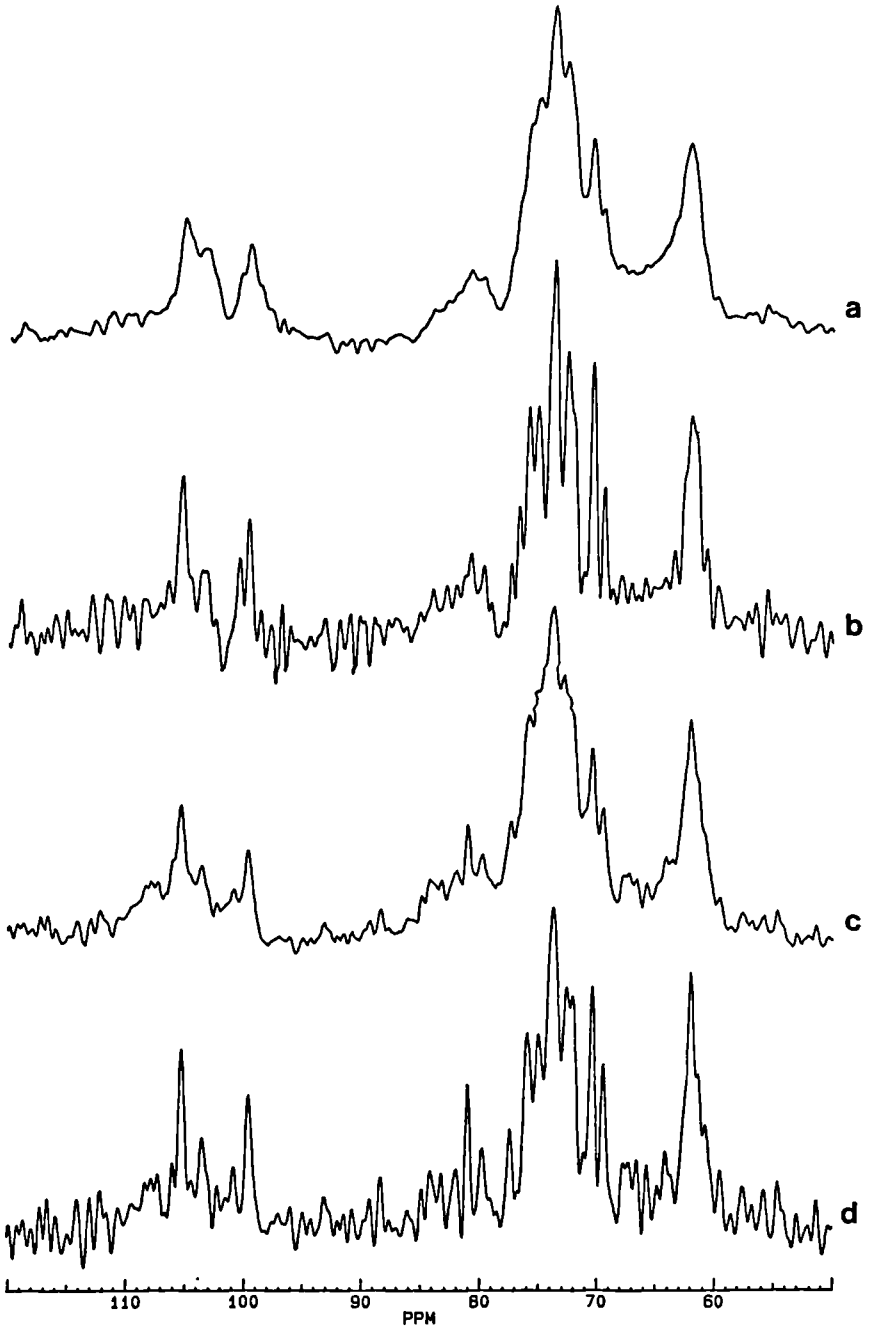

(a) Hydrated cellulose/xyloglucan composite formed in the presence of 0.5% low mwt xyloglucan ex. *A.aceti* ssp. *xylinum* (cf Figure 6.3) under magic angle spinning and dipolar decoupling conditions; (b) as (a), with resolution enhancement (line broadening -40 Hz, Gaussian multiplication 0.5); (c) as (a) but formed in the presence of 2.0% low mwt xyloglucan (cf Figure 6.4); (d) as (b) of (c). All illustrate essentially identical chemical shifts to Figure 6.10c and a similarity in C-1 chemical shift for xyloglucan glucosyl residues and cellotetraose (Figure 6.10d).

that the majority of the xyloglucan is located on the surface or within cellulose fibres and with ^{13}C NMR data (section 6.3.5) which indicates profound effects on the molecular organisation of the cellulose component, implying intimate association between the two polymers. Taken together therefore, the data indicates an intimate, intrafibre association between cellulose and xyloglucan, similar to that seen in the cell wall.

The oligomeric composition of the xyloglucan dissociated from the composite by alkali treatments was determined by *endo*-glucanase digestion into component oligomers followed by Dionex analysis. For all alkali treatments, no structural differences were detected compared to the controls (data not shown). There is apparently no structural feature of tamarind xyloglucan which determines whether it associates within, on the surface of, or between cellulose fibres.

Use of deep-etch freeze-fracture TEM to monitor removal of xyloglucan from the composite using alkali was unsuccessful (data not shown). There was no consistency of network architecture at the μm scale and hence no information was obtained on whether cross-linking xyloglucan was preferentially removed at lower alkali concentrations.

6.3.6.2 Ground Pellicles

Mechanical grinding of cellulose/xyloglucan pellicles removed a substantial proportion of the xyloglucan component, giving a cellulose:xyloglucan ratio of 1:0.18. This is essentially all the xyloglucan that is removed by 0.5M KOH treatment (Table 6.2), and is confirmed by the data presented in Table 6.3 which shows that 0.5M and 1.0M KOH remove only a small amount of xyloglucan from the ground complex. This effect does not correlate with the situation in the cell wall, where mechanical deconstruction of plant material leaves the cellulose/xyloglucan network of comminuted cell walls intact. This suggests a protective role for pectins in the cell wall; in their absence this data suggests that the cellulose/xyloglucan complex may be much more susceptible to

perturbation. As was seen with intact pellicles, very little xyloglucan is further extracted by 1.0M KOH treatment and fibre swelling by 4M KOH (Chambat *et al*, 1984; Edelmann & Fry, 1992a) is required for complete dissociation (Table 6.3).

Table 6.3: Extraction of Xyloglucan by Increasing Alkali Concentration from Mechanically Ground Composites

Alkali Treatment	Cellulose:Xyloglucan Ratio
2 x 0.5 M KOH	1:0.157 ± 0.01
2 x 1.0M KOH	1:0.140 ± 0.01
2 x 4.0M KOH	1:0.017 ± 0.005

6.3.6.3 Cellulose/Xyloglucan Composites Bound in vitro

Consistent with the proposal that the low levels of binding between cellulose and high and low mwt xyloglucan achieved *in vitro* are indicative of surface binding only (Hayashi *et al,* 1987), the reconstituted complexes were almost completely dissociated at lower alkali concentrations than composites formed in the fermentation system. The cellulose:xyloglucan ratio of high mwt xyloglucan complexes was slightly reduced from 1:0.035 to 1:0.031 ± 0.004 by 2 x 0.5M KOH treatment. For low mwt xyloglucan complexes, the ratio was reduced from 1:0.049 to 1:0.031 ± 0.0005. Stronger alkali treatments (2 x 1.0M KOH) further reduced the xyloglucan component of both complexes to very low levels (cellulose:xyloglucan ca. 1:0.01); significantly however some xyloglucan remained associated. This is inconsistent with previous reports that 1M KOH is sufficient to fully dissociate *in vitro* bound complexes (Hayashi *et al,* 1987), however this experiment was performed once only and needs to be repeated before conclusions can be drawn, particularly as the amount of xyloglucan remaining is at the limit of detection of this technique.

6.3.7 Enzymic Dissociation of Cellulose/High Mwt Xyloglucan Complexes

The cellulose:xyloglucan ratio of the intact pellicle starting material was somewhat lower than previously calculated (1:0.25), due possibly to the fact that this material had been stored in a solution of 0.05% NaN_3 at 1°C for several weeks, which may have allowed some leaching of the xyloglucan component. Incubation of intact cellulose/high mwt xyloglucan pellicles with *endo*-1,4-β-glucanase reduced the cellulose:xyloglucan ratio to 1:0.137 ± 0.02. In contrast, much less xyloglucan was removed by enzyme action on ground cellulose/xyloglucan pellicles, ratios being reduced from 1:0.18 to 1:0.16. This suggests that mechanical perturbation of the composite dissociates the majority of the xyloglucan available for enzymic hydrolysis in the intact pellicle, and that the material which requires 4M KOH for extraction and is therefore presumably located within cellulose fibres is not available for enzyme attack over the time period of this experiment. The result is somewhat at variance with that reported by Hayashi & Maclachlan (1984) and Baba *et al* (1994a) who showed almost complete dissociation of native cellulose/xyloglucan complexes by *endo*-glucanase, however, much longer time periods (3,6 and 7 days) were used by these authors. Analysis of the oligomeric composition of the xyloglucan released by enzyme action showed no structural difference from that of the bulk starting material (cf section 6.3.6.1 and 6.3.6.2).

6.4 Discussion

The *Acetobacter* system provides an elegant method for examining the association of xyloglucan with cellulose. Using high molecular weight xyloglucan composite structures are formed which have network architectures similar to those seen for native cellulose/xyloglucan complexes (McCann *et al*, 1990; McCann & Roberts, 1991). The presence of high mwt xyloglucan in the composite introduces lateral order and maintains spatial organisation of the cellulose fibres, consistent with the role proposed for xyloglucan in many models of the plant cell wall (eg Carpita & Gibeaut, 1993; McCann & Roberts, 1991; Talbott & Ray, 1992a), with the modifying polymer being visualised as forming cross-linkages between cellulose fibres of a similar size to those seen in the primary wall (McCann *et al*, 1990).

Interestingly, lower mwt tamarind xyloglucan does not have a similar effect on molecular architecture; lateral order is not evident, and very few cross-linkages between adjacent cellulose fibres are seen (Figures 6.3 and 6.4). This suggests that, because of the overlapping molecular weight profiles of low and high mwt xyloglucan (Figure 6.8) only the higher mwt polymers are in fact involved in cross-linking and aligning cellulose fibres. In the primary cell wall however, extracted xyloglucan molecules are typically of a much lower molecular weight than either of the xyloglucans used in this study (eg Sakurai & Nevins, 1993; Talbott & Ray, 1992a; Chapter 9, this thesis). In this system, we predict that the physical properties of high mwt tamarind xyloglucan are sufficient to allow cross-bridge formation (see later). *In muro* however, other physical (see below) or biological factors such as the enzyme XET (Fry *et al*, 1992; Nishitani & Tominaga, 1991; Smith & Fry, 1991), may be involved in modifying the cellulose/xyloglucan network architecture (see also section 1.5.2 for further discussion).

When *Acetobacter* cellulose is synthesised in the presence of the charged cellulose derivative CMC, normal fasciation of micriofibrils into ribbons (Figure 6.1) is prevented (Haigler *et al,* 1982). This leads to a reduction in ribbon dimensions, apparent at the gross morphological level as a reduction in cohesiveness and order (Chapter 8, this thesis). Xyloglucan from both tamarind (Uhlin *et al,* 1995; Yamamoto & Horii, 1994) and pea (Hayashi *et al*, 1987) has been previously reported to have a similar effect. This study provides no evidence for reduction in fibre width in the presence of low or high mwt xyloglucan for the Acetobacter strain 53524. The level of incorporation of both polymers is similar to that found in primary cell walls, but is higher than would be expected from examination of the micrographs, suggesting that most of the xyloglucan is not visible as cross-linkages. We infer from the micrographs that much of the xyloglucan is intimately associated with the cellulose, either at the surface or woven into the fibres. This is supported by the data from ^{13}C NMR which implies an intimate association between the two polymers and the requirement for concentrated alkali, sufficient to cause microfibril swelling (Edelmann & Fry, 1992a), for full dissociation of the complex, is also consistent with intrafibril interactions. This suggests that, in the cell wall, the presence of xyloglucan may not be critical for determining cellulose microfibril dimensions. Attempts have been made to synthesise cellulose *in situ* on EM grids as described by Haigler *et al* (1982), allowing measurement of

ribbon width immediately after synthesis in the presence and absence of xyloglucan, as this was the method used by the above authors. However this strain of bacteria proved impossible to grow under these conditions (see section 5.3.5). Hence, this question remains unresolved, and further work needs to be done in this area.

In the abiotic system, levels of incorporation of high and low mwt xyloglucans are very much lower. This is consistent with surface binding only, as predicted by Hayashi *et al*, (1987). NMR indicates no effect on the molecular organisation of the cellulose component when the two polymers are combined *in vitro*, and the vast majority of the xyloglucan is removed at 1M KOH, implying a superficial interaction. Slightly higher binding was achieved with the lower mwt xyloglucan. Adsorption of very low mwt xyloglucan (4 oligosaccharide units) to microcrystalline cellulose is high compared to polymeric xyloglucan, probably because of the ability of these small fragments to penetrate the smaller pores of cellulose (Vincken *et al*, 1995). Lower mwt xyloglucan would be predicted to have improved access to binding sites over xyloglucan of a higher mwt. Conversley, levels of association in the fermentation system were slightly lower than with the high mwt xyloglucan, however this may be due in part to differences in rates of cellulose production for different cultures rather than a molecular wight effect *per se*, an issue which needs to be addressed more fully (see Chapter 11). More work on different molecular weight xyloglucans is required to elucidate the relationship between binding capacity and molecular size.

The deposition of cellulose into a fermentation medium containing xyloglucan is, compared with the cell wall, a highly dilute system. This implies a powerful energetic driving force for cellulose/xyloglucan association. Furthermore, the formation of cross-linkages by high (but not low) mwt xyloglucan in both the fermentation *and* the abiotic system means that not only association, but also cross-bridge formation, must occur purely as the result of physico-chemical forces. Note however the possible involvement of other forces *in muro* (see above). The driving force for alignment of xyloglucan with cellulose must be enthalpic. Equally however, there must also be a driving force for

dissociation, such that a xyloglucan molecule effectively 'lifts-off' a cellulose fibre and become available to cross-link another. Dissociation may be mediated in one of two ways. Firstly, specific sequences within the xyloglucan molecule itself may confer the ability to bind or not to bind to cellulose. This has been addressed by Finkenstadt *et al* (1995) using molecular modelling. Depending on the conformation of the xylose-glucose (1→6) linkage, modelling suggests that galactose (and fucose) residues on side chains modulate binding, potentially facilitating the formation of cross-linkages. Alternatively, dissociation may be due solely to entropic factors. These need not require any chemical difference between mobile (high entropy) and bound (low entropy) segments, as exemplified in gels of the linear polysaccharide amylose, which contain a balance of rigid and mobile regions (Gidley, 1989). The apparent regularity of cross-bridges, the lack of evidence for periodic structural irregularity in primary structure of tamarind xyloglucan on the 30-50 nm distance scale, and uniformity of the oligomeric composition of xyloglucan that is either loosely or tightly associated with the cellulose component favours, we believe, an arguement for purely entropic effects.

Entropic factors may also be used to explain why lower mwt xyloglucan did not form cross-linkages between adjacent cellulose fibres in this system. Gidley & Bulpin (1989) report that shorter chain lengths (< DP 110) of the linear polysaccharide amylose form precipitates, whilst cross-linking gel networks are formed with longer molecules. In the highly dilute fermentation system, the enthalpic driving force for alignment of cellulose and xyloglucan will be strong, however the force dictating dissociation ie derivation of the lowest free energy for the system by introducing entropy in the form of cross-linkages, will be reduced for smaller molecules. In the much more concentrated cell wall environment, where the mechanism by which cellulose and xyloglucan are co-localised allowing their association remains unclear, it is feasible that regions of these shorter xyloglucan molecules associate with cellulose microfibrils, but binding of a portion of the molecule does not automatically lead to binding of the full length. Hence, isolated regions of the molecule could be bound to the cellulose whereas other regions are not, introducing the typical cross-linked structure. The length of these cross-links would be expected still to be a function of persistence length, which for cell wall-derived

xyloglucans would be similar to that reported for tamarind xyloglucan (Gidley *et al*, 1991a), since C∞ is primarily a function of side chain substitution (see below).

Xyloglucan bridge lengths observed with high mwt xyloglucan are similar to those reported for the primary cell wall (McCann *et al*, 1990). The length of xyloglucan molecules suggests that a single molecule may participate in the formation of more than one cross-link (McCann and Roberts, 1991; McCann *et al*, 1990; 1992b). The distance between each xyloglucan bridge is approximately the same size as the cross-bridge length and therefore, between each cross-link, an equivalent length of the polymer is assumed to be aligned with the the fibre (not visible on micrographs). Measurement of C∞ (characteristic ratio) of tamarind xyloglucan by static light scattering gives a value of 110 (Gidley *et al*, 1991a). This is extremely high (an order of magnitude greater than for CMC, Robinson *et al*, 1982) and is probably a reflection of the high level of bulky glycosyl substitution of this molecule. In solution this means that the molecule has a hydrodynamic behaviour equivalent to that of approximately 60nm rigid segments (the persistence length) connected by universal joints (Burton & Brant, 1983) and it may be inferred that chain lengths of the order of the persistence length are required for significant segmental mobility. In reality, segmental mobility will be more evenly distributed than the above description suggests, however it can be inferred that, at the 10-20nm distance scale, tamarind xyloglucan is highly persistent. There would therefore be little entropic advantage conferred by bridge lengths less than 20nm. Equally, the strong enthalpic driving force for association would presumably limit the length of cross-bridges to that required for effective entropy gain, ie not much longer than the persistence length and probably less than 100nm.

The similarity of the hydrodynamic chain persistence with the bridge lengths in cellulose/xyloglucan networks is suggestive of a cause and effect relationship. Certainly, the stiffness of the molecule menas that, in the presence of cellulose, it is entropically more favourable for tamarind xyloglucan to associate compared with a less rigid molecule such as CMC. This may partially explain the difference in the behaviour of these two molecules when combined with cellulose (see also Chapter 8).

The model for cellulose/xyloglucan binding proposed by Levy *et al* (1991) implies a role for a fucosylated trisaccharide side chain in locally flattening out a region of the xyloglucan backbone into a cellulose-like conformation. This allows hydrogen bonding between the xyloglucan backbone and the cellulose, and is hypothesised to act as a point of cross-linking. The results presented here, using non-fucosylated xyloglucan, indicate that fucose is not a fundamental requirement either for association with cellulose or for the formation of cross-linkages. Recent evidence (Levy, 1995) does predict a higher rate of binding for fucosylated xyloglucan *in vitro*, although final binding levels are unaffected by the presence of the fucose residue. It will be interesting to investigate whether this also occurs in the fermentation system, which is a more accurate mimic of the cell wall.

NMR data (Figures 6.9-6.12) show that cellulose/xyloglucan networks produced by fermentation contain rigid segments composed of cellulose and 80-85% of the high mwt xyloglucan with chemical shifts (particularly glucosyl C-1) which differ from those found for the more segmentally flexible portion of xyloglucan. The relatively broad lines exhibited by segmentally mobile xyloglucan, the copious washing of composites prior to analysis and the lack of observable single-chain molecules by microscopy, all argue against the trapping of non-associated molecules and argue for assignment of the flexible segments to cross-bridges in the high mwt xyloglucan complex. A similar argument persists for complexes formed using low mwt xyloglucan, however in this case the very low xyloglucan levels visible in the SP/MAS spectrum are attributed to loose xyloglucan polymer chain ends (the bulk of the polymer being associated on the surface or within cellulose fibres).

Consistency of chemical shifts from cellotetraose solution through xyloglucan solutions and ceoncentrated (30% w/w) hydrates to CP/MAS visible xyloglucan within composites suggests a common conformational state. In accordance with reported minima in energy calculations of cello-biose (Kroon-Batenburg *et al*, 1993; Levy *et al*, 1991), we assign this to the 'twisted conformation' described by Levy *et al*, 1991).

The inferred chemical shift for glucosyl C-1 of xyloglucan associated with cellulose is essentially identical to that of cellulose, suggessting a common conformation. This interpretation of chemical shift effects implies that glycosidic conformation is the determining feature rather than xyloglucan substituents or hydrogen bonding patterns. This coincidence of cellotetraose and xyloglucan glucosyl C-1 shifts and the lack of a separate resonance for the 25% of the glucose residues which are not xylose substituted (even when resolution is increased by depolymerisation (Gidley *et al*, 1991a)) suggests that xyloglucan glucosyl C-1 shifts are not influenced directly by branch substituents. The very similar chemical shifts for C-1 of celluloses with both non-crystalline and a range of crystalline forms suggests that this resonance is insensitive to the hydrogen bonding pattern differences which define these various states of cellulose. NMR data on cellulose/xyloglucan composites therefore provide evidence for a transition from 'twisted' to 'flat' conformations of xyloglucan upon binding to cellulose. Molecular dynamics simulations show that this transition is feasible (Kroon-Batenburg *et al*, 1993; Levy *et al*, 1991) and preliminary *ab initio* nuclear shielding calculations for the glycosidic linkage in β-(1→4) glucans, using the approach described by Durran *et al* (1995) for α-(1→4) glucans, predict a relative chemical shift effect of the appropriate magnitude and direction (Durran, Howlin, Webb and Gidley, unpublished results).

The presence of xyloglucan has a major effect on the molecular state of cellulose produced by fermentation. In the absence of xyloglucan, NMR analysis suggests approximately 57%Iα, 25% Iβ and 18% non-crystalline. Xyloglucans reduce both crystallinity and the proportion of the Iα component, calaculations giving 21% Iα, 32% Iβ, and 47% non-crystalline, 22% Iα, 32% Iβ and 44% non-crystalline and 20% Iα, 29% Iβ and 51% non-crystalline for composites formed using high mwt, 0.5% low mwt and 2.0% low mwt xyloglucan respectively. The major overall change is therefore a shift from the Iα to the non-crystalline form and the 35-37% of cellulose which is lost from the Iα form therefore represents the minimum amount of cellulose which ends up in a different state of organisation as the result of the presence of xyloglucan. For composites formed using high mwt xyloglucan, the total xyloglucan contained was measured to be 38% of the cellulose level, with the amount associated with cellulose in a 'cellulosic' conformation of 33%. In this case, xyloglucan causes

at least an equal weight of cellulose to be affected by its presence even though much of it is relatively loosely associated (ca. 50% is removed by 0.5M KOH or *endo*-glucanase treatments). For lower mwt xyloglucan, the presence of xyloglucan perturbs the organisation of significantly more than its equivalent weight of cellulose suggesting that a greater proportion of smaller sized molecules may be more effective at causing defiects within the crystal lattice structure.

The level of incorporation of xyloglucan in an actively producing cellulose fermentation system is of the same order as that found by analysis of primary cell walls (Redgwell & Selvendran, 1986; Talbott & Ray, 1992). Furthermore, it is only in the presence of xyloglucan that cellulose molecular order resembles that found in primary cell walls. Analysis of apple cell walls by Newman *et al* (1994) suggested 62% non-crystalline and approximately equal (ca. 20% each) contents of Iα and Iβ. For onion bulb and tomato pericarp cell walls, NMR analysis again suggested similar Iα and Iβ contents with non-crystalline levels close to 60% (onion) and 80% (tomato) (Foster *et al*, 1996). The main difference between cellulose/xyloglucan composites and primary cell wall cellulose is the higher non-crystalline component of the latter. It is possible that cell wall components other than xyloglucan act to reduce crystallinity further and this will be looked at in future studies.

The tightness of the association between cellulose and xyloglucan in this system, as evidenced by the effect on molecular order and the requirement for strong alkali for full dissociation, together with the level of incorporation and the formation of cross-linkges imparting lateral order to the structure suggests that *Acetobacter aceti* ssp. *xylinum* is a very useful model for the self-assembly of cell walls. It complements approaches based on assembly of cellulose/xylan composites (Vian *et al*, 1994) more representative of secondary cell walls. Use of other xyloglucans will shed more light on the molecular basis of cross-bridge formation. Recent studies have indicated that xyloglucan-modified composites exhibit very different mechanical behaviour from controls, the presence of xyloglucan apparently creating a more pliable structure (see Chapter 10). This is again consistent with a role for xyloglucan in a wall which needs to undergo rapid turgor-driven expansion and reinforces the conclusion that

structures formed using, in particular, high mwt xyloglucan, are representative of native cellulose/xyloglucan networks.

Chapter 7: Cellulose/Glucomannan Composites

Ultrastuctural and Molecular Features

7.1 Introduction

The formation of composite structures of cellulose and tamarind xyloglucan using cultures of *Acetobacter aceti* ssp. *xylinum* undergoing active cellulose synthesis was described in Chapter 6. Ultrastructural and molecular evidence was presented for similarities between these networks and the cellulose/xyloglucan networks proposed for primary plant cell walls (McCann *et al*, 1990; McCann & Roberts, 1991). Work in this chapter will describe the use of an alternative modifying polysaccharide, glucomannan, which is a major hemicellulose component of other cell wall types. Differences in network properties obtained will be discussed with respect to the possibility of specific functionality of hemicelluloses in their interaction with cellulose, which may reflect differing cell wall structural requirements.

Glucomannan is the major hemicellulose component of the secondary cell wall of gymnosperms (Brett & Waldron, 1991) and has been localised in the cell walls of a number of species by immunogold labelling (Baba *et al*, 1994b). It has also been identified in other plant tissues, in particular storage organs such as tubers and bulbs and also in the seeds of some species (Meier & Reid, 1982). Glucomannan belongs to the mannan family of polysacharides, with a linear structure of β-1,4-linked mannose interspersed with β-1,4-linked glucose. There is wide interspecific variation in mannose:glucose ratio, ranging from 2-6:1 in gymnosperms to approximately 2:1 in dicotyledons (Ishizu, 1983). In contrast with xyloglucan, very little information on the structural role of glucomannan in cell walls is available.

Commercially, konjac glucomannan is used in the food industry as a gelling agent (Dea & Morrison, 1975). Konjac glucomannan is acetylated (Chanzy *et al*, 1982), having typically 1 acetyl group/16 monosaccharide residues (Gidley *et al*, 1991b). Deacetylation using aqueous alkali followed by freeze-thaw treatment facilitates gelation (Gidley *et al*, 1991b). The crystalline (Frei & Preston, 1968; Chanzy *et al*, 1982) and molecular (Gidley *et al*, 1991) aspects of glucomannan conformation have been well characterised, making this a useful polysaccharide for incorporation into the *Acetobacter* cellulose-synthesising system. Hackney *et al* (1994) incorporated glucomannan into the *Acetobacter* system, reporting alteration of the cellulose component of cellulose/glucomannan composites.

7.2 Materials and Methods

7.2.1 Preparation of Konjac Glucomannan

Konjac glucomannan was prepared from Konjaku flour by overhead stirring in deionised water (12g/l) containing 0.05% NaN_3 for 2 hours at 80°C. After centrifugation at 40000g the supernatant was decanted, dialysed extensively against deionised water at 1°C and freeze-dried. The Man:Glc ratio was determined using alditol acetates method 3 (Section 2.9)

7.2.2 Preparation of Cellulose/Glucomannan Composites

Composite structures were prepared using the method described in Chapter 6 (6.2.1), substituting glucomannan for xyloglucan. All incubation and purification protocols are identical to those used in Chapter 6.

7.2.3 Monosaccharide Analysis

Composites were freeze-dried and the monsaccharide composition determined using the alditol acetates method 2 (Section 2.8). Analyses were performed in triplicate using the products of 4 different fermentations.

7.2.4 Deep-Etch Freeze-Fracture TEM

The ultrastructure of fully hydrated cellulose/glucomannan composites was examined according the the method described in Chapter 2 (Section 2.12.5).

7.2.5 ^{13}C NMR Spectroscopy

^{13}C NMR spectroscopy was performed on hydrated samples (ca.4.4% dry weight) as described in Chapter 2 (Section 2.13).

7.3 Results

After incubation for 2 days at 50rpm and 30°C, a thick pellicle was formed on the surface of the culture medium, similar to that seen in control and xyloglucan-containing incubations (Chapter 6). Using the Man:Glc ratio of 62:38 determined, which was identical to that reported by Gidley *et al* (1991b) for konjac glucomannan, the cellulose/glucomannan ratio for composites was calculated as 1:0.43 ±0.06. This figure is higher than that for xyloglucan-modified composites (Chapter 6) and is greater than reported by Hackney *et al* (1994). These authors give a cellulose:xyloglucan ratio of 1:0.32, however they used salep glucomannan, with a slightly different Man:Gal ratio of of 1.63:1, which may affect incorporation.

7.3.1 Ultrastructure

The network architecture of cellulose/glucomannan composites was examined by the deep-etch freeze-fracture TEM technique. Micrographs reveal a heterogeneous structure (Figure 7.1). There are many regions of highly compact structures (Figure 7.1a) in which the cellulose and glucomannan components cannot be distinguished. These are interspersed with some areas of less dense material where individual cellulose fibres are clearly visible (Figure 7.1b). Occasionally, cross-linkages between cellulose fibres, similar to those seen in xyloglucan-modified networks, are evident (Figure 7.1b). This suggests that glucomannan may have the ability to function as a cross-linking polymer, but examination of many micrographs shows that this is clearly not the predominant effect.

7.3.2 Molecular Organisation

The ^{13}C CP/MAS spectrum of hydrated cellulose/gluomannan composites is shown in Figure 7.2a. Clear differences between this spectrum and that for unmodified bacterial cellulose (Figure 7.2b) are seen, with several additional signals appearing as shoulders on the C-1 peak, and a dramatic alteration of the crystalline/non-crystalline ratio of the cellulose component from both C-4 and C-6 peaks. There is also evidence for a broadening of the signal at non-crystalline cellulose C-4 sites. Hydrated glucomannan shows no discrete signals for C-4 sites at > ca. 80ppm (Gidley *et al*, 1991b) and it is possible that the observed broadening is due to overlap with signals from a different conformational structure of glucomannan (see below). An alternative possibility is suggested from the data of Hackney *et al* (1994) who measured ^{13}C longitudinal relaxation times of glucomannan-modified and native bacterial cellulose and inferred an overall reduction in lateral crystallite dimensions in the presence of glucomannan. An increase in crystal surfaces should increase the relative proportion of signal at ca. 84ppm (Earl & VanderHart 1981; Newman *et al*, 1994) as is seen in Figure 7.2b. Broader peaks at C-4 are attributed to an increase in disorder or poorly-ordered surfaces in cellulose I (Newman & Hemmingson, 1995) and increasing disorder is observed to move the C-4 signal closer to the 80ppm chemical shift observed for cellulose in solution (Horii *et al*, 1984) (Figure 7.4b). The observed broadening (Figure 7.2b) of the C-4 signal may therefore reflect increasing disorder in the cellulose

Figure 7.1 Micrographs of Cellulose/Glucomannan Composites

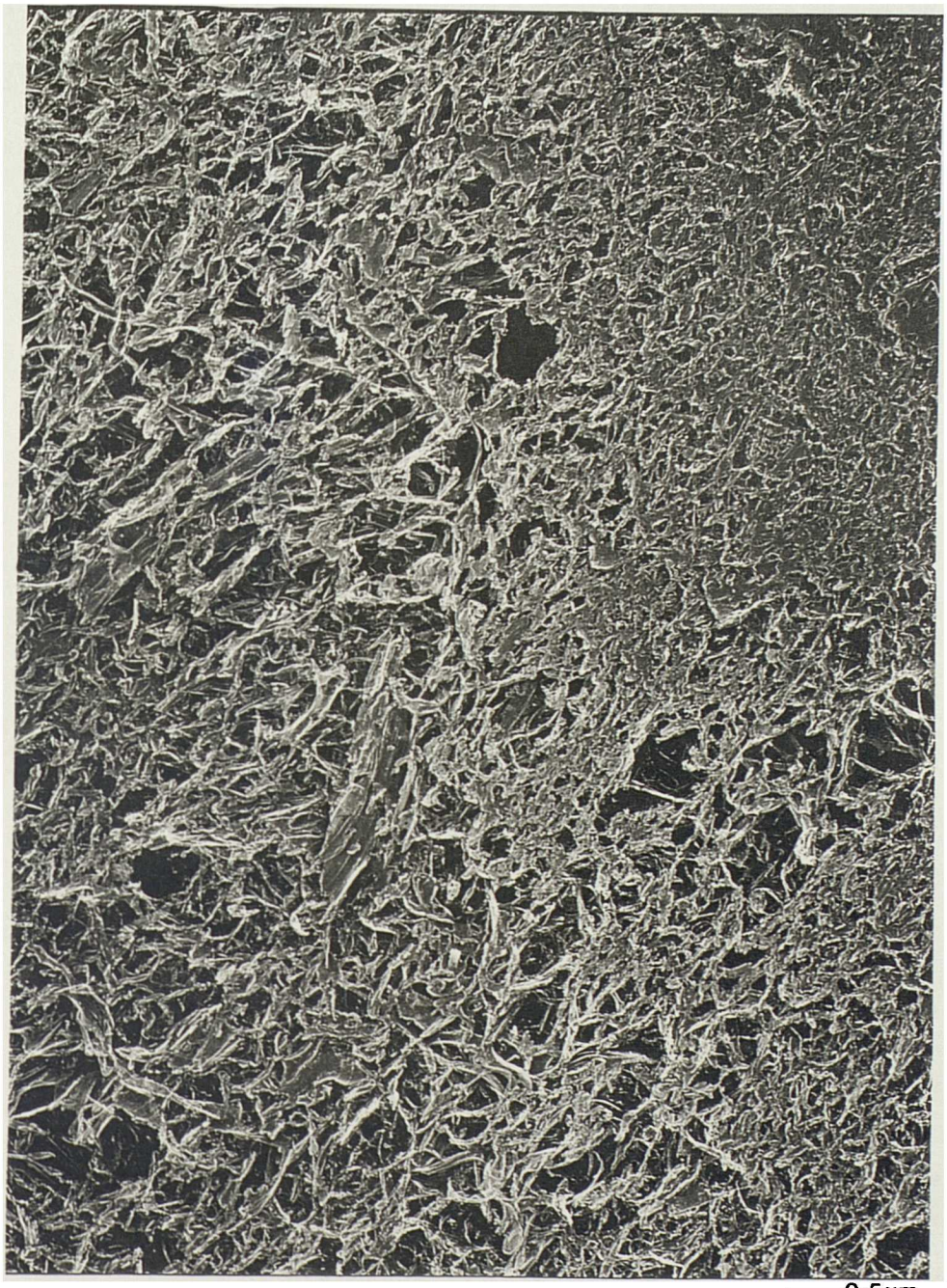

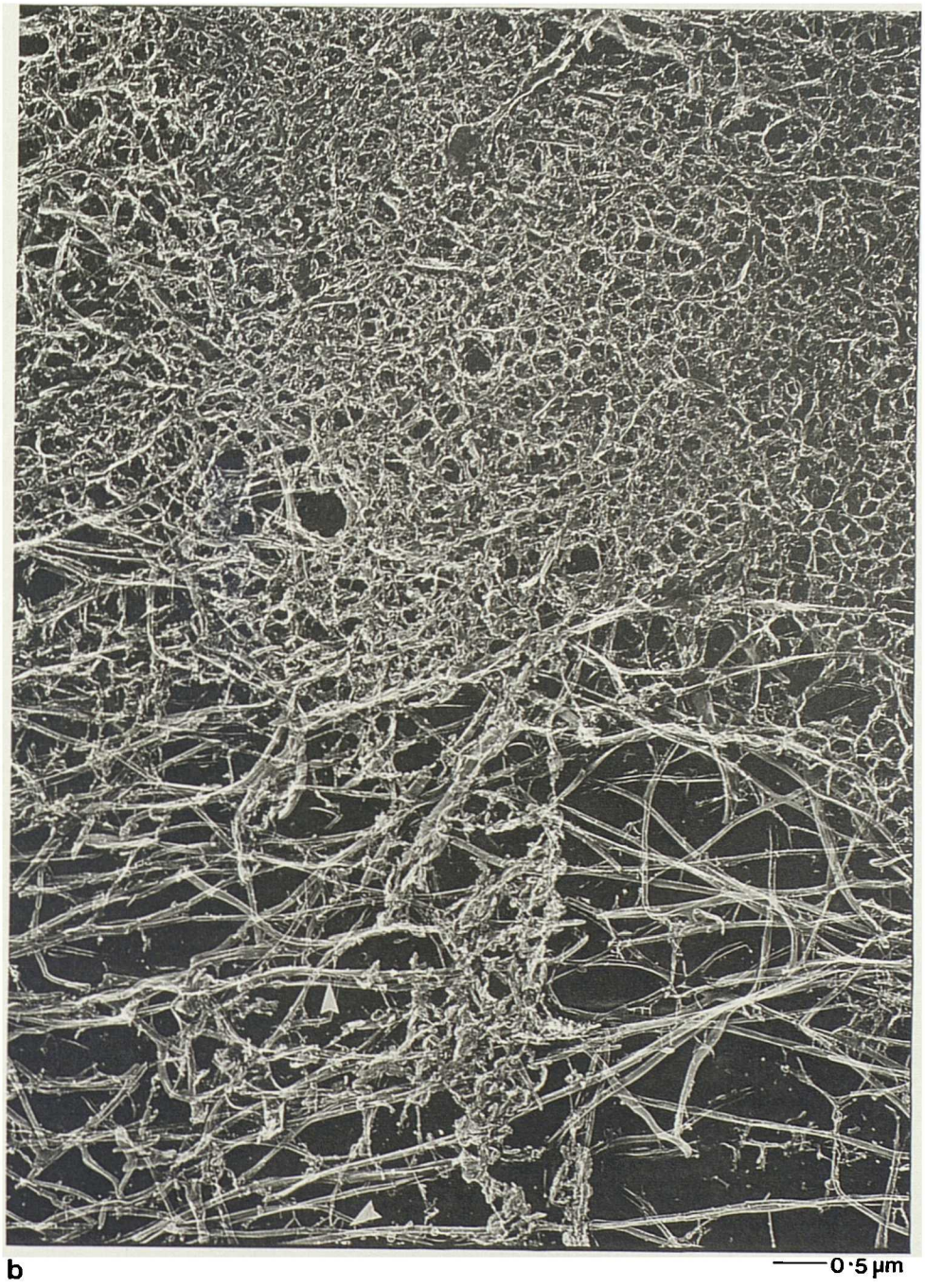

Micrographs of tungsten tantalum/carbon replicas (printed in reverse contrast) of networks produced by *Acetobacter aceti* ssp. *xylinum* incubated in the presence of konjac glucomannan showing regions of densely packed material in which cellulose and glucomannan cannot be distinguished (a) and regions of more dispersed material (b). Putative cross-linkages are shown by the arrows.

component. This broadening of the signal means that calculation of crystalline/non crystalline ratios for the cellulose component is less accurate than was possible for native (Chapter 5) and xyloglucan-modified cellulose (Chapter 6). Integration of C-4 signals at 88-91 and 84-86 ppm for crystalline and non-crystalline material respectively gives an approximate crystalline content for glucomannan-modified cellulose of ca. 25%. This compares with a crystalline content of ca. 80-85% for native cellulose (Chapter 5). A large reduction in overall crystallinity of the cellulose component in cellulose/glucomannan composites is in agreement with the results of Hackney *et al* (1994).

Application of resolution enhancement (Figure 7.2c) to determine the Iα/Iβ ratio of the crystalline component of the cellulose gave less conclusive results than seen for xyloglucan-modified composites (Chapter 6). The much reduced level of crystallinity in this sample confers a weaker signal at 88-90 ppm than seen in either control or xyloglucan modified materials. Comparison of this signal with published quantified signal patterns (Debzi *et al*, 1991; Yamamoto & Horii, 1993) gives a Iα/Iβ ratio of approximately 60:40 although these results should be treated with caution due to the poor signal : noise ratio. Collating the above information gives an overall molecular description for cellulose synthesised in the presence of konjac glucomannan of ca. 15% Iα, 10% Iβ and 75% non-crystalline compared with 57% Iα, 25% Iβ and 18% non-crystalline for native cellulose. At least 57% of cellulose resonance sites are therefore altered by the presence of glucomannan in the composite 1e more than one cellulose site is perturbed on average by each glucomannan site.

Resonances at ca. 101.0 and 103.8ppm for mannosyl and glucosyl residues respectively are reported for a 30% (w/v) hydrate of konjac glucomannan (Gidley *et al*, 1991b). A signal at ca.101ppm can be identified as a shoulder on a broad C-1 peak on the cellulose/glucomannan composite spectrum (Figure 7.2a). The signal for glucose of glucomannan cannot be distingushed as is is overlapped by signals from non-crystalline cellulose at C-1. There is also the appearance of an additional signal at ca. 102.46ppm which does not correspond with signals from glucomannan in the solution state spectrum of the composites (Figure 7.4a) or hydrated glucomannan (Gidley *et al*, 1991b). However it is

Figure 7.2: ^{13}C CP/DD/MAS Spectra of Composites of Bacterial Cellulose and Konjac Glucomannan

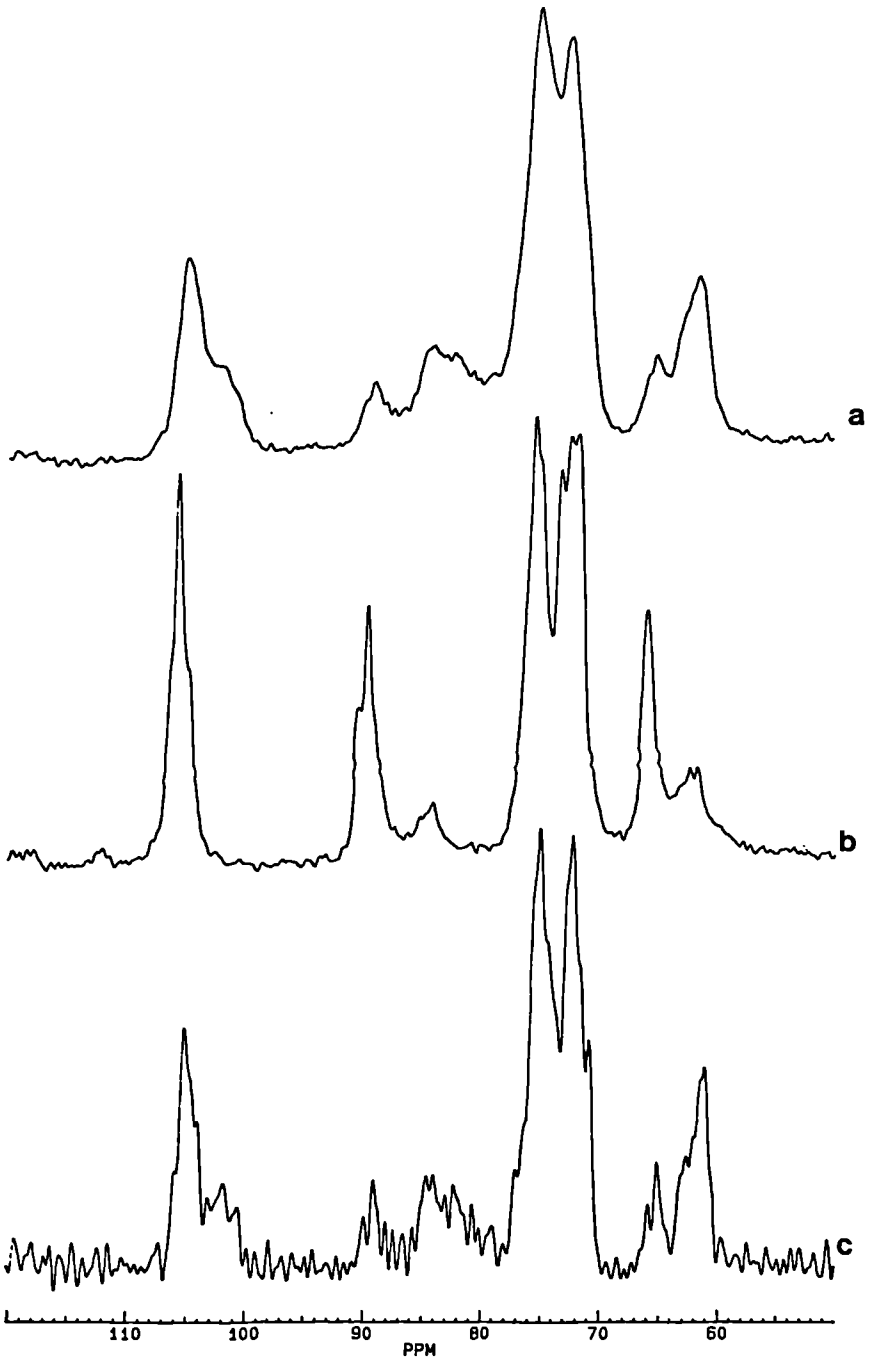

Spectra of (a) hydrated cellulose/glucomannan composites ex. *A.aceti* ssp. *xylinum* showing overall reduction in crystallinity of the cellulose component and the appearance of additional resonances as shoulders on a broad C-1 peak compared to (b) hydrated cellulose ex. *A.aceti* spp. *xylinum*, (c) resolution enhancement (line broadening -70Hz, Gaussian multiplication 0.5) of (a) illustrating some fine structure on C-1 (ca. 105ppm) and C-4 (88-92 ppm) and showing slight alteration of the Iα/Iβ ratio of the cellulose component, but ambiguity in separation of signals for cellulose and glucomannan.

coincident with that for C-1 of the mannan I polymorph from ivory nut mannan reported as ca. 102.2ppm (Marchessault *et al*, 1990; Gidley *et al*,1991b) and is assigned here to C-1 of mannan structural units with extended 'cellulosic' conformatios as found in crystalline mannan I (Chanzy *et al*, 1982, 1987). Appearance of a signal at ca. 102ppm was also observed by Kim and Newman (1995) upon mixing glucomannan and Avicel microcrystalline cellulose. This provides evidence for a possible conformational change in glucomannan on association with cellulose as was seen with xyloglucan in cellulose/xyloglucan composites (Chapter 6); molecular ordering of the glucomannan may have been imposed due to their proximity to crystallite surfaces (Chanzy *et al*, 1982). Application of resolution enhancement (Figure 7.2c) gives a poor quality spectrum due to the poor signal:noise ratio, although putative resonances for the C-1 mannosyl and glucosyl residues of glucomannan (ca. 101.0 and 103.8ppm) and also C-1 of mannan I can be distinguished. The mannan I polymorph also has a resonance at ca. 81.5 ppm, probably corresponding to C-4 sites, which does not correspond to a major signal in hydrated glucomannan (Gidley *et al*, 1991b). Although this cannot be distinguished in the composites, there is a marked broadening of the C-4 signal, possibly due to overlapping of C-4 signals for non-crystalline cellulose and mannan I.

Foster *et al* (1996) used variable cross-polarisation times in a CP/MAS experiment to show differences in intensity between components in the cell wall which are relatively rigid, which probes relative segmental flexibility within the CP/MAS spectrum. Figure 7.3 shows ^{13}C CP/MAS spectra of cellulose/glucomannan composites obtained with contact times of 4, 2 and 1ms, designed to establish variation in flexibility between the cellulose, glucomannan and mannan I segments. The results indicate little difference in mobility between the cellulose and glucomannan components suggesting that they share a common relaxation pathway ($^1HT_{1\rho}$). The signal for the mannan I polymorph at ca. 102.2ppm is better resolved at 2ms contact time relative to glucomannan signals, suggesting that it may be more restricted than the glucomannan component.

Figure 7.3 ^{13}C CP/MAS Spectra of Cellulose/Glucomannan Composites obtained using Variable Contact Times

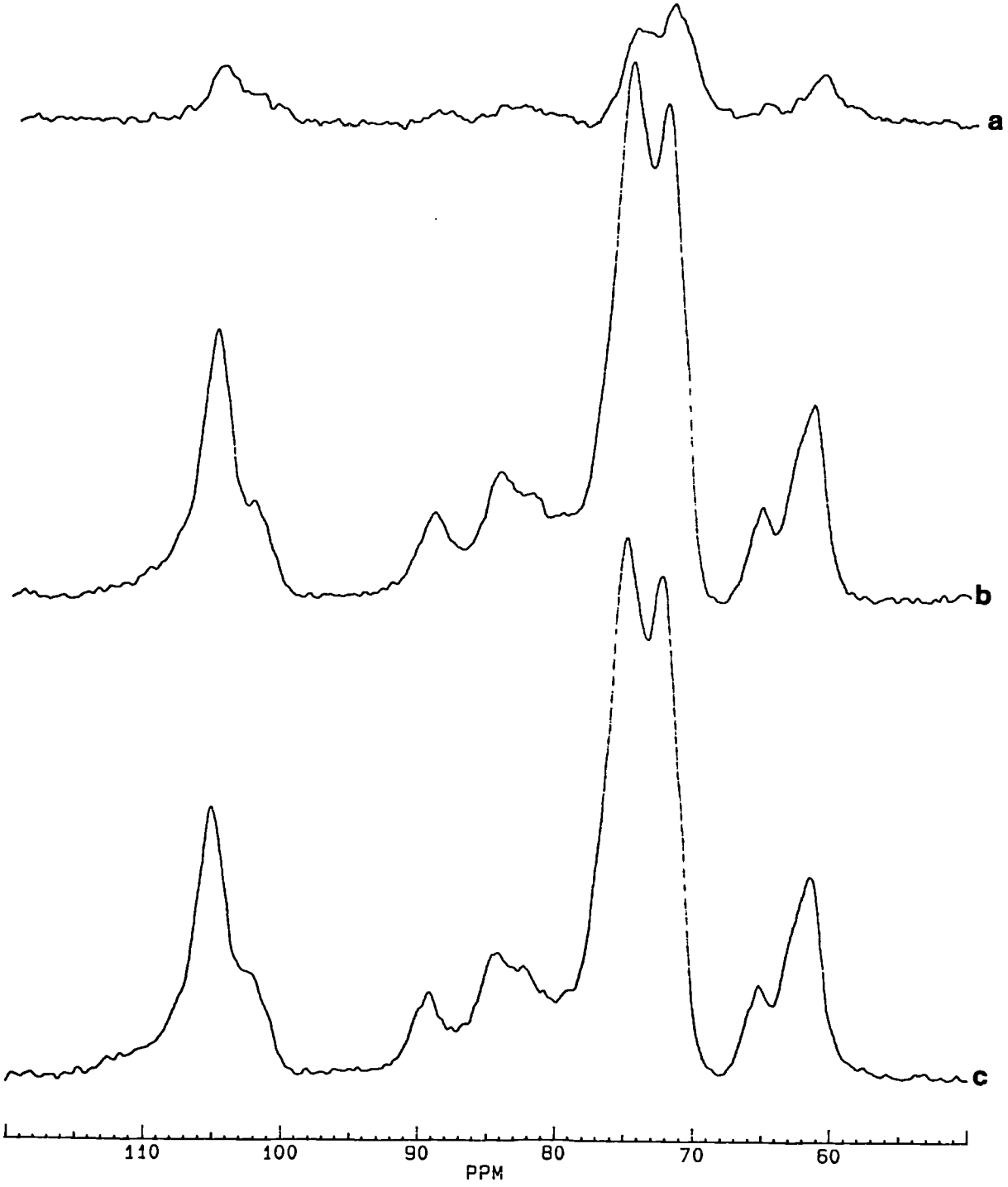

Spectra of cellulose/glucomannan composites ex. *A.aceti* spp. *xylinum* obtained using contact times of (a) 4ms, (b) 2ms and (c) 1ms showing little discrimination between cellulose and glucomannan components suggesting similar relaxation behaviour

Figure 7.4: ^{13}C SP/MAS Spectra of Cellulose/Glucomannan Composites

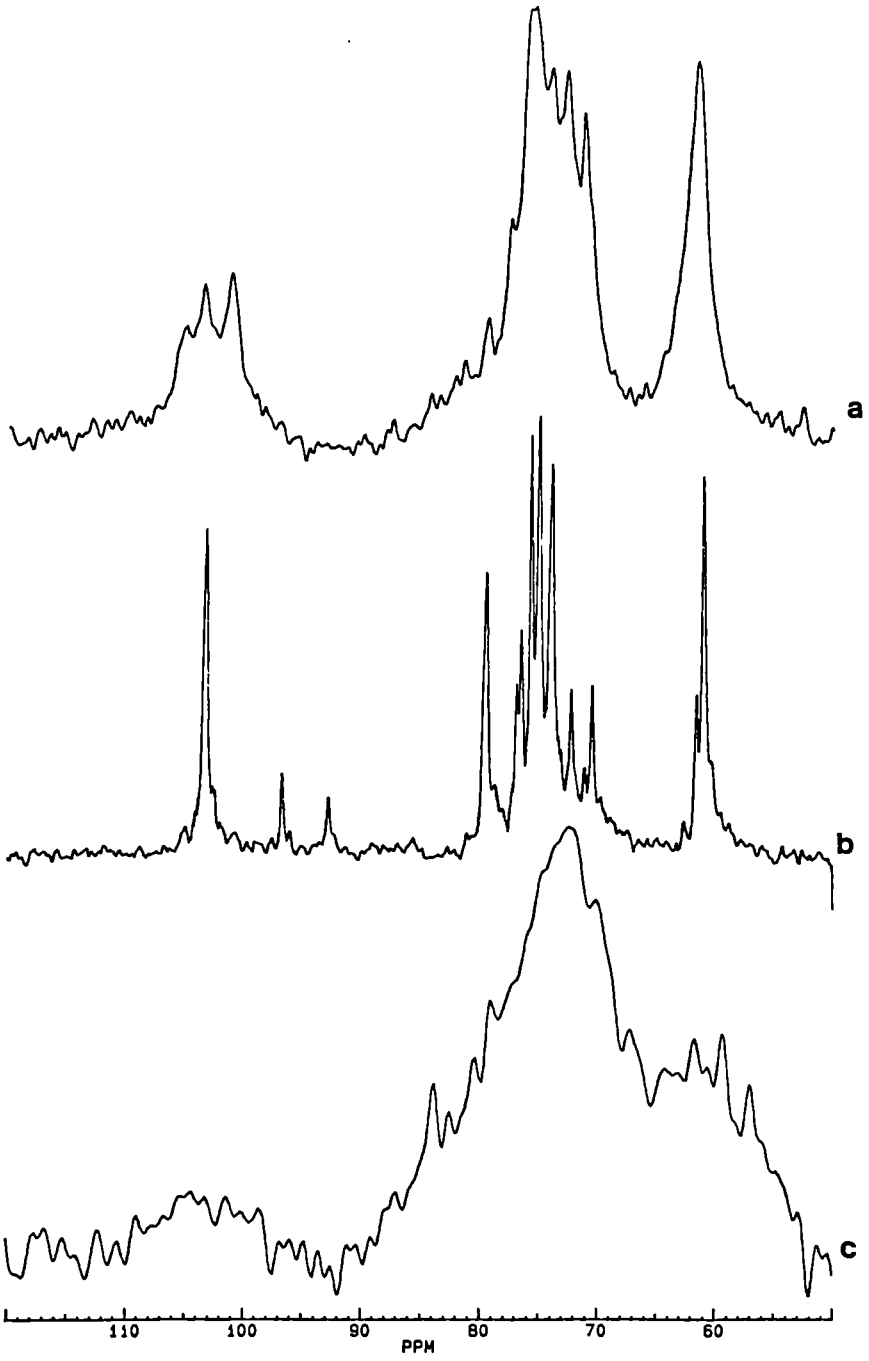

Spectra of cellulose/glucomannan composites ex. *A.aceti* ssp. *xylinum*, (a) SP/MAS showing chemical shifts at ca. 103.8 and 101.1ppm assigned to glucosyl and mannosyl residues respectively and a highly unusual signal at ca. 105.5ppm corresponding to C-1 of Iα cellulose; (b) 5% w/v solution of cellotetraose at 333K under scalar decoupling conditions illustrating a similarity in C-1 chemical shift (103-104ppm) with peaks assigned to glucomannan glucosyl residues in (a) and C-4 chemical shifts at ca. 80ppm; (c) SP sepectrum with no MAS of cellulose/glucomannan composites showing that the signal at 105.5ppm is assigned to a component more rigid than the glucomannan component

The SP/MAS spectrum of the cellulose/glucomannan composite is shown in Figure 7.4a, with the appearance of signals at ca. 101.1 and 103.8ppm corresponding to mannosyl and glucosyl residues respectively (Gidley *et al*, 1991b). No signal at ca. 102.2 ppm is observed, implying that the putative mannan I polymorph structure formed in association with cellulose in this system is relatively rigid, as suggested by the results for the CP/MAS spectra above. A resonance at 105.5ppm is seen in this spectrum which is coincident with the chemical shift for C-1 of Iα cellulose (Debzi *et al*, 1991; VanderHart & Atalla 1984). This is different from the major C-1 chemical shift at 103.3ppm seen in the SP/MAS spectrum for a solution of cellotetraose (Figure 7.4b) which is essentially identical to the shifts seen for related glucosyl residues in solutions and hydrates of glucomannan (Gidley *et al*, 1991). The appearance of a cellulosic signal in an SP/MAS spectrum is highly unusual and is not seen in spectra of native cellulose or cellulose/xyloglucan composites (Chapter 6). An SP spectrum with no MAS is shown in Figure 7.4c The cellulose signal at C-1 is eliminated, suggesting that it is relatively more rigid than the glucomannan component.

7.4 Discussion

Secondary walls are deposited around the primary walls of many plant cells after the process of cell expansion is complete functioning to impart increased strength and rigidity to tissues. In contrast to primary walls, in which the wall itself provides limited mechanical strength supplemented greatly by the turgor pressure of the cell, secondary walls are structures which can provide structural support independently of turgor. The hemicellulose composition of primary and secondary walls differs markedly. Whilst deposition of lignin in secondary walls contributes greatly to strength, cellulose is a major load-bearing molecule in both wall types and it is logical to assume that differences in functionality between primary and secondary walls are due substantially to differences in the hemicellulose composition and how they interact with the cellulose component.

The network architecture of composites formed in the presence of glucomannan is very different to xyloglucan-modified structures (Chapter 6). The predominant effect is a pulling-together of cellulose fibres to form a much more compact structure than either the control (Chapter 5) or xyloglucan-modified (Chapter 6) networks. The structure is also slightly less hydrated (ca. 4.4% w/v) than xyloglucan-modified (ca. 2.9% w/v) or native (ca. 3.3%) materials. ^{13}C NMR spectroscopy indicates that the presence of glucomannan in the composites has a profound effect on the molecular organisation of the cellulose component, suggesting extensive interaction between the two polymers. In contrast to xyloglucan, which caused an alteration in the $I\alpha I\beta$ ratio with a slight reduction in overall crystallinity, the major effect of glucomannan was to increase the non-crystalline component, concurring with the results of Hackney *et al* (1994).

Examination of both ultrastructure and molecular organisation of composites formed using glucomannan indicates that. like xyloglucan, extensive and intimate interaction between the cellulose and the modifying polymer are apparent, but that the nature of the interaction is very different. In Chapter 6 and Whitney *et al* (1995), xyloglucan is described as acting as a molecular tether, pulling adjacent cellulose fibres together into a more organised structure. In the light of results presented in this chapter, xyloglucan may perhaps be better described as a molecule which holds cellulose fibres *apart* in an organised network. A more open, hydrated structure would better facilitate enzyme access and deposition of newly synthesised wall material, two processes important in cell wall expansion. However, a less hydrated, more densely-packed network may be advantageous in secondary walls which are less dynamic and have a role in the imparting of mechanical strength.

Clearly, glucomannan and xyloglucan have interacted with newly synthesised cellulose in this system in very different ways. The nature of the interactions seem to provide molecular architectures appropriate for the function of primary and secondary cell walls. These results suggest that the *Acetobacter aceti* ssp. *xylinum* cellulose-synthesising system can be expanded to look at different cell

wall types and provide some evidence that hemicelluloses play an important role in determining the ultrastructural and molecular organisation of cellulose and, by inference, the entire cell wall.

Chapter 8: Influence of Polymeric Additives on Architecture and Molecular Organisation of Networks Produced by *Acetobacter aceti* ssp. *xylinum* Cultures

8.1 Introduction

Acetobacter aceti ssp. *xylinum* (ATCC 53524) synthesises very pure, highly crystalline, predominantly Iα cellulose as an extracellular polysaccharide in agitated liquid cultures, which forms a densely packed network of apparently randomly oriented strands (Chapter 5). Addition of high molecular weight tamarind xyloglucan to the incubation medium resulted in the formation of networks in which cellulose fibres, showing greater alignment than in the controls, were connected by cross-linking xyloglucan molecules (Chapter 6). These structures had a similar architecture to that proposed for cellulose/xyloglucan networks in primary type I cell walls (Carpita & Gibeaut, 1993; McCann *et al*, 1990; McCann & Roberts, 1991). Coupled with observations of altered molecular organisation of the cellulose component of the composite to become more 'plant-like', this system was proposed to be a valuable model for primary cell wall construction (Chapter 6; Whitney *et al*, 1995). In Chapter 7, this proposal was extended to include other cell wall types. Networks formed in the presence of glucomannan, a major hemicellulosic polysaccharide of secondary cell walls, had a very different architecture to those formed using xyloglucan. These differences could be partially reconciled with contrasting structural requirements of primary and secondary cell walls. Work outlined in this chapter discusses the effect of a range of polymers on network structure in this system.

Carboxymethyl cellulose (CMC) is a cellulose derivative in which free hydroxyl groups on glucose residues of a cellulosic backbone are substituted to a greater or lesser degree with carboxymethyl substituents, rendering these polysaccharides water-soluble. CMC was demonstrated to perturb ribbon assembly in *A.xylinum* (Ben-Hayim & Ohad, 1965) and its prevention of the normal fasciation of

microfibrils into ribbons in this system led to a model for cellulose ribbon biogenesis as a hierarchical, cell-directed self assembly process (Benziman *et al*, 1980; Haigler & Brown, 1981; Haigler *et al*, 1982). Yamamoto & Horii (1994) reported a similar effect on the molecular organisation of the cellulose component when CMC was added to cultures of *A.xylinum* (ATCC 23769) to that seen with xyloglucan, namely a reduction in the Iα component. CMC was proposed to reduce cellulose lateral crystallite dimensions coupled with an increase in the relative abundance of the Iβ allomorph (Uhlin *et al*, 1995). As a well-characterised polymeric additive in the *Acetobacter* system, experiments using CMC help to validate the conclusions drawn from other, less well researched, additives.

Pectins are a highly heterogeneous and complex set of polymers, which form a major component of type I primary cell walls. Typically, treatment of isolated cell walls with chelating agents and mild alkali results in the extraction of the majority of the pectic component whilst leaving the chemical and structural integrity of the cellulose/xyloglucan network intact. It was observations such as these which led to the multi-domain model for plant cell walls, in which the pectin network is independent from, but co-extensive with, the cellulose/xyloglucan framework (Carpita & Gibeaut, 1993; McCann & Roberts, 1991; McCann *et al*, 1990; Talbott & Ray, 1992a). However, even after extraction of isolated cell walls with concentrated alkali (4M KOH), sufficient to remove the majority of the hemicelluloses, a pectic fraction is retained (Mitchell, J, Unilever Research, pers. comm.; Redgwell & Selvendran, 1986; Ryden & Selvendran, 1990; Seymour *et al*, 1990). This pectic component remains associated with the α-cellulosic fraction even after either increasing the alkali concentration, although the action of pectin-degrading enzymes such as polygalacturonase (PG) can effect almost total removal (Mitchell, J., Unilever Research, pers.comm.). The high level of resistance to extraction exhibited by this component suggests an intimate interaction with cellulose and it is therefore of interest to examine the effect of pectin as a polymeric additive in this system.

Two other common hemicelluloses, xylans and mixed-linkage glucans were described in Chapter 1 (sections 1.7.1 and 1.7.2). Glucuronoxylans have already been demonstrated to asscociate with

cellulose microfibrils from quince mucilage *in vitro*, causing the spontaneous formation of helicoid arrays (Reis *et al*, 1994; Vian *et al*, 1994), and there is evidence for glucuronoxylans directing a helicoidal array *in vivo* (Vian *et al*, 1992). Conformational changes of xylans upon sorption to cellulose *in vitro* have been reported (Mitikka *et al*, 1995) and the alteration of *Acetobacter* cellulose to become more like higher plant cellulose when xylans were incorporated into the cellulose synthesising system has also been demonstrated (Atalla *et al*, 1993). Uhlin *et al* (1995) propose that xylans and xyloglucans interact with cellulose in the *Acetobacter* system in a similar way, ie that they co-crystallise with the cellulose component during aggregation, causing defect structures within the crystal lattice. CMC acts in a different way, lowering the degree of cellulose crystallinity by decreasing crystallite size.

The function of mixed-linkage glucans in wall structure remains unresolved; their transient appearance during cell elongation has been interpreted as implying a role for these polymers as molecular threads which interlock microfibrils during elongation of Type II cell walls (Carpita & Gibeaut, 1993), but equally they may act as storage polymers within the wall, which are degraded after cessation of elongation (Roberts, K., John Innes Institute, pers.comm.). Incorporation of this polymer into the *Acetobacter* system may help elucidate its role in the Type II cell wall.

The interaction of glucomannan with *Acetobacter* cellulose was described in Chapter 7. Work in this chapter describes the use of two different galactomannans. Guar galactomannan has a Man:Gal ratio of ca. 1.5 and is therefore not predicted to form intermolecular associations (Dea & Morrison, 1975; Dea *et al*, 1986). This polymer was incorporated into the system simply to determine the effect of the presence of a high molecular weight polysaccharide, not predicted to associate with the cellulose component, on cellulose biogenesis. In contrast, galactomannan from locust bean gum (LBG), has a much higher Man:Gal ratio (ca. 4.0) facilitating intermolecular interactions (Dea & Morrison, 1975; Dea *et al*, 1986). Furthermore LBG galactomannans have been shown to interact with other polysaccharides, such as carrageenans (Fernandes *et al*, 1991; Goycoolea *et al*, 1995; Murayama *et al*, 1995a,b; Stading & Hermansson, 1993, Viebke, 1995). The interaction of LBG galactomannan with

cellulose, particularly in regard to alterations of molecular conformation of the galactomannan component in the presence of a cellulose template (cf glucomannan conformational changes in the presence of cellulose, Chapter 7, this thesis), is of interest.

8.2 Materials and Methods

8.2.1 Raw Materials

8.2.1.1 Carboxymethylcellulose (CMC)

Carboxymethylcellulose (CMC, 4M6F) was obtained from Hercules, UK.

8.2.1.2 Pectin

A relatively highly esterified pectin (DE 65%) derived from apple fruit was supplied by Biocon (Ireland)

8.2.1.3 Xylan

Xylan derived from birchwood was supplied by Sigma, UK. Monosaccharide analysis (Alditol Acetates Method 3, section 2.10) detected no neutral sugars other than xylose, contrasting with the report of Sjostrom (1971) who demonstrated a (1→3)-α-L-rhamnose unit and a (1→2)-α-D-galactose unit before the reducing end unit of xylose for birch xylan. Methanolysis analysis (section 2.7) gave a glucuronic acid substitution level of ca. 5%, less than reported by Duckert *et al*, (1988).

8.2.14. Mixed-Linkage Glucan

Mixed-linkage glucan derived from barley was obtained from Biocon (Ireland).

8.2.1.5 Guar and LBG Galactomannan

Guar galactomannan (Man:Gal 62:38) was a commercial sample obtained from Hercules (UK). The LBG galactomannan was obtained by fractionation of commercial LBG samples (Hercules, UK) by D. Cooke, Unilever Research. The native sample was extracted at 25°C (LBG_{25} fraction), 45°C ($LBG_{25\text{-}45}$ fraction) and 80°C ($LBG_{45\text{-}80}$ fraction). Each extraction was performed in deionised water (1% w/v solution) and the isolated fractions were collected as supernatants after centrifugation at 27,500g for 30

minutes. Extracted galactomannans were recovered by precipitation in propan-20ol (IPA), precipitates were washed extensively with pure IPA, vacuum filtered, soaked in pure acetone overnight to remove excess water and dried at 40°C under vacuum. The $LBG_{45\text{-}80}$ fraction (Man:Gal 83:17) was incorporated into the *Acetobacter* fermentation system.

8.2.2 Construction of Cellulose/Polysaccharide Composites

Experimental cultures in media containing 2% glucose and either 0.5% pectin, CMC and mixed-linkage glucans, or 0.5% or 2.0% birchwood xylan, or 0.2% guar or LBG galactomannan were performed as described in Chapter 6 (section 6.2.). After two days incubation, pellicles were removed and washed extensively in sterile deionised water. Material produced in the presence of CMC, which did not form a discrete pellicle, was collected and washed by cenrifugation in a bench-top centrifuge at 3000 rpm.

8.2.3 Monosaccharide Analysis

The sugar composition of the composites was determined using alditol acetates Method 2 (section 2.8).

8.2.4 Deep-Etch Freeze-Fracture TEM

High resolution microsopy was performed on the cellulose/polysaccharide composites as described in Chapter 2 (section 2.12.5)

8.2.5 ^{13}C NMR Spectroscopy

CP/MAS and SP/MAS ^{13}C NMR spectroscopy on the composites was performed as described in Chapter 2 (section 2.13). High resolution ^{13}C NMR of isolated polymers was performed as described in Chapter 9 (section 9.2.).

8.3 Results

8.3.1 CMC

Already reported as disrupting ribbon assembly in the *Acetobacter xylinum* strain ATCC 23769 (Haigler *et al*, 1992), CMC substantially alters both the gross morphology and network features of cellulose synthesised by strain ATCC 53524. Rather than forming a discrete pellicle, modified cellulose appears as a slime throughout the medium. This lack of cohesion is reflected in a network where fibres are associated in an open, porous structure (Figure 8.1). Although cellulose and CMC cannot be distinguished in the micrographs; in agreement with Haigler *et al*, (1982); Uhlin *et al*, (1995) and Yamamoto & Horii (1994) the presence of CMC has apparently substantially reduced fibre dimensions. This is consistent with the proposed effect of CMC in preventing fasciation of cellulose microfibrils into ribbons (refer to Figure 6.1).

The ^{13}C NMR spectra of cellulose/CMC composites are shown in Figure 8.2. The effect of the presence of CMC inferred from the micrographs (Figure 8.1) is of an alignment of the two polymers such that they are indistinguishable microscopically. This intimate interaction is predicted from the effect on fibre morphology in this system and as previously reported (Haigler *et al*, 1982). The CP/MAS spectrum (Figure 8.2a) shows no discrete signals for CMC (Figure 8.3). This suggests either a conformational alteration of CMC in the presence of cellulose, as was seen with the glucosyl backbone residues of xyloglucan (Chapter 6 and Whitney *et al*, 1995) or the absence of any cellulose/CMC interaction. The microscopic evidence favours, we believe, the former interpretation, although more work is required on this system.

Integration of signals at 88-91 and 84-86ppm, corresponding to C-4 sites in crystalline and non-crystalline environments respectively (VanderHart & Atalla, 1984) in Figure 8.2a gives a crystalline content of ca. 68%. This is reduced compared with the crystalline content of native bacterial cellulose

Figure 8.1: Micrographs of Composites Formed in the Presence of CMC

Micrographs of tungsten/tantalum/carbon replicas of composites produced by fermentation of *A.aceti* ssp. *xylinum* (ATCC 53524) in the presence of carboxymethyl cellulose illustrating an open porous structure and showing neither discrete cross-bridges or overall strand alignment (contrast Figure 6.2), but a reduction in strand width compared to native cellulose networks (Figure 5.7)

Figure 8.2: ^{13}C CP/MAS NMR Spectra of Bacterial Cellulose/CMC Composites

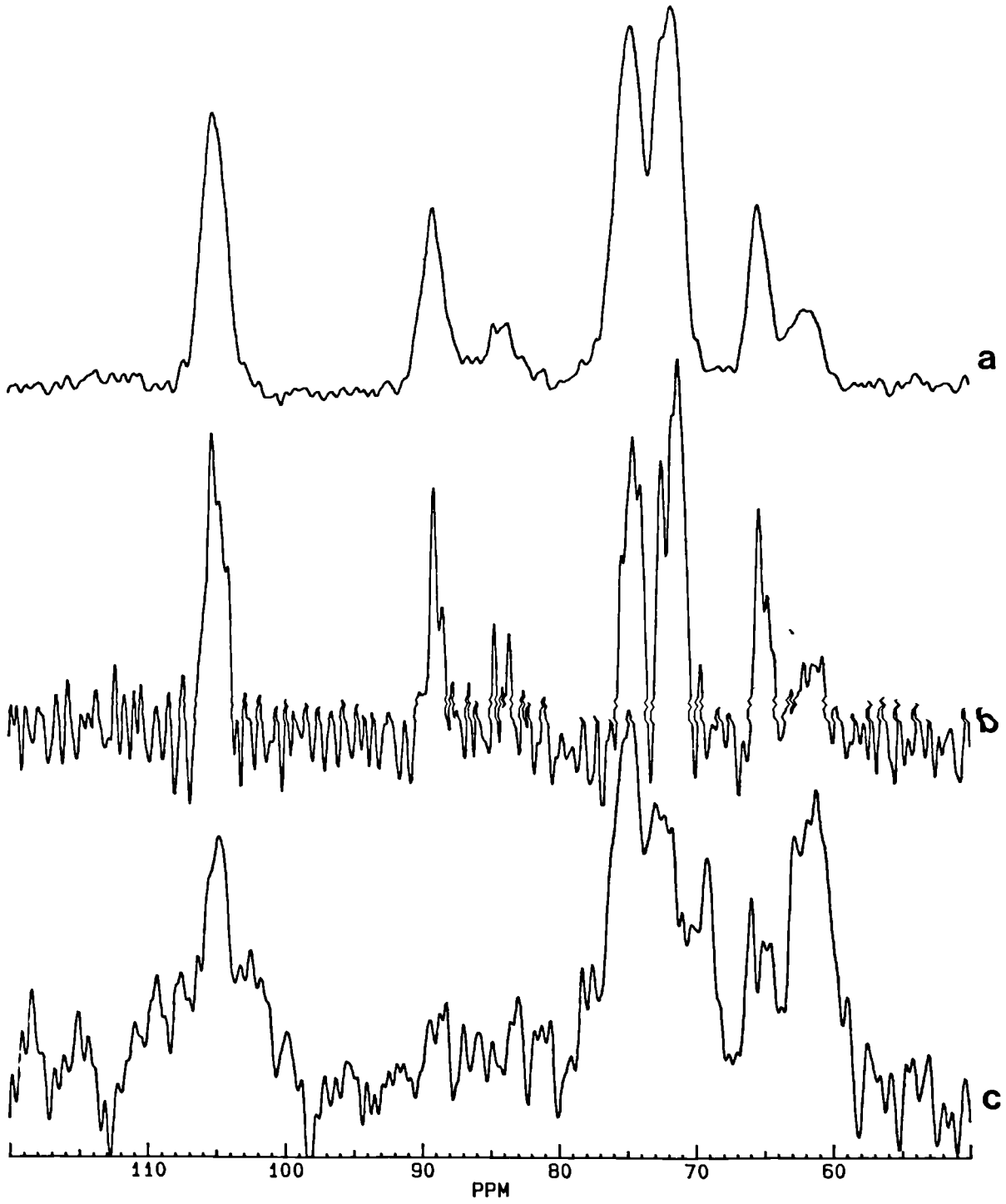

(a) hydrated cellulose/CMC composite ex. *A.aceti* ssp. *xylinum* (ATCC 53524) (cf Figure 8.1), (b) resolution enhancement (line broadening -70Hz, Gaussian multiplication 0.5) of (a) showing altered fine structure of cellulose signals compared with Figure 5.3b and the absence of discrete CMC signals (comapre Figure 8.3) suggestive of conformational alignment of CMC with the cellulose component, (c) SP/MAS spectrum comprising only signals for CMC, indicating a proportion of the CMC is not associated with the cellulose component

Figure 8.3: High Resolution ^{13}C NMR Spectrum of CMC

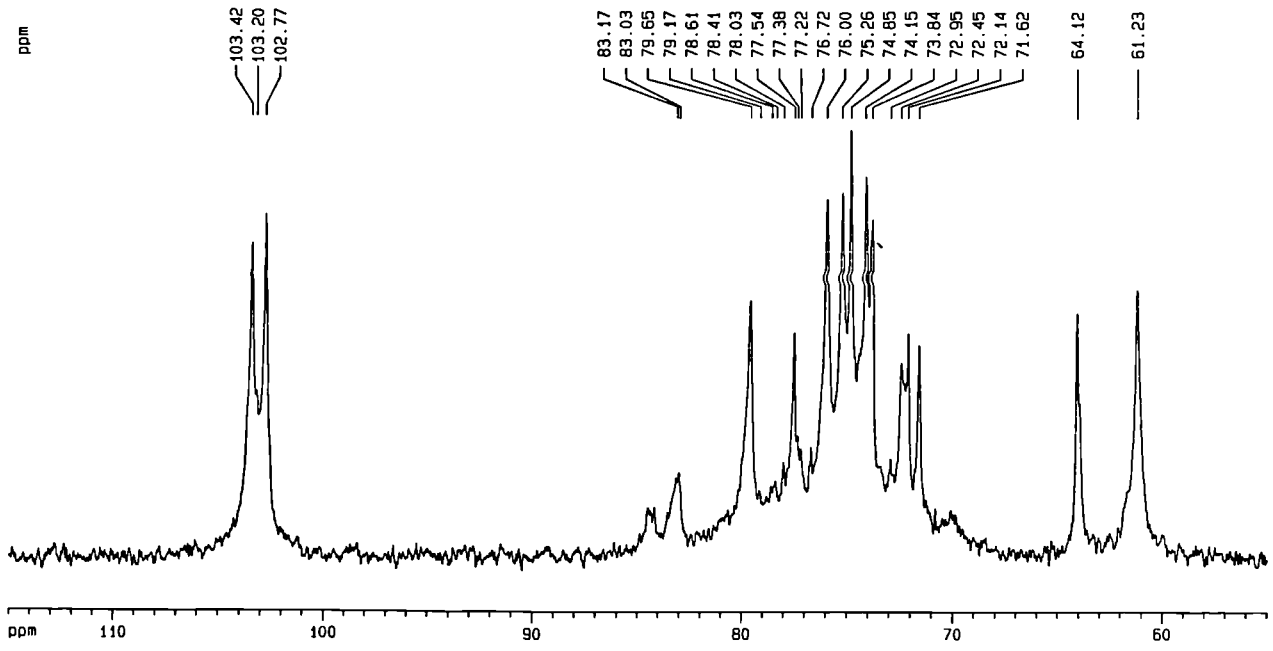

High resolution spectrum of a 4% (w/v) solution of CMC (4M6F), line broadening 5Hz

(80-85%), and concurs with the results of Yamamoto & Horii, (1994) and of Uhlin *et al* (1995), the latter authors proposing that the reduced coherence of order in the presence of CMC is a result of reduction of crystallite size. The resolution enhanced CP/MAS spectrum shown in Figure 8.2b is of poor quality, however comparison of C-4 signals with published quantified signal patterns (Debzi et al, 1991; Yamamoto & Horii, 1993) gives a Iα/Iβ ratio of ca. 40/60. The conversion of the metastable Iα allomorph into the more stable Iβ form is of a similar magnitude to that seen in the presence of xyloglucan (Chapter 6 and Whitney *et al*, 1995) and is in agreement with the results of Yamamoto & Horii (1994) who showed a similar reduction in the mass fraction of Iα for cellulose cultured in the presence of CMC. In the presence of CMC therefore, the cellulose component has an altered molecular organisation of 27% Iα, 41% Iβ and 32% non-crystalline compared with controls (57% Iα, 25% Iβ and 18% non-crystalline). This profound effect on the molecular organisation of the cellulose in the presence of CMC implies an intimate interaction between the two components (cf xyloglucan, Chapter 6, Whitney *et al*, 1995) and provides indirect evidence that the absence of discrete CMC signals in the CP/MAS spectrum (Figure 8.2a) is due to a conformational rearrangement of the CMC component. The SP/MAS spectrum of the composite (Figure 8.2c) is typical of that obtained for pure CMC (Figure 8.3) and indicates that not all CMC in the composite is aligned with cellulose. The poor quality of this spectrum indicates low levels of material, indirect evidence for significant association with cellulose, although the absence of cellulose:CMC ratios precludes confirmation.

8.3.2 Pectin

Cellulose synthesis in the presence of pectin produced a structure very similar to that seen in control incubations, ie a densely-packed network of apparently randomly oriented strands (Figure 8.4). Prior to chemical analysis, the apparent increase in width of fibres and increase of dark (relative to the light, electron dense cellulose fibres) colour around fibres was interpreted as the formation of a hydrated pectin sheath around individual fibres. However, monosaccharide analysis could not detect the presence of sugars other than glucose (>99%) in the composites, and NMR spectroscopy (Figure 8.5)

Figure 8.4: Micrograph of Composites Formed in the Presence of Apple Pectin

Micrograph of tungsten/tantalum carbon replicas of composites produced by fermentation of *A.aceti* ssp. *xylinum* (ATCC 53524) in the presence of apple pectin illustrating an apparently randomly oriented network of cellulose fibres (cf controls, Figure 5.7) and the apparent presence of water around individual fibres (darker regions of the micrograph)

Figure 8.5 ^{13}C NMR Spectra of a Putative Bacterial Cellulose/Pectin Composite

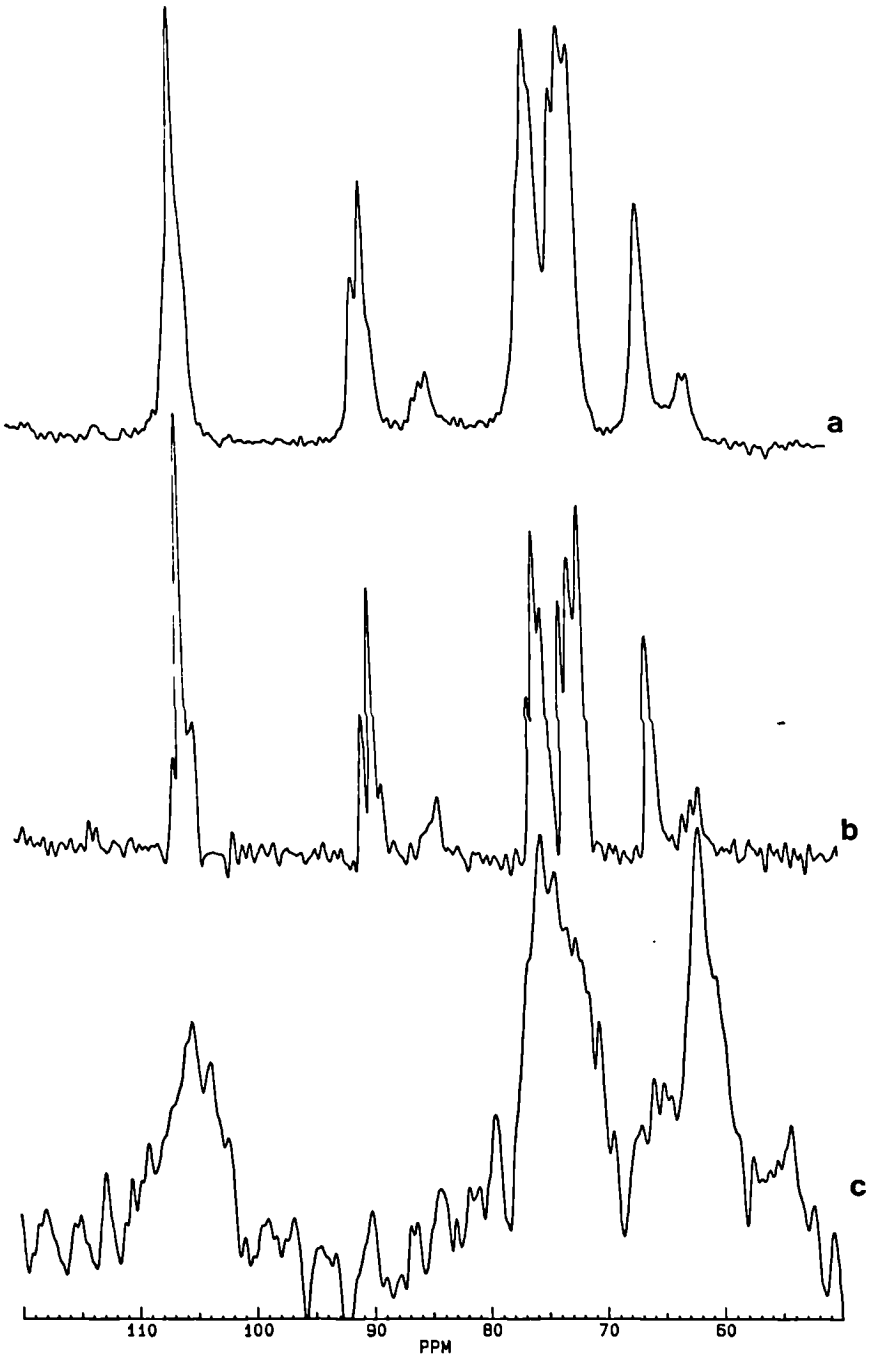

(a) CP/MAS spectrum of hydrated putative cellulose/pectin complex ex *A.aceti* ssp. *xylinum* (ATCC 53524) (cf Figure 8.4) and (b) after application of resolution enhancement (line broadening -70Hz, Gaussian multiplication 0.5) illustrating no signals attributable to pectin and unaltered cellulose fine structure relative to native bacterial cellulose (Figure 5.3), (c) SP/MAS spectrum of (a) showing the appearance of a putative cellulose C-1 signal at ca. 105ppm

Figure 8.6: High Resolution ^{13}C NMR Spectrum of Apple Pectin

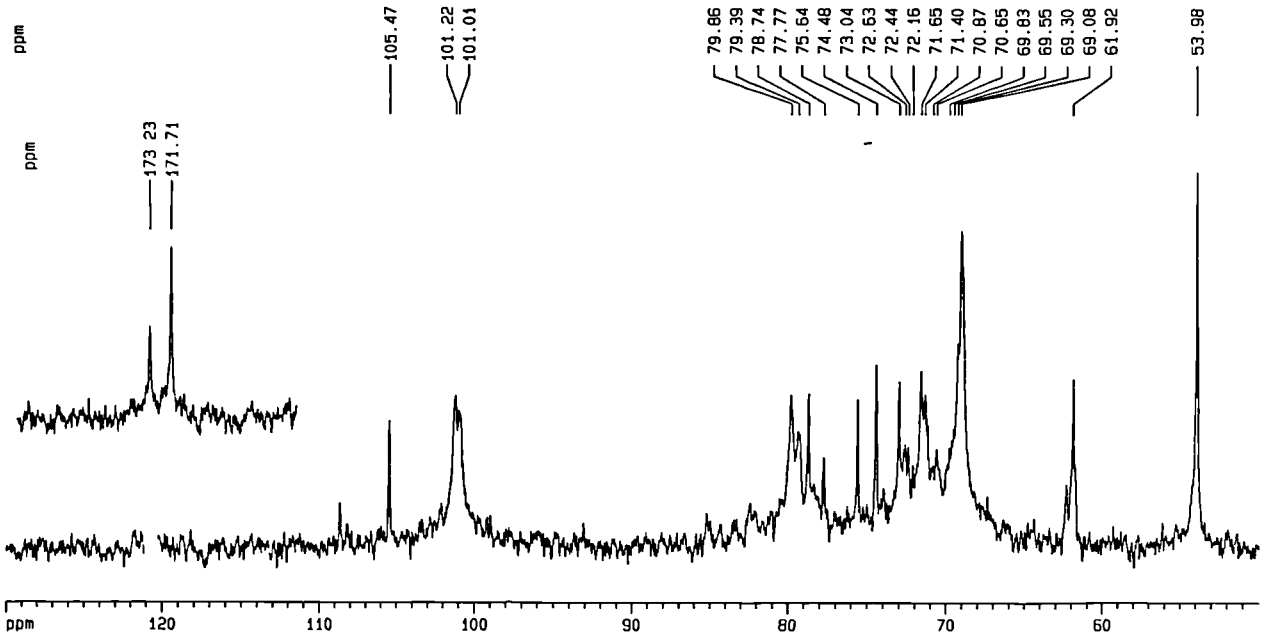

provides no evidence for pectin signals in the CP/MAS spectrum. Integration of signals at C-4 sites and comparison of C-4 signals with published, quantified spectra (cf section 8.3.1) indicates that the molecular organisation of the cellulose composite is identical to that of native cellulose (Chapter 5). The SP/MAS spectrum indicates a peak at ca. 105ppm, coincident with both the cellulose C-1 peak and a peak in the high resolution ^{13}C NMR spectrum of the native pectin starting material corresponding to (1→4)-β-D-galactan (Figure 8.6). As monosaccharide analysis detected only glucose, this may in fact be cellulosic material. This is highly unusual, but the appearance of cellulose signals in the SP/MAS spectrum of cellulose/glucomannan composites was reported in Chapter 7. There is insufficient evidence to fully explain the appearance of this signal in the SP/MAS spectrum with the data available. If it is cellulosic, the absence of signals from ca. 83-89ppm indicates that it is present as solvated single chains (as in cellotetraose, Figure 6.10d).

The chemical evidence obtained on the composite formed in the presence of pectin suggests that the hydrated areas identified around cellulose fibres may be artefactual. However, the possibility that the presence of pectin in the medium may have affected the interaction of water with the cellulose indirectly, perhaps by increased entrapment of water within the structure, cannot be excluded.

8.3.3 High Mwt Xyloglucan + Pectin

A single incubation of *Acetobacter* in the presence of both 0.5% high mwt xyloglucan (see Chapter 6) and 0.5% apple pectin was performed. The characteristic interaction of cellulose with xyloglucan in this system, namely cross-linkage formation and alignment of cellulose fibres, was seen (Figure 8.7a). Somewhat more unusual structures, in which the modifying polymer(s) apparently interacted were also seen (Figure 8.7b). However this first crude attempt at regenerating a primary cell wall was essentially unsuccessful. Unfortunately, monosaccharide analysis was not performed on this sample as it became contaminated in the NMR rotor, but NMR data (Figure 8.8) indicates comparable effects, both with respect to incorporation levels and molecular properties of the cellulose and xyloglucan components as was seen for composites produced in the presence of 0.5% high mwt xyloglucan only (Figure 6. 9).

Figure 8.7: Micrographs of Composites Formed in the Presence of High Mwt Tamarind Xyloglucan and Apple Pectin

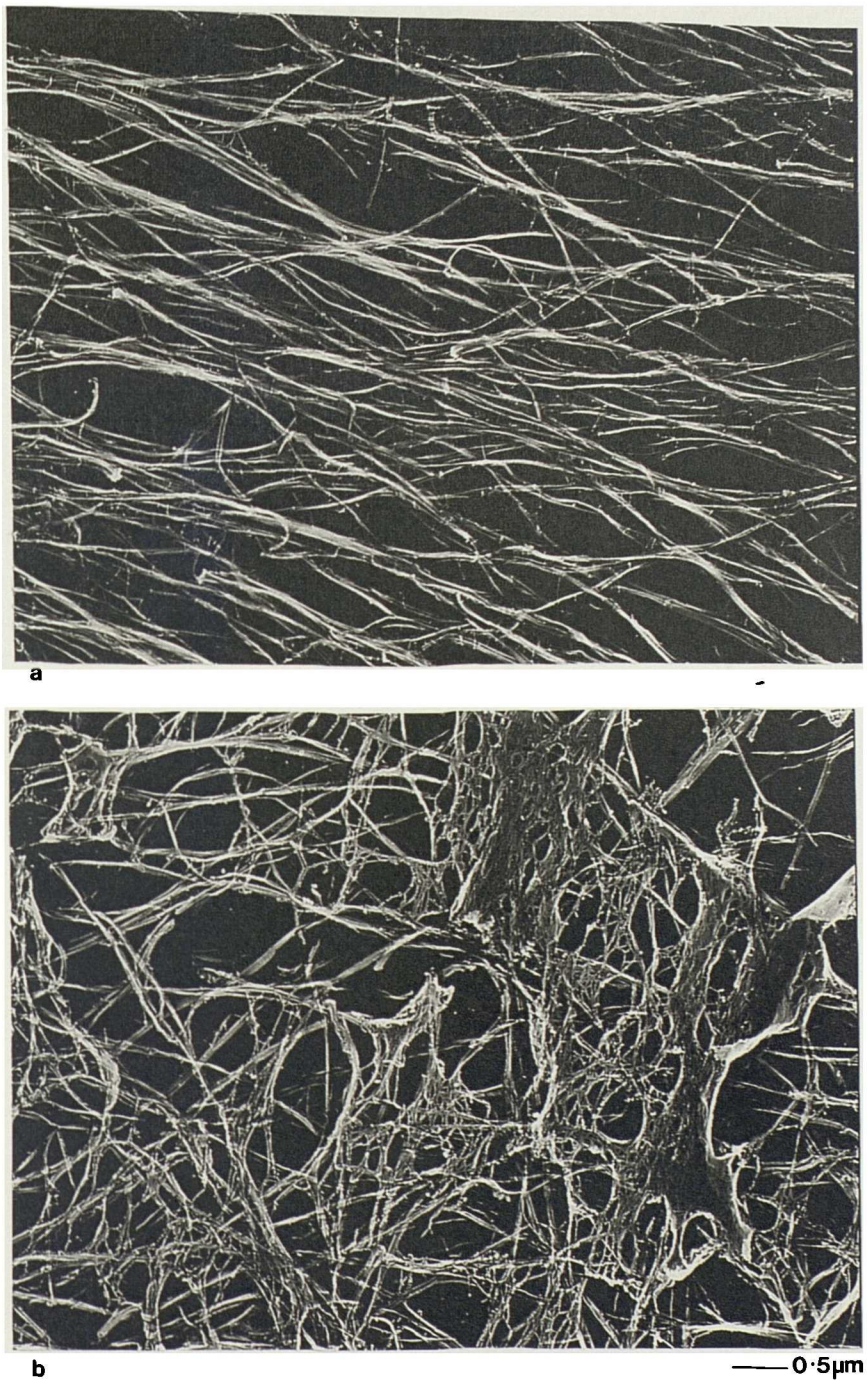

Micrographs of tungsten/tantalum/carbon replicas of composites produced by fermentation of A.aceti ssp. xylinum (ATCC 53524) in the presence of 0.5% high mwt tamarind xyloglucan and 0.5% apple pectin, showing some alignment and cross-linking between cellulose fibres (a) and unusual structures possibly caused by the aggregation of the pectin (b), but no evidence for a structure similar to that seen for primary cell walls (eg McCann & Roberts, 1992; McCann *et al*, 1990).

Figure 8.8: ^{13}C NMR Spectra of a Putative Bacterial Cellulose/Xyloglucan/Pectin Composite

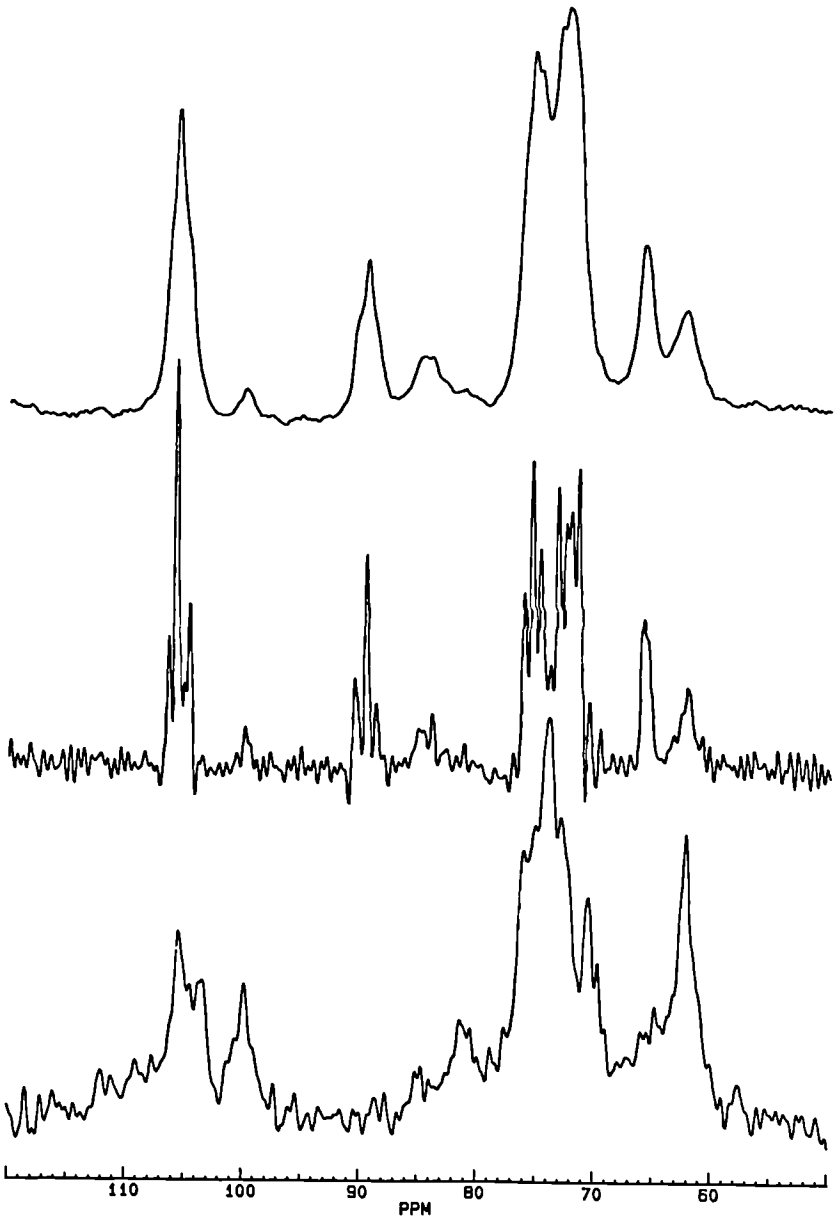

(a) CP/MAS spectrum of hydrated cellulose/xyloglucan/pectin composite and (b) after application of resolution enhancement (line broadening -70Hz, Gaussian multiplication, 0.5) and (c) SP/MAS spectrum showing essentially identical formed to spectra obtained from cellulose/xyloglucan composites (Figure 6.7), but the appearance in (c) of a putative methyl ester signal at ca. 65.5ppm, which indicates some pectin incorporation, as is inferred by the micrographs (Figure 8.7).

Interestingly, the NMR data indicates the presence of a methyl ester signal at ca. 65.5ppm in the SP/MAS spectrum, which must originate from pectin. In the absence of monsaccharide analysis, no firm conclusions can be drawn, but the appearance of this signal may suggest that the presence of xyloglucan facilitates pectin incorporation.

8.2.4 Xylans

At the ultrastructural level, the presence of 0.5% birchwood xylan in the culture medium of *Acetobacter* has little effect on network architecture (Figure 8.9) compared to controls (Figure 5.7). Isolated regions where cellulose fibres appear to align into bundles are occasionally observed (Figure 8.9b) but, from examination of many micrographs, structures essentially identical to controls predominate (Figure 8.9a). Similarly, when the initial concentration is increased to 2.0%, the majority of the composite exhibits no ultrastructural change (Figure 8.10a) although areas where the presence of a second polymer is apparent can be identified (Figure 8.10b). The micrographs provide no evidence for helicoidal arrays (Reis, *et al*, 1994; Vian *et al*, 1994) or reduction in cellulose fibre width.

Overall incorporation of xylan into the composite structure was very high, monosaccharide analysis giving a cellulose:xylan ratio of 1:0.25 ± 0.04 and 1:1.54 ± 0.11 for fermentations containing initial xylan concentrations of 0.5% and 2.0% respectively. This indicates that the rate of incorporation is increased at higher xylan concentrations, as incorporation at 2.0% after 2 days is greater than the four-fold increase in starting concentration. Despite the presence of significant amounts of xylan in the composite structure, very few regions are seen microscopically where individual xylan molecules can be identified (eg Figure 8.10b). This may be partly a function of the very low mwt of birchwood xylan (ca DP8, Uhlin *et al*, 1995), which would be difficult to visualise using this technique, but is also consistent with bulk alignment with cellulose.

The ^{13}C NMR spectra of cellulose/xylan composites produced in the presence of 0.5% xylan are shown

Figure 8.9: Micrographs of Composites Formed in the Presence of 0.5% Birchwood Xylan

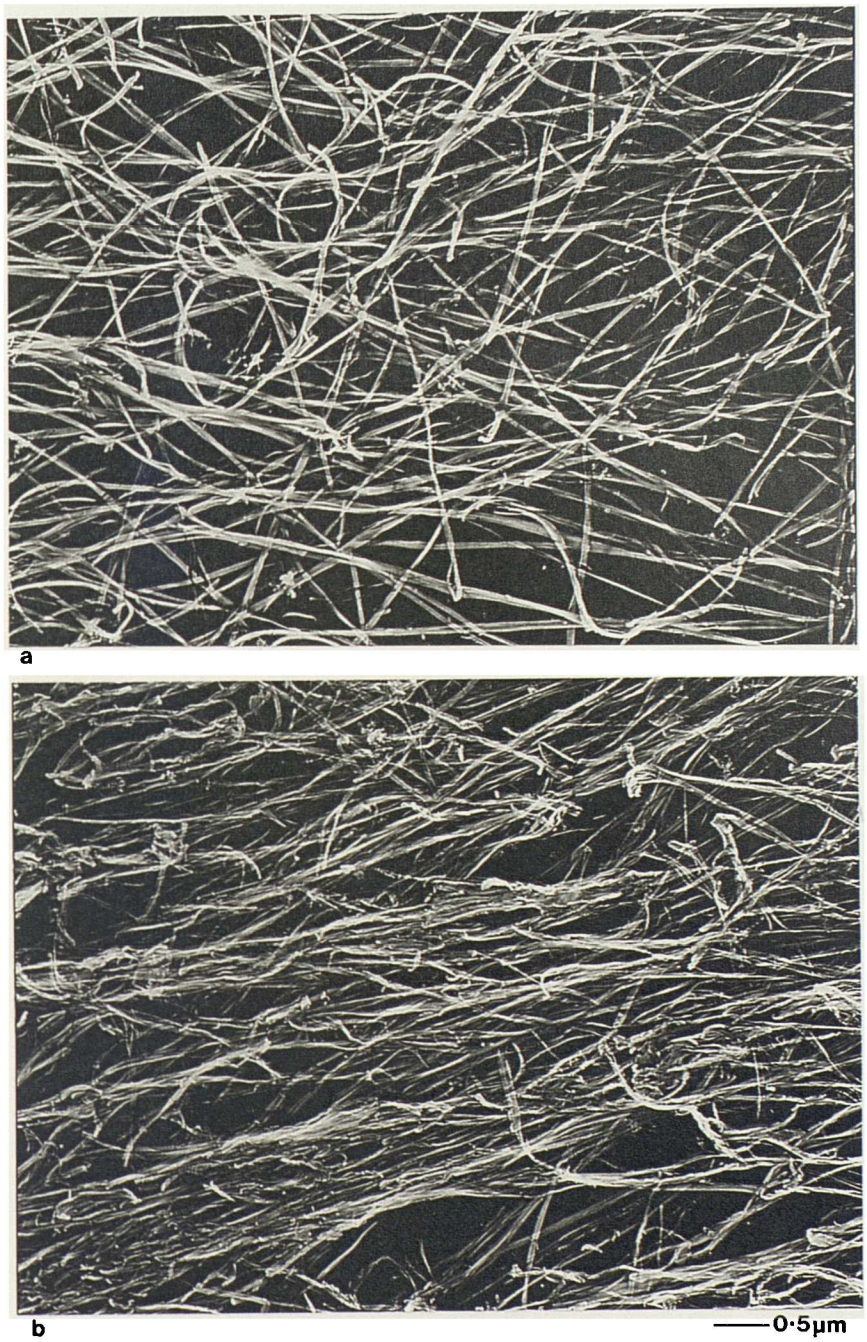

Micrographs of tungsten/tantalum/carbon replicas of hydrated cellulose/xylan composites produced by fermentation of *A.aceti* ssp. *xylinum* (ATCC 53524) in the presence of 0.5% xylan showing the bulk effect (a) to be the production of network architectures essentially identical to controls (Figure 5.7) but isolated regions (b) where fibres are aligned into composite ribbons.

Figure 8.10: Micrographs of Composites Formed in the Presence of 2.0% Birchwood Xylan

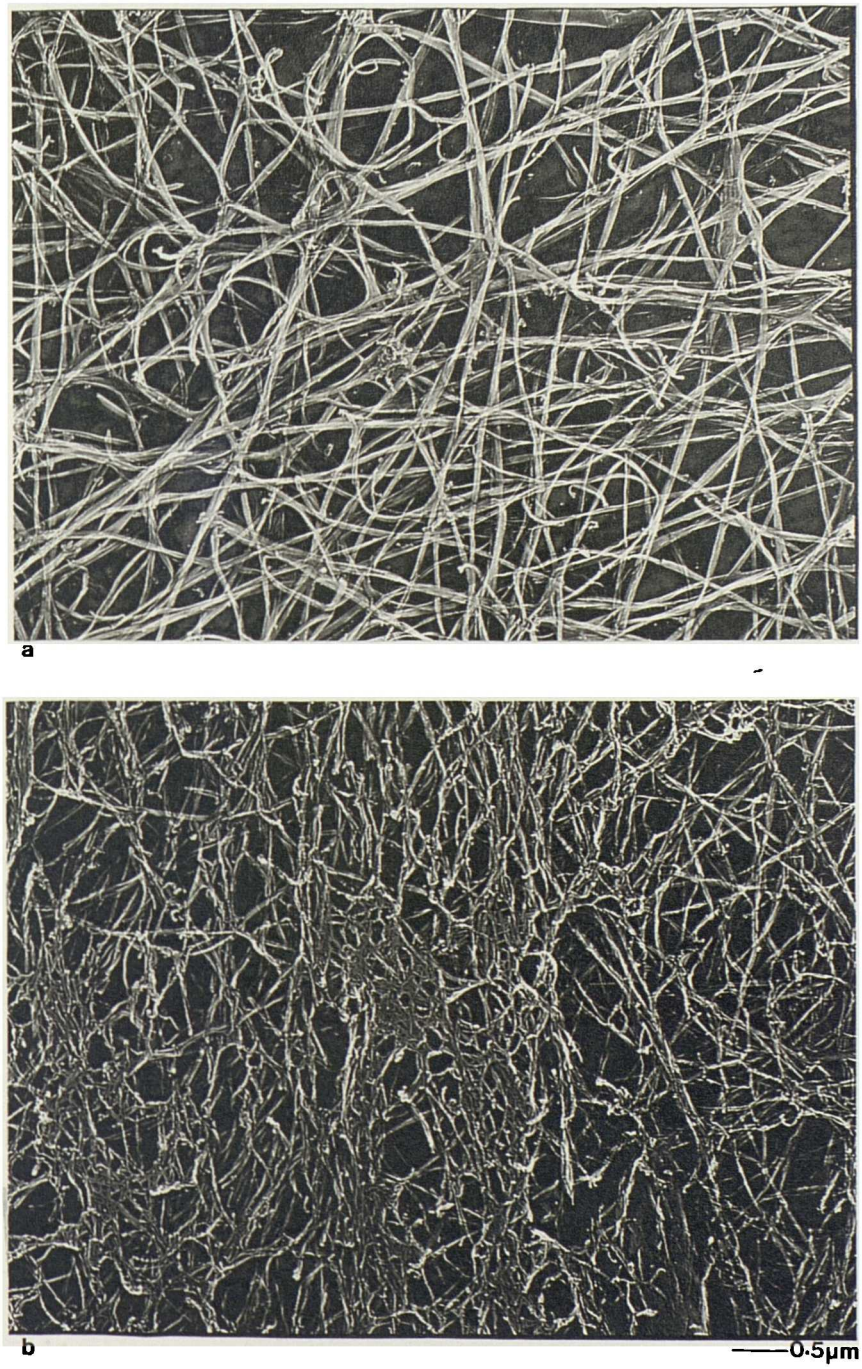

Micrographs of tungsten/tantalum/carbon replicas of hydrated cellulose/xylan composites produced by fermentation of *A.aceti* ssp. *xylinum* (ATCC 53524) in the presence of 2.0% xylan showing the bulk effect to be unaltered network architecture compared to controls (Figure 5.7 and cf Figure 8.9a), but isolated regions (b) where the presence of xylan is tentatively identified

Figure 8.11: ^{13}C NMR Spectra of Bacterial Cellulose/Xylan Composites (0.5% Xylan)

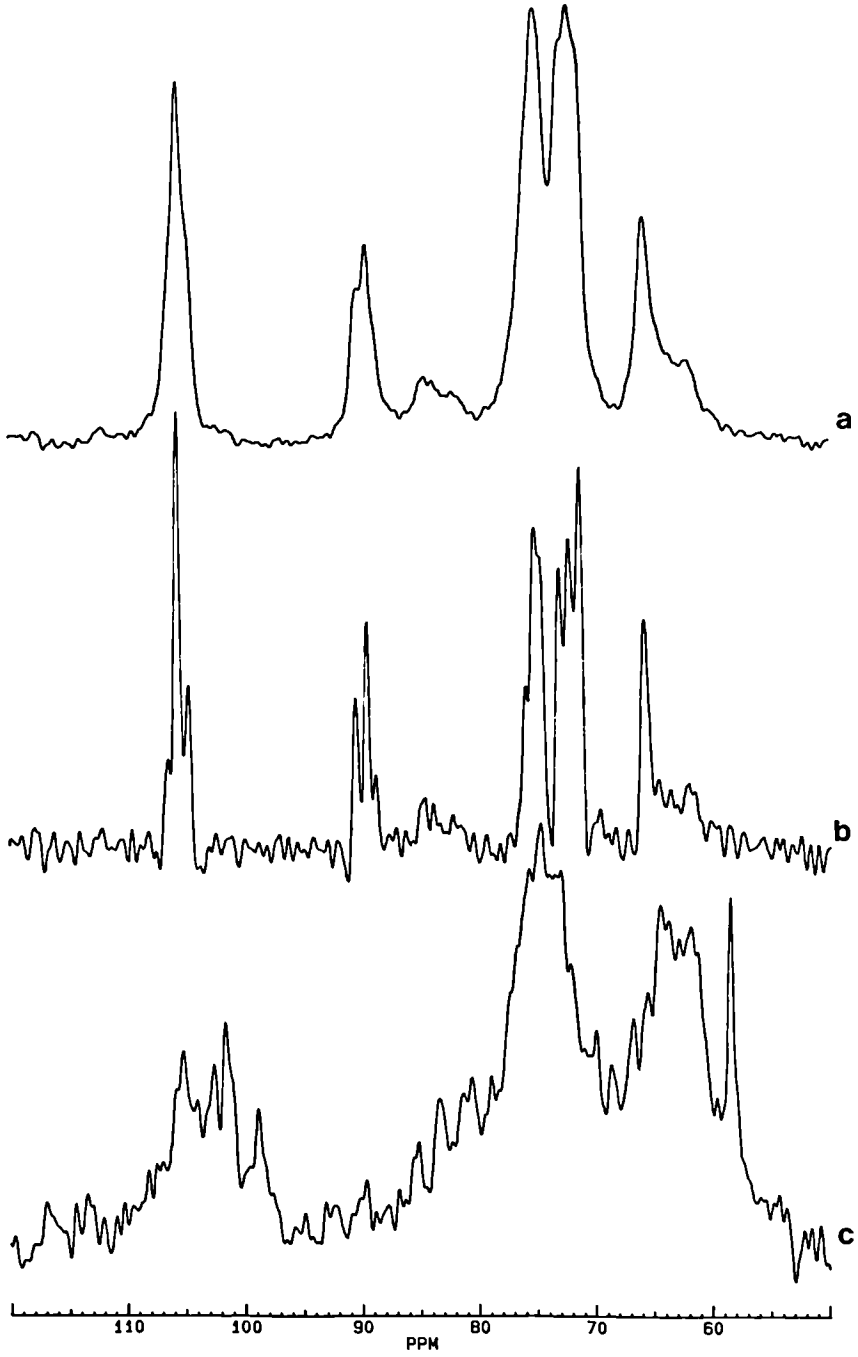

(a) ^{13}C CP/MAS spectrum of hydrated cellulose/xylan composites ex. *A.aceti* ssp. *xylinum* (ATCC 53524) produced in the presence of 0.5% birchwood xylan (cf Figure 8.9) and (b) as (a) after application of resolution enhancement (line broadening -70Hz, Gaussian multiplication 0.5) showing no unambiguous signals for xylan (compare Figure 8.15), apart from a possible broadening of the signal at C-4, and no effect on the molecular organisation of the cellulose component compared with controls (Figure 5.3). Poor signal:noise ratios of the SP/MAS spectrum (c) preclude signal assignment.

in Figure 8.11. Comparison of the CP/MAS spectrum (Figure 8.11a) with that obtained for native bacterial cellulose (Figure 5.3), integration of C-4 signals at 88-91 and 84-86ppm, corresponding to crystalline and non-crystalline environments of the cellulose component respectively (VanderHart & Atalla, 1984) and comparison of the splitting of the C-4 crystalline signal after resolution enhancement (Figure 8.11b) with published, quantified signal patterns (Debzi *et al*, 1991; Yamamoto & Horii, 1993) indicate essentially identical molecular organisation of the cellulose in the composite. The broadeningof the C-4 signal may be due to the presence of a C-4 signal for xylan. A significant downfield chemical shift of the C-4 signal of xylan from ca. 77ppm (Figure 8.13) to ca. 83ppm upon alignment with cellulose has been recently reported (Mitikka *et al*, 1995); no data on a corresponding shift for C-1 is currently available, although the evidence from composites produced in the presence of 2.0% xylan is that the shift is not significant (Figure 8.12). The CP/MAS spectra suggest that a significant proportion of the xylan may be present as a relatively mobile component, not aligned with cellulose and hence visible in the SP/MAS spectrum (Figure 8.11c). Poor signal:noise ratios in this spectrum preclude accurate signal assignment. The presence of significant quantities of xylan not associated with cellulose was not inferred from the micrographs unless, as described above, individual xylan molecules are present but cannot be visualised.

In contrast to Figure 8.11, the ^{13}C NMR spectra of composites produced in the presence of 2.0% xylan indicates the presence of significant quantities of xylan in the CP/MAS spectrum, consistent with its alignment with cellulose (Figure 8.12a). The chemical shift for the C-1 of xylan is recorded as 101.85 and a signal at 75.895 is assigned to C-4, essentialy identical to the chemical shifts for xylan in solution (Figure 8.13), after differences in internal referencing (ca. 1ppm) are taken into account. Identical chemical shifts are identified in the SP/MAS spectrum, which comprises relatively mobile (solution-state) xylan within the composite. However, this data does not support a conformational transition of xylan in the presence of cellulose, as reported by Mitikka *et al* (1995); since the appearance of such low mwt xylan in the CP/MAS spectrum is conclusive evidence of alignment with the cellulose component. The work of Mitikka *et al* (1995) used xylans from a different source (pulp wood) and examined sorption isotherms of *in vitro* binding, nevertheless, these chemical shift differences between

Figure 8.12: ^{13}C CP/MAS Spectra of Bacterial Cellulose/Xylan Composites (2.0% Xylan)

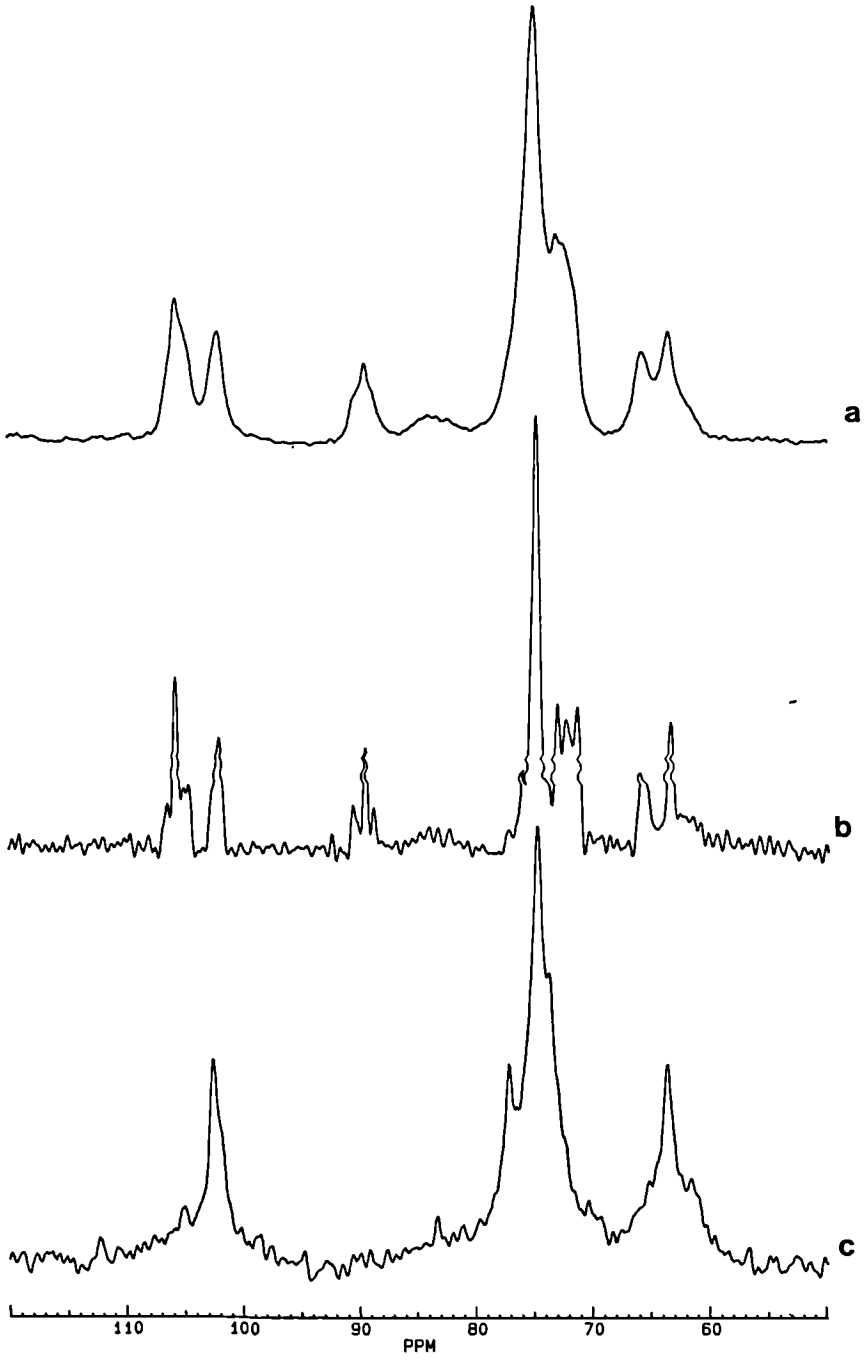

(a) CP/MAS spectrum of hydrated cellulose/xylan composite ex. *A.aceti* ssp. *xylinum* (ATCC 53524) produced in the presence of 2.0% xylan and (b) as (a) after application of resolution enhancement (line broadening -70Hz, Gaussian multiplication 0.5) showing signals at C-1 and C-4 coincident with the equivalent shifts for xylan in the solution state spectrum (c), indicating significant association of xylan with the cellulose component in the absence of conformational alterations of the xylan component

Figure 8.13: High Resolution ^{13}C NMR Spectrum of Birchwood Xylan

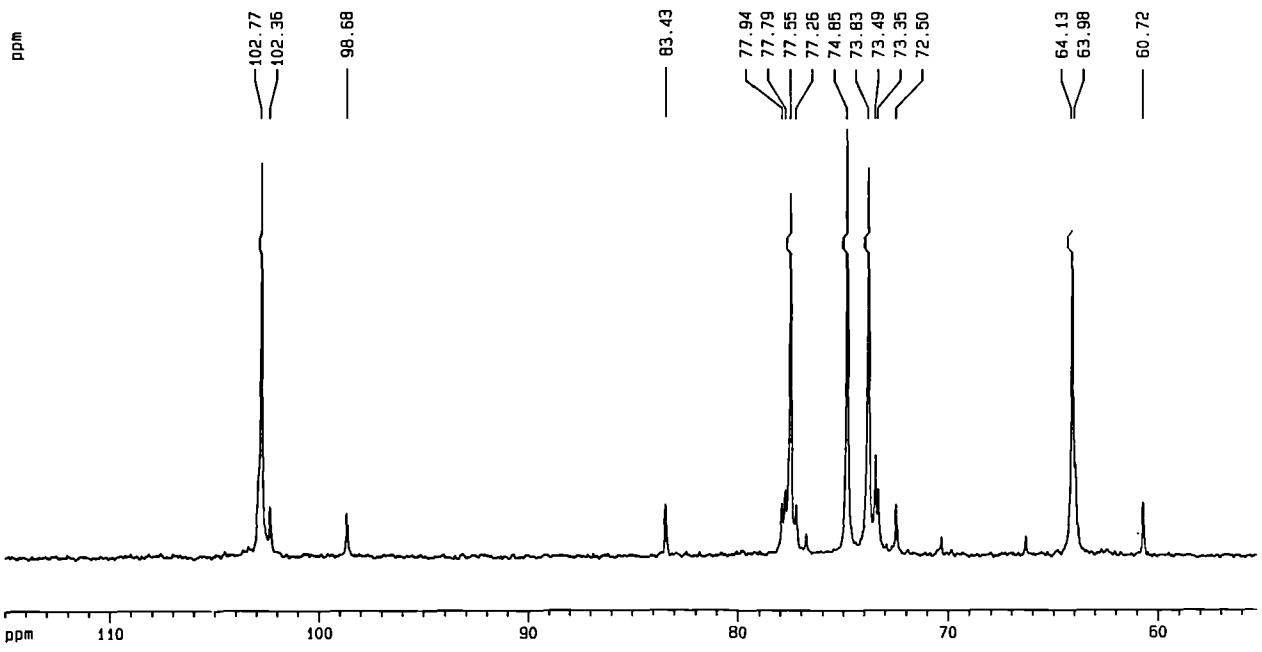

the two experimental protocols are difficult to reconcile in the absence of further data. The molecular organisation of the cellulose component in the cellulose/xylan composite is essentially unaltered (Figure 6.12a and b) relative to control cellulose (Figure 5.3b). A slight reduction in the crystallinity of the cellulose was recorded (to ca. 70%); accurate determination of thepercentage crystallinity was hampered by the broadness of the C-4 signal. This does not concur with the data of Uhlin *et al* (1995) who showed comparable effects on cellulose as was seen with xyloglucan. Since xylans used in both studies came from the same source, it is clear that much more work needs to be done on examining the interaction of xylans with cellulose in this system before definite conclusions can be be drawn.

8.3.5 Mixed-Linkage Glucans

As was mentioned in the introduction, the precise role of mixed-linkage glucans in type II cell walls remains unclear. Incorporation of these polysaccharides into the *Acetobacter* system was intended to provide evidence for whether mixed-linkage glucans could act as a molecular tether between cellulose fibres in a similar way as was demonstrated for xyloglucans (Chapter 6, Whitney *et al*, 1995). Transient molecular tethering of type II cell walls during elongation by these polysaccharides has been proposed (Carpita & Gibeaut, 1993).

The presence of mixed-linkage glucans in the fermentation medium apparently has no effect on the orientation of cellulose fibres within the structure (Figure 8.14). There is some evidence for association of cellulose fibres in isolated regions, but the overall alignment and cross-linking between cellulose fibres that was demonstrated with xyloglucan (Chapter 6, Whitney *et al*, 1995) is not apparent. The occurrence of very short polymer chain lengths emerging laterally from cellulose fibres is a consistent and unique feature of composites formed in the presence of mixed-linkage glucans, bing observed in the products of four separate fermentations. These may represent spliced regions of β-(1→3)-linked residues, cellodextrin-rich regions which would have no affinity for cellulose but, because of the conformation of the β-(1→3)-linkage, are regions of flexibility (Buliga *et al*, 1986). The function of

Figure 8.14: Micrographs of Composites Formed in the Presence of Mixed-Linkage Glucan

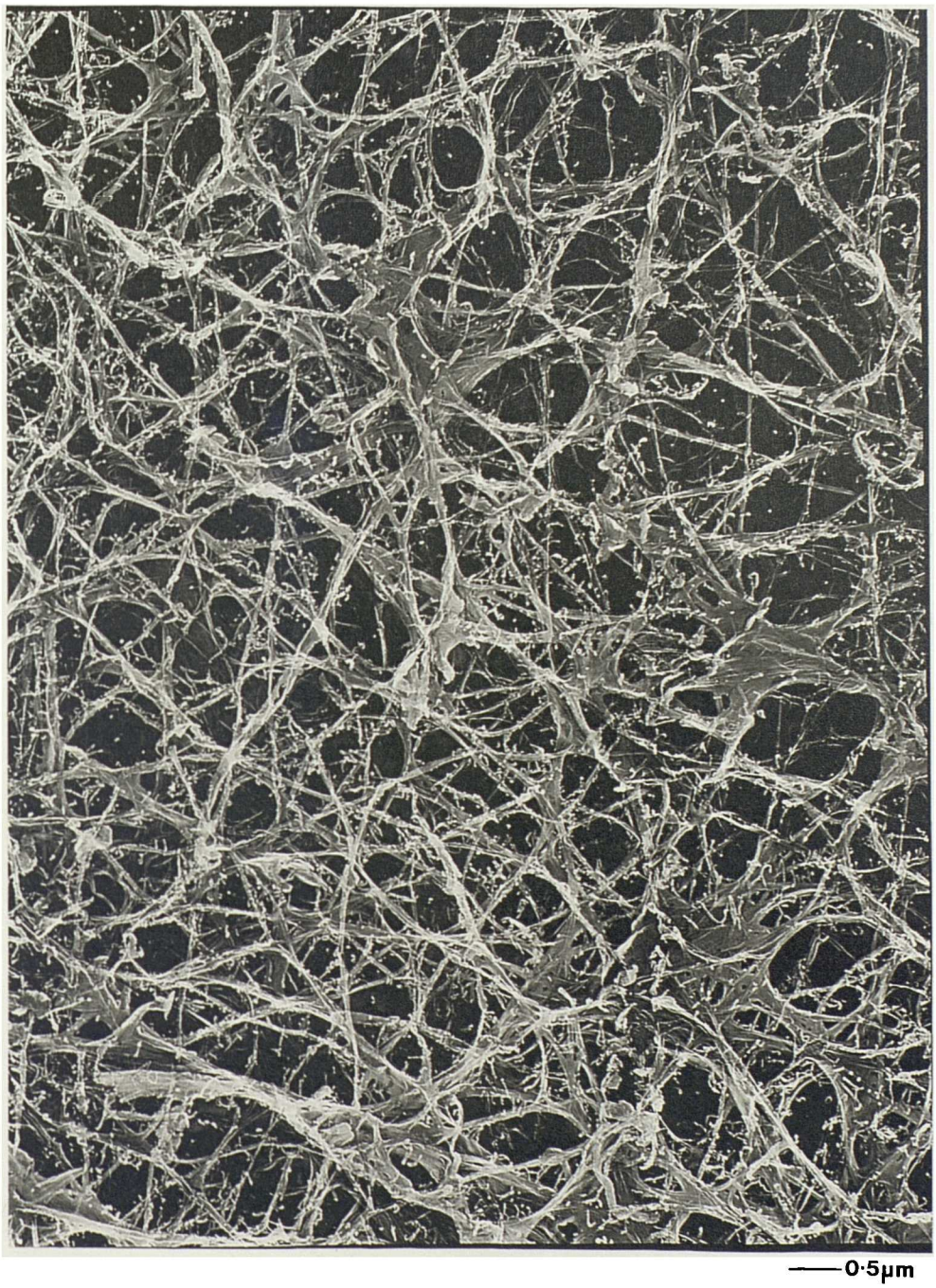

Micrograph of a hydrated cellulose/mixed-linkage glucan composite produced by fermentation of *A.aceti* ssp. *xylinum* (ATCC 53524) showing no evidence for overall fibre alignment or inter-fibre cross-linking (contrast Figure 6.2), but isolated regions of inter-fibre association and the unique presence of short polymer chain ends, believed to be mixed-linkage glucan, emerging laterally from cellulose fibres.

such regions located seemingly at the end of the molecule, remains unclear.

The ^{13}C CP/MAS spectrum of the cellulose/mixed-linkage glucan composite indicates the presence of a significant amount of mixed-linkage glucan that is relatively immobile and is therefore presumably aligned with the cellulose component (Figure 8.15a). The consistency of chemical shifts for mixed-linkage glucan in both the CP/MAS and SP/MAS (Figure 8.15c) imply a common conformational state and are indicative, therefore, of no transition in molecular conformation of the polymer on association with cellulose. The possibility that some of the mixed-linkage glucan component shares a cellulosic conformation cannot however be excluded, as chemical shifts would be coincident with those of cellulose. Regions rich in contiguous β-(1→4)-linkages might be predicted to have a cellulosic conformation in the presence of a cellulose template. The C-1 chemical shift for β-(1→3)- and β-(1→4)-linkages cannot be separated under those conditions, although they are effectively split using high resolution conditions, giving shifts at 103.66 and 103.43ppm for β-(1→3) and β-(1→4)-linkages respectively (Figure 8.16 and Bock *et al*, 1991). The lack of spectral resolution in the solid state spectra therefore precludes accurate assignment of relatively immobile or relatively mobile mixed-linkage glucans to regions rich in β-(1→4)- or β-(1→3)-linkages respectively. The mass fraction of mixed linkage glucan incorporated could be calculated by determining polymer ratios from the total weight of the pellicle vs. the weight of the assed glucan. This assumes that all the glucan is incorporatied, ie there is no turnover. Use of low temperature CP/MAS, coupled with the above information would allow integration of signals at ca. 105 and 103ppm, which would enable any conformational transition of the (1→4)-linkage to a cellulosic conformation to be determined

Analysis of the resolution enhanced CP/MAS spectrum (Figure 8.15b) indicates that the relative proportions of Iα and Iβ cellulose remain unaltered. The crystalline content of the composite cannot be determined due to overlapping signals for non-crystalline cellulose and mixed-linkage glucans, but could be if the above-mentioned analyses are performed.

Figure 8.15 ^{13}C NMR Spectra of Bacterial Cellulose/Mixed-linkage Glucan Composites

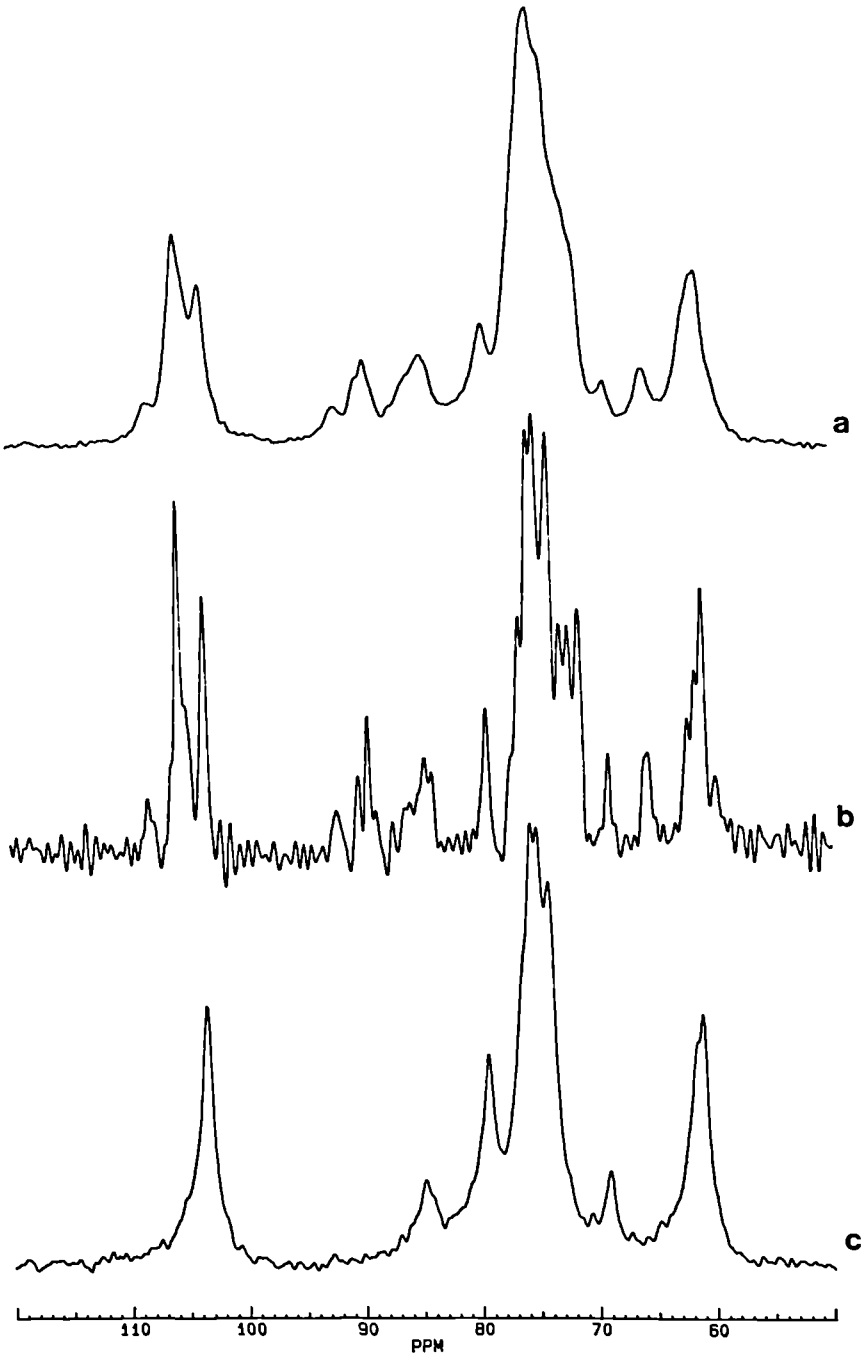

(a) CP/MAS spectrum of hydrated cellulose/mixed-linkage glucan composite ex. *A.aceti* ssp. *xylinum* (ATCC 53524) and (b) as (a) after application of resolution enhancement (line broadening -70Hz, Gaussian multiplication 0.5) showing signals for mixed-linkage gluacn, inferring alingment with cellulose, but with a consistency of chemical shifts for mixed linkage glucan in the SP/MAS spectrum (c) indicating a proportion of the mixed-linkage glucan is not in a cellulosic conformation. Minimal alteration of the molecular organisation of the cellulose component is apparent.

Figure 8.16: High Resolution ^{13}C NMR Spectrum of Barley Mixed-Linkage Glucan

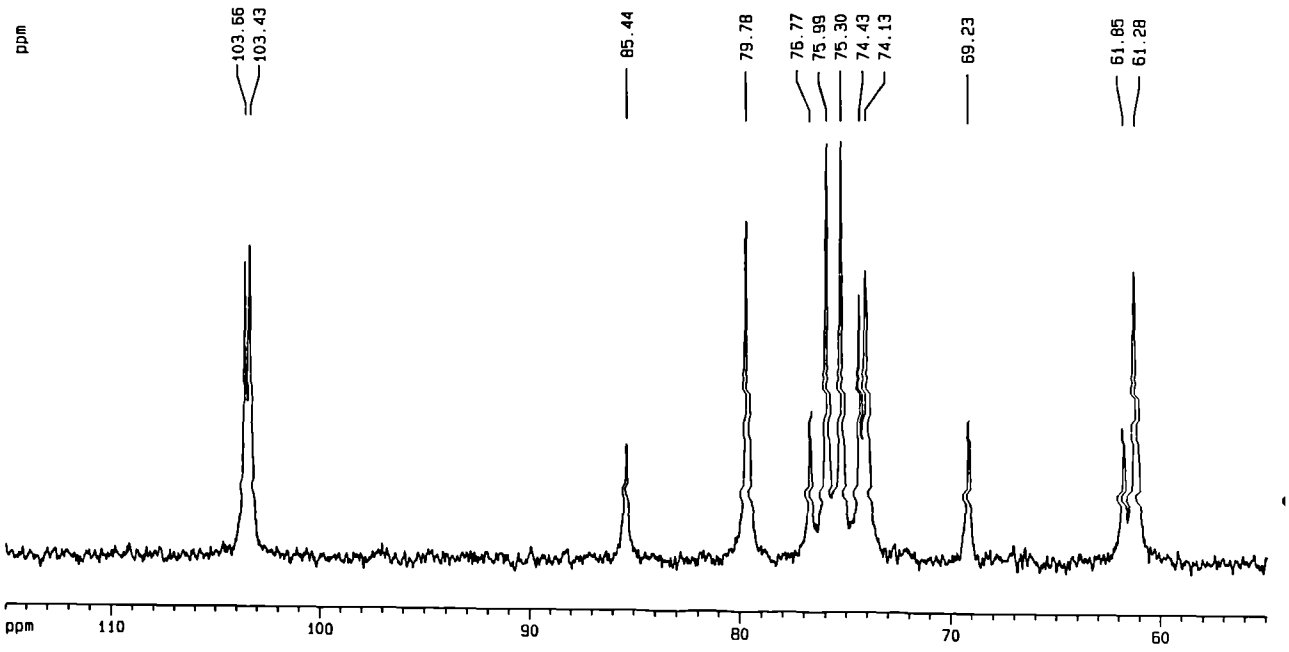

8.3.6 Galactomannans

Composites produced in the presence of 0.2% guar gum have apparently randomly oriented cellulose fibres similar to that seen in control incubations (Figure 5.7) interspersed with much thinner strands, approximately the width expected for single polysaccharide chains (Chapter 6, Whitney *et al,* 1995) (Figure 8.17). These thinner strands are attributed to guar galactomannan. The architecture of the cellulose/guar composite is consistent with the presence of two, discrete, independent networks,indicative of the absence of significant molecular interaction between the two composites. As galactomannans with a galactose content of greater than 30% (guar galactomannan Man:Gal = 62:38, Gidley *et al*, 1991b) show no evidence for intermolecular association (Dea & Morrison, 1975; Dea *et al*, 1986), we predict that the apparent network formed by guar in this system is not in fact a true gel network, but rather an entangled system of polymers trapped within the cellulose framework.

Figure 8.18 shows the ^{13}C NMR spectra of cellulose/guar composites. Signal:noise ratios are poor, particularly after application of resolution enhancement (Figure 8.18b). Calculation of crystalline:non-crystalline and Iα/Iβ ratios as previously described (section 8.3.1) gives a molecular organistaion for the cellulose component essentially identical to the controls (section 5.3.3). A putative signal at ca. 101ppm is identified, although the signal is weak and almost indistinguishable from the noise. The presence of a mannosyl C-1 signal in the CP/MAS spectrum is inferred from the SP/MAS spectrum, which shows resonances at both ca. 99.9 and 101.0ppm corresponding to galactosyl and mannosyl residues respectively (Figure 8.18c), but the proportions of the signals are very different from sugar analysis predictions ie there is greater intensity for the galactosyl resonance. The greater proportion of galactosyl signal in the SP/MAS spectrum indicates that a proportion of the mannosyl residues exhibit reduced mobility and may therefore be involved either in association with cellulose or in forming a gel network, consistent with visibilty in the CP/MAS spectrum. As was seen for hydrated (but not dry or milled) guar galactomannan which had the galactose content reduced by the action of α-galactosidase, there is a consistency of chemical shifts for mannosyl residues in solid-like and solution-like segments (Gidley *et al*, 1991b) and, in contrast to Konjac glucomannan (Chapter 7, this thesis) these authors also provide no evidence for a conformational change to a mannan I 'extended cellulosic' conformation

Figure 8.17: Micrograph of Composites Formed in the Presence of Guar Galactomannan

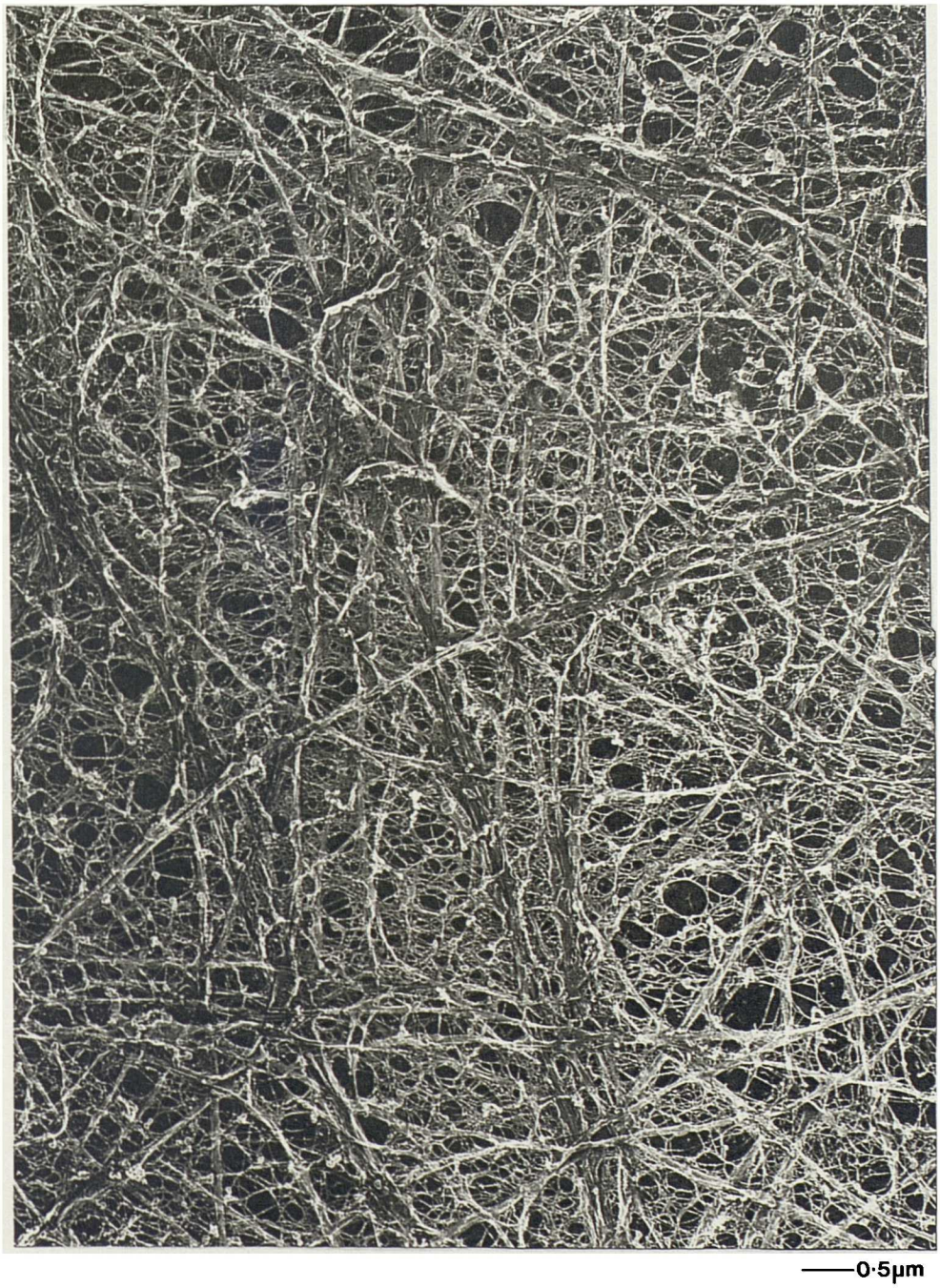

Micrograph of tungsten/tantalum/carbon replica of composites produced by fermentation of. *A.aceti* ssp. *xylinum* (ATCC 53524) produced in the presence of 0.2% guar, showing an apparently randomly oriented network of cellulose fibres independent of a guar galactomannan network comprising single polysaccharide strands. Man:Gal ratios predict that the majority of the galactomannan network arises from entanglement of strands within a cellulose framework rather than a true gel structure

Figure 8.18 ^{13}C NMR Spectra of a Celluose/Guar Composite

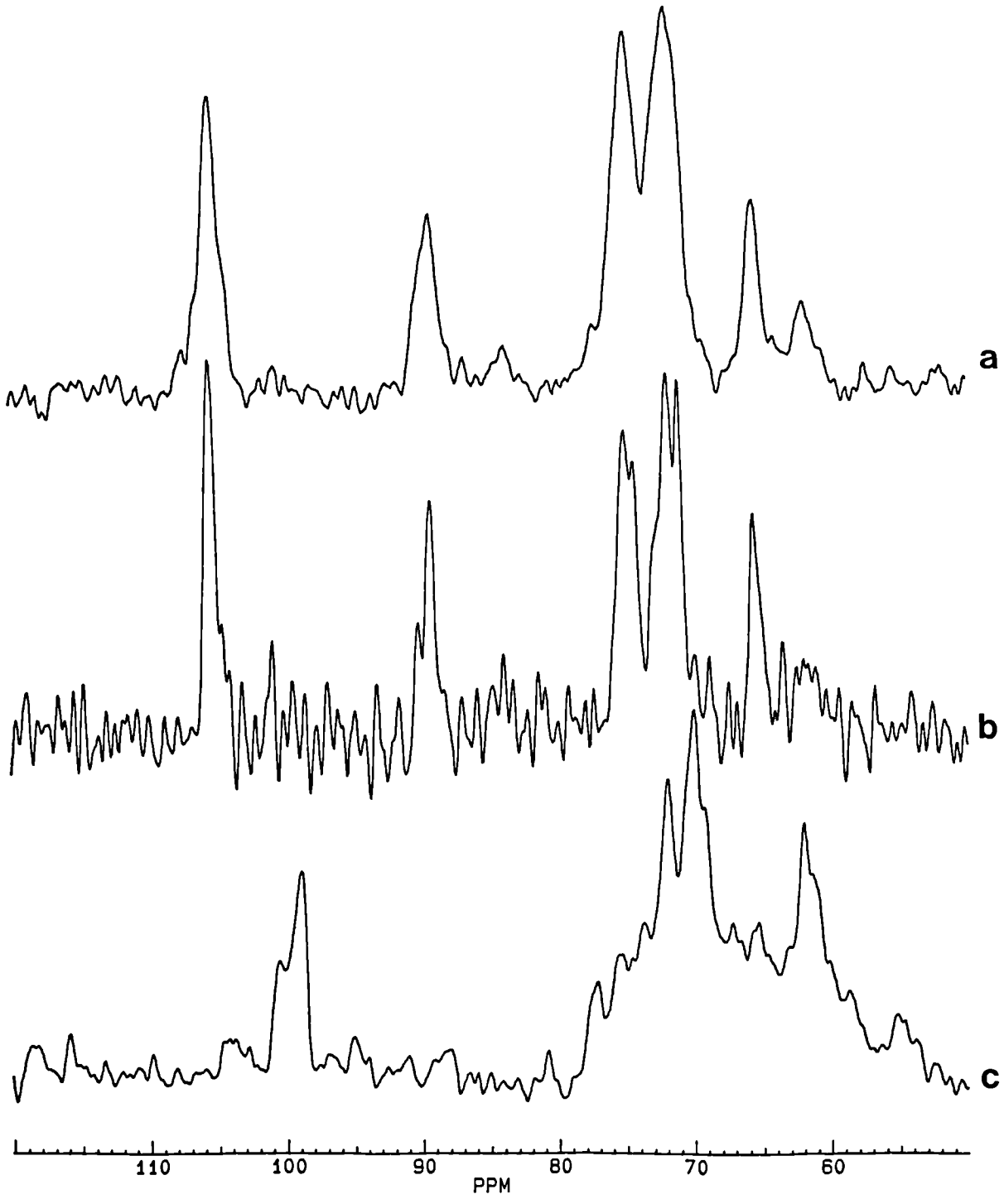

(a) ^{13}C CP/MAS NMR spectrum of cellulose ex. *A.aceti* spp. *xylinum* (ATCC 53524) produced in the presence of 0.2% guar (cf Figure 8.16) showing unaltered crystallinity of the cellulose component compared to controls (Figure 5.3b) and a putative mannosyl residue at ca. 101ppm; (b) as (a) after application of resolution enhancement (Line broadening -70Hz, Gaussian multiplication 0.5) illustrating similar fine structure to controls (Figure 5.5a), (c)SP/MAS spectrum of (a) illustrating signals at ca. 100 and 101ppm assigned to galactosyl and mannosyl residues respectively (Gidley *et al*, 1991b), but in a different proportion to that inferred by sugar analysis, indicating preferential involvement of mannosyl residues in forming 'solid-like' structures

Figure 8.19: Micrographs of a Cellulose/LBG Galactomannan Composite

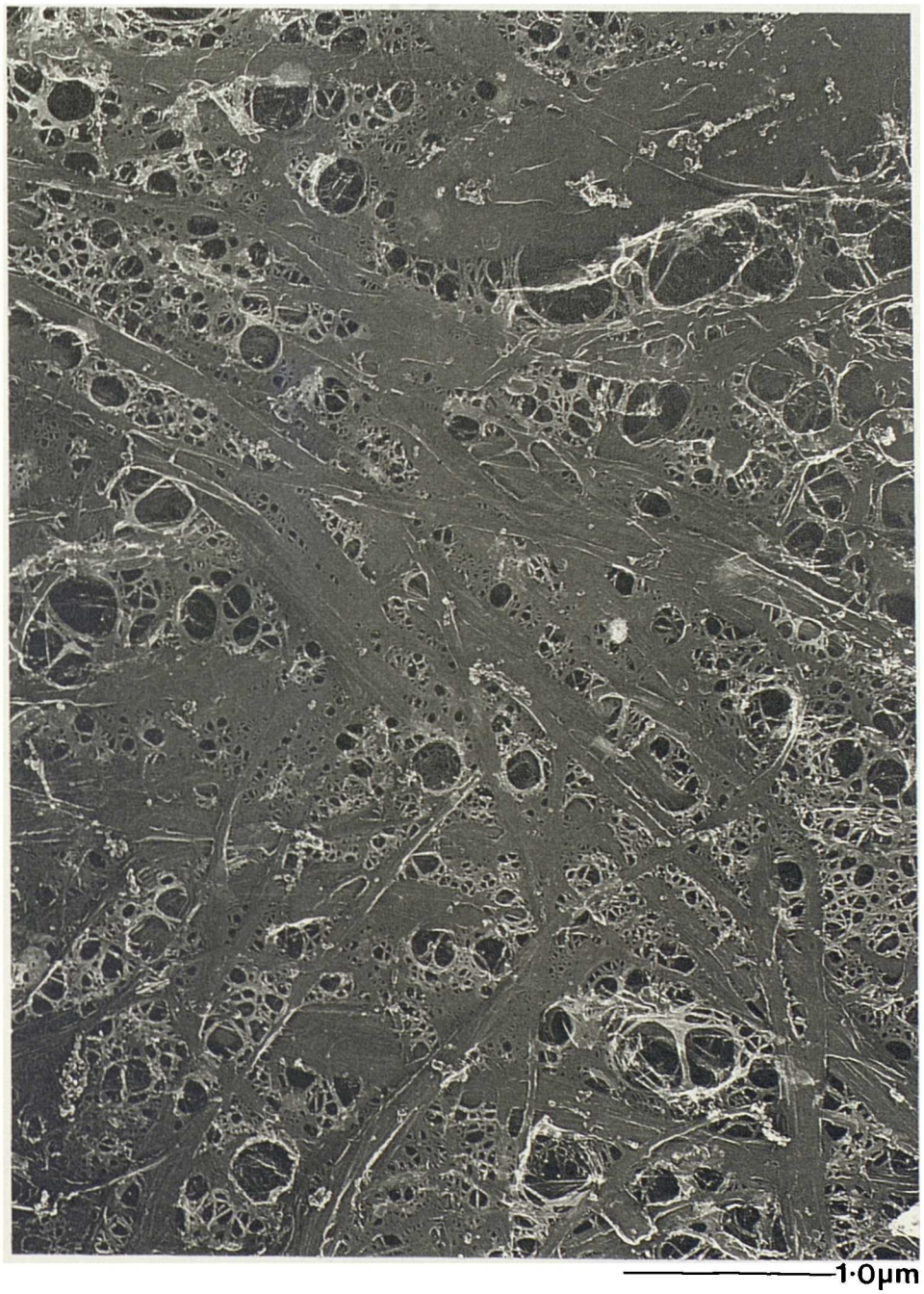

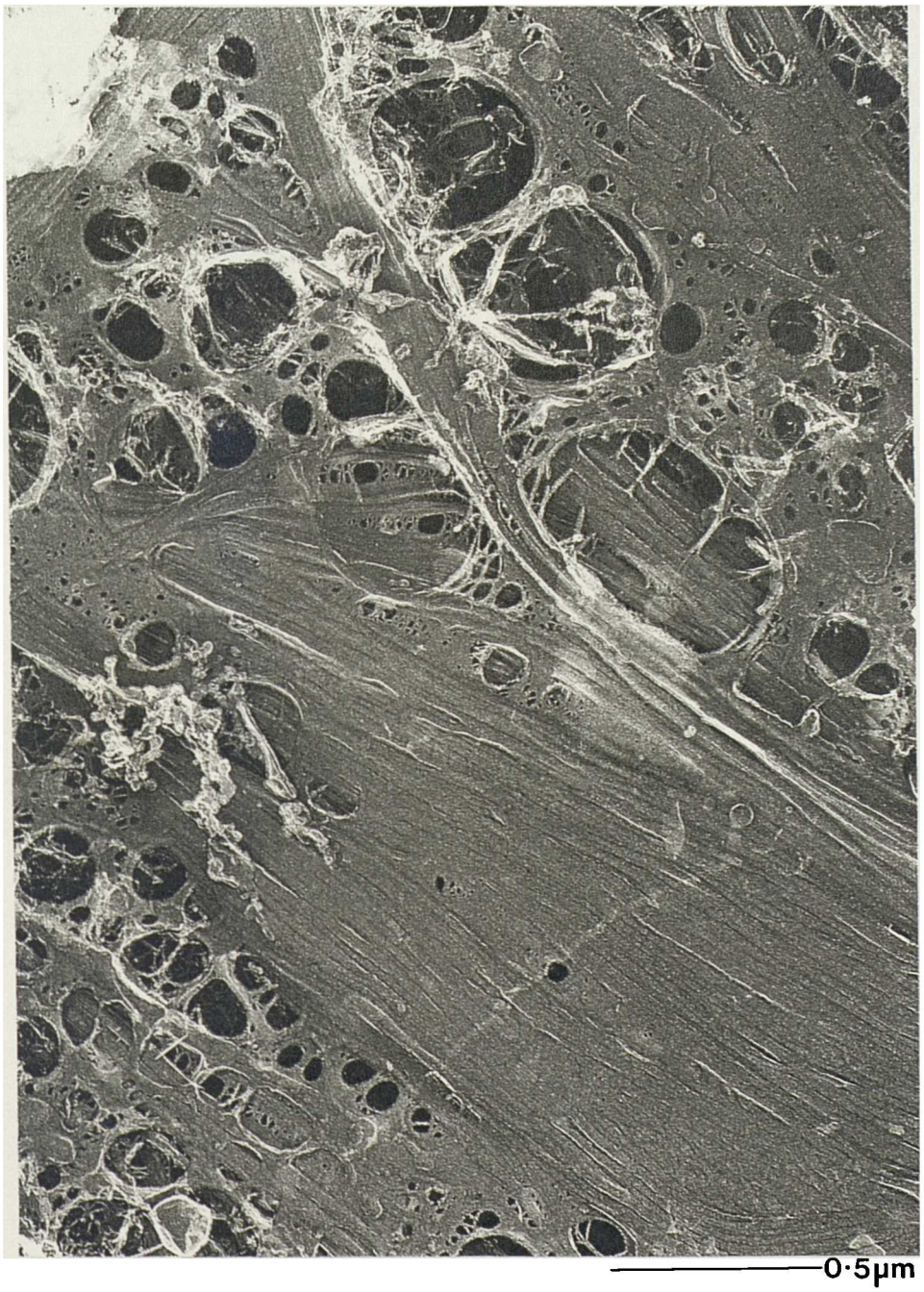

Micrographs of tungsten/tantalum/carbon replicas of composites produced by fermentation of *A.aceti* ssp. *xylinum* (ATCC 53524) in the presence of 0.2% LBG galactomannan, illustrating a randomly oriented network of cellulose fibres and a network of LBG galactomanna, with some evidence for LBG/cellulose association (a) and regions in which the presence of LBG has apparently constrained the cellulose fibres such that they are forced into parallel alignment (b)

Figure 8.20: ^{13}C CP/MAS Spectra of Cellulose/LBG Galactomannan Composites

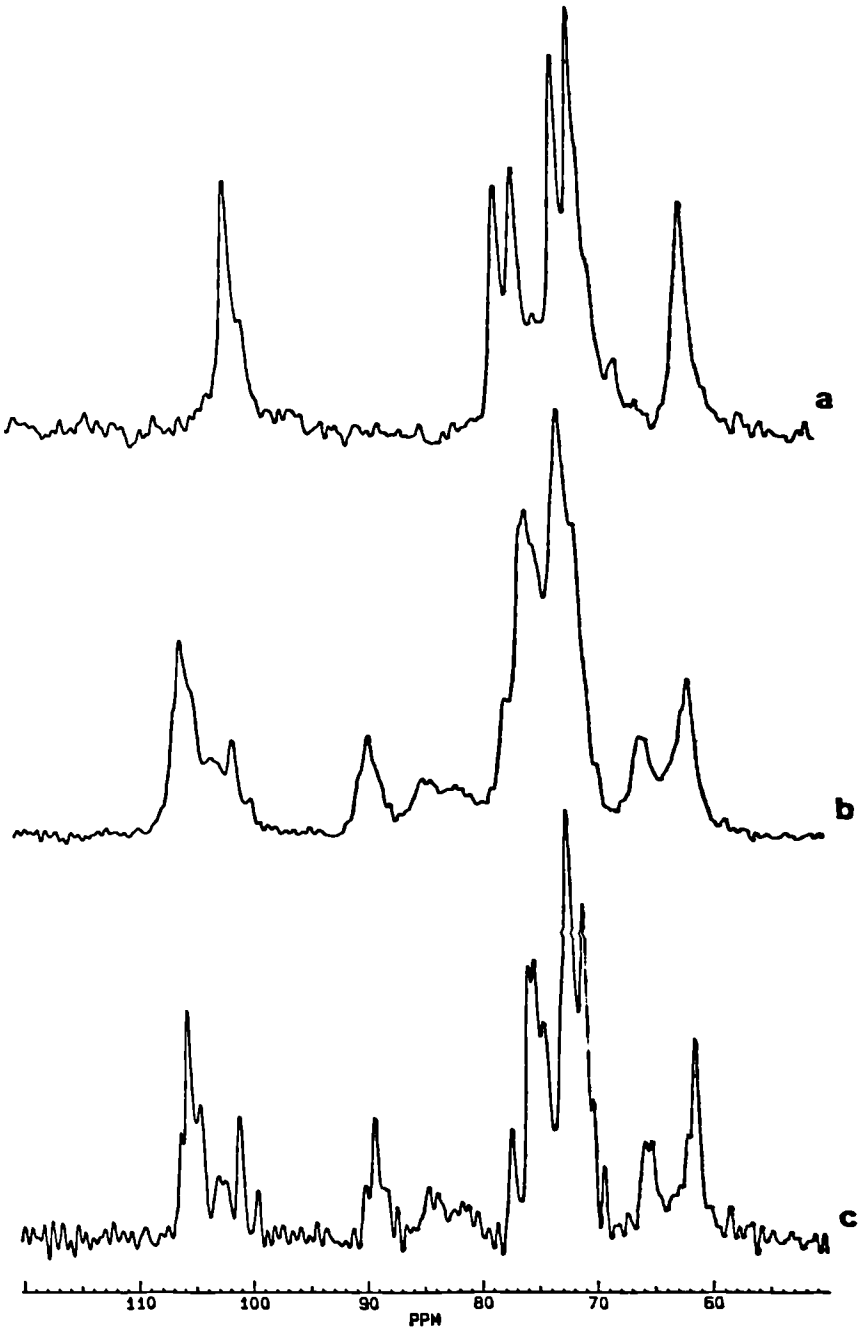

(a) Spectrum of LBG gel showing signals at ca. 101 and 100ppm assigned to C-1 of mannosyl and galactosyl residues respectively, (b) hydrated cellulose/LBG composite ex. *A.aceti* ssp. *xylinum* (cf Figure 8.18) showing an reduction in the crystallinity of the cellulose component, the presence of signals at ca. 101.0 and 99.6ppm consistent with the formation of an LBG gel and the appearance of additional signals at ca. 102.8 and 102.5ppm, the latter signal assigned to mannosyl C-1 of mannan I, (c) as (b) after application of resolution enhancement (line broadening -70Hz, Gaussian multiplication 0.5) showing altered fine-structure on C-4 indicative of altered Iα/Iβ ratios

Figure 8.21: ^{13}C SP/MAS Spectra of Cellulose/LBG Galactomannan Composites

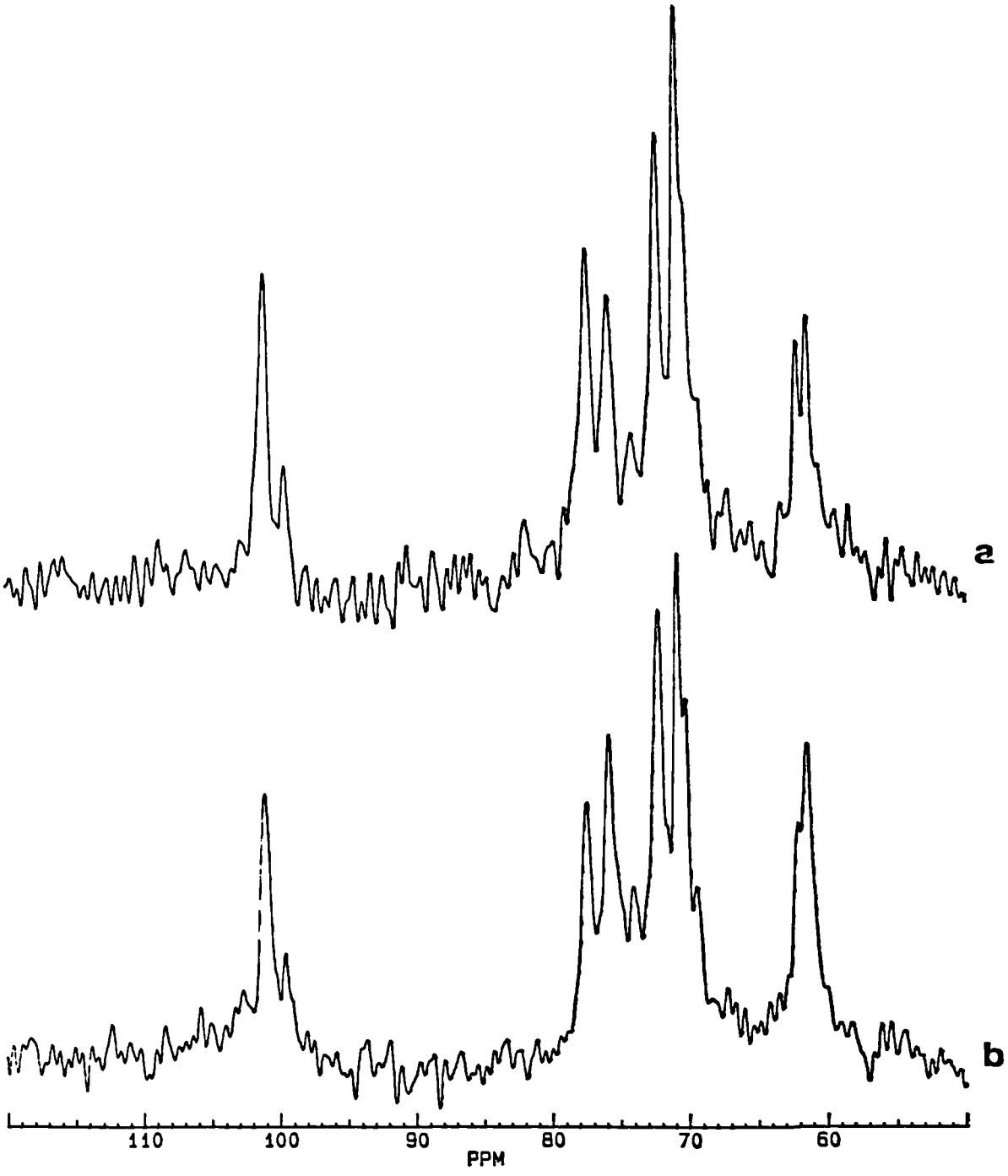

Spectra of (a) native LBG gel and (b) hydrated cellulose/LBG composite ex *A.aceti* ssp. *xylinum* showing a consistency of chemical shifts for mannosyl and galactosyl C-1 signals (ca. 101 and 99.6ppm respectively) between (a) and (b) and LBG gel (Figure 8.18a and b)

(Chanzy *et al*, 1982). Combining NMR and microscopical evidence it appears that, contrary to prediction, therefore there has apparently been some association of guar galactomannan into a gel-like structure.

After incubation with LBG galactomannan a composite with a very different molecular architecture is formed (Figure 8.19). Galactomannan apparently self associates, as predicted from its Man:Gal ratio (Dea & Morrison, 1975; Dea *et al,* 1986), but there is also evidence for inter-fibre association mediated by galactomannan. There is also evidence that the presence of an LBG network can force the cellulose fibres into parallel alignment, creating thick bundles of fibres (Figure 8.19b). These structures are unique to the cellulose/LBG system and the occurrence of this entropically unfavourable event is probably a reflection of the constraining effect of the formation of a permanent gel network concomitant with cellulose synthesis on cellulose fibre orientation.

As predicted from the micrographs, the ^{13}C CP/MAS spectrum of the cellulose/LBG composite (Figure 8.20b) illustrates the presence of signals for mannosyl and galactosyl residues (ca. 101.0 and 99.6ppm respectively) with chemical shifts coincident with equivalent signals in a native LBG gel (Figure 8.20a). As predicted there is relative enrichment of the mannosyl signal in the gel spectrum (Gidley *et al*, 1991b). The appearance of a signal at ca. 102.5ppm is consistent with an induced conformational alteration of LBG in the presence of a cellulose template, the chemical shift of this signal being essentially coincident with that reported for mannosyl C-1 of the mannan I 'extended cellulosic' conformation (Chanzy *et al*, 1982). The slight chemical shift difference may be due to differences between mannan-mannan and cellulose-mannan interactions. The additional signal slightly downfield (ca. 102.8ppm) may also be due to mannosyl C-1 in a similar chain conformation

The presence of LBG alters the molecular conformation of the cellulose component when crystalline:non-crystalline ratios are determined (see section 8.3.1). Crystallinity is reduced to 55% compared with controls (section 5.3.3) and the Iα/Iβ ratio changed to ca. 50:50, giving an overall

molecular description for cellulose synthesised in the presence of LBG of 27.5% Iα, 27.5% Iβ and 45% non-crystalline, compared with 57% Iα, 25% Iβ and 18% non-crystalline for controls (section 5.3.3).

A consistency of chemical shifts is seen for relatively mobile LBG in both a pure gel and in the cellulose/LBG composite (Figure 8.21). The evidence from ^{13}C NMR spectroscopy closely correlates with the interpretation of the electron micrographs (Figure 8.19) namely that, in the composite, LBG forms an independent gel network with identical molecular characteristics to native gels, but a proportion also associates with the cellulose, causing conformational alteration of LBG to an 'extended-cellulosic' conformation and having profound effects on the molecular organisation of the cellulose component.

8.4 Discussion

The aim of this chapter was to characterise, at the ultrastructural and molecular level, the effect of addition of a range of polymeric additives to *Acetobacter aceti* ssp. *xylinum* in an attempt to determine the potential of the fermentation system for examining interactions with cellulose. It is clear from the results that, for most of the polymers added, much more characterisation work on the composites is required than was performed for this thesis. Nevertheless, for a number of additions, some useful information has been gained.

The interaction of CMC with *Acetobacter* cellullose has been previously described (Haigler et al, 1982; Uhlin *et al*, 1995; Yamamoto & Horii, 1994). It was encouraging that, in the presence of CMC, overall fibre dimensions were seen to reduce, in concurrence with published results (Haigler *et al*, 1982). This suggests that the unaltered fibre dimensions seen in the presence of xyloglucan (Chapter 6) which contrasted with previously published data (Hayashi *et al*, 1987; Uhlin *et al*, 1995; Yamamoto & Horii,

Chapter 6, discussion). CMC has a β-1,4-linked backbone, substituted with charged carboxymethyl groups. The backbone of CMC could, in principle, associate with cellulose by hydrogen bonding between the β-glucan chains, but further association between cellulose subunits may be impeded by the presence of charged substituent groups, either by steric hindrance or electrostatic repulsion (Haigler *et al*, 1982), resulting in alteration of normal microfibril fasciation into ribbons. That there is a profound effect on cellulose molecular organisation in the presence of CMC concurs with results from other groups (Uhlin et al, 1995; Yamamoto & Horii, 1994) and provides strong evidence for an intimate association between the two components. Evidence obtained in this study is therefore shown to agree closely with other results (Haigler *et al*, 1982; Uhlin *et al*, 1995; Yamamoto & Horii, 1994).

A small percentage of the total pectin in plant cell walls remains associated with the cellulose component, even after concentrated alkali treatments (Mitchell, J., Unilever Research, pers.comm.; Redgwell & Selvendran, 1986; Ryden & Selvendran, 1990; Seymour *et al*, 1990). The chemical basis for this interaction has yet to be elucidated. In the bacterial fermentation system, there was no evidence for cellulose/pectin association. However, pectins within the cell wall are highly heterogeneous and the use of just one model pectin may not give the correct chemnical characteristics enabling binding to cellulose. Moreover, although pectin with a relatively high DE was used in this study, it is thought that, in the cell wall, pectin may be deposited as a completely esterified molecule and subsequently de-esterified, as is seen during cell plate deposition (Roberts, K., John Innes Institute, pers.comm.). The failure to incorporate this particular pectin and hence, the inability to synthesise a model 'cell-wall' by the addition of pectin and xyloglucan, is more likely to be due to use of an inappropriate pectin source. Future work in this laboratory will extend this investigation to look at pectins of different types.

The interaction of cellulose with glucuronoxylans has been extensively studied by Vians group (Reis *et al*, 1991;1992;1994; Vian *et al*, 1992, 1994). Glucuronoxylans are believed to coat cellulose microfibrils, imparting a negative charge which may be necessary for maintaing intra-microfibril spacing necessary for orientation in a cholesteric mesophase (Vian *et al*, 1992) and are proposed to

play a key role in composite cholesteric assembly, acting as a 'twisting agent' (Reis *et al*, 1994). No evidence is provided for helicoidal asembly of celluloses fibres in this system.

It is of concern that, in examining the interactions of cellulose and birchwood xylan in this system there is no evidence for alteration of cellulose fibre dimensions or molecular organisation of the cellulose component. Previous work (Uhlin *et al*, 1995) reported significant reduction in the size of cellulose fibres in the presence of birchwood xylan, although it should be noted that similar reductions were observed with xyloglucan by these authors, which are not demonstrated in this system. It could be envisaged that a glucuronoxylan with a greater negative charge than this sample could interfere with microfibril fasciation in a similar way as described for CMC (see above). Furthermore, the molecular organisation of the cellulose component is essentially unchanged, in direct contrast to previous work (Atalla *et al*, 1993; Uhlin *et al*, 1995), even though there is evidence for alignment of xylan with the cellulose (conferring visibility in the CP/MAS spectrum). Additionally this study provides no evidence for a conformational transition of xylan in the presence of a cellulose template (contrast Mitikka *et al*, 1995). It is clear that the interaction of xylan with cellulose in this system needs considerably more investigation. The study of higher mwt xylans from different sources would be useful in this context.

The role of mixed-linkage glucans in the Type II cell wall (Carpita & Gibeaut, 1993) has not been elucidated in this study. The unique appearance of 'loose polymer chain ends' in cellulose/mixed-linkage glucan composites, prompted the suggestion that these may in fact be cello-dextrin rich regions, which are highly flexible and would not bind to cellulose. Contiguous β-(1→3)-linkages have been previously proposed be facilitate the molecule to act as a molecular thread during elongation (Carpita & Gibeaut, 1993), however, from examination of the micrographs, the very short polymer chains are unlikely to be available for cross-linking. In the presence of suitable enzymes however, which could splice these ends together (Buliga *et al*, 1986), these polymer ends could be connected to form a thread which interlocks cellulose fibres. The lack of spectral resolution precluded assignment of

bound and free mixed-linkage glucan to β-(1→4)- and β-(1→3)-rich regions respectively to further validate this hypothesis.

Galactomannans have been shown to interact strongly with other polysaccharides to form 'mixed-gels' (Fernandes *et al*, 1991; Goycoolea *et al*, 1995; Murayama *et al*, 1995a,b; Stading & Hermansson, 1993; Viebke, C., 1995). Incorporation of LBG galactomannan into cellulose-synthesising cultures of *Acetobacter* has provided evidence of association at the molecular level, with cellulose acting as a template for conformational transitions of the galactomannan component, similar to that seen with glucomannan (Chapter 7, this thesis).

From the above discussion, it is apparent that added polymers interact with newly synthesised cellulose in specific ways. The work presented is essentially preliminary data, but provides encouragement that *Acetobacter aceti* ssp. *xylinum* may indeed prove very useful in elucidating cellulose-polysaccharide interactions in a range of different systems.

Chapter 9: Purification and Characterisation of Xyloglucan from Tomato (*Lycopersicon esculentum*) and Pea (*Pisum sativum*) Stem

9.1 Introduction

As a major hemicellulose of dicotyledonous and non-graminaceous moncotyledonous plants, the chemical structure of xyloglucan has been extensively investigated. Probably the best studied xyloglucans have been obtained from suspension-cultured sycamore cells by Albersheims group (Bauer *et al*, 1973; Hisamatsu *et al*, 1991, 1992; York *et al*, 1988, 1990, 1995), but xyloglucans from other sources such as legume seedling stems (Kato & Matsuda, 1976, 1980b; Paully *et al*, 1995), tamarind seeds (Gidley *et al*, 1991; York *et al*, 1993) and apples (Renard *et al*, 1992) have also been characterised. The structure and functions of xyloglucan have been comprehensively reviewed by Fry (1989) and Hayashi (1987).

The basic chemical structure of xyloglucan was described in Chapter 1 (Section 1.5.1). The cellulosic backbone of β-1,4-linked glucan is substituted at position 6 with α-D-xylopyranose, with xyloglucan from dicotyledons and non-graminaceous monocotyledons typically being much more heavily substituted than that isolated from graminaceous monocotyledons (Hayashi, 1987). Further species-specific substitution of xylose with galactose, galactose-fucose or arabinose residues may also occur and variation of xyloglucan oligosaccharide composition between populations of the same species has been reported (Buckeridge *et al*, 1992). Some xyloglucan oligosaccharides, particularly those with a fucose residue, have biological activity (Farkas & Maclachlan, 1988a; McDougall & Fry, 1988, 1989a,b, 1990, 1991; York *et al*, 1984) ie they are 'oligosaccharins' (Aldington & Fry, 1993). It has been demonstrated that an *Arabidopsis Fuc*$^{-}$ mutant (Reiter *et al* 1993) can functionally replace fucose with galactose, giving the side chain Gal (1→2)-Gal-(1→2)-Xyl-(1→6)-Glc or , in current

nomenclature, J (York *et al* 1996). The oligosaccharide XXJG shows comparable biological activity to XXFG (York *et al*, 1996).

As a major world producer, Unilever has a particular interest in tomato fruit. Work is in progress in this laboratory to establish the cell wall architecture of different tomato varieties at different ripening stages, with the aim of correlating this structure with textural attributes of tomato pastes. In conjunction with this research, cell wall modifying enzymes are being characterised and transgenic plants containing genes encoding these enzymes produced. As a component of the major load-bearing cell wall network, whose modification might be predicted to profoundly affect network architecture and hence textural properties, xyloglucan and its modifying enzymes have been a particular focus for research. Xyloglucan comprises ca. 7% of total cell wall carbohydrate of the processing tomato variety 6203 (Mitchell, J. Unilever Research, pers.comm.). The molecular mass of xyloglucan in red tomato fruit is half that of green (Sakurai & Nevins, 1993, 1995), and it has been suggested that xyloglucan hydrolysis contributes to fruit softening (Sakurai & Nevins, 1993). Despite its commercial importance however, tomato fruit xyloglucan has not been extensively characterised. Seymour *et al* (1990) report that, unlike most dicotyledonous primary cell wall xyloglucan, tomato xyloglucan is non-fucosylated. As a member of the Solanaceae, it might be predicted that tomato xyloglucan is either an arabinoxyloglucan as seen in tobacco (Akiyama & Kato, 1982; Eda & Kato, 1978; Eda *et al*, 1983; Mori *et al*, 1979; Sims & Bacic, 1995) or an arabinogalactoxyloglucan as found in potato (Ring & Selvendran, 1981; Vincken *et al*, 1996). The first part of this chapter focuses on the characterisation of xyloglucan obtained from mature green processing tomato fruit.

The second half of this chapter descibes work involved in purification of xyloglucan from dark-grown pea stems. Unlike tomato xyloglucan, pea xyloglucan has been extensively characterised. In common with other primary cell wall xyloglucans from dicotyledons and non-graminaceous monocotyledons, pea xyloglucan is fucosylated and was reported by Hayashi & Maclachlan (1984) to comprise the two oligosaccharides XXXG and XXFG in equimolar proportions. More recently, Pauly *et al* (1995) have

shown that the structure is more complicated than this, with other oligosaccharides such as XLFG, XXLG, XLXG, XXG, XG, GXXG and GXFG being identified. The oligosaccharides XXLG and/or XLXG, XXFG and XLFG are mono-*O*-acetylated.

The main reason for pea xyloglucan purification was as a source of fucosylated polysaccharide for incorporation into the *Acetobacter* cellulose-synthesising system. In Chapter 6, it was reported that, despite molecular modelling predictions to the contrary (Levy *et al*, 1991), fucose residues on the xyloglucan molecule are not required for formation of cross-linkages between adjacent microfibrils. However, fucosylated xyloglucan apparently binds cellulose at a much higher rate than xyloglucan lacking a fucose residue (Levy, 1995) and we were interested in monitoring the rate of incorporation into the *Acetobacter* system. The second reason for wishing to add pea xyloglucan to the cellulose-synthesing system was to help explain an apparently anomalous result described in Chapter 6. Hayashi *et al* (1987) reported a reduction in cellulose ribbon width in the *Acetobacter* system by the addition of pea xyloglucan, consistent with it interacting with cellulose at the point of microfibril fasciation as seen with CMC (Haigler *et al,* 1982). Similar findings have been reported more recently (Uhlin *et al*, 1995; Yamamoto & Horii, 1994). However, despite the intimate interaction between tamarind xyloglucan and cellulose in this system, as evidenced by the high levels of incorporation, the profound effect on the molecular organisation of the cellulose componant and the requirement for high alkali concentrations for effective polymer dissociation components, no reduction in ribbon width was observed. This could be due either to the point at which ribbon widths were determined ie after network formation rather than immediately after synthesis or a strain specific difference (see Chapter 6 discussion).

9.2 Materials and Methods

9.2.1 Purification of Tomato Xyloglucan

A 6M KOH extract of mature green tomato (*Lycopersicon esculentum* var. 6203) was prepared as described in Chapter 2 (Section 2.10). This extract was further purified essentially according to the method of Kato & Matsuda (1976).

9.2.1.1 Removal of Starch and Proteins

The extract from 9.2.1 was dissolved in 0.02M phosphate buffer pH 6.9 and 0.1U of α-amylase (E.C. 3.1.1.1, Sigma) per 100mg extract was added. After the addition of a few drops of toluene, the sample was incubated with constant stirring at 40°C for 16 hours. The reaction was terminated in a boiling water bath for 5 minutes. The pH was subsequently adjusted to 7.2 and 0.1U Pronase E (Sigma) added per 250mg extract. After a further 16 hours incubation at 40°C the reaction was terminated as above. Denatured protein was precipitated by centrifugation at 27,100g for 10 minutes at 4°C, the supernatant decanted and dialysed against deionised H_2O at 1°C for 7 days. The dialysate was recovered and freeze-dried.

9.2.1.2 Iodine Precipitation

The extract from 9.2.1.1 was dissolved in 5.9M $CaCl_2$ (10ml/100mg extract). 1ml 3% I_2 in 4% KI per 10ml was added and, after thorough mixing, left to stand for 2 hours at 1°C. The precipitate was recovered by centrifugation at 27,100g for 30 minutes at 4°C, redissolved in hot deionised water, neutralised with sodium thiosulphate and dialysed at 1°C. The precipitation step was repeated and, after dialysis, the recovered material was freeze-dried.

9.2.1.3 DEAE Sephadex Ion Exchange Chromatography

DEAE Spehadex ion-exchange media, supplied with a Cl^- counter-ion, was converted to the PO_4^- counter-ion by exchanging 5 times in 0.5M potassium phosphate at RT. After conversion, the media was swelled in 10mM phosphate buffer pH 6.00 in a boiling water bath for 2 hours. The swelled media was cooled to RT and poured into a 1 x 10 cm column and packed at a flow rate of 1.5ml/min for 2 hours using 10mM phosphate buffer as eluent. The sample from 9.2.1.2 was dissolved in buffer and passed through the column at a flow rate of 1ml/min using buffer as eluent. 2ml fractions were collected using a Bio-Rad 2128 Fraction Collector and assayed using the phenol-sulphuric acid test (Section 2.1). Carbohydrate-containing fractions were pooled, dialysed and freeze-dried as before.

9.2.1.4 Removal of Glucomannan, Arabinan, and Arabinoxylan Contaminants

A glucomannan, arabinan and possibly an arabinoxylan co-purified with xyloglucan through purification steps 9.2.1-9.2.3. These were removed by incubation with β-mannanase, endo-arabinase and β-xylanase enzymes (all supplied by Megazyme Pty, Australia) at pH 4.5 in 25mM sterilsed sodium acetate buffer.

9.2.2 Purification of Pea Xyloglucan

A 4M KOH extract was obtained from dark grown pea (*Pisum sativum* var. Arolla) cell walls as described in Chapter 2 (Section 2.12). This was further purified by incubation with β-mannanase (4U) and endo-arabinase (3U) (Megazyme Pty, Australia) per 150mg extract for 16 hours at 40°C in 25mM sterilised sodium acetate buffer pH 4.3. Polymeric material was recovered by precipitation with 75% ethanol.

9.2.3 Separation of Vascular and Parenchyma Cells from Tomato Fruit

Mature green processing tomato fruit var. 6203 were cut into 1/4's, the skin and locular tissue removed and the pericarp tissue finely diced. Parenchyma cells were separated from vascular tissue by orbital agitation of the diced pericarp in 0.05M CDTA/0.5M mannitol/0.4% MS salt solution (100ml/10g fresh weight pericarp) for 5 days at RT. Separated cells were collected by passing through a 750μm sieve. Cell wall material was prepared from separated parenchyma cells as described for complete pericarp tissue (Section 2.11.1). Cell walls were prepared from vascular tissue as for parenchyma cells, but a preliminary grinding step in liquid nitrogen using a mortar and pestle was incorporated.

9.2.3 1 Light Microscopy of Separated Cells

Isolated parenchyma and vascular cells were suspended in deionised water and placed on a glass microscope slide. Cells were visualised with a Lieca microscope.

9.2.4 Monosaccharide Analysis

The neutral sugar composition of all samples was determined using alditol acetates method 3 as described in Chapter 2 (Section 2.9).

9.2.5 Molecular Weight Analysis

The molecular weight of samples was determined using high performance size-exclusion chromatography with multi-angle laser light scattering (HPSEC-MALLS) as described in Chapter 6 (Section 6. 2.8).

9.2.6 Oligomeric Composition

The oligomeric composition of samples was determined by hydrolysis with *endo*-1,4-β-glucanase and analysis of the hydrolysis products using HPAEC (Dionex) according to the method described in Chapter 2 (Section 214).

9.2.7. NMR Characterisation

Solid state ^{13}C NMR was performed on 30% w/v hydrates of tomato 6M KOH extract using conditions described in Chapter 2 (Section 2.13). High resolution NMR was performed on a Bruker AMX400 (400 Mhz) machine operating at 60°C. ^{1}H-NMR spectra were obtained with an aquisition time of 2.9s, a delay (DI) of 1.1s, pulse angle (PI) of 40° and 32 scans, referenced to external DSS (4,4-dimethyl-4-silapentane sodium sulphonate). ^{13}C NMR spectra were obtained with acquisition time of 0.7s, a recycle delay of 2s, a pulse width of 50° and 22,000 scans.

9.2.8 Incorporation into the Acetobacter *System*

Purified pea xyloglucan was incorporated into the *Acetobacter* system at a concentration of 0.5% as described in Chapter 6 (Section 6.2.1). Deep Etch, Freeze-fracture TEM of the composites was performed as described in Chapter 2 (Section 2.12.5).

9.3 Results

9.3.1 Tomato Xyloglucan

9.3.1.1 Monosaccharide Analysis

Monosaccharide analysis of the partially purified 6M KOH extract (from 9.2.1.3) gave a neutral sugar composition of Ara (6%), Man (12.75%), Gal (15.55%), Xyl (19.8%) and Glc (45.9%). After incubation with β-mannanase, the composition was altered to Ara (12%), Gal (23.8%), Xyl (34.8%)

and Glc (26.9%). The elimination of mannose and the reduction of the total amount of glucose confirms the co-purification of a glucomannan. If it is assumed that, after β-mannanase treatment, only the mannose and glucose contents are altered, glucomannan can be calculated to compose ca. 44% of the partially purified 6M KOH extract, and has an approximate Glu:Man ratio of ca. 70:30, which is high compared with, for example, Konjac glucomannan (Chapter 7, this thesis). Further purification with β-xylanase and endo-arabinase gives a monosaccharide composition of Ara (7.25%), Xyl (27.55%), Gal (22.1%) and Glc (43.1%). The presence of a large amount of arabinose is consistent with the presence of an arabinoxyloglucan as seen in tobacco (Akiyama & Kato, 1982; Eda & Kato, 1978; Eda *et al*, 1983; Mori *et al*, 1979; Sims & Bacic, 1995). Some of the galactose may be derived from xyloglucan if tomato xyloglucan is like that of potato ie an arabinogalactoxyloglucan (Ring & Selvendran, 1981; Vincken *et al*, 1996), but the total amount of galactose is too high to be fully accounted for as a xyloglucan component. This suggests a significant amount of galactan has co-purified during the purification procedure.

9.3.1.2 Molecular Weight Determination

The molecular weight profile of the 6M KOH extract (before purification) and purified xyloglucan (from 9.2.1.4) are shown in Figure 9.1. The 6M KOH extract (a) shows the presence of two discrete peaks of peak molecular weight of 16,100 Da and 58,100 Da, although NMR clearly identifies at least three major polysaccharides (xyloglucan, glucomannan and arabinan/galactan/arabinogalactan). Sakurai & Nevins (1993) report, however, that all the mannose in the hemicellulose fraction of mature green tomato fruit eluted with low mwt material, suggesting that either the glucomannan is the lower mwt peak or is too small to be detected. The molecular weight profile of purified xyloglucan is shown in Figure 9.1b. The higher mwt peak is assigned to xyloglucan as it forms the bulk of the material, with a peak mwt of 48,000. The lower mwt peak is assigned to galactan. The peak mwt of xyloglucan is much lower than has been reported for other primary cell wall xyloglucans such as pea (Talbott and Ray, 1992a). but, is in approximate agreement with data presented by Sakurai and Nevins (1993) who quoted a molecular weight of slightly under 73 kDa. There is evidence of aggregation of the xyloglucan and/or galactan components (data not shown); this has the effect of distorting the results as

Figure 9.1: Molecular Weight Analysis of Tomato Fruit 6M KOH Extract and Purified Tomato Xyloglucan

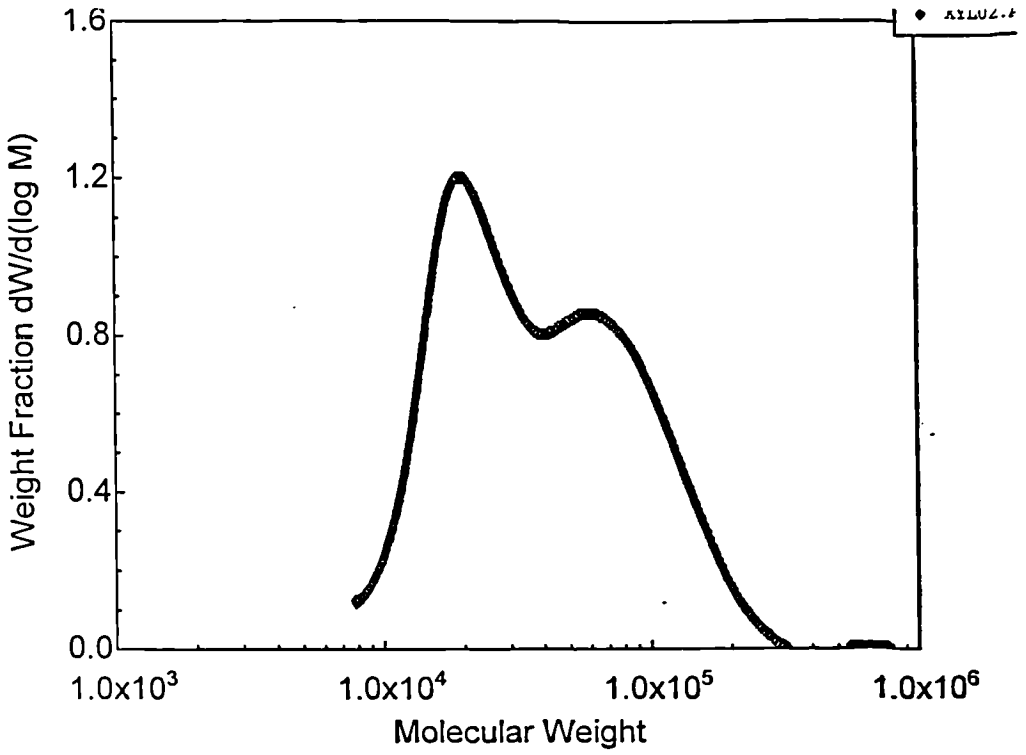

a

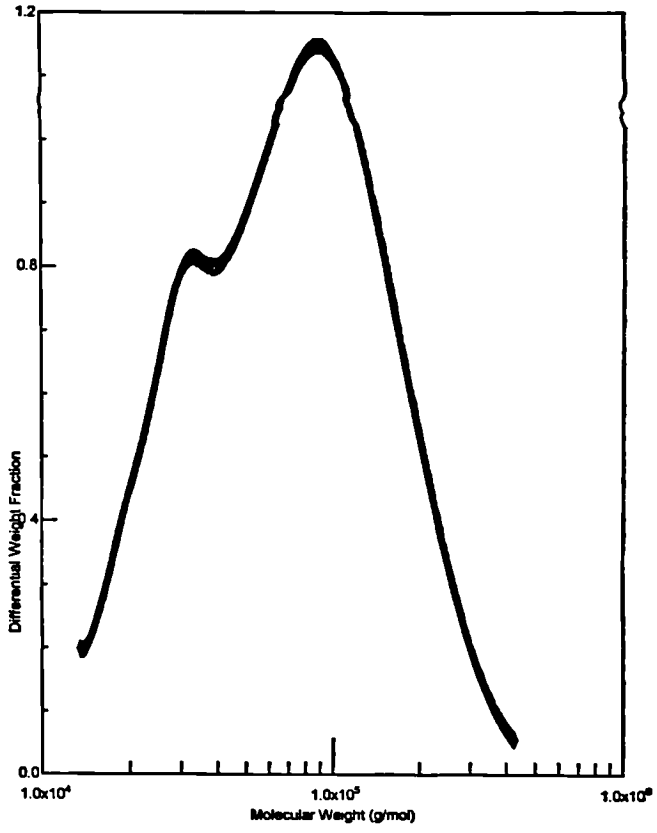

b

· Molecular weight profile of (a) the crude 6M KOH extract from mature green tomato fruit and (b) after several purification processes

aggregates, although they may form a small percentage of the total, scatter a very large amount of light. A similar aggregation event is seen for pea xyloglucan (section 9.3.2.2) and low mwt tamarind xyloglucan (section 6.3.4). The result suggests that different eluent conditions should be investigated.

9.3.1.3 Oligomeric Composition

The oligosaccharide composition of the partially purified 6M KOH fraction (from 9.2.1.3) is shown in Figure 9.2a and is much more complex than is seen for either tamarind (Figure 9.2b) or pea (Figure 9.2c) xyloglucan. A complicated range of hydrolysis products after *endo*-glucanase digestion is more typical of xyloglucan derived from monocotyledons (Hayashi, 1987), but similar complexity has been observed for potato (Vincken *et al*, 1996) and tomato (York *et al*, 1996) xyloglucan. A 1:1 mixture of tamarind and tomato extract hydrolysis products indicated no overlapping oligomer signals (data not shown).

The 4 oligomers generated from tomato 6M KOH extract eluted at ca. 22 minutes (Figure 9.2a) are essentially identical in relative intensity to those seen for tamarind xyloglucan eluted at ca. 15 minutes (Figure 9.2b). It was suggested that these tomato xyloglucan oligomers may in fact be the same as derived from tamarind xyloglucan, but are present as dimers containing an α-L-Ara$_f$ residue attached directly to the backbone, as described by York *et al* (1995) rendering them resistant to *endo*-glucanase attack. However, NMR data provided no evidence for an α-L-Ara$_f$ residue attached to the backbone (9.3.1.5) and the apparent absence of galactose in tomato xyloglucan (9.3.1.4) suggests that these oligosaccharides cannot be dimers of tamarind xyloglucan oligosaccharides.

In the light of sugar analysis results which indicated the presence of a significant quantity of glucomannan, an *endo*-glucanase digest of Konjac glucomannan is shown in Figure 9.3a. By comparison of this spectrum with that of Figure 9.3c, two peaks are tentatively identified as deriving from glucomannan. More glucomannan-derived oligomers may be present, but cannot be identified

Figure 9.2 Oligomeric Composition of Partially Purified Tomato Xyloglucan

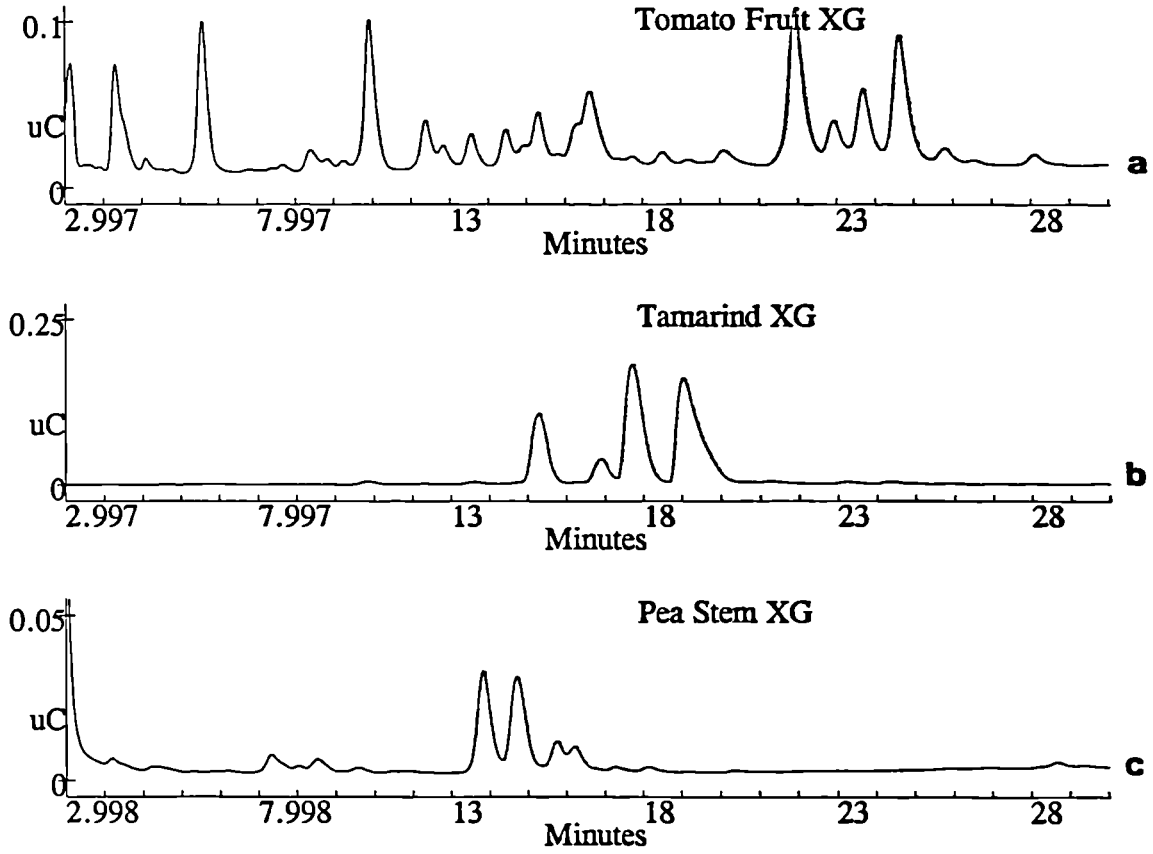

Dionex profiles of oligomers generated by the action of endo-1,4-β-glucanase on (a) partially purified tomato xyloglucan, (b) tamarind xyloglucan and (c) partially purified pea xyloglucan revealing a complex mixture of hydrolysis products in (a) not seen with other souces of xyloglucan.

Figure 9.3: *endo*-Glucanase Hydrolysis Products of Konjac Glucomannan and Cellulose Oligomers

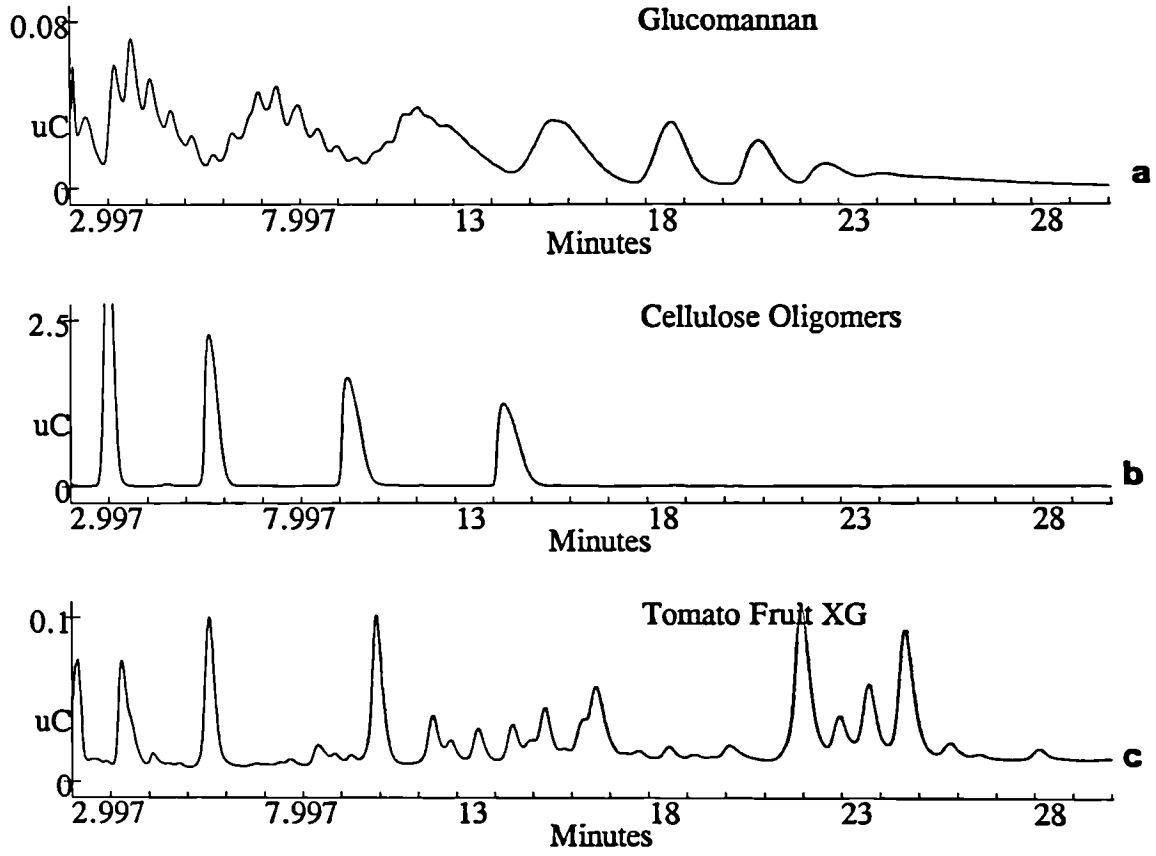

Oligomers generated by the action of endo-glucanase on konjac glucomann (a). Separation of lower molecular weight oligomers is poor as gradient conditions were kept at those optimal for xyloglucan oligosaccharide separation. Three glucomannan peaks are tentatively assigned to components in the partially purified tomato xyloglucan digest (Figure 9.4). Comparison with cello-oligomers (b) allows assignment of cellobiose and cellotetraose in the tomato xyloglucan spectrum (c). Cellotriose is *not* present in (c)

due to the absence of suitable standards. Cello-oligomer standards were also characterised (Figure 9.3b) and comparison with spectrum 9.3c reveals cellobiose and cellotetraose as hydrolysis products of the tomato extract. This latter result suggests that a signifcant amount of the xyloglucan may be unsubstituted as seen with monocotyledon-derived xyloglucan, but the possibility that these oligomers are derived from the glucomannan component cannot be eliminated. Peak 2 (Figure 9.4) was shown not to be cellotriose as it did not co-elute with cellotriose in a 1:1 mixture of cellulose oliglomers and partially purified tomato xyloglucan (data not shown). A chromatogram showing partial oligomer assignments is shown in Figure 9.4.

Figure 9.5b shows the *endo*-glucanase digest of purified tomato xyloglucan (from 9.2.1.4) compared with the partially purified polymer (Figure 9.5a). Relative intensities of peaks assigned to glucomannan and cellobiose (Figure 9.4) have reduced although interestingly, cellotetraose remains a major component. Since cellotetraose should be hydrolysed by *endo*-glucanase to cellobiose, this data suggests that the peak may have been incorrectly assigned, but this was not confirmed.

The purified tomato xyloglucan was submitted to J.-P. Vincken at the Agricultural University of Wageningen for comparison with xyloglucan puruified from potato. Two *endo*-glucanases from *Trichoderma viride* (endoIV and endoV), which had been demonstrated to yield different ranges of xyloglucan hydrolysis products (Vincken *et al*, 1996) were used to hydrolyse tomato xyloglucan. The results shown in Figure 9.6 demonstrate significant similarity between the two xyloglucans.

9.3.1.4 ^{13}C-NMR Analysis

A solid state ^{13}C NMR spectrum of partially purified tomato xyloglucan (from 9.2.1.3) is shown in Figure 9.7. Three major C-1 peaks are identified at ca. 105.5, 103.4 and 100.1ppm, correlating with chemical shifts reported for galactose, glucose and xylose residues for tamarind xyloglucan (Gidley *et al*, 1991a). A minor C-1 peak at ca. 110.5ppm is tentatively assigned to the arabinose residue of

Figure 9.4: Partially Assigned Oligomer Profile of Partially Purified Tomato Xyloglucan

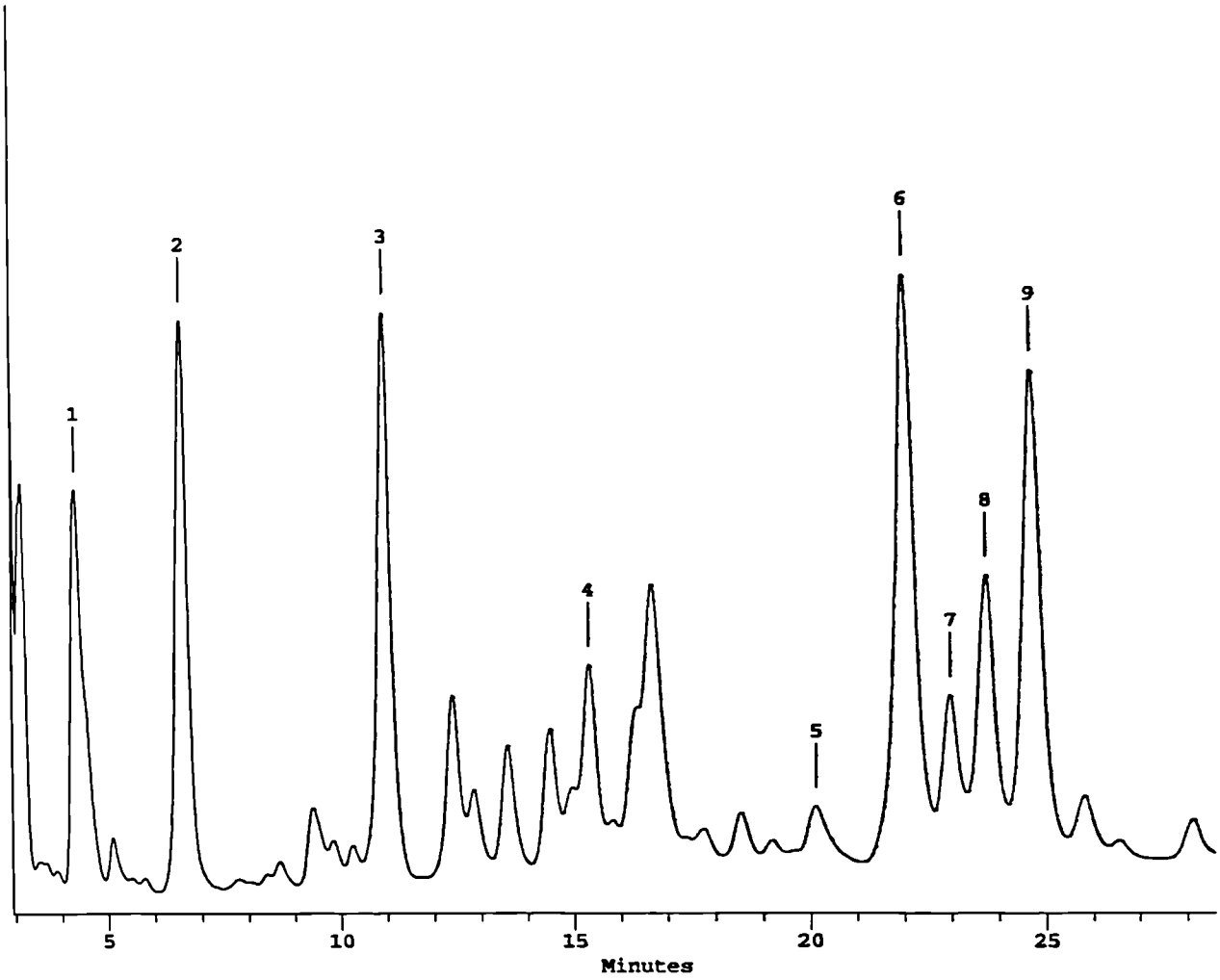

Spectrum of partially purified tomato fruit xyloglucan showing partial peak assignments. Peak 1 (cellobiose), peak 2 (unidentified, but is very much less significant in the pure polymer (Figure 9.5)), peak 3: cellotetraose; peak 4: glucomannan; peak 5: glucomannan. Peaks 6-9 are confirmed by NMR not to be dimers of tamarind xyloglucan oligosaccharides

Figure 9.5: *endo*-Glucanase Digest of Partially Purified and Fully Purified Tomato Fruit Xyloglucan

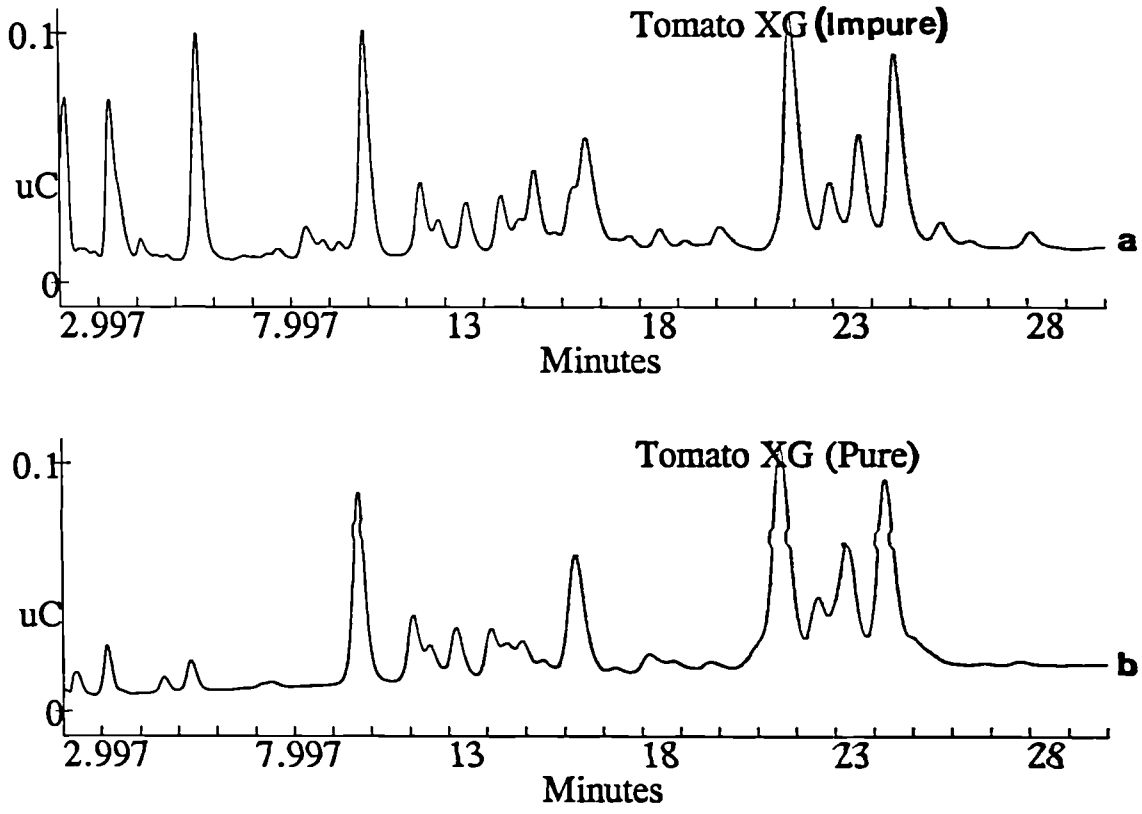

Partially purified (a) and fully purified (b) tomato xyloglucan showing a reduction in relative intensities of peaks assigned to glucomananan and cellobiose (Figure 9.4) but not cellotetraose, suggesting that this peak may be incorrectly assigned (see text)

Figure 9.6: Comparison of the Degradation Products of Tomato and Potato Xyloglucan

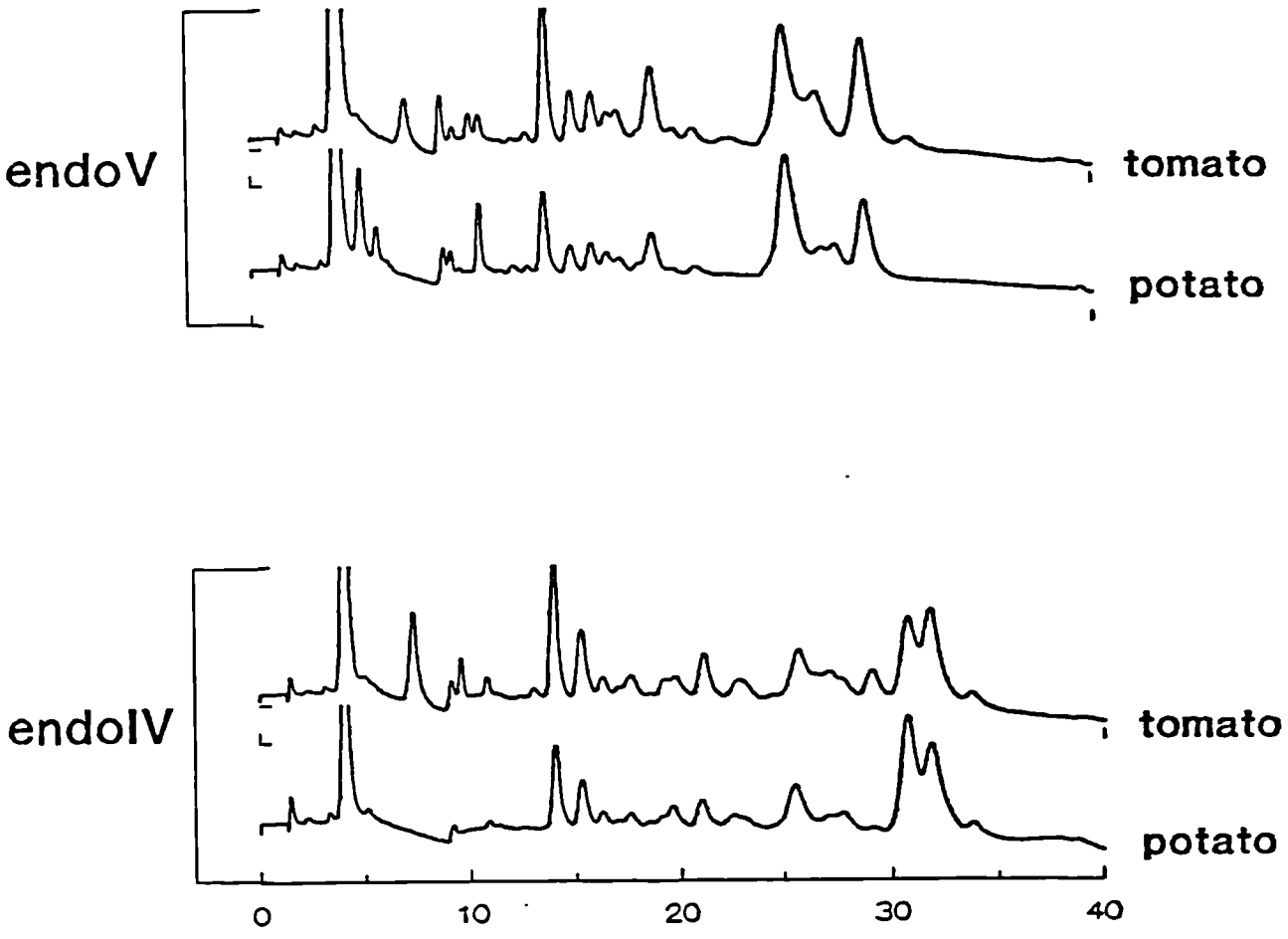

Hydrolysis products using two *endo*-glucanases shown to have differing modes of action against xyloglucans (Vincken *et al*, 1996). Reproduced with permission from J.-P. Vincken, Wageningen Agricultural University, The Netherlands

arabinoxyloglucan This correlates with the chemical shift of 110.2ppm for the Ara C-1 of the oligosaccharide $AraXyl_2Glc_3$ generated by *endo*-glucanase digestion of tobacco xyloglucan from Mori *et al* (1981). It should be noted however that these authors report a significantly different chemical shift (111.2ppm) for Ara C-1 of the polymeric arabinoxyloglucan. No chemical shifts for glucomannan could be unequivocally identifed in this spectrum. Hereafter, all spectra are obtained using high resolution solution-state NMR for more accurate signal assignment.

Figure 9.8a shows a high resolution ^{13}C NMR spectrum of partially purified tomato xyloglucan (from 9.2.1.3). The signal at 101.00ppm is assigned to the mannosyl C-1 of glucomannan, in accordance with Gidley *et al* (1991b). Signals at 110.20, 105.41, 103.38 and 99.86 ppm are assigned to Ara, Gal, Glc and Xyl of xyloglucan as described above.

The ^{13}C NMR spectrum of the 6M KOH extract after β-mannanase digestion is shown in Figure 9.9, with correct internal referencing. The signal for mannosyl C-1 identified in Figure 9.8 has been completely eliminated. The C-1 signal at 102.77ppm is assigned to the C-1 xylosyl residue of xylan (see Chapter 7) indicating a significant quantity of xylose which is not associated with the xyloglucan component. A signal is present at 108.69ppm, essentially identical to that reported by Capek *et al* (1983) for a (1→5)-linked arabinan isolated from *Althaea officinalis* L. and shifts coincident with (1→5)-arabinofuranosyl residues are identified for C-2 through to C-6 (Seymour *et al*, 1990). The absence of further signals between 107-109ppm indicate that this contaminating arabinan is unbranched (Capek *et al*, 1983).

The signal at 105.47 was initially assigned to the C-1 of the galactosyl residue of xyloglucan as reported by Gidley *et al* (1991a). However, a signal at 78.74ppm is identified, essentially identical to that reported by Pressey & Himmelsbach (1984) for a 1→4-linked galactose, the 1→4 linkage causing a characteristic downfield shift of ca. 10ppm for C-4 galactosyl residues. Further signals for C-2, C-3,

Figure 9.7: Solid State ^{13}C-NMR Spectrum of a 6M KOH Extract of Mature Green Tomato Fruit Xyloglucan

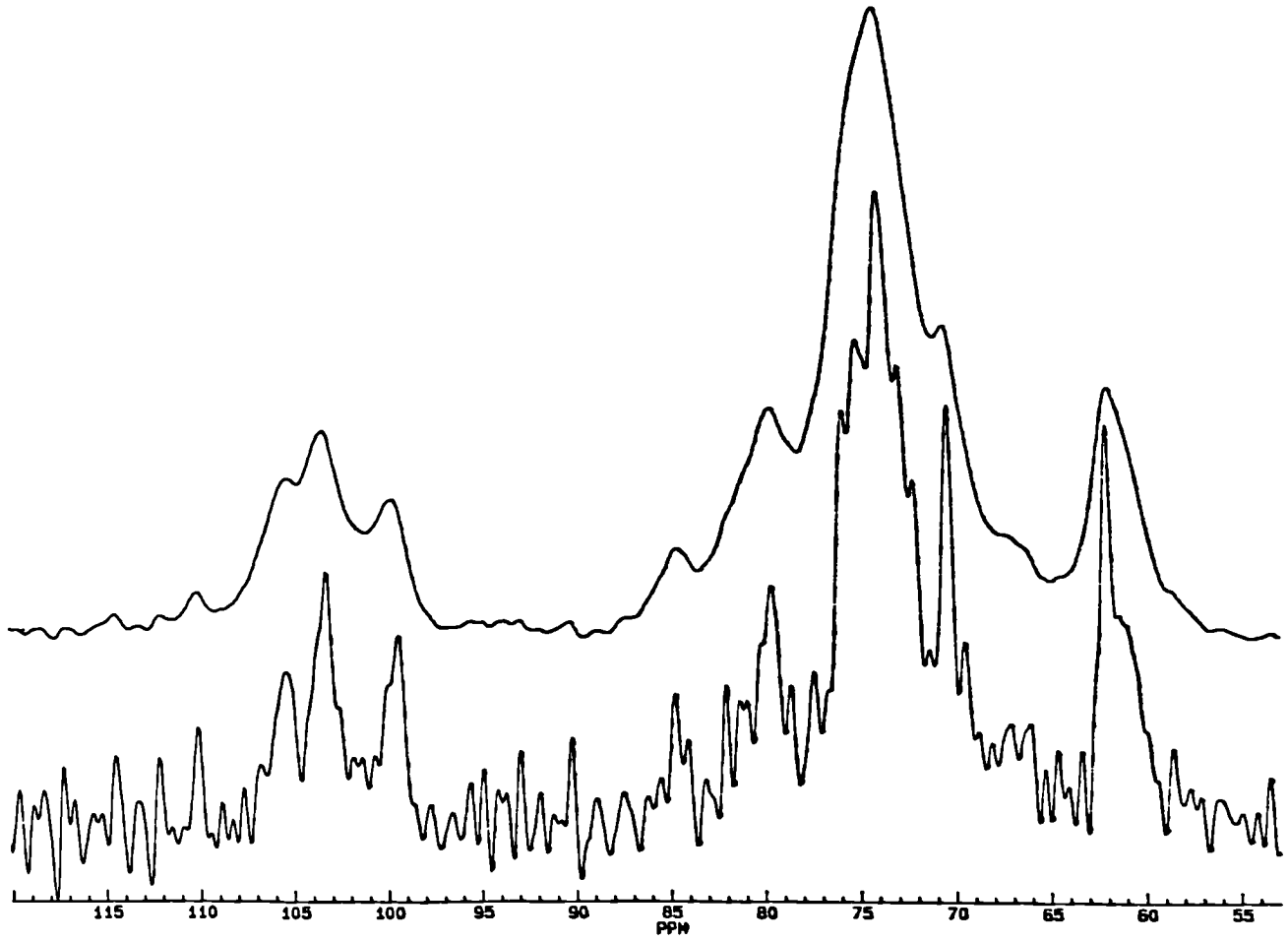

Solid state spectrum of a 30% (w/v) hydrate of partially purified tomato xylogluacn showing characteristic signals at ca. 105.5, 103.8 and 100.1ppm assigned to galactose, glucose and xylose residues of xyloglucan respectively, a minor signal at ca. 110.2ppm tentatively assigned to arabinose of an arabinoxyloglucan, but no unambiguous signals are identified for glucomannan

Figure 9.8 High Resolution ^{13}C NMR Spectra of a 6M KOH Extract of Mature Green Tomato Fruit Cell Walls

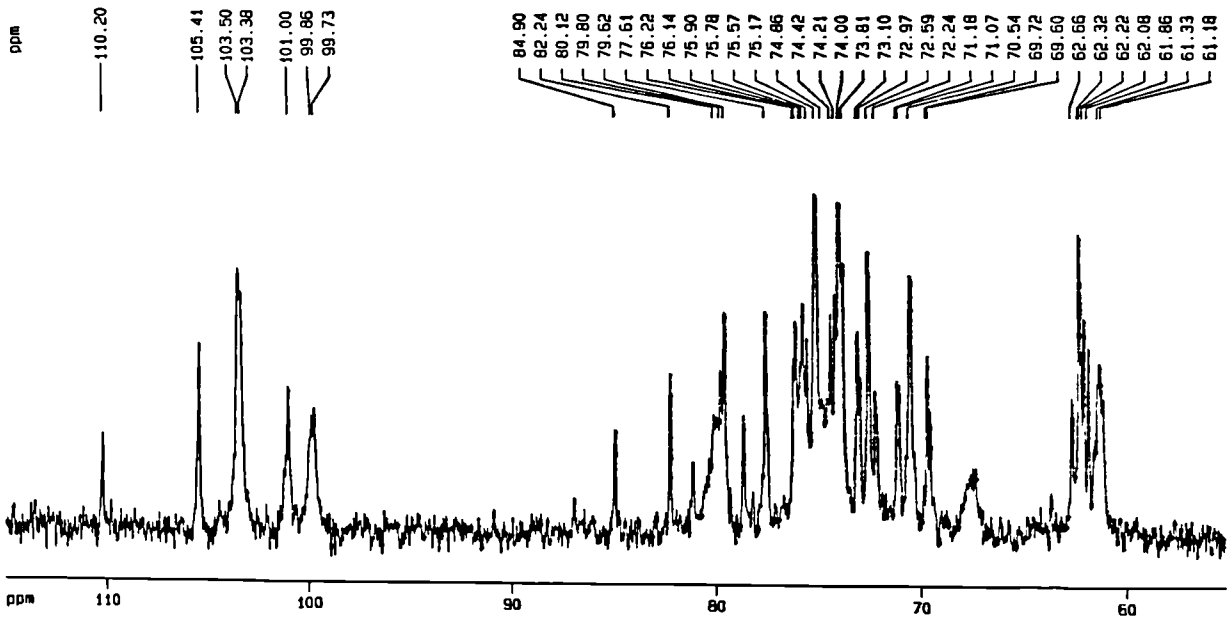

High resolution ^{13}C-NMR spectrum (line broadening 3Hz) of 6M KOH extract from tomato cell walls (cf Figure 9.7), showing signals for glucomannan and a putative arabinogalactoxyloglucan (see text).

Figure 9.9 High Resolution ^{13}C NMR Spectrum of a 6M KOH Extract Partially Purified by β-Mannanase Digestion

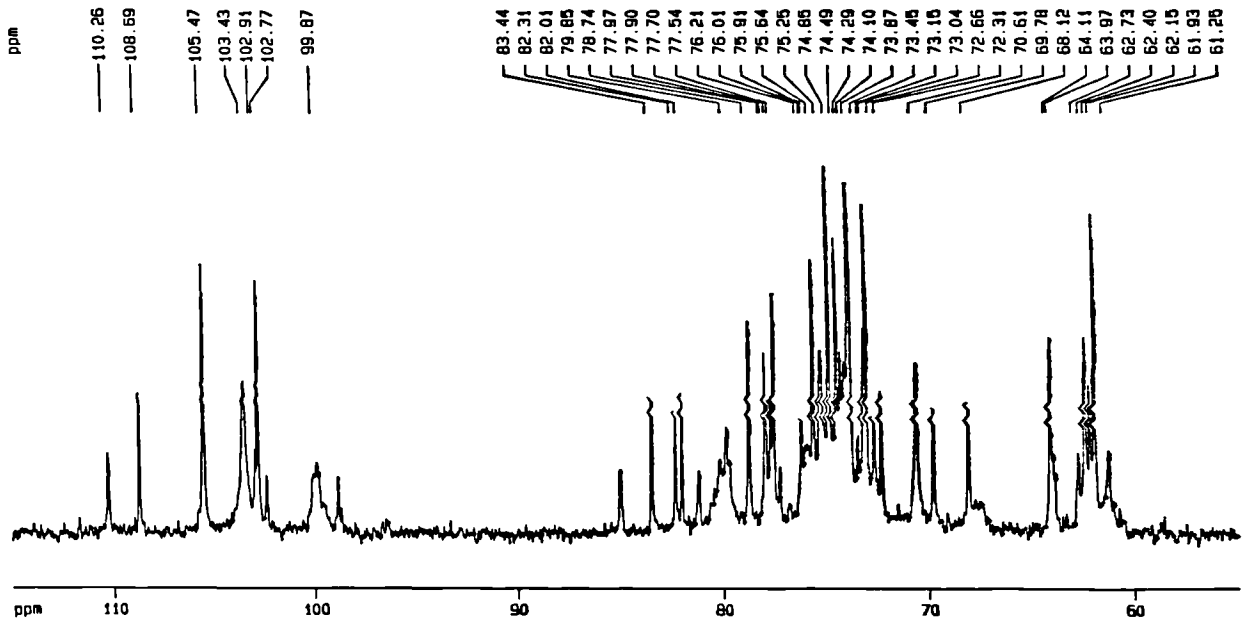

^{13}C NMR spectrum (line broadening 3Hz) of the 6M KOH extract (from 9.2.1.3) after β-mannanase digestion showing elimination of the glucomannan signal and the presence of signals for α-(1→5)-arabinan : 108.69 (C1), 82.01 (C2), 77.97 (C3), 83.44 (C4) and 68.12 (C5) and for β-(1→4)-galactan: 105.47 (C1), 73.04 (C2), 74.49 (C3), 78.74 (C4), 75.64 (C5) and 61.93 (C6)

C-5 and C-6 can be identified with chemical shifts coincident with those reported by Seymour *et al* (1990) for a β-1,4-linked galactan. This, combined with approximately equal intensities for C-1 through C-6 galactose signals (galactan) and the absence of unambiguous signals for C-2 - C-6 coincident with galactose residues of xyloglucan oligosaccharides (York *et al*, 1993), suggests that the vast majority of the galactose which co-purifies with tomato xyloglucan is present as β-1,4-galactan. The possibility that galactose is present as a minor xyloglucan component, insufficient for detection by NMR, cannot be fully discounted (see pea xyloglucan, section 9.3.2.3).

The signals for arabinan and galactan identified above could be derived from an arabinogalactan. Chemical shifts are coincident with signals described for a polysaccharide obtained from tomato fruit by the action of pectinesterase and polygalacturonase, which was described as containing relatively long, homogeneous blocks of α-(1→5-linked arabinofuranosyl and β-(1→4)-linked galactopyranosyl residues (Pressey & Himmelsbach, 1984). However, digestion with *endo*-arabinase (Figure 9.10) failed to eliminate the β-1,4 galactan, suggesting either that the arabinan and galactan are separate polymers or that contiguous blocks of galactose residues are of sufficient length to be precipitated with ethanol. After digestion with *endo*-arabinase and xylanase enzymes, a spectrum of xyloglucan and β-(1→4) galactan is obtained (Figure 9.10). The presence of a signal at 102.69 indicates some residual xylan suggesting that a proportion of the xylose identified by monosaccharide analysis for this extract (9.3.1.1) may not be associated with the xyloglucan. Tomato xyloglucan may therefore have less xylosyl substitution than the Glc_4/Xyl_3 pattern seen for most xyloglucans isolated from dicotyledonous and non-graminaceous monocotyledonous plants and in this respect, may be more similar to that isolated from monocotyledons (Hayashi, 1987).

9.3.1.5 ^{1}H-NMR Analysis

The *endo*-glucanase digest of tomato xyloglucan (Figure 9.2) showed a complex range of oligosaccharides. This is confirmed in recent reports from Albersheim's group that tomato xyloglucan has many different sidechains, including one not previously characterised (York *et al*, 1996).

Figure 9.10: High Resolution ^{13}C-NMR Spectrum of Tomato Fruit Xyloglucan

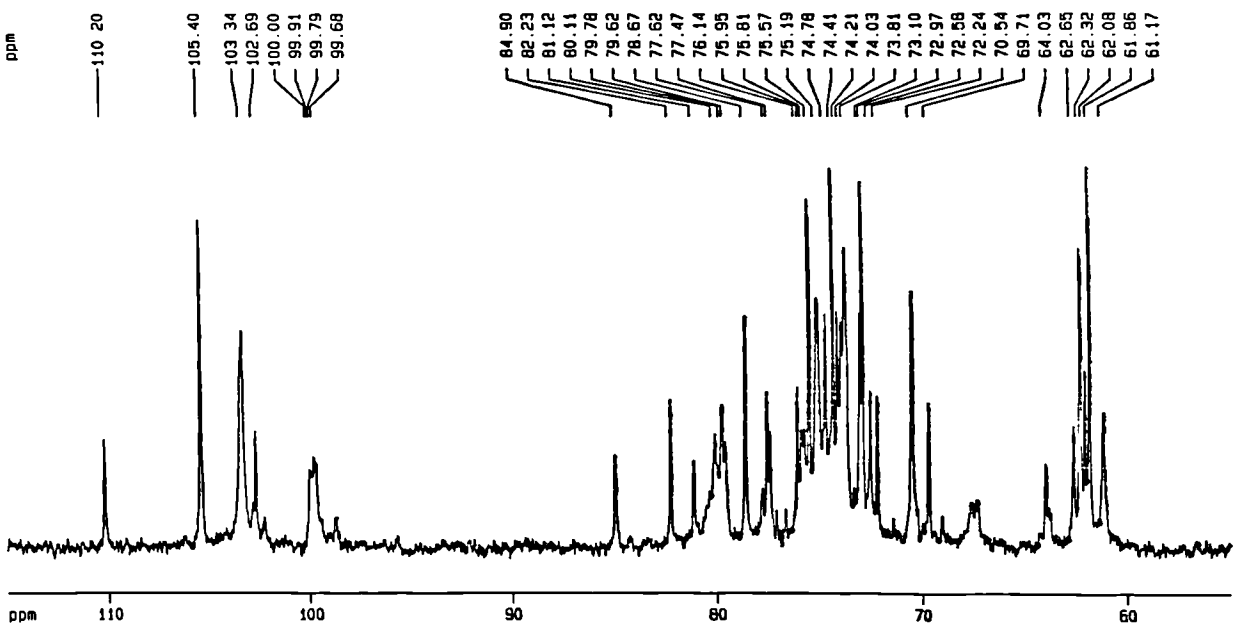

Spectrum of tomato xyloglucan after *endo*-arabinase and β-xylanase purification treatments showing elimination of signals for (1→5)-arabinan and reduction in relative intensity of β-(1→4)-xylan. β-1,4-galactan signals are identified (C1 = 105.40) and β-(1→4)-xylan (C-1 = 102.69) remains a minor contaminant

Assignment of ^{1}H-NMR signals against known xyloglucan oligosaccharides (Hisamatsu *et al*, 1992; York *et al*, 1990; 1992) is therefore incomplete.

A ^{1}H NMR spectrum of purified tomato xyloglucan (cf Figure 9.10) is shown in Figure 9.11. The signal at 4.615 ($J_{1,2}$ 7.8Hz) is in the region assigned to the H-1 of 2-linked β-gal as defined by Hisamatsu *et al* (1992). The coupling constant is identical to that for galactose substituted by fucose in the side chain Fuc-(1→2)-Gal-(1→2)-Xyl-(1→6)- (York *et al*, 1990), but tomato xyloglucan does not contain fucose. In light of the unequivocal ^{13}C NMR evidence that most galactose is present as β-(1→4)-galactan this doublet is assigned to galactan. It should be noted that the same doublet appears in purified pea xyloglucan (Figure 9.14). Whilst β-(1→4)-galactan remains a significant contaminant in this purified preparation, galactose is undoubtedly an, albeit relatively minor, component of pea xyloglucan (Hayashi & Maclachlan 1984; Pauly *et al*, 1995). This suggests that the doublet contains components from both 4,-linked and 2,-linked Gal and means that tomato xyloglucan cannot be confirmed as an arabino- or an arabinogalactoxyloglucan on the data available. Treatment with galactanase was not possible as the galactanase we had available showed *endo*-1,4-β-glucanase side activity.

H-1 of terminal α-xylose attached at C-6 of 4,6-linked glucose is identified at 4.936 ($J_{1,2}$ 3.6Hz) as according to Hisamatsu *et al* (1992). The assignment of the α-xylose doublet at 5.061 ($J_{1,2}$ 3.3Hz) is ambiguous. This doublet is not present in either pea (Figure 9.16) or tamarind (Gidley *et al*, 1991a) xyloglucan, both of which lack arabinose, but the downfield chemical shift of 0.125ppm is greater than that of 0.04 quoted for α-xylose attached at the 2-position with α-Ara$_f$ (Kiefer *et al*, 1990). Recent reports of a unique oligosaccharide identified in tomato xyloglucan (York *et al*, 1996) with a side chain α-Ara$_f$ (1→2)-α-Ara$_f$-(1→2)-α-Xyl$_p$-(1→6)- imply that this signal may represent the α-xylose of this unusual sidechain. The signal at 5.1366 is in the region assigned to H-1 of 2-linked α-Xyl with 2-linked β-Gal at C-2 (Hisamatsu *et al*, 1992). The low amount of xyloglucan-associated galactose in this sample however means that this relatively high intensity putative α-xylose signal cannot be identified.

Figure 9.11: Partial ^{1}H-NMR Spectrum of Purified Tomato Xyloglucan

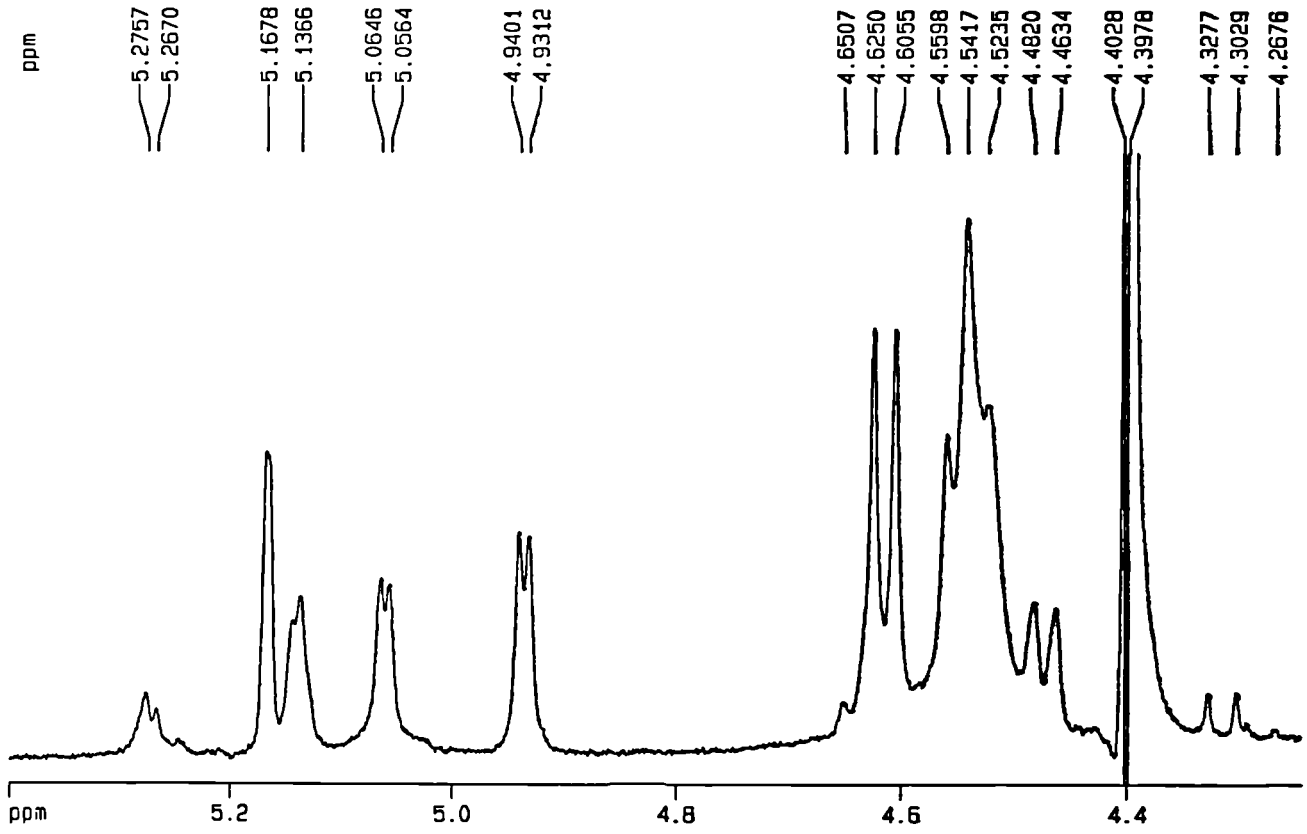

The doublet at 5.1678 is not unambiguously assigned. The H-1 signal of α-Ara found in sycamore xyloglucan is typically located between 5.3-5.4ppm (Hisamatsu *et al*, 1992), which are absent in this spectrum. However, the small $J_{1,2}$ value and large relative intensity of this peak are suggestive of this being arabinose. The two signals at 5.2757 and 5.2670 are located within the region assigned to H-1 of terminal α-Fuc and cannot therefore be assigned.. Each signal appears as a strongly coupled doublet suggesting that these may be arabinose signals in this non-fucosylated polysaccharide.

The absence of signals at 5.34-5.37 and 5.32-5.34 suggests that the sidechains α-L-Araf-(1→2)-Glc and α-L-Ara-(1→3)-β-D-Xyl-(1→2)-Glc respectively, identified in sycamore xyloglucan (Hisamatsu *et al*, 1992), are not present in tomato xyloglucan.

9.3.1.5 Separation of Parenchyma and Vascular Cells

Agitation of diced tomato pericarp in CDTA for 5 days effected complete dissolution of parenchyma and vascular tissue. Examination of a suspension of parenchyma cells under the light microscope revealed large (200-400nm wide), thin-walled single cells with their cell contents intact, indicating that CDTA had caused cell separation by dissolution of the middle lamella (Figure 9.12a). Strands of intact vascular tissue were also obtained (Figure 9.12b), which remained tightly associated with a sheath of tightly packed cells, very much smaller than the parenchyma cells seen in Figure 9.12a. Further treatment of this vascular tissue with CDTA failed to dissociate the vascular bundles from these cells (data not shown).

After measuring the dry weights of cell walls isolated from parenchyma and vascular tissue, a ratio of 12.6:1 parenchyma:vascular cell walls was obtained. Mannose comprised 6.9% of the neutral sugar composition of parenchyma cell walls and 4.3% of vascular tissue cell walls, compared to 6.4% for complete mature green tomato pericarp as determined by monosaccharide analysis. This suggests that

Figure 9.12: Micrographs of Mature Green Tomato Fruit Parenchyma and Vascular Cells Separated by CDTA Treatment

a

b

Thin walled parenchyma cells (a) 200-400µm wide and vascular tissue (b) which is intimately associated with a layer of much smaller parenchyma cells

the significant quantity of glucomannan isolated in the 6M KOH extract is not derived from the secondarily thickened vasculature, but is equally a component of the primary cell wall from the parenchyma cells.

9.3.2 Pea Xyloglucan

9.3.2.1 Monosaccharide Composition

The monosaccharide composition of a crude 4M KOH extract of pea stem cell walls had a neutral sugar composition of Rha (1.4%), Fuc (3.2%), Ara (18%), Xyl (23%), Man (6.5%), Gal (19.5%) and Glc (29%). Treatment of this preparation with *endo*-arabinase and β-mannanase effectively eliminated the arabinose and mannose components, giving a sugar composition of Fuc (5%), Ara (2%), Xyl (33%), Gal (17%) and Glc (43%). Apart from the high galactose content which is believed to be due to the presence of a neutral galactan (cf tomato fruit), the ratio of Glc:Xyl:Fuc (8.6:6.6:1) is close to the ratio predicted by Hayashi & Maclachlan (8:6:1) for an equimolar mix of XXXG and XXFG. Some alteration of this ratio is inferred by the results of Paully *et al* (1995) who identify a more complex mixture of component oligosaccharides. No attempt was made to further purify the sample, as the galactanase enzyme supplied by Megazyme Pty showed side activity against xyloglucan. Galactan can be clearly identified with chemical shifts distinct from that of galactose in xyloglucan using NMR (see section 9.3.1.4) and β-1,4-galactan does not associate with cellulose so should not interfere with incorporation into the *Acetobacter* system.

9.3.2.2 Molecular Weight Determination

The molecular weight distribution profile of pea xyloglucan (after arabinase and mannanase purification treatments) is shown in Figure 9.13. The peak molecular weight (31,780) is very much lower than that previously reported (Talbott & Ray, 1992a), probably because the conventional methods of measurement, using dextran standards, are poor models for stiff, linear xyloglucan

Figure 9.13: Molecular Weight Profile of Purified Pea Xyloglucan

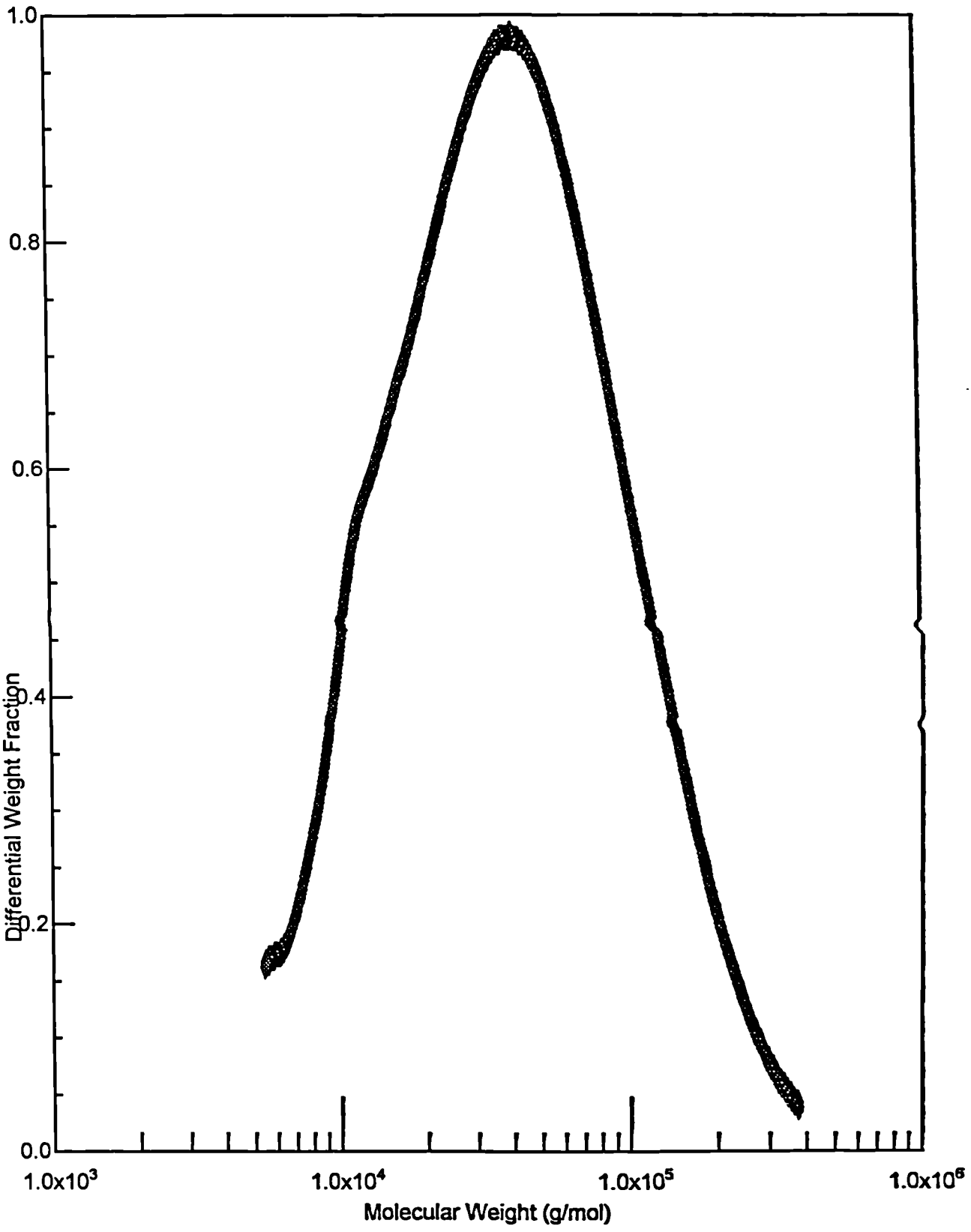

Figure 9.14: Oligomeric Composition of Pea Xyloglucan

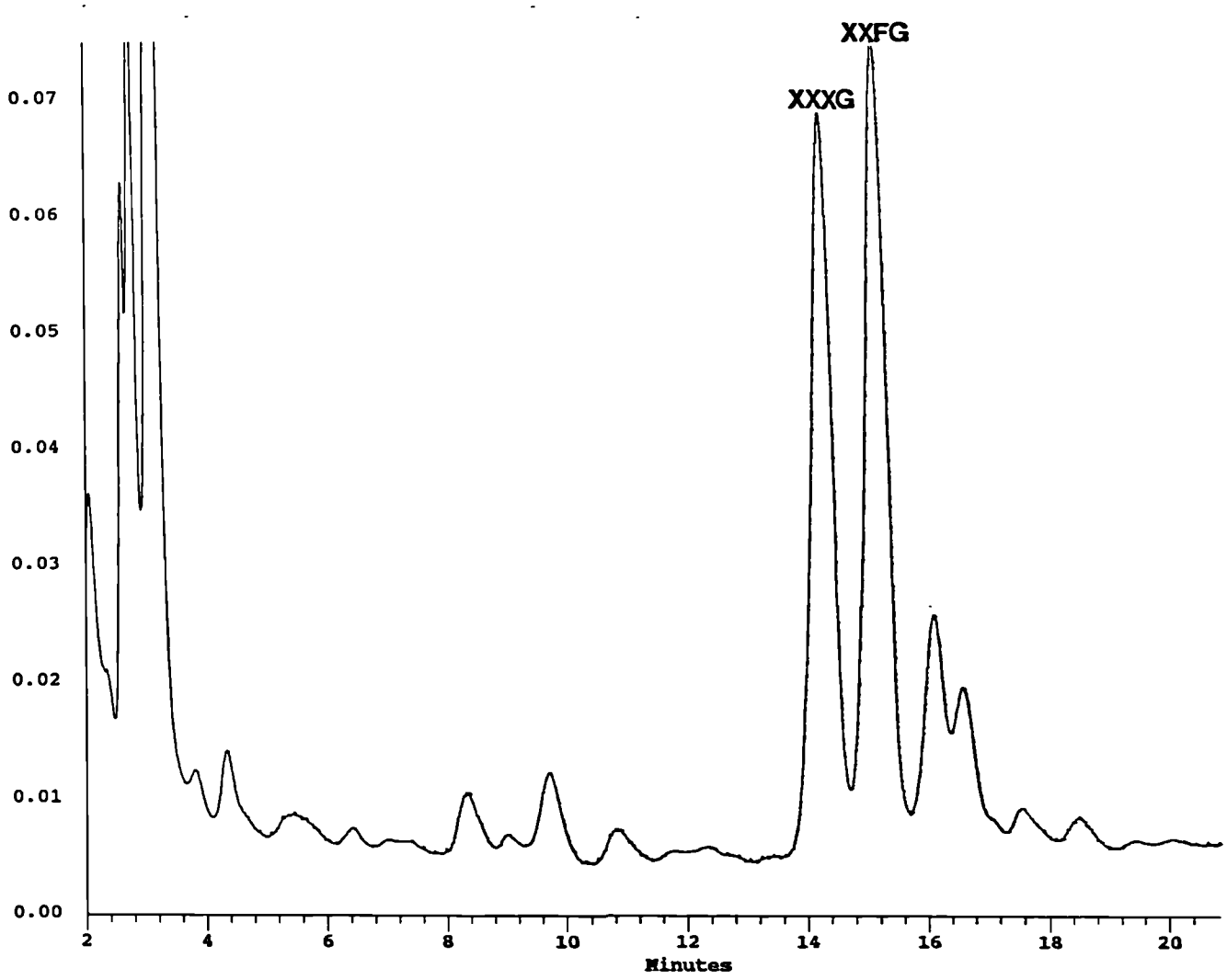

endo-glucanase digestion products of pea xyloglucan

molecules. Again, as was seen for tomato xyloglucan (section 9.3.1.2), significant aggregation of the polymer under these eluent conditions is apparent, which has the effect of distorting the results at the high mwt end, but does not affect the result for peak mwt.

9.3.2.3 Oligomeric Composition

Compared to the oligomer profile obtained for tomato xyloglucan (Figure 9.2a), *endo*-glucanase treatment of pea xyloglucan generates a simple range of hydrolysis components, with two major and two minor oligosaccharide components (Figure 9.14a). By comparison with tamarind xyloglucan (Figure 9.2b) and data obtained from mung bean xyloglucan (Downie, 1994) the two major peaks are assigned as XXXG and XXFG respectively. The two minor peaks could not be unambiguously assigned.

9.3.2.3 ^{13}C NMR Characterisation

Figure 9.15 shows a high resolution ^{13}C NMR spectrum of pea 4M KOH extract. A C-1 signal at 108.7ppm in the 4M KOH extract is assigned to arabinan (cf 9.3.1.3), and the presence of a minor signal at 108.35 suggests that this arabinan may, unlike that seen in the tomato 6M KOH extract, be branched (Capek *et al*, 1983). A minor signal at ca.101 ppm is also identified in this spectrum, which is tentatively assigned to glucomannan (Gidley *et al*, 1991b). Both of these signals are eliminated after enzyme treatment (Figure 9.16) in concurrence with sugar analysis data (9.3.2.10).

C-1 signals at 100.01 and 103.58ppm (Figure 9.16) are assigned to xylose and glucose residues of xyloglucan respectively (Gidley *et al*, 1991). A signal corresponding to C-4 of (1→4)-galactan is identified at 78.75ppm (Pressey & Himmelsbach, 1984) and further signals for β-(1→4)-galactan can be assigned (Seymour *et al*, 1990). C-2 to C-5 signals for xyloglucan-associated galactose (York *et al*, 1993), known to be a component in pea xyloglucan, are not positively identified. However, this may be due to the relatively low abundance of galactose in pea xyloglucan (only 6% in a polymer containing

XXXG:XXFG in equimolar proportions). The appearance of a minor signal at ca. 102.8ppm indicates the presence of a contaminating xylan (see Chapter 7) and the predicted Glc:Xyl:Fuc ratios as described in Section 9.3.2.1 may therefore be incorrect.

9.3.2.4 ^{1}H NMR Characterisation

The ^{1}H-NMR spectrum of purified pea xyloglucan is shown in Figure 9.17. Signals at 4.616 ($J_{1,2}$ 7.72Hz) and 4.935ppm ($J_{1,2}$ 3.4) are assigned to H-1 of 2, or 4-linked β-Gal and terminal α-Xyl of 4,6-linked β-Glc as described in 9.3.1.5. The signal at 5.113 ($J_{1,2}$ 3.2Hz) is assigned to H-1 of α-Xyl of the sidechain α-L-Fuc-(1→2)-β-D-Gal-(1→2)-α-D-Xyl-(1→6)-Glc and the signal at 5.2742 ($J_{1,2}$ 3.72 Hz) to terminal α-Fuc (York *et al*, 1990). This result suggests the majority of pea xyloglucan comprises the two oligosaccharides XXXG and XXFG as proposed by Hayashi & Maclachlan (1984) and suggested by the *endo*-glucanse digestion results (Figure 9.13).

9.3.2.5 Incorporation into the Acetobacter *System*

Only a very small amount of purified pea xyloglucan was available for incorporation into the Acetobacter system, sufficient for a single fermentation. Unfortunately, this fermentation became contaminated and only a small amount of putative cellulose/pea xyloglucan complex was obtained. Examination of the complex using deep-etch, freeze-fracture TEM (Figure 9.15) revealed no lateral organisation of cellulose fibres or xyloglucan cross-linkages, although there is some evidence that the width of fibres may be somewhat reduced compared to tamarind-xyloglucan/cellulose composites. In the absence of sugar analysis data to define association levels, these results cannot be further interpreted.

Figure 9.15: High Resolution ^{13}C-NMR Characterisation of a 4M KOH Extract from Pea Stem

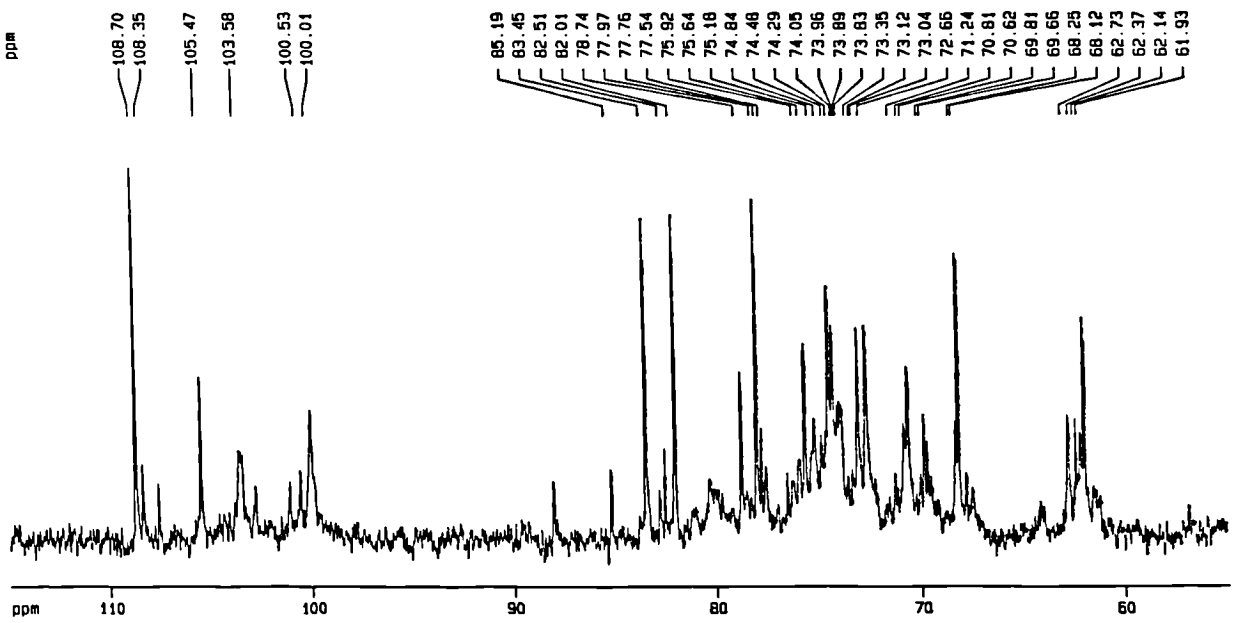

^{13}C-NMR spectrum (line broadening 3Hz) of a crude pea stem 4M KOH extract. The signal at 108.7 ppm is assigned to arabinan and a putative C-1 signal for mannosyl C-1 at ca. 101ppm identified, tentatively assigned to glucomannan (see text).

Figure 9.16: High Resolution ^{13}C NMR Characterisation of Partially Purified Pea Xyloglucan

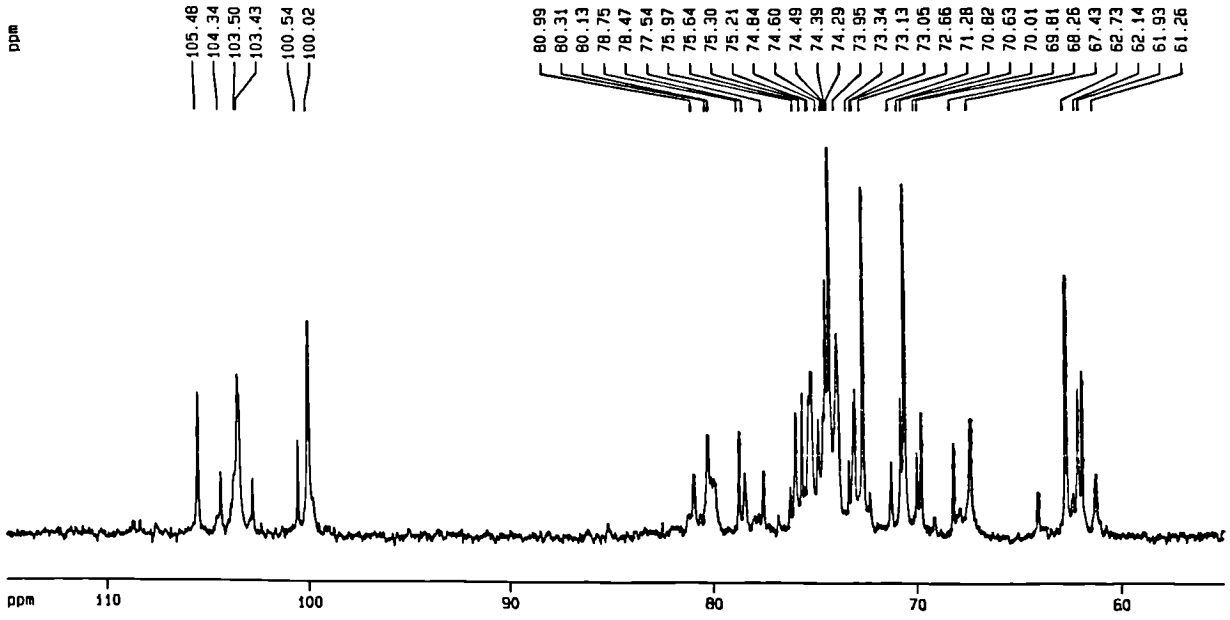

^{13}C NMR Spectrum (line broadening 3Hz) of a 4M KOH extract from pea stem (cf Figure 9.15) after purification with with β-mannanase and *endo*-arabinase enzymes. The signal at 108.7 assigned to arabinan in Figure 9.15 is eliminated togtether with the putative C-1 mannosyl signal at ca. 101ppm. Signals for β-(1→4)-galactan (C1 = 105.48; C-4 = 78.17ppm) and xylosyl (C1 = 100.02) and glucosyl (C1 = 103.5) residues of xyloglucan are identified, but galactosyl and fucosyl residues of xyloglucan are not assigned.

Figure 9.17: ^{1}H-NMR Spectrum of Partially Purified Pea Xyloglucan

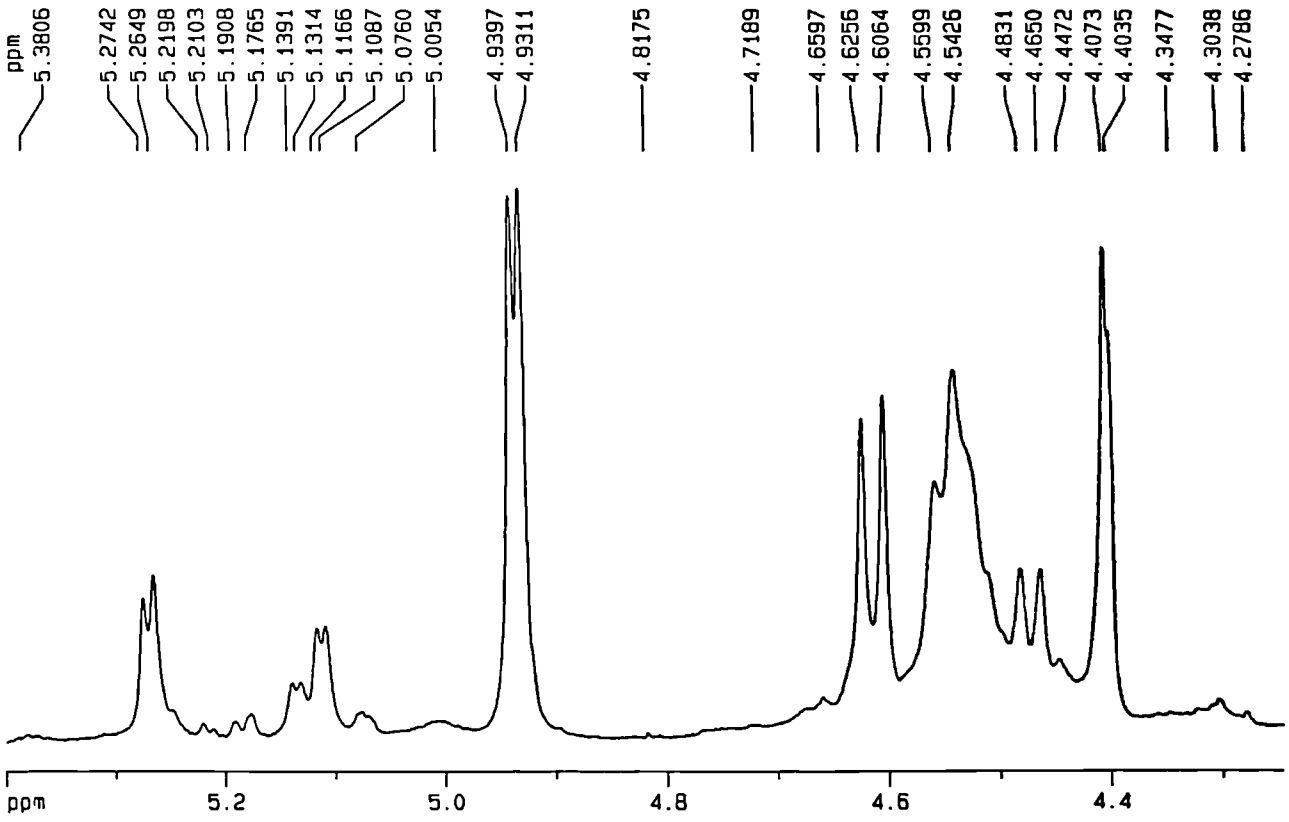

Figure 9.18: Deep-Etch Freeze Fracture TEM of a Putative Cellulose/Pea Xyloglucan Complex

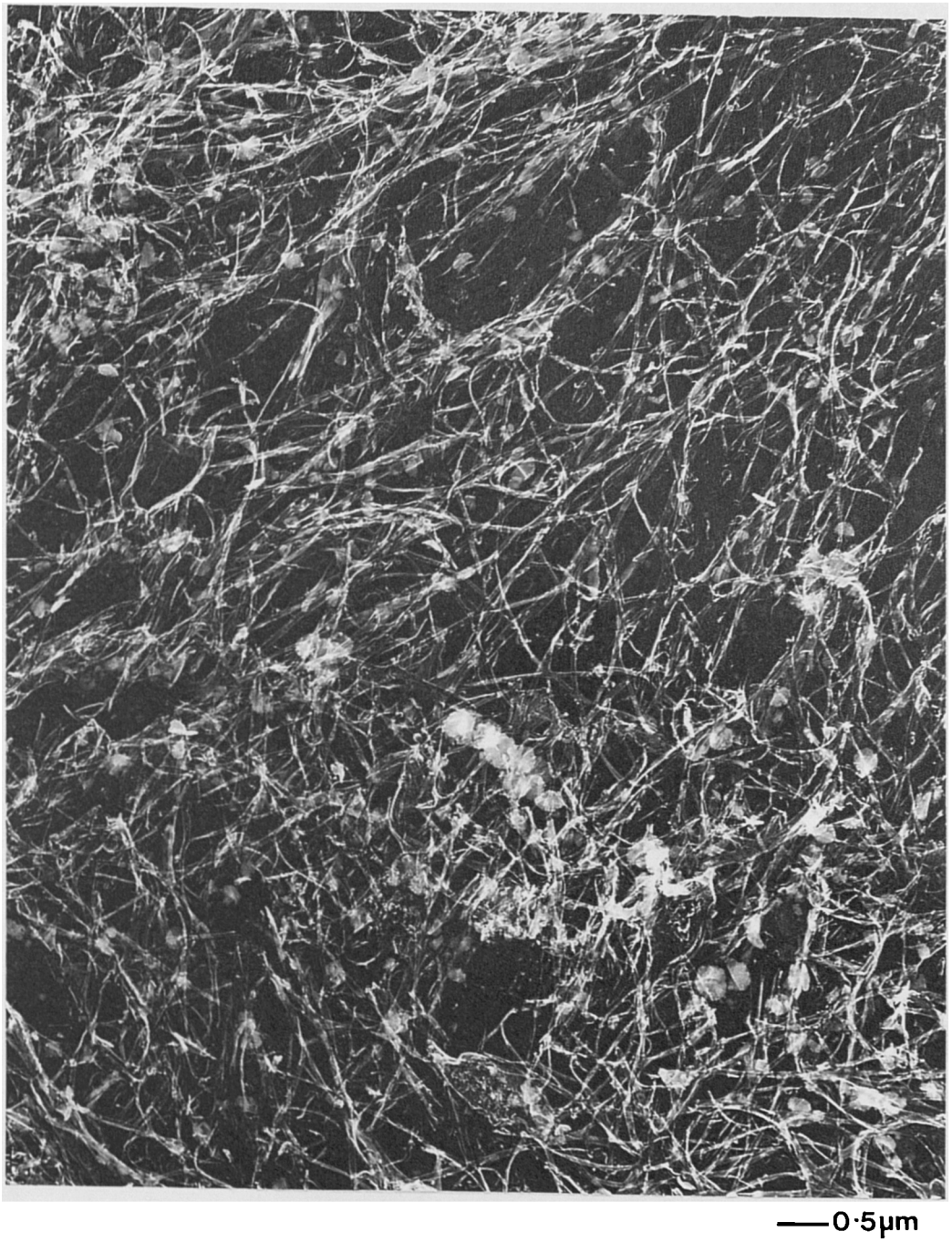

An electron micrograph of cellulose synthesised by *Acetobacter aceti* ssp. *xylinum* in the presence of pea xylo glucan showing no evidence of lateral organisation of cellulose fibres or cross-linkages between adjacent fibres. There is some evidence for reduction in cellulose fibre width in this composite compaed with that formed in the presence of high mwt tamarind xyloglucan (Chapter 6, Figure).

9.4 Discussion

From the complexity of the hydrolysis products of tomato xyloglucan (Figure 9.2, section 9.3.1.3) and the difficulty in complete assignment of the ^{1}H NMR spectrum of the almost pure polysaccharide (Figure 9.11, section 9.3.1.5), the structure of tomato xyloglucan remains only partly determined. There is significant similarity of *endo*-glucanase hydrolysis products with those obtained from potato, another member of the Solanaceae (Figure 9.6), suggesting commonality of structure, however the evidence that, like potato xyloglucan, tomato xyloglucan is galactosylated, is not unequivocally established. The monosaccharide and NMR analyses indicate that the tomato xyloglucan backbone may in fact be less xylose-substitued than is typical for xyloglucans sourced from other dicotyledons (Hayashi, 1987). As there is no evidence for arabinose residues attached to the backbone as had been identified in sycamore extracellular polysaccharides (Hisamatsu *et al*, 1992), this suggests that the backbone may have an overall lower level of side chain substitution, such as is more usually seen in xyloglucan from monocotyledons (Hayashi, 1987). Complete structural assignment of tomato xyloglucan is beyond the scope of this thesis and the results from Albersheims group on tomato xyloglucan characterisation, some of which were presented at the Keystone Symposium, Colorado (York *et al*, 1996), are awaited with interest.

Of particular interest is the occurrence of significant quantities (approximately equivalent to the total amount of xyloglucan) of the hemicellulose glucomannan, which is present as a primary cell wall component in mature green tomato fruit. Since glucomannan is also a substrate for *endo*-glucanase enzymes, measured effects of these enzymes on tomato cell walls cannot be attributed solely to action against xyloglucan. Knowledge of the structural attributes imparted by the presence of glucomannan, offers scope for modifications aimed specifically at the glucomannan component (see also Chapter 7).

In contrast to the highly complex nature of tomato xyloglucan, pea xyloglucan extracted by alkali treatments is relatively simple in structure. It is becoming clear however, that the native structure is

more complex than this, particularly in the presence of mono-*O*-acetyl groups on side chains, which are removed under alkaline conditions (Paully *et al*, 1995) such as those used in this study. The major aim of purification and characterisation of pea stem xyloglucan was as a source of fucosylated polysaccharide, more typical of primary cell wall xyloglucan than that isolated from tamarind seeds, for incorporation into the *Acetobacter* system. Preliminary results obtained were inconclusive and precluded interpretation in terms of altered cellulose fibre dimensions in the presence of fucosylated vs. non-fucosylated polysaccharide (see Chapter 6, discussion). It became clear however that isolation of xyloglucan from pea stems is extremely labour-intensive for low polymer yields. For this reason, it is hoped that fucosylated xyloglucan will be obtained from suspension cultures of *Phaseolus vulgaris* cells, in collaboration with the CCRC, Athens, Georgia.

It will be of great interest to examine the effects of tomato and pea/bean xyloglucan, both of which have very different structures to tamarind xyloglucan, on the molecular organisation and network architectures of cellulose/xyloglucan composites formed using *Acetobacter*. However, the molecular weights of both polysaccharides are very much lower than that of high mwt tamarind xyloglucan (see section 6.3.4). Results presented in Chapter 6 demonstrated a significant molecular weight effect on the behaviour of chemically identical xyloglucans in the fermentation system, such that lower mwt tamarind xyloglucan did not introduce cross-linking into the cellulose/xyloglucan network. This could be explained in terms of differeing entropy requirements for relatively short and relatively long molecules in this system although it was emphasised that, in the cell wall environment, other physical and biological factors may influence binding and cross-linking phenomena. The evidence from Chapter 6 suggests that the relatively low mwt xyloglucans purified from cell walls may show different association characteristics with cellulose in the fermentation system compared with cell walls.

Chapter 10: Comparative Rheology of Comminuted Cell Wall Material and Bacterial Cellulose Composites

10.1 Introduction

As described in earlier chapters, primary plant cell walls comprise slender, tough rods of cellulose microfibrils, intimately associated with hemicellulose components and embedded in a matrix of complex and heterogeneous pectic polymers (Carpita & Gibeaut, 1993; McCann *et al*, 1990; Talbott & Ray, 1992a). Primary plant walls are dynamic structures, surrounding cells undergoing expansion during which cell volume can be increased by 10-100 times their original size (Taiz 1994). However, expansion is driven by turgor pressure, an essential pre-requisite for plant growth (Boyer, 1968; Cosgrove, 1987); this may range from 0.3-1MPa depending on species and growing conditions (Cosgrove 1993b) and, due to the geometry of the cell, turgor-mediated tensional stresses within primary walls may be in excess of 100MPa (Cosgrove, 1993a, 1993b). Hence, primary walls must fulfill the apparently conflicting requirements of substantial mechanical strength in a dynamic structure.

The architectural basis for fulfilment of this function remains unclear as there is no clear consensus on which is the major load-bearing network in plant cell walls. Structurally, cell walls resemble modern man-made materials such as fibreglass, reinforced concrete and graphite-fibre reinforced resin and, traditionally, the cellulose/hemicellulose matrix is described as the network bearing the majority of tensional stresses in the wall (Fry 1989). However, walls deficient in cellulose and hemicellulose components can form a functional wall with greater tensile strength than controls (Shedletzky *et al*, 1992) , suggesting that cell walls possess remarkable flexibility in their structure.

10.1.1 Wall Mechanical Properties and Correlation with Textural Attributes

Cell walls apparently derive their mechanical strength from the structural components of the wall and the nature of their interaction. There are several mechanisms by which interactions between components can be perturbed whilst the ability to withstand tensional stress is unimpaired, for example during cell growth. For the plant, cell walls impart mechanical strength to an organism lacking an endo- or exoskeleton; as a food, the textural character of plant tissues is believed to be attributable, in part, to the properties of these cell walls. For example, the textural differences between a ripe and unripe tomato fruit are obvious and these are correlated with well documented changes in wall chemistry and physiology (eg Seymour *et al,* 1990). Much progress has been made in elucidating chemical and architectural properties of cell walls (eg McCann & Roberts 1991; McCann *et al*, 1990, 1995; Redgwell & Selvedran, 1986), but the challenge for the food technologist is to *predictably* relate these to the textural attributes of a plant tissue. One of the major problems with this is a matter of scale ie correlating changes in nms or μms with mechanical properties measured at the mm or cm distance scale. In an attempt to bridge this a variety of mechanical testing methodologies are employed, using large and small deformation techniques on intact tissues, isolated cell walls and even isolated cells. Even this array of procedures falls short of a continuous mechanical spectrum from molecules to tissues. We are still unable to relate, for example, the mechanical properties of comminuted cell walls, which may be comprehensively defined at the molecular and ultrastructural level, to whole tissues which contain a variety of cells of different types, in which the wall functions as a continuous matrix.

In chapters 6 and 7 bacterial cellulose synthesised *in situ* was shown to be induced to form networks with added hemicellulose polymers with ultrastructural and molecular features akin to plant cell walls of different types. We are therefore able to controllably and predictably generate continuous materials which, we believe, may bridge the gap between isolated walls and a wall matrix as seen in plant tissues. Most evidence from cell expansion studies suggests that the cellulose/hemicellulose network may indeed be the major load-bearing network in cell walls and therefore our ability to recreate these networks in a controllable fashion may provide crucial information on mechanical properties conferred

by these structures. Work in this chapter outlines mechanical testing, using both small and large deformation techniques, of these composites and discusses how results obtained can be correlated with those obtained for comminuted cell walls. It is pertinent at this point to discuss briefly the principles behind mechanical testing and the limits of interpretation of results in these complex systems.

10.1.2 Rheology

Rheology was defined by Professor E.C. Brigham as "the study of the flow and deformation of matter' and was recognised as a science in its own right with the formation of the Rheological Society in the US in 1929. Rheological testing involves the application of force to the sample under investigation and measurment of the deformation or, conversely, application of deformation and measurement of resistance. Results can be interpreted in terms of interactions at the molecular level by comparison with data from simple 'well-behaved' systems and for plant materials, which are extremely complex, it is hoped that some general material properties can be defined using such techniques.

It is important to note that, in all rheological testing, timescale is a particularly important variable. For example, we generally regard glass as a solid structure yet, over a suitable time period, glass in a window will flow under the force of gravity, as evinced by medieval and Roman glass windows which have, over a period of many hundreds of years, flowed so that they are much thicker at the bottom than at the top. Contrast a sugar syrup which will respond to gravity or another applied force over a time period of seconds. The same processes are occurring, the only variable is time.

Before looking at the application of rheology to complex polymer systems it is worth considering two idealised extremes. The perfect elastic solid was described by Robert Hooke in 1678 in his 'True Theory of Elasticity'. A true Hookean solid is perfectly elastic ie all energy put into the system when deformation is applied is returned when that deformation is released. The stress generated in resisting deformation is directly proportional to the magnitude, but independent of the rate of deformation

(Barnes *et al*, 1993). Perfect 'Newtonian' liquids were described by Isaac Newton in 'Principia' in 1687 and in these liquids resistance to deformation is directly proportional to the rate of movement, but independent of the magnitude (Barnes *et al*, 1993). For true Hookean solids, the ratio of stress (force per unit area) to strain (amount of deformation, dimensionless) indicates the rigidity of the material, for Newtonian liquids this ratio gives the viscosity of the liquid (Morris, 1983). In reality, no true Hookean solids and very few Newtonian liquids exist and most materials therefore exhibit a rheological behaviour which contains components of both a viscous and an elastic response ie they are viscoelastic. Growing plant cell walls could be described as having viscoelastic-liqiud behaviour ie they do not return to their original shape and size after removal of applied deformation, whereas a mature wall responds more like an elastic solid, returning almost completely to its original size and shape after cessation of stress application (Cosgrove 1993b).

10.1.3 Small Deformation (Oscillatory) Rheology

For polymer systems, there is generally a low strain region in which stress generated in resisting applied deformation shows a linear relationship to strain (Morris, 1983). At higher strains, the slope of the stress-strain curve decreases and at sufficiently high strains samples will irreversibly fail. Large deformation rheology operates at high strains leading to flow and fracture/failure and can give information on bulk material properties. Small deformation rheology uses very much lower strain conditions, which cause less perturbation of the structure and can generate information about the molecular behaviour of components in a system. No net deformation of the sample under test occurs.

10.1.3.1 The Theory of Oscillatory Rheology.

The oscillatory rheometer used in this chapter uses parallel plates and is described in greater experimental detail in section 10.2.3. It is relevant at this point to discuss how results are interpreted. Figure 10.1a shows a sine wave similar to that which would be generated by the oscillatory motion if a

Figure 10.1 Sine Waves Produced by Plotting the Postion or Velocity of the Bottom Plate of an Oscillatory Rheometer against Time

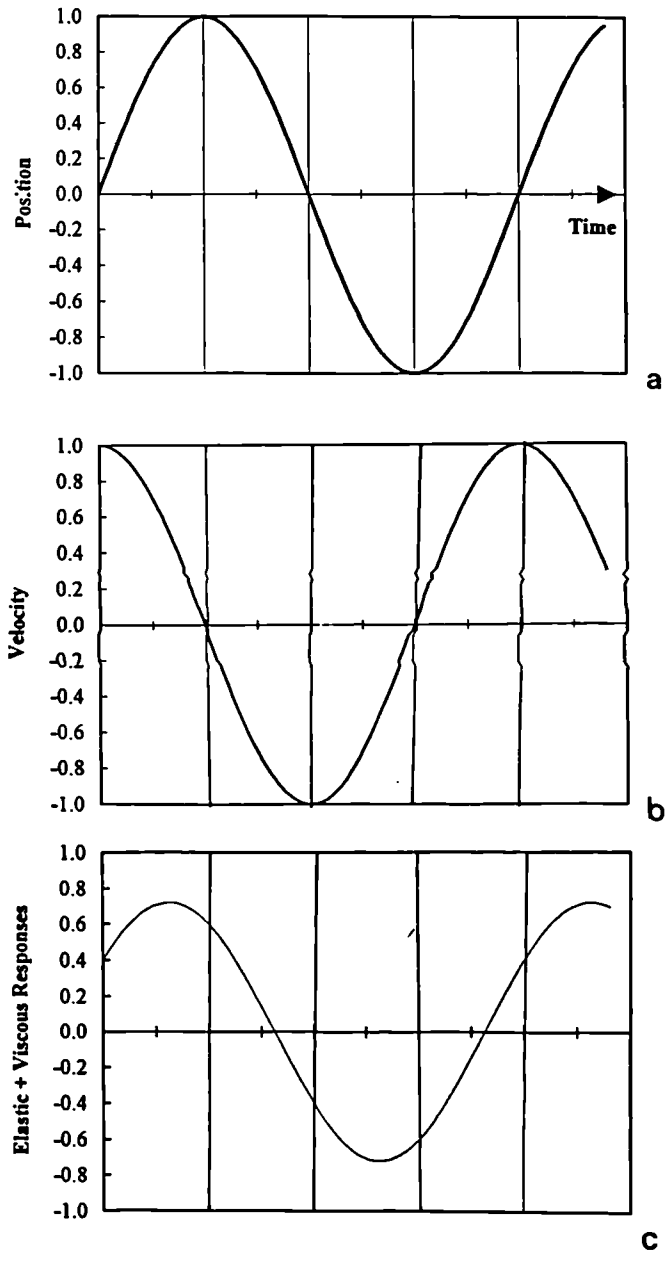

The sine wave plotting the position of the rheometer plate (a) or the velocity of the plate (b) (cosine of (a). Perfect Hookean solids would generate output wave a ie 0° out of phase with the original input signal from the bottom plate, perfect Newtonian liquids output wave b (90° out of phase) and viscoelastic materials would produceanywhere between 0° and 90° out of phase depending on the relative contributions from the 'liquid-like' and 'solid-like' components

mark was made on the outer edge of the bottom plate and its position relative to its starting point plotted over time. If, however, the velocity of the plates' motion is plotted in a similar way, a cosine wave exactly 90° out of phase is generated (Figure 10.1b). For a Hookean solid, development of stress will follow the positional sine wave of Figure 10.1a, a Newtonian liquid will follow the velocity cosine wave 90° out of phase shown in Figure 10.1b. For viscoelastic materials the sine wave output will be somewhere between 0° and 90° out of phase with the original input signal. Plotting of the phase angle of the viscoelastic response as a resultant vector allows the relative contribution of the solid-like and liquid-like components of a viscoelastic material to be calculated. The viscous component is termed the 'loss modulus' G'', and the elastic component the 'storage modulus', G'.

10.1.4 Use of Oscillatory Rheology to Probe Plant Cell Walls

Use of small deformation oscillatory rheology to probe mechanical properties of plant cell walls has been a subject of interest in this laboratory for several years. Testing has been performed at three levels, on tissues using discs of tomato pericarp, comminuted cell wall preparations and isolated intact cells (Tim Foster, Michelle Gothard, Unilever Research, pers. comm.). Of these, most work has been performed on cell wall preparations, where attempts to correlate mechanical properties measured by using small deformation rheology with the extensive chemical (eg Redgwell & Selvendran, 1986), architectural (eg McCann *et al*, 1990) and molecular (eg Foster *et al*, 1996) information available for these systems have met with limited success (see discussion). In this chapter, the use of small deformation rheology to monitor enzymic degradation of cell walls will be shown, together with the correlation of this data with chemical measurements. The bulk of the work however, focuses on the use of the bacterial cellulose composites to mimic continuous cell wall networks under rheological testing

10.2 Materials and Methods

10.2.1 Material Preparation

10.2.1.1 Plant Cell Walls

Tomato cell walls were prepared from mature green tomato fruit (*Lycopersiocon esculentum* var. 6203) as described in Chapter 2 (Section 2.11.1) Pea cell walls were prepared from the third internode of dark-grown pea stem (*Pisum sativum* var. Arolla) as previously described (Section 2.12.1). Both cell wall preparations were sequentially extracted to remove most of the pectin component ie to the second sodium carbonate extraction (Section 2.11) to produce cell wall 'ghosts'.

10.2.1.2 Bacterial Cellulose Composites

Bacterial cellulose was produced as described in section 2.13.4 and modified with xyloglucan or glucomannan as described in sections 6.2.1 and 7.2.2. Intact pellicles were washed with deionised water containing 0.05% NaN_3 and stored at 1°C. Comminuted material was produced by grinding with an Ultra-Turrax T-25 (Janke & Kunkel) in deionised water followed by centrifugation at 27,100g at 4°C. Large quantities of cellulose material for concentration-dependence studies was obtained by incubating 5ml bacterial inoculum in 95ml Hestrin-Schramm medium (Hestrin & Schramm, 1954) in Roux bottles at 30°C as described in section 2.13.2 for seed culture production.

10.2.2 Hydrolysis of Pea Cell Wall Ghosts using endo-1,4-β-Glucanase

Approximately 1g of hydrated pea cell wall ghost material (5.4% dry weight) was weighed exactly into a screw-capped vial. The total amount of xyloglucan in the ghost material was estimated by monosaccharide analysis as 12% (w/w) and sufficient *endo*-1,4-β-glucanase enzyme (from *Trichoderma viride*, Megazyme Pty, Australia) added to hydrolyse all the xyloglucan component in 24 hours, assuming that the insoluble xyloglucan is as readily hydrolysed as soluble CMC (4M6F,

Hercules, UK) against which enzyme activity was assayed. In fact, it is known that solubilised XG is a much less effective substrate than solubilised CMC (Hayashi *et al*, 1984) and the total amount of enzyme was increased to 0.01U from 0.002U based on CMC to reflect this. The total volume was made up to 7ml with sterilised 50mM sodium acetate buffer pH 4.5 and the vial incubated with constant agitation at 40°C.

500µl aliquots of homogenous suspension were removed at t=15, 30, 45, 60, 90, 120, 180, 270, 360, 480, and 1440 minutes after enzyme addition. Aliquots were placed in screw-capped eppendorf tubes and the enzyme inactivated by placing in a boiling water bath for 5 minutes. Samples were centrifuged in a Centaur Microfuge for 5 minutes, the supernatant removed and incubated for 16 hours with 0.005U of *Trichoderma viride endo*-1,4-β-glucanase (Megazyme Pty Australia). After enzyme deactivation as above, 100µl was injected onto the Dionex HPAEC system (Dionex Corp., USA) using the gradient conditions for xyloglucan oligosaccharide separation described in section 2.13.7. Xyloglucan peaks were identified by comparison with spectra obtained for purified pea xyloglucan (Chapter 9). These were quantified by integration and comparison with peak areas for a tamarind xyloglucan oligosaccharide sample of known concentration.

10.2.3 Small Deformation (Oscillatory) Rheology

All small deformation measurements were made using a Rheometrics RDA II ( ). Figure 10.2 shows a schematic representation of an oscillatory rheometer. Samples are placed between circular parallel plates with defined radius, thereby imparting a defined sample geometry. The distance between the plates can be controlled, giving a known sample depth (gap setting). Mechanical measurements are made by oscillating the bottom plate via a geared drive at a preset frequency and displacement (strain) and the force required to do so (stress) is calculated. Strain and stress are transmitted through the sample to the top plate which is connected to a motion sensor, in the case of the RDA II a torsion bar

Figure 10.2 Schematic Representation of an Oscillatory Rheometer

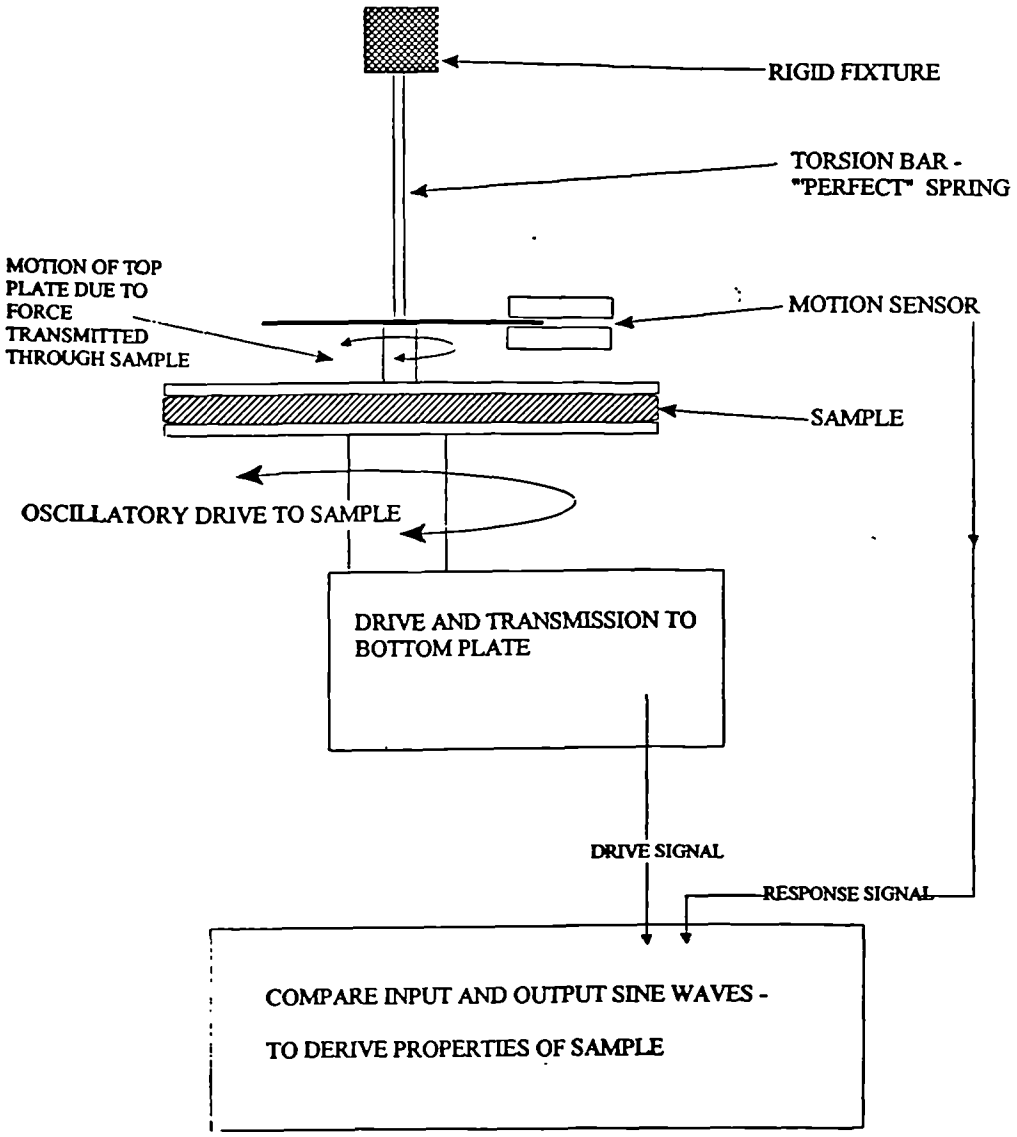

with a defined spring constant. Force can therefore be calculated by the degree of twist occurring at the base of the bar. The output signal is recorded and compared to the input signal; from this data various rheological parameters such as storage modulus (G'), loss modulus (G''), complex (shear) modulus (G* (= $\sqrt{G'^2 + G''^2}$)), dynamic viscosity (η^* (= G^*/ω)) and the loss tangent ($\tan\delta$ (= G''/G')) can be calculated as a function of time, frequency and temperature.

10.2.4 Small Deformation Rheology of Depectinated Tomato Cell Walls

1.5g depectinated comminuted cell wall samples (7,5% or 4% dry weight) were placed between 25mm parallel plates (gap setting 2.000mm). Liquid paraffin was applied to the edge of the sample to prevent dehydration and the plates enclosed and kept at 40°C during all measurements. Strain sweeps were recorded from 0.05-200% strain and frequency sweeps (mechanical spectra) from 0.5-200 $rad.s^{-1}$ at 0.5% strain. Timesweeps were performed for 2 hours at 0.5% strain and 6.28 $rad.s^{-1}$ (1Hz).

Endo-1,4-β-glucanase (*Trichoderma viride*, Megazyme Pty, Australia) quantities were calculated for depectinated tomato cell walls as described for depectinated pea stem cell walls (10.2.2) giving a basal enzyme quantity of 0.1U/1.5g material (7.5% dry weight). Enzyme was added either by injection directly into the sample on the plate at t = 250s or prior to placement on the plate followed by whirli mixing. Frequency sweeps were performed immediately after enzyme addition at t=0 and at t=2 hours at 0.5% strain and timesweeps as above. Chemical analysis of material after testing was not possible due to the use of liquid paraffin to prevent dehydration.

10.2.5 Small Deformation Rheology of Bacterial Cellulose Composites

10.2.5.1 Intact Pellicles

Pellicles as obtained were 1.5-3mm thick with irregular outlines and an average diameter of ca. 3cm. Pellicles syneresed readily when placed on the plates. No attempt was made to cut pellicles into regular

geometries to avoid pre-stressing an already apparently weak structure. 25mm radius parallel plates were used to increase sensitivity and the possibility of sample slippage reduced by attaching fine emery paper to the surface of the plates. To allow direct comparison with cell wall material strain and frequency sweeps were conducted under the same conditions as in 10.2.4. All experimentation was performed at 20°C

10.2.5.2 Comminuted Composite Material

Comminuted material was produced by retrieving intact pellicles after mechanical measurements, pooling replicates, and homogenising material using an Ultra-Turrax T25 as described in section 10.2.1.2. Single measurements were made for each sample as there was insufficient material to allow testing at a range of concentrations (cf 10.2.5.3). Mechanical measurements were performed as described in section 10.2.5.1, but using 12.5mm radius plates. Dry weights were determined by drying overnight at 70°C under vacuum.

10.2.5.3 Concentration Dependence

The concentration dependence of rheological behaviour was determined using comminuted cellulose. Concentrations were varied either by the addition of deionised water followed by vigourous vortexing or by blotting with glass fibre filter paper (Whatman). Rheological measurements were made as previously described (10.2.5.1) using 12.5mm radius plates and dry weights determined as above (10.2.5.2).

10.2.6 Large Deformation Rheology Testing of Bacterial Cellulose Composites

The rheological behaviour of bacterial cellulose composites was examined using tensile testing. Portions of intact pellicle were excised using a sharp razor blade to give a rectangular strip of material. Ideally for tensile testing the length/width ratio should be ca. 10, however due to the weakness of the

material and difficulties encountered in accurate cutting due to sample slippage, sample geometries were highly variable. The two ends of the excised samples were placed between vice-grips in a Minimat (Polymer Laboratories, Loughborough, UK) and the grips moved apart at a constant speed of 10mm/minute using a 20N load beam. The behaviour of the sample under tension was recorded in real time using a video camera.

10.3 Results

10.3.1 Release of Xyloglucan from Pea Cell Wall Ghosts by endo-*Glucanase Action*

The oligomeric composition of material released by *endo*-1,4-β-glucanase action after t=480 minutes is shown in Figure 10.3a with comparison spectra of material released after t=90 minutes, purified pea xyloglucan and tamarind xyloglucan in Figure10.3 b-d respectively. Peaks 1-3 decrease in abundance relative to peaks 4-7 during the time course of the experiment and, after comparison with reference spectrum c are not assigned to xyloglucan. In accordance with the data presented in Chapter 10, peaks 4 and 5 are assigned as XXXG and XXFG respectively. Peaks 6 and 7 cannot be unambiguously assigned (see Chapter 9 discussion). Apart from t=30 minutes the relative ratio of peaks 4:5:6:7 remains approximately constant at 1.00 :1.08 ± 0.03: 0.3 ± 0.03: 0.26 ± 0.04 indicating that there is no structural difference between xyloglucan which is readily hydrolysed and that which is more resistant to hydrolysis. Significant quantities of low molecular weight material is eluted at ca. 2-4 minutes, some of which may be cellobiose (eluted at ca.2 minutes using this gradient) produced by the action of *endo*-1,4-β-glucanase on cellulose microfibrils.

Figure 10.4 shows the time course of xyolglucan released by the action of *endo*-1,4-β-glucanase. Even after 24 hours only approximately 8% of the total xyloglucan was released. The amount of xyloglucan released is much lower than that reported by Hayashi & Maclachlan (1984) and Baba *et al* (1994a) on

Figure 10.3 Dionex Profile of the Oligomeric Composition of Xyloglucan Released from Pea Cell Wall Ghosts by endo-1,4-β-glucanase Action

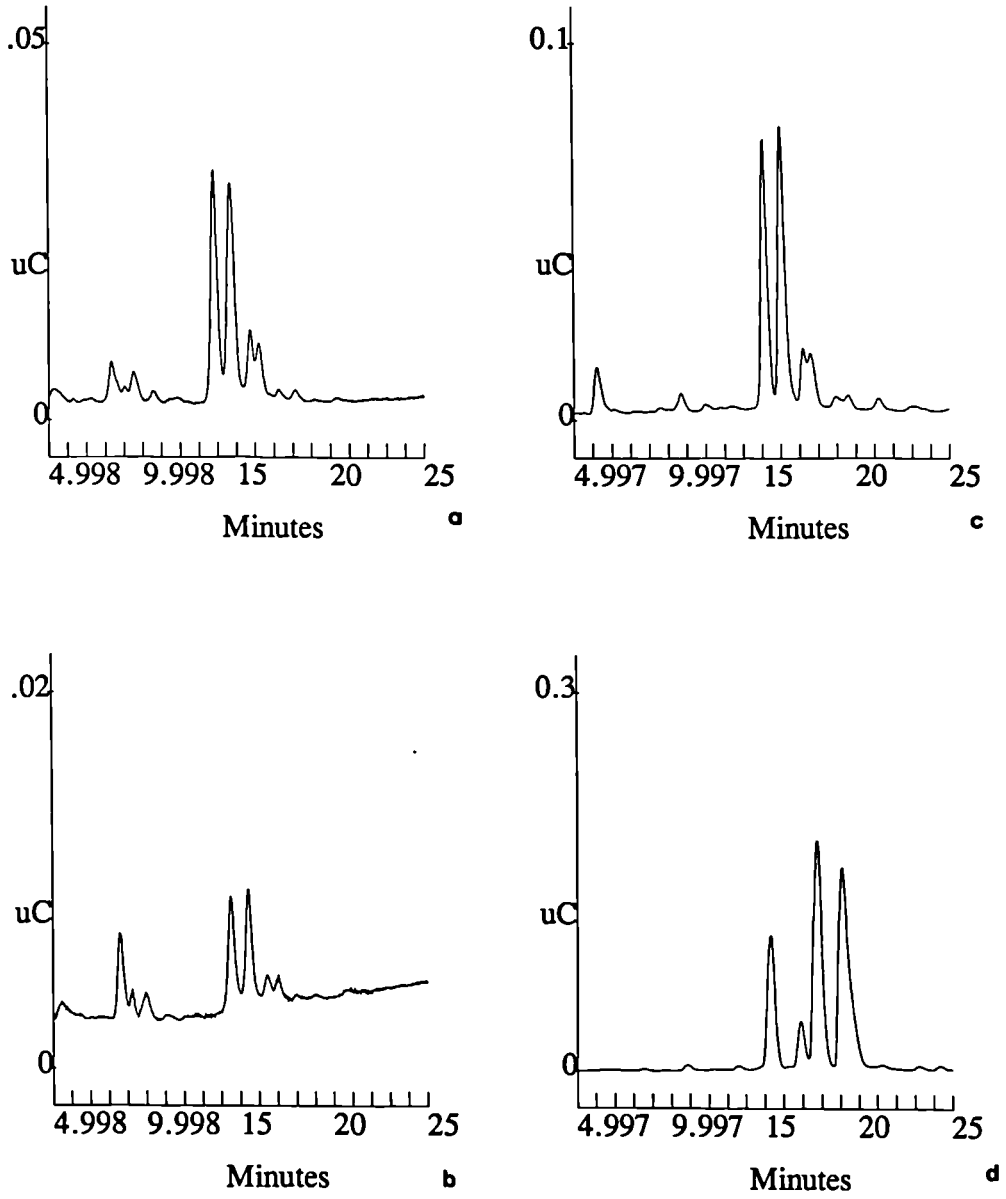

Oligomeric composition of xyloglucan released by enzyme action after 480 minutes (a) compared with composition at 90 minutes (b). Purified pea and tamarind xyloglucan oligomers are shown in (c) and (d) respectively. Peaks 1-3 of (a) do not appear in (c) and are not assigned to xyloglucan. Peaks 4-7 are assigned to xyloglucan by reference to (c). The relative ratio of 4:5:6:7 remains unchanged with time, but the total amounts of these peaks increase relative to peaks 1-3 (compare (a) and (b))

Figure 10.4 Time Course of Xyloglucan Degradation by *endo*-1,4-β-Glucanase Action on Pea Cell Wall Ghosts

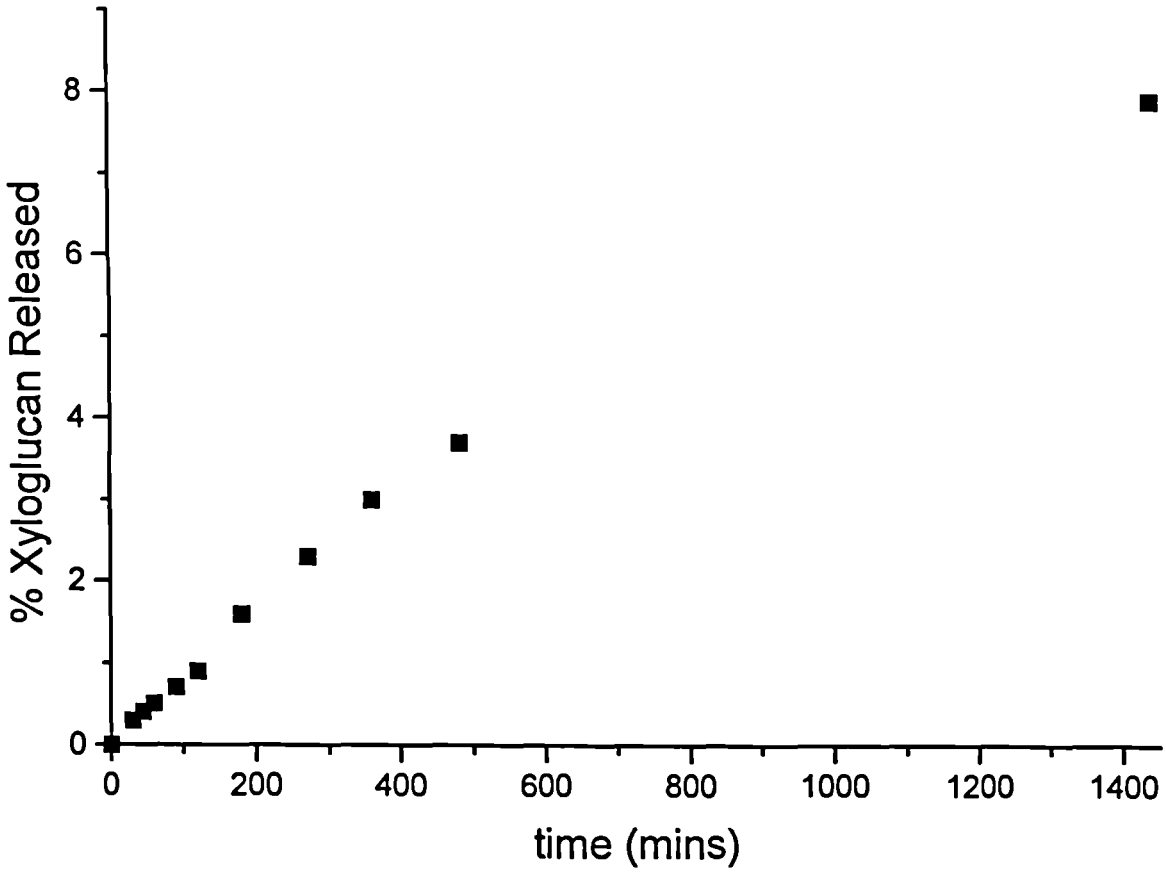

a similar system, however they used material which had been extracted with 4% KOH and performed experiments over 3,6 and 7 day time periods.

10.3.2 Small Deformation Rheology of Depectinated Mature Green Tomato Cell Walls

10.3.2.1 Cell Wall Properties

Figure 10.5 shows a typical strain sweep for depectinated tomato cell wall material at 7.5% dry weight. The storage modulus (G') is approximately an order of magnitde greater than the loss modulus (G'') which is normally considered to be indicative of a well-ordered system. Strains at which G' and G'' show strain-independence (the linear region) are sufficiently non-perturbing as to not degrade the sample structure. A strain of 0.5%, well within this linear region, was chosen to record the mechanical spectra of these samples.

The mechanical spectra (frequency sweeps) of depectinated tomato cell wall material are shown in Figure 10.6 at 7.5% (a) and 4% (b) dry weight concentration. Qualitatively, spectra are very similar, although the absolute modulus G' (1Hz) reduces from 31011MPa at 7.5% dry weight to 9397 MPa at 4% dry weight indicating a marked concentration dependence of G'. Tomato cell wall material has been shown to exhibit a concentration-dependence behaviour which can be fitted to the Hermans gelation model (Clark *et al*, 1983; Herman 1965) suggesting that dispersions of walls are highly cross-linked and/or entangled structures even after removal of some polymer components by sequential extraction procedures (M.Gothard, Unilver Research, pers.comm.). For both concentrations, G' is very much greater than G'' ie the materials are exhibiting a predominantly solid-like response over the experimentally accessible frequency range. For a true gel system G' and G'' would show frequency independence over a wide range as the network can be regarded as permanent (Morris, 1983). Clearly, from Figure 10.6 a and b, G' and G'' are not truely frequency-independent; G' has a slight frequency dependence and G'' shows a marked up-turn at higher frequencies. The slope of η^* is calculated as

Figure 10.5: Strain Sweep of Depectinated Mature Green Tomato Pericarp Cell Wall Material

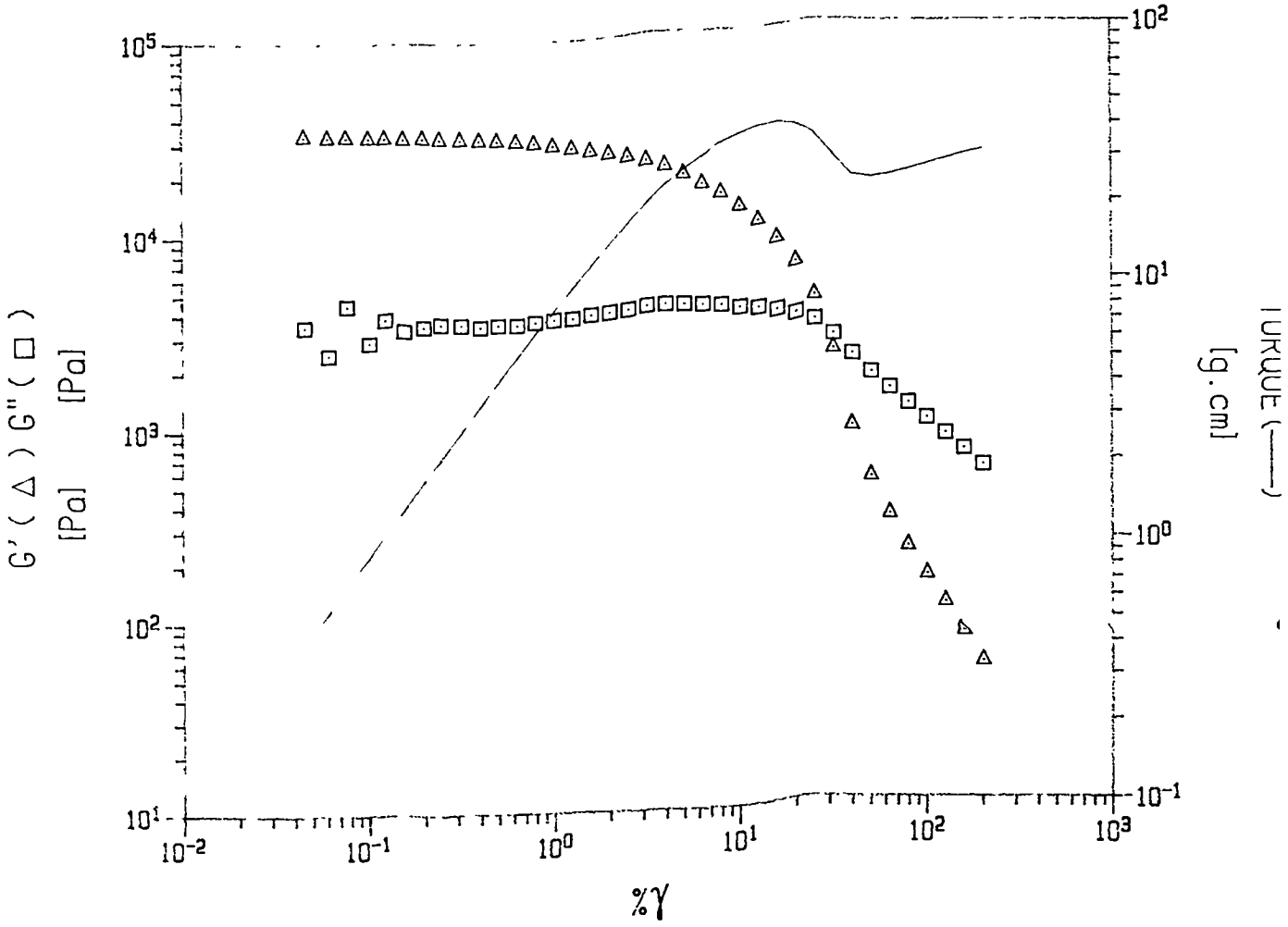

Strain sweep of material at 7.5% dry weight concentration showing strain independence over a wide range and an order of magnitude difference between G' and G'' indicative of a cross-linked system.

Figure 10.6 Mechanical Spectra of Depectinated Tomato Cell Walls at Different Dry Weight Concentrations

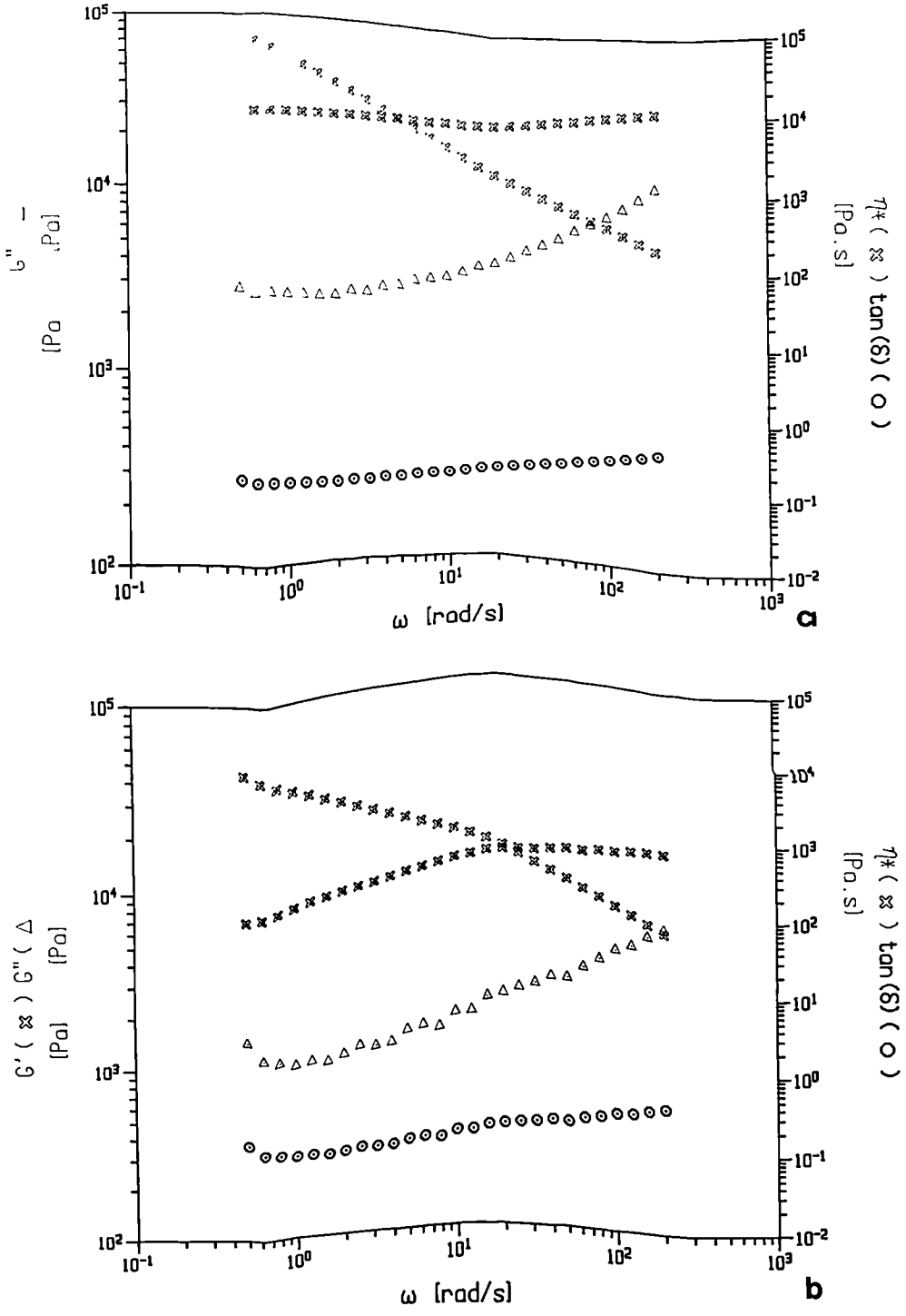

Mechanical spectra (frequency sweeps) of cell wall material at 7.5% (a) and 4.0% (b) dry weight concentrations. G' is significantly higher than G" indicating a well ordered system. Frequency independence of G' and G" is not maintained at higher frequencies ie the system is not a true gel. Tan δ values are low, which implies a low loss system

-0.88 for 7.5% dry weight and -0.92 for 4% dry weight, reasonably close to the value of -1 predicted for perfectly elastic networks (Morris 1983). Values for tan δ are low (ca. 0.14 at 1Hz for both concentrations) indicating a low loss system. When compared with results for cell wall material obtained by laboratory co-workers, depectinated mature green cell wall material has a mechanicalspectrum typical of the plateau zone on the theoretical frequency response (Figure 10.16)

10.3.5.2 Effect of endo-*1,4*-β-*Glucanase Treatment on Rheological Behaviour*

The effect of injection of enzyme directly into a sample of 4% dry weight depectinated cell wall material followed by incubation for 2 hours at 40°C is shown in Figure 10.7. From the control experiment the value of G' remains approximately constant over the 2 hour time period which indicates minmal water loss from the system and that no rheologically-significant sample degradation had occurred. Injection of 1.0U (20x basal enzyme requirement) or 10.0U (200x basal enzyme requirement) of *endo*-glucanase failed to cause a significant reduction in G' either initially or throughout the time course of the experiment. Frequency sweeps were performed on each sample at t=0 at t=2 hours and results are shown in Figure 10.8 a-f and Table 10.1

Table 10.1 Effect of Injection of *endo*-Glucanase into Depectinated Cell Wall Samples on Rheological Behaviour

Sample	G' (1Hz) MPa	η^*/ω	tan δ
Control t=0	9397	-0.92	0.14
Control t=2	11207	-0.92	0.11
Enzyme (1U) t=0	9494	-0.92	0.12
Enzyme (1U) t=2	11281	-0.92	0.11
Enzyme (10U) t=0	11132	-0.92	0.14
Enzyme (10U) t=2	11690	-0.93	0.11

Slight increases in G' over the two hour time period may be due to water loss. It is clear from Figure 10.7 and 10.8 and Table 10.1 that injection of *endo*-glucanase directly into depectinated cell wall samples has no significant effect on the rheological behaviour and, by inference, the network structure of the material.

Figure 10.7: Effect of Injection of *endo*-1,4-β-Glucanase into Cell Wall Samples *in situ*

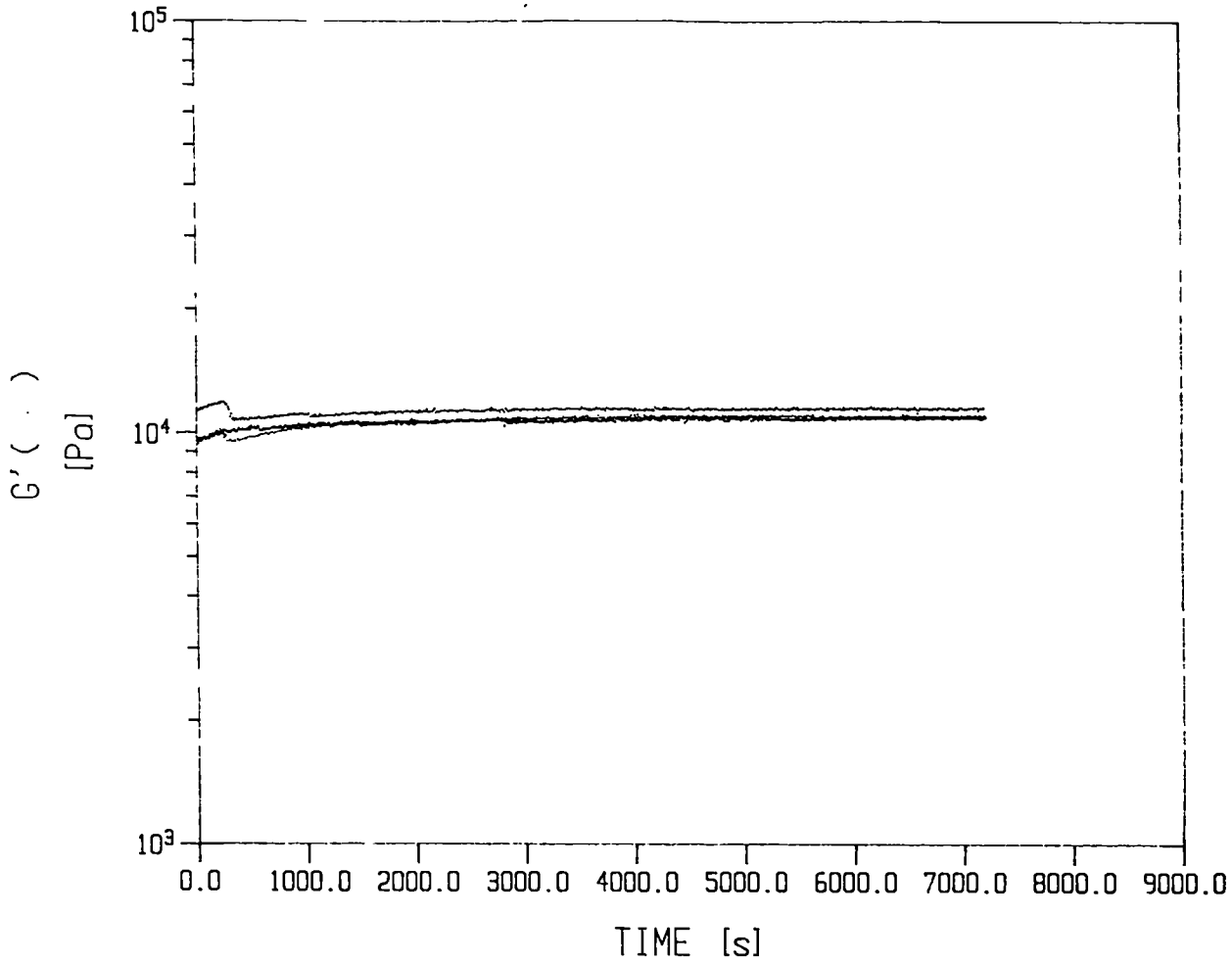

Figure 10.8: Mechanical Spectra of Cell wall Material Before and 2 Hours After Incubation with *endo*-1,4-β-Glucanase added by Injection

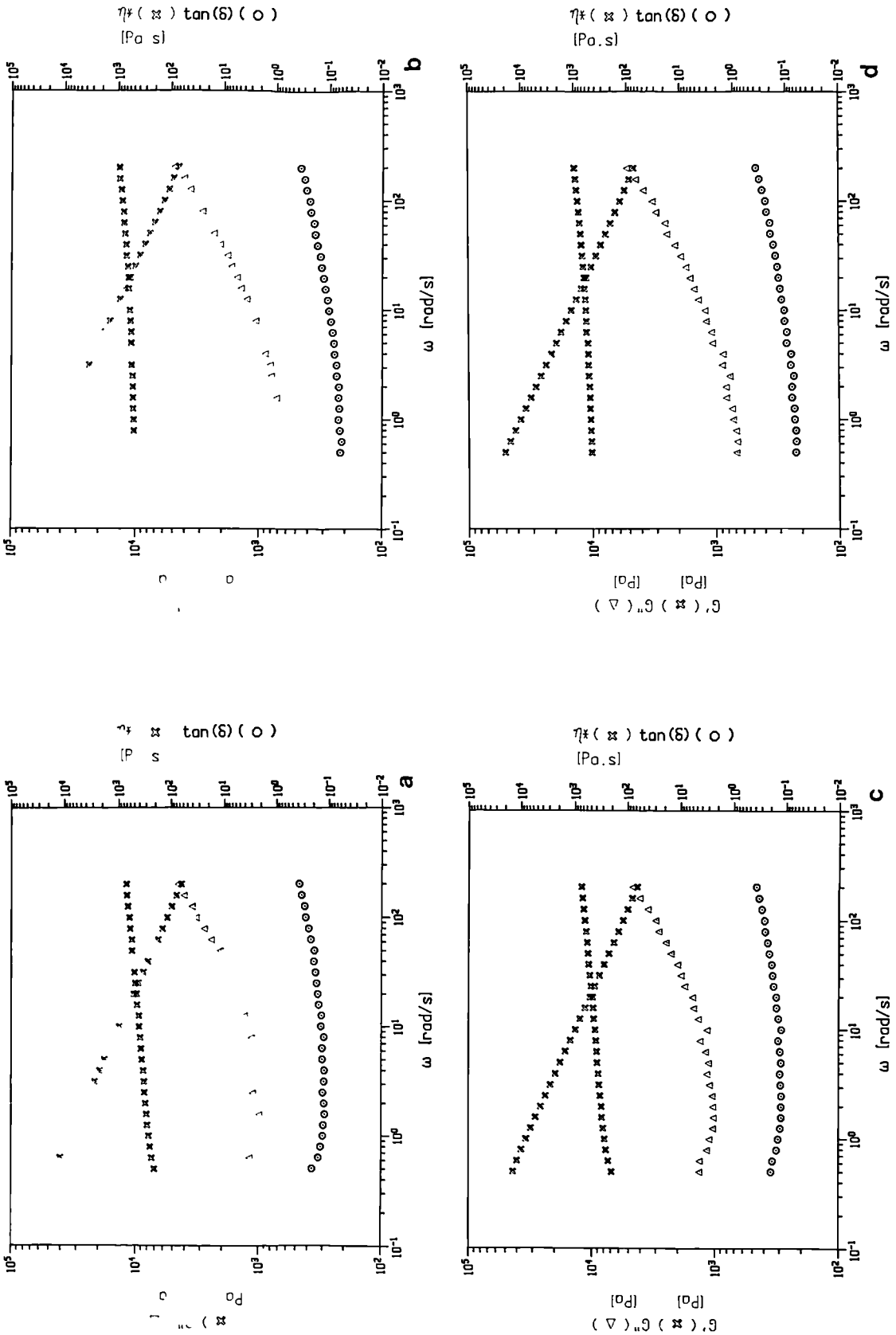

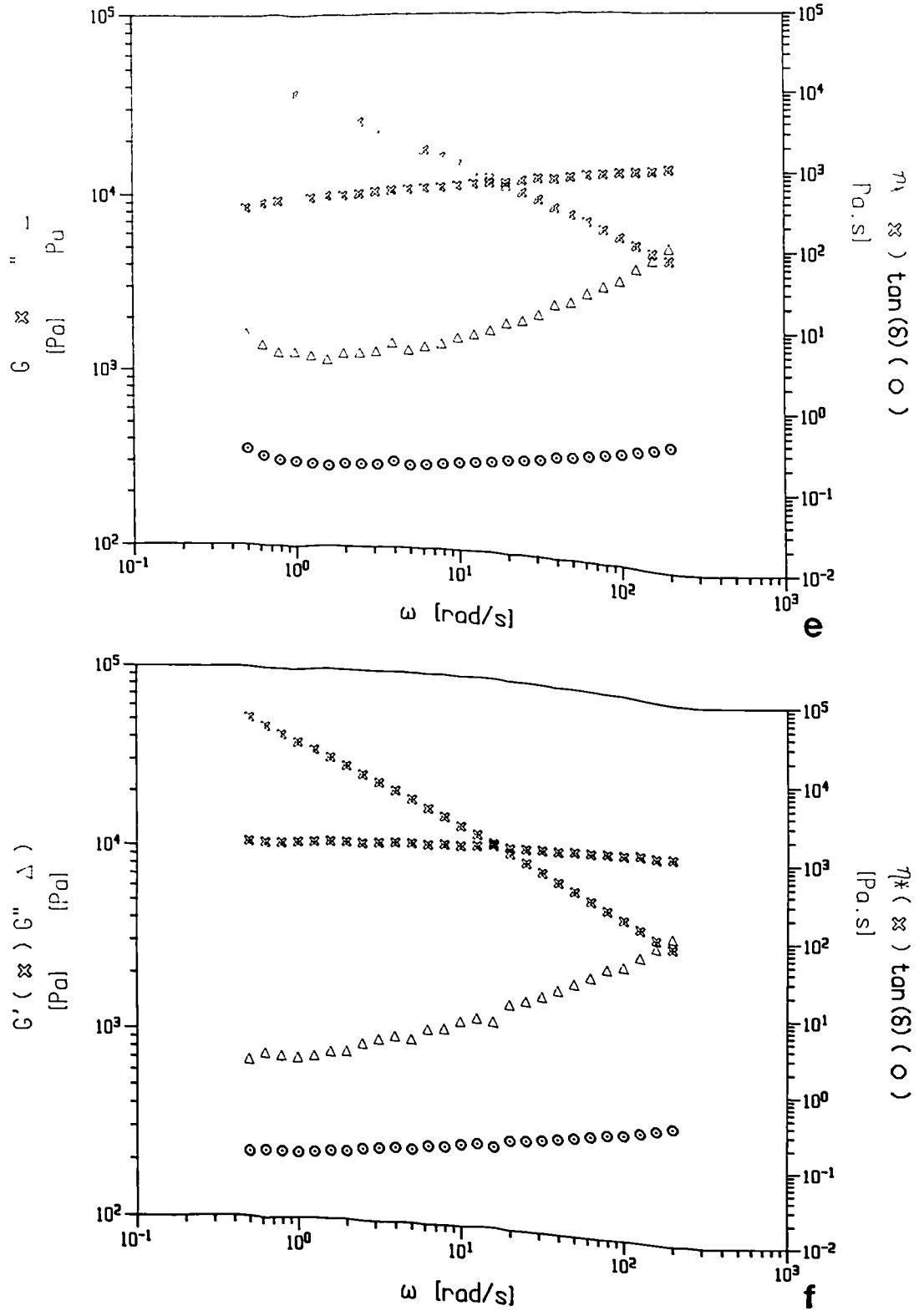

Control samples before (a) and aftre (b) 2 hours incubation at 40°C, o.5% strain, 6.28 rad.s-1. (c) and (d) are spectra of samples before and 2 hours after addition of 1U enzyme respectively; (e) and (f) as (c) and (d) but using 10U enzyme.

The above results suggest that either the enzyme has impaired access to the substrate or the effect of its action cannot be detected rheologically. To determine whether accessibility is a problem, enzyme was added to samples prior to placement on the Rheometrics plate. Dispersion of the enzyme throughout the substrate was facilitated by vortexing.

Figure 10.9 shows the time course experiment for samples which have enzyme added prior to placement on the plate. Samples which have had 0.05U (1x basal quantity) or 0.5U (10x basal quantity) show a slight reduction in modulus compared to the control but, throughout the time course of the experiment, this initial reduction in modulus is not continued. This result can be explained in one of two ways. Either the enzyme is apparently having an almost instantaneous effect at the time of addition and initial vortexing, but no rheologically detectable effect during the experiment. This suggests that *endo*-glucanase action on cell wall ghosts can be detected rheologically but the enzyme has an effect only when it first sees the substrate. Possibly the enzyme becomes irreversibly bound to the substrate very quickly. Alternatively, 4% depectinated mature green tomato cell walls will undoubtably follow the Hermans concentration dependence model (Figure 10.15a). As 4% dry weight is in the terminal behaviour region, even slight changes in concentration (such as by enzyme addition) will have large effects on the moudulus. Table 10.2 and Figure 10.10 show that, although *endo*-glucanase addition has lowered the modulus of samples the rheological behavior of the samples is virtually unchanged. A slight increase in G' over 2 hours may indicate a degree of water loss.

Table 10.2 Rheological Parameters of Depectinated Cell Wall Samples Treated with *endo*-1,4-β-Glucanase for 2 Hours

Sample	G' (1Hz) MPa	η^*/ω	tan δ
Control t=0	9397	-0.92	0.14
Control t=2	11207	-0.92	0.11
Enzyme (0.05U) t=0	8054	-0.89	0.15
Enzyme (0.05U) t=2	9000	-0.92	0.13
Enzyme (0.50U) t=0	6896	-0.92	0.15
Enzyme (0.50U) t=2	7688	-0.92	0.12

Figure 10.9: Effect of Incubation of Depectinated Cell Walls with Varying Quantities of *endo*-1,4-β-glucanase Added Prior to Placement on the Plates

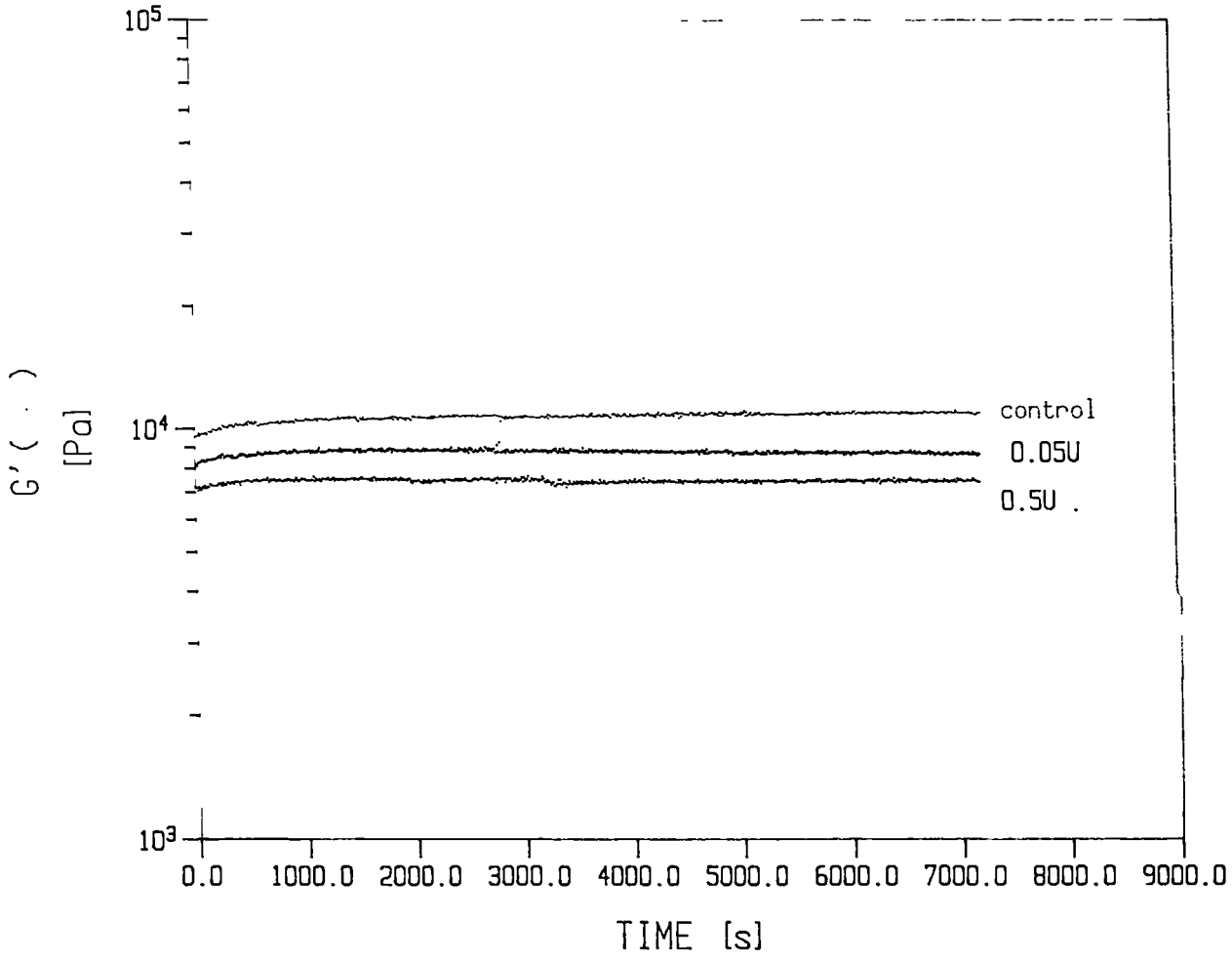

Figure 10.10 Mechanical Spectra Before and After 2 Hours *endo*-1,4-β-Glucanase Treatment

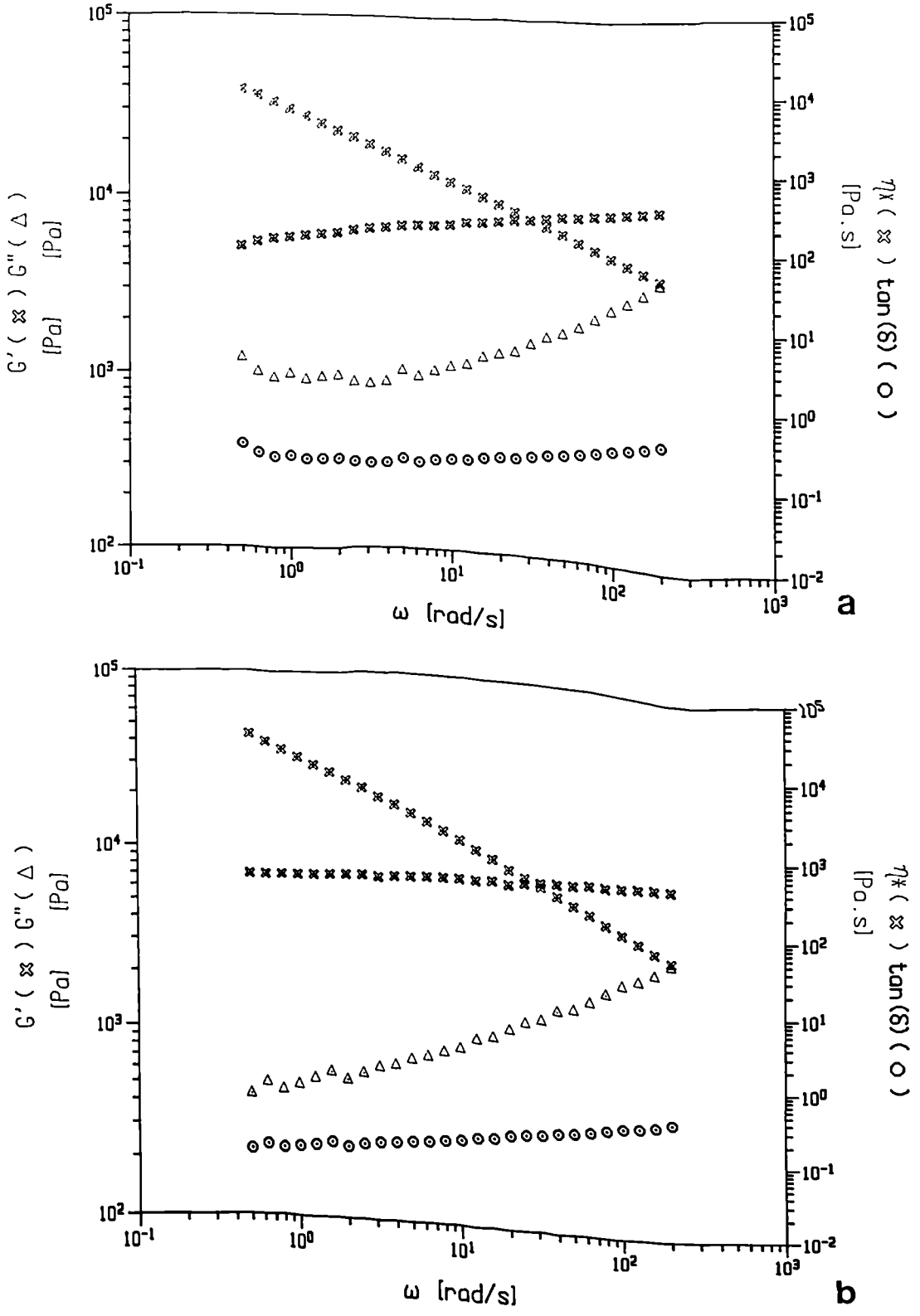

Spectrum (a) of cell wall sample immediately after addition of 0.5U enzyme and (b) after 2 hours at 40°C, 0.5% strain, ω = 6.28 rad.s^{-1}, showing no significant difference between (a) and (b) or when compared to Figure 10.8 (a) and (b) apart from reduction in absolute moduli values. Spectra for samples incubated with 0.05U are qualitatively identical (data not shown).

Even if a vast excess of enzyme is added (686x basal quantity) the initial reduction in G' does not increase over time (Figure 10.11a.). Absolute moduli values are decreased, but rheological paramaters remain remarkably constant (Table 10.3 and Figure 10.11 b,c). . As suggested previously, some of the effect may be attributable to dilution. The massive amount of enzyme used suggests that this result is not due to enzyme becoming rapidly and irreversibly bound to the substrate, but that there is a problem with access of the enzyme to substrate sitesThis may be due partly to the relatively concentrated system (4% dry weight) used, but this is probably less than the cell wall itself although the relative concentration within individual particles may be much higher. Even in a much more dilute system, *endo*-1,4-β-glucanase has a limited effect (Section 10.3.1). For all enzyme experiments where enzyme is added prior to placement on the plates, rheologically detectable differences occur only during the time between enzyme addition and transfer to the rheometer (30 seconds max).

Table 10.3 Effect of Addition of a Vast Excess of *endo*-1,4-β-Glucanase on Rheological Parameters of Depectinated Tomato Cell Walls

Sample	G' (1Hz) Mpa	η^*/ω	tan δ
Control t=0	9397	-0.92	0.14
Control t=2	11207	-0.92	0.11
Enzyme (34U) t=0	2790	-0.90	0.17
Enzyme (34U) t=2	3144	-0.89	0.13

10.3.6 Small Deformation Rheology of Bacterial Cellulose Composites

10.3.6.1 Intact and Comminuted Pellicles

Figure 10.12 shows the strain response curves of intact pellicles. When compared with the strain response of depectinated mature green tomato cell walls (Figure 10.5), intact pellicles are somewhat more strain dependent. The absolute moduli of the continuous pellicles is very much less than cell wall material, possibly due to the lower solid contents in the pellicles (<1% dry weight),. There are no significant difference in strain response between pellicles modified with xyloglucan or glucomannan and controls. 0.5% strain, as was used for the mechanical spectra of depectinated cell walls, is well within the linear regions of the strain response curves of the intact pellicles. Hence identical conditions can be used when obtaining spectra from pellicles, allowing direct comparison with data from cell

Figure 10.11: Time Course and Mechanical Spectra of Depectinated Tomato Cell walls Treated with a Vast Excess of *endo*-1,4-β-Glucanase

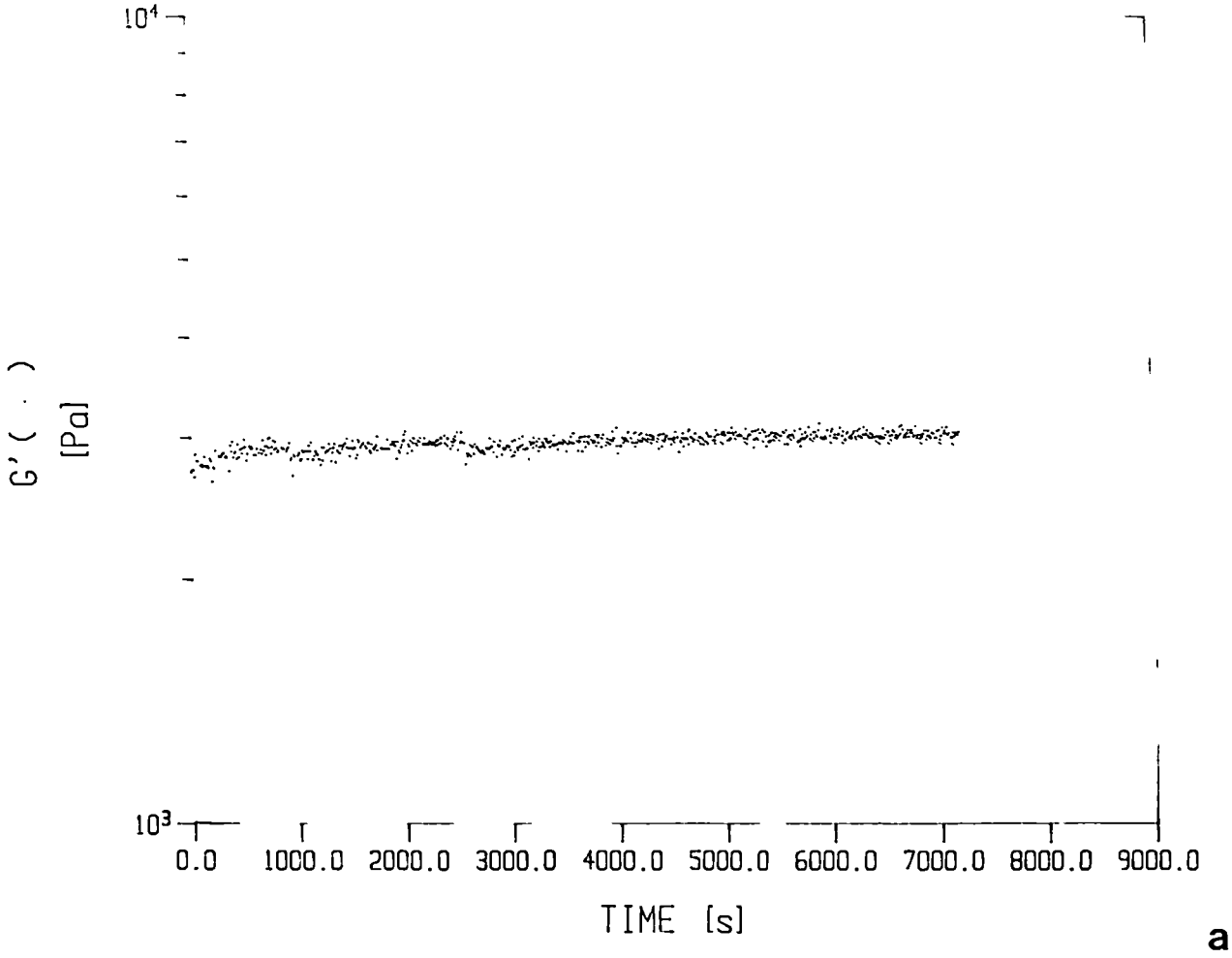

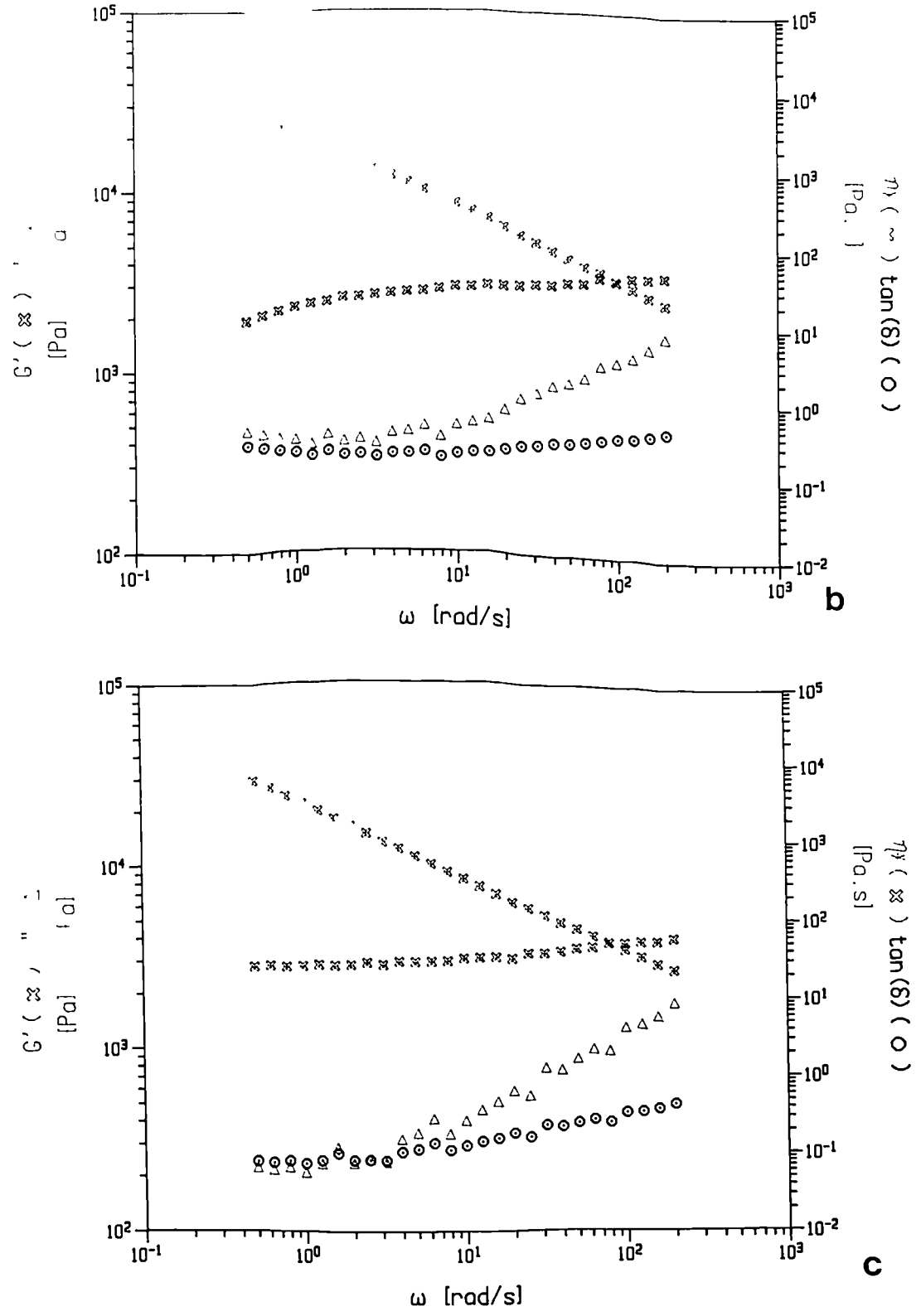

Time course (a) of material incubated with a vast excess of enzyme showing an immediate reduction in G' compared to controls (Figure 10.7 and 10.9) and mechanical spectra of these samples immediately after enzyme addition (b) and at t=2 hours (c) showing no significant difference in rheological behaviour between each other and compared to controls (Figure 10.8 a,b).

Figure 10.12 Strain Response Curves of Intact Bacterial Composite Pellicles

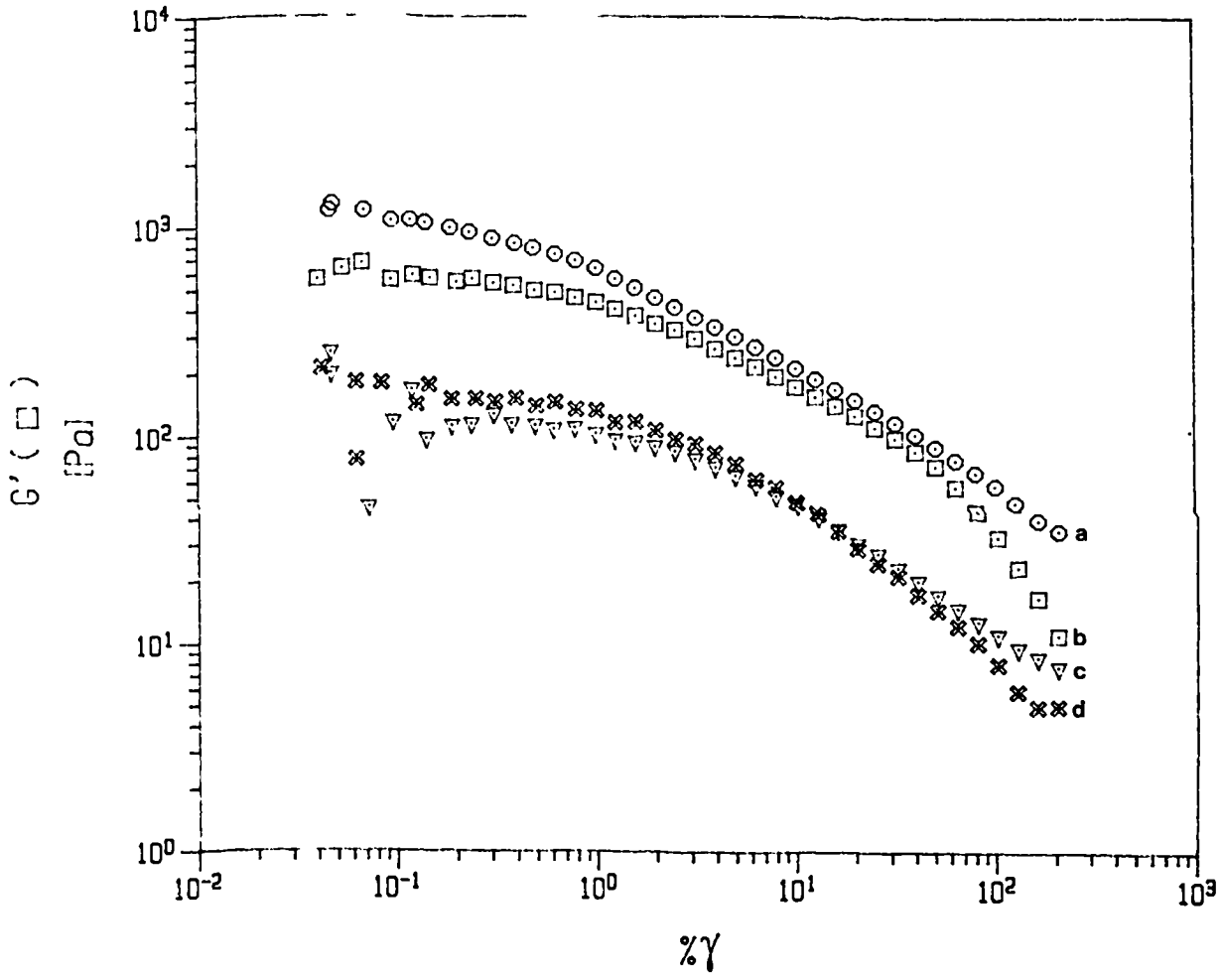

Strain response curves of cellulose pellicles grown for 2 (a) and 3 (b) days, cellulose grown in the presence of tamarind xyloglucan (c) and konjac glucomannan (d) showing similar response behaviour for all samples. O.5% strain, as used for mechanical spectra of cell walls is within the linear regions of all intact pellicles

walls. After the strain test, pellicles remained intact with no evidence of crack propagation or bulk failure, although syneresis had occurred.

Typical mechanical spectra for intact pellicles in the presence and absence of modifying polysaccharides are shown in Figure 10.13 with calculated rheological parameters in Table 10.4.

Table 10.4 Rheological Parameters of Intact Pellicles in the Presence and Absence of Hemicelluloses

Sample	G' (1Hz) MPa	η^*/ω	tan δ
Cellulose 2 days 1	290	-0.77	0.3
Cellulose 2 days 2	63	-0.80	0.3
Cellulose 2 days 3	762	-0.80	0.3
Cellulose 2 days 4	37	-0.80	0.2
Cellulose 3 days 1	189	-0.82	0.3
Cellulose 3 days 2	241	-0.83	0.2
Cellulose 3 days 3	621	-0.82	0.2
Cellulose/XG 1	113	-0.73	0.2
Cellulose/XG 2	54	-0.72	0.2
Cellulose/XG 3	180	-0.72	0.2
Cellulose/XG 4	21	-0.71	0.3
Cellulose/GM1	128	-0.76	0.2
Cellulose/GM 2	76	-0.80	0.2
Cellulose/GM 3	103	-0.79	0.1
Cellulose/GM 4	116	-0.76	0.2

The mechanical spectra of intact pellicle material are very similar in form to those for depectinated cell walls ie G' is greater than G'' for all frequencies measurde, the slope of η^* is relatively close to -1 and tan δ is low (0.2 - 0.3) indicating that the pellicles are well ordered, low loss systems. G' and G'' are not truely frequency-independent, G' shows a slight increase at high frequency and G'' shows the same upturn at higher frequencies seen in mechanical spectra of depectinated cell wall material (Figure 10.6) and for other tomato cell wall material types (M.Gothard Unilever Research, pers.comm.). Absolute moduli values for pellicles are very much lower than cell wall ghosts, again probably a reflection of the very low dry weight contents. Within replicates, significant variation in G' is seen, but values for the slope of η^* and tan δ are highly reproducible. These within replicate variations in G' are probably due to dry weight content differences; the concentrations were not determined as material was limited and these samples were pooled for measurements on comminuted material.

Figure 10.13 Mechanical Spectra of Intact Pellicles of Bacterial Cellulose in the Presence and Absence of Modifying Hemicelluloses

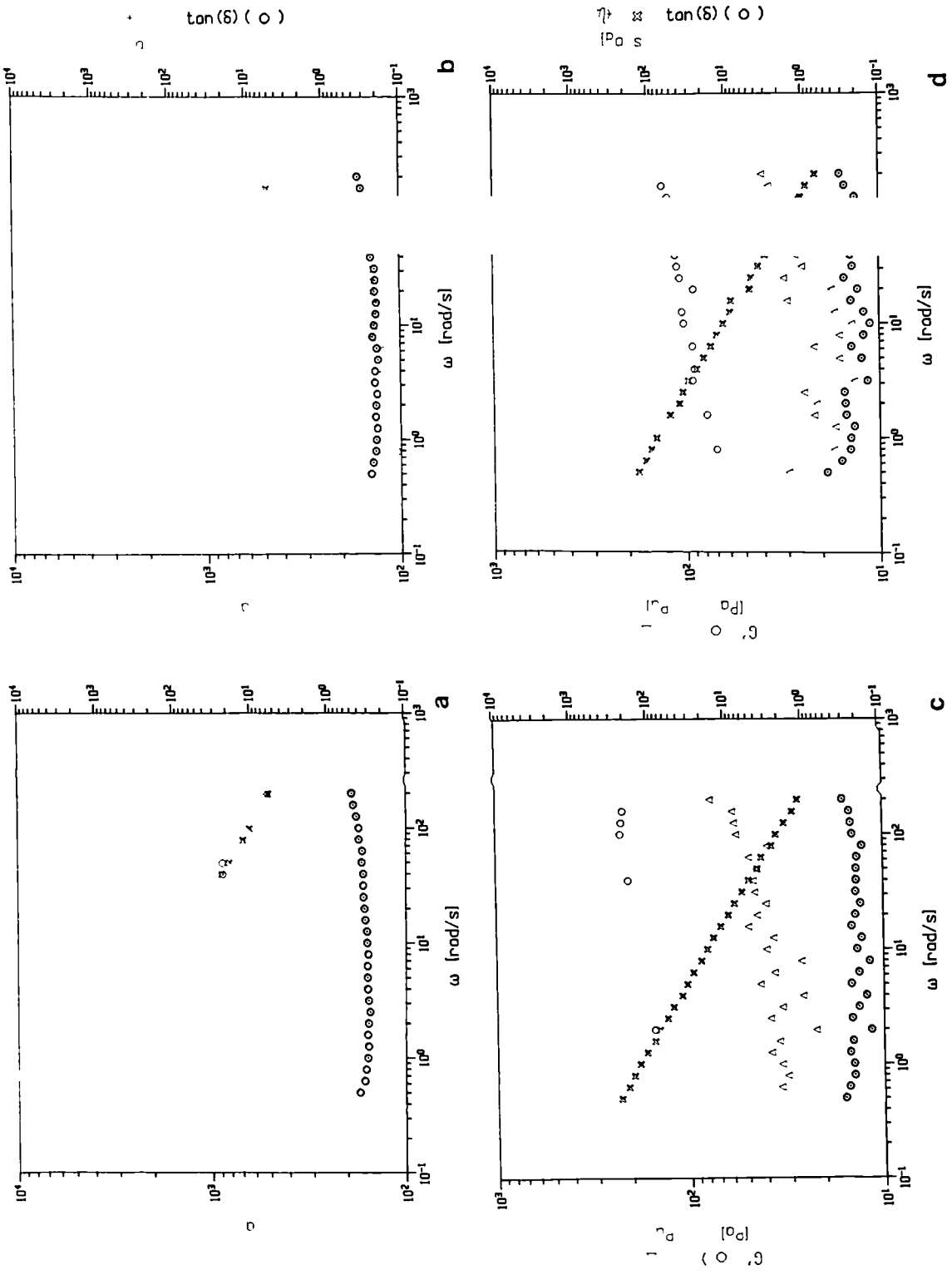

Mechanical spectra of (a) cellulose pellicle grown for 2 days, (b) as (a) but grown for 3 days, (c) cellulose-xyloglucan pellicle and (d) cellulose-glucomannan pellicle (d) showing very similar rheological behaviour to depectinated tomato cell wall material (Figure 10.6) Rheological behaviour under small deformation conditions is apparently not affected by the presence of other polymers (compare (a) and (b) with (c) and (d))

Between replicates (Figure 10.13) the form of mechanical spectra is remarkably conserved; it appears that, under small deformation rheological conditions, the presence of other polymers in the system is not detected and suggests that the cellulsoe component defines the rheological behaviour of these samples. This is somewhat surprising in light of the significant ultrastructural and molecular organisational changes evoked by the presence of hemicelluloses (Chapters 6 and 7). There is possibly a slight reduction in G' in xyolglucan-or glucomannan-modified pellicles, but in the absence of dry weight data, this result is inconclusive. The slopes of η^* for xyloglucan-modified composites is less than for the other materials; this suggests that this material is least gel-like or ordered in its frequency response. This is at variance with ultrastructural data for cellulose-xyloglucan composites (Chapter 6), electron micrographs revealing structures very much more ordered than the control or glucomannan-modified pellicles.

Material from the above experiments was pooled to give a single measurement for comminuted material (Figure 10.14 and Table 10.5). Remarkably, the mechanical spectra for these comminuted materials are superimposable on spectra obtained from intact pellicles (Figure 10.13) and depectinated tomato cell walls (Figure 11.6). Absolute moduli values are higher due to greater dry weight concentrations. The value of G' obtained for cellulose after 2 days is anomalous, the dry weight concentration is very low, but the value from the modulus obtained is almost twice that of the other materials. Also the value for the slope of η^* is slightly lower, indicating a less ordered structure which would be expected to give a lower G' value. As this experiment was not repeated, the significance of this result cannot be assessed.

Table 10.5 Rheological Data of Comminuted Cellulose Composites

Sample	% Dry Weight	G' (1Hz) MPa	η^*/ω	tan δ
Cellulose 2 days	1.7	8960	-0.78	0.3
Cellulose 3 days	2.1	3329	-0.80	0.2
Cellulose/XG	3.1	4709	-0.81	0.2
Cellulose/GM	3.3	4856	-0.81	0.2

Figure 10.14: Mechanical Spectra of Comminuted Bacterial Cellulose Composites

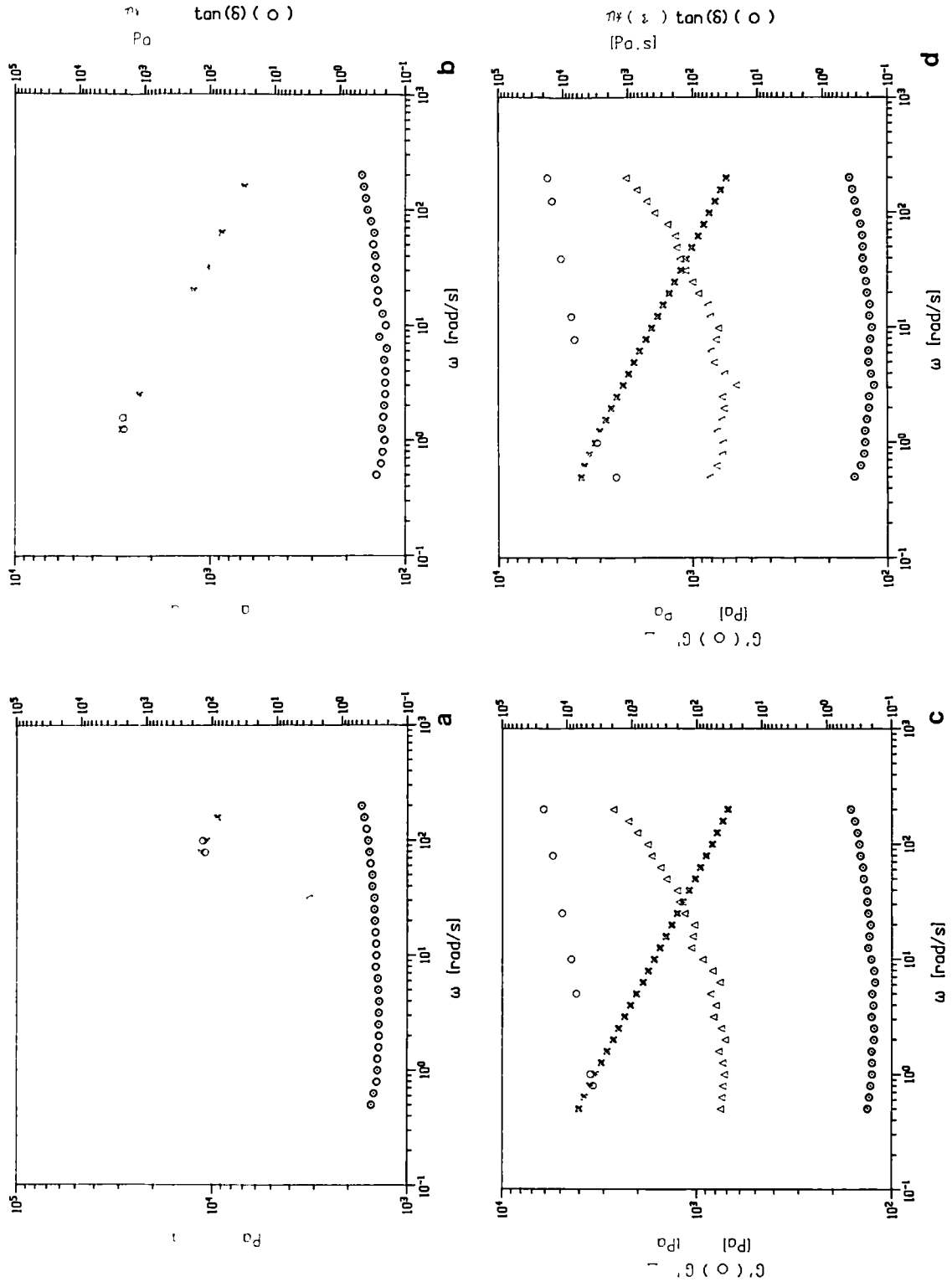

Mechanical spectra of (a) comminuted cellulose material pooled from intacct pellicles from 2 day old cultures; (b) as (a) but from 3 day old cultures; (c) as (a) but from xyloglucan-modified composites; (d) as (a) but from glucomannan-modified composites showing similar rheological behaviour to continuous pellices from which they were derived (Figure10.13) and depectinated cell walls (Figure 10.6) differing only in absolute modulus due to concentration differences

10.3.6.2 Concentration-Dependent Behaviour of Bacterial Cellulose

Red and green comminuted tomato cell walls show concentration-dependent rheological behaviour similar to non-extracted walls and walls after sequential extraction of cell wall components, which can be fitted to the Hermans gelation model for the development of G' (Hermans, 1965; Clark *et al*, 1983) (T. Foster, M. Gothard, Unilever Research, pers. comm.). A similar concentration dependence behaviour is exhibited by comminuted cellulose fibres and the data for comminuted and continuous composites can be fitted to this curve (Figure 10.15). Although data was not fitted to the Hermans glation model, the concentration-dependence graph for cellulose can be superimposed on that for cell walls, suggesting that isolated fibres behave according to the model (M. Gothard, Unilever Research, pers. comm.). Caution should be applied in extrapolating the terminal (lowest) concentration which could effectively be from the single point data obtained for modified composites. Due to differences in density of particle packing revealed in micrographs (Chapter 6 and 7) the concentration-dependence behaviour may have different terminal zones.

10.3.7 Large Deformation Rheology of Bacterial Cellulose Composites

In contrast to small deformation rheology, which did not detect major differences in mechanical behaviour imparted by the presence of hemicelluoses in the composites, large deformation rheology revealed highly significant differences in mechanical behaviour (Figure 10.16). Cellulose samples were relatively strong under tension compared with cellulose-xyloglucan and cellulose-glucomannan composites. Apparent Youngs modulus was calculated, ranging from 2.22-2.8MPa for cellulose alone, to 0.5-1.3MPa for xyloglucan-modified materials and 0.35-0.46 MPa for glucomannan composites (Table 10.5). Cellulose appeared to be more brittle than xyloglucan- or glucommannan-cellulose composites, having a more defined failure point, and glucomannan composites are apparently the most pliable. Results should be interpreted with caution as no attempts were made to standardise materials in terms of polymer concentration and samples were substantially different in geometry to the ideal 10:1 length:width ratio, however the difference in strength under tension between cellulose and modified cellulose does appear to be significant. This large deformation technique is clearly able to detect

Figure 10.15 Concentration Dependence of Comminuted Cellulose Fibres

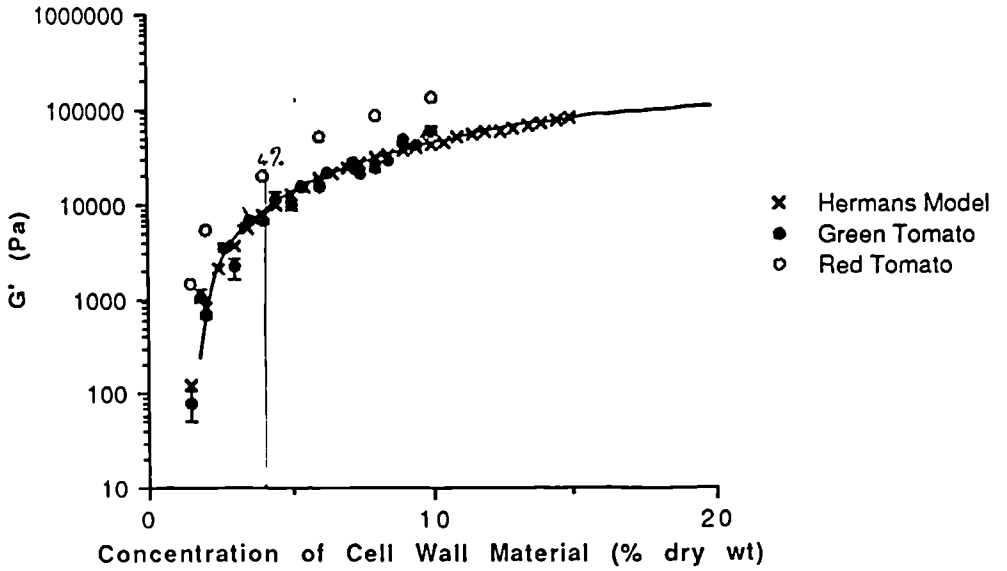

a

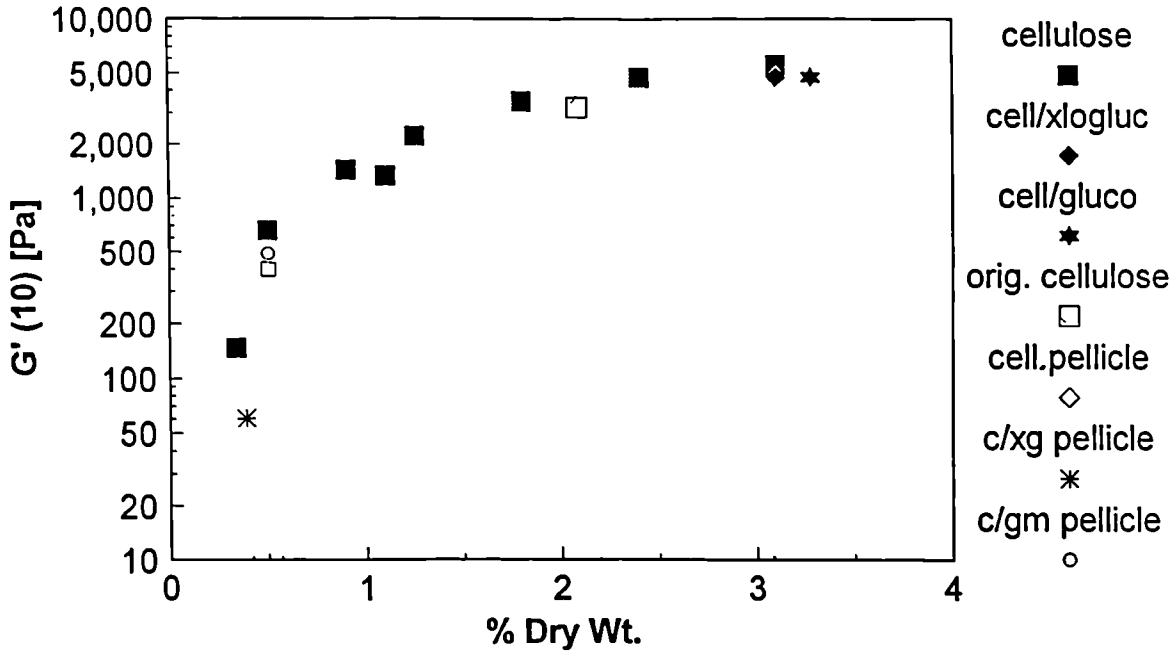

b

Concentration-dependence data of comminuted cellulose can be superimposed on that for cell wall material which has been fitted to the Hermans gelation model (a). Moduli from intact and and comminuted pellicles can be firtted to the curve (b), but the dry weights of the pellicles were not accurately determined and have been estimated. Figure 10.15a is reproduced from a report by S.Doran with permission.

Figure 10.16: Tensile Testing of Cellulose and Modified-Cellulose Pellicles

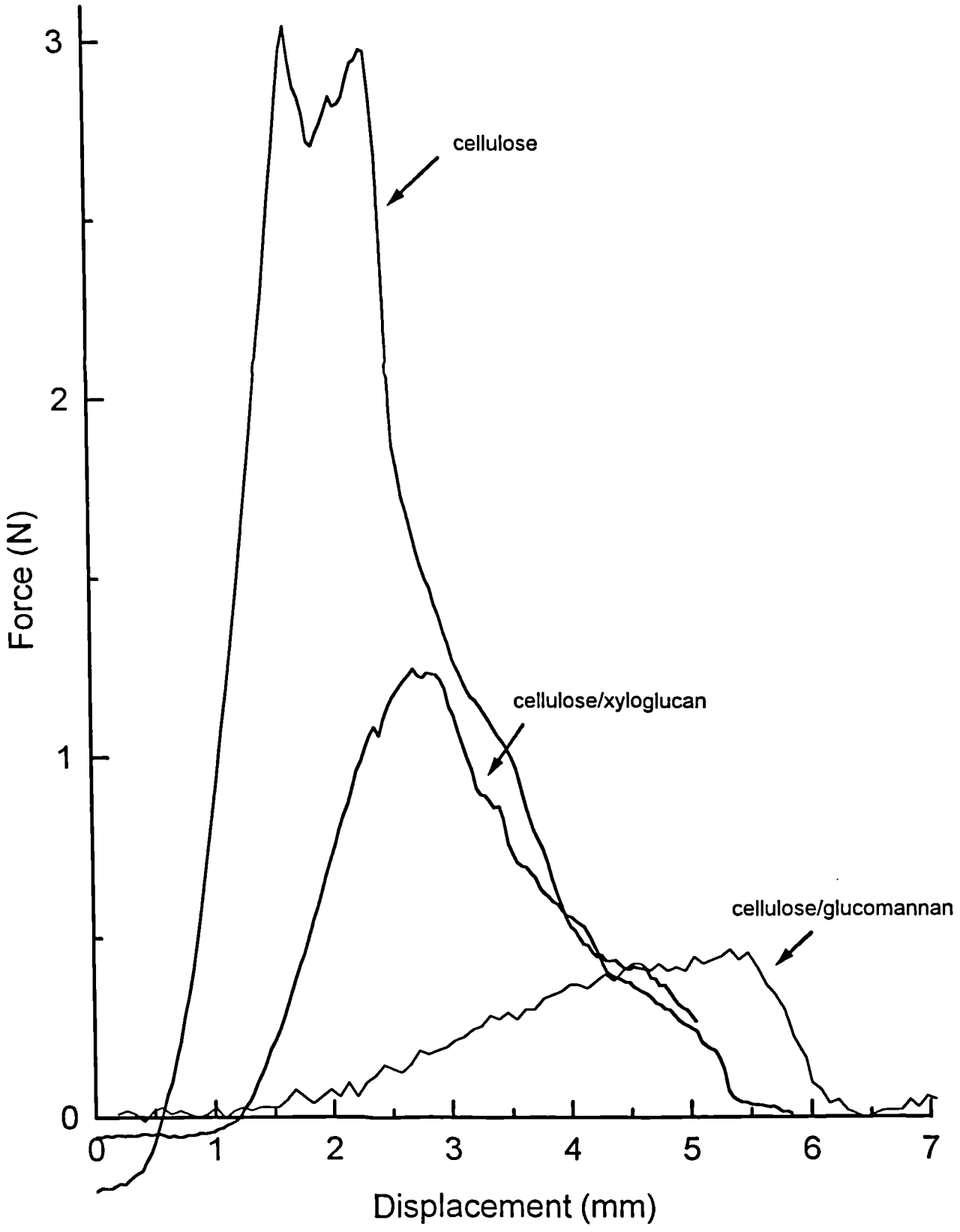

differences induced by the presence of hemicelluloses which were not apparent under small deformation conditions.

Table 10.5 Apparent Youngs Modulus of Cellulose Composites under Tensile Testing

Sample	Apparent Youngs Modulus (MPa)
Cellulose 1	2.22
Cellulose 2	2.80
Cellulose 3	2.50
Cellulose/XG 1	0.82
Cellulose/XG 2	0.50
Cellulose/XG 3	0.78
Cellulose/XG 4	1.30
Cellulose/XG 5	1.00
Cellulose/GM 1	0.35
Cellulose/GM 2	0.46
Cellulose/GM 3	0.43

10.4 Discussion

10.4.1 Endo-Glucanase Treatment of Depectinated Cell wall Material

Treatment of depectinated pea stem cell wall material with *endo*-1,4-β-glucanase released a small proportion of the total xyloglucan into the medium. Despite the dilute conditions and the excess of enzyme used however, most of the xyloglucan was not hydrolysed, suggesting that it is unavailable for enzyme attack. Xyloglucan can only be detected after it has been completely dissociated from the cell wall complex ie xyloglucan chains which have been cut by the enzyme in one region, but remain attached to the cell wall will not be measured. It is possible therefore that the enzyme was in fact far

more active than the data suggests, but the majority of 'cuts' were single cuts per xyloglucan molecule, with the molecule remaining attached to or embedded within the cellulose microfibrils. This may partially explain the discrepancy between this data and that presented by Hayashi & Maclachlan (1984) who measured a massive increase in reducing chain ends (generated by single cuts). Furthermore, these authors used 4% KOH extracted material which may have a slightly looser structure caused by alkali-induced swelling possibly facilitating enzyme action, and experiments were performed over days rather than hours.

Hayashi & Maclachlan (1984) report that 92% of total xyloglucan in pea stems is resistant to extraction by 4% KOH whereas 8% is removed at this stage. This may represent material less tightly associated with cellulose microfibrils and the correlation of this data with the amount of xyloglucan released by enzyme action in this experiment suggests that, under these conditions, the enzyme hydrolysed only that component which is susceptible to 4% KOH extraction ie relatively loosely associated. By analogy with the cell wall models for cellulose/xyloglucan networks (Carpita & Gibeaut, 1993; McCann *et al*, 1990; Talbott & Ray, 1992a) we tentatively propose that this may be xyloglucan involved in cross-linking.

Pea cell wall material contains a small amount of 1,4-linked xylose indicating the presence of xylan in the hemicellulose fraction (Talbott & Ray 1992a). All xylose present in depectinated pea stem cell walls was attributed to xyloglucan in this experiment suggesting that we may have overestimated the total amount in the ghosts and therefore underestimated the effectiveness of the enzyme. A better indication of the action of the enzyme would have been attained by determining the sugar composition of the ghosts after incubation. Unfortunately, this was not done. Coupled with the fact that the experiment was only performed once, all results should be interpreted with caution, however it does appear that the majority of the xyloglucan present cannot be cut twice by the enzyme ie a portion of each of the majority of xyloglucan molecules are embedded within microfibrils.

Measurement of *endo*-glucanase action on depectinated tomato cell walls (pea stem cell walls could not be used due to limited material availability) using small deformation rheology failed to detect significant differences in rheological behaviour, even if vast excesses of enzyme were used. Reductions in G' detected showed that enzyme as effective only in the time between addition and measurement on the rheometer plates and the magnitude of the reduction was not great considering the amount of enzyme used. These results are the same as seen for enzyme-treated whole cell walls (S. Doran, T.Foster, Unilver Research pers.comm.). It had been hoped that removal of the majority of the pectic component would open the structure sufficiently to allow enzyme action and therefore measurable alterations in rheology; clearly this was not the case.

Work in this laboratory suggests that much of the rheological behaiviour of comminuted cell wall preparations can be explained by interactions between particles. For example, red tomato cell wall material has a slightly higher modulus than green, although they are obviously softer in the intact state (T.Foster, M.Gothard Unilever Research, pers.comm.).. We believe that this can be explained by increased 'hairiness' of particles in red fruit. Ripening is accompanied by heightened hydrolytic enzyme action which may expose polymers in a looser structure thereby increasing the possibility of interaction by physical entanglement (M. Gidley, Unilever Research pers. comm.). Similar explanations can be evoked for apparently anomalous behaviour in sequentially extracted fruit materials (M. Gidley, Unilevr Research, pers.comm.) although data obtained for bacterial cellulose composites may provide an alternative hypothesis (see below). For comminuted wall material therefore, particle-particle interactions apparently predominate in small deformation rheological behaviour, with alterations in polymer composition within particles having a secondary effect. The slight reduction in modulus caused by cellulase action may therefore be due to action on exposed polymers at the surfaces of particles, reducing hairiness and, by inference, particle-particle interaction. Any action of endo-glucanase within particles may not be detected by this technique. Shomer *et al* (1984) reported a massive degradation of the microfibrillar system of cell walls of tomato pericarp as measured by the collapse of tomato juice precipitate after treatment with a crude cellulase preparation. This precipitate collapse would be predicted to result in a significantly lower modulus (not determined

by these authors). Use of a crude enzyme preparation could have resulted in multiple enzymes acting in concert, which may increase hydrolysis within particles, reducing particle integrity and effective hydrodynamic volume.

10.4.2 Rheological Behaviour of Bacterial Cellulose Composites

Previous chapters have characterised in some detail the ultrastructural and molecular features of composites produced using high molecular weight tamarind xyloglucan and konjac glucomannan. Both polymers have a profound effect on these characteristics. However, the obvious differences in network architecture invoked by these polymers are essentially undetectable using small deformation oscillatory rheology. The most apparently ordered and cross-linked system, that of xyloglucan, gives the least gel-like response in terms of η^*, exactly the opposite of what might have been expected. However, although the cellulose/xyloglucan composites appear to be the most ordered due to the formation of H-bonded lengths, in the timescales accessible by the frequency range of the rheometer, the 'random' entanglements such as those occurring in the cellulose control sample may in fact exist for long enough to appear permanent ie they do not dissociate. In the case of such a random entanglement system there may be as many or more 'permanent' entanglements (over the experimentally accessible frequency range) as ther are truely permanent junctions in the xyloglucan-modified composite. These results suggest that it is the cellulose component which dominates the rheological behaviour of these composite structures. The reults obtained for sequentially extracted (M. Gothard Unilever Research, pers.comm.) and enzyme-treated (S. Doran, T.Foster, Unilever Research, pers. comm. and above) cell walls, which show little alteration in behaviour with polymer extraction, may therefore be due in part to the fact that cellulose, which is not extracted or hydrolysed, is the dominant polymer in rheological terms. It should be noted however that the cellulose fibres in the composites are much thicker than seen in cell walls (ca. 36nm compared to ca. 5-10nm) and are many microns long. This suggests that, in the composites, cellulose may have a greater contribution to rheological behaviour than the cellulose in cell walls. In contrast, large deformation rheology detects significant alterations in network structure in

the presence of hemicelluloses, implying that, under these conditions, cellulose is not the primary determinant of mechanical behaviour.

Spectra of continuous and comminuted cellulose composites are qualitatively identical to each other and to comminuted cell walls. Normally, for a gel-like system, mechanical disruption of the network results in a dramatic alteration in rheological behaviour (slope η^* moves closer to 0, tan δ increases and overall modulus decreases at comparable concentrations) as linkages which contribute to the gel response are destroyed (Morris, 1983). For composites, there is no alteration in behaviour. Whilst this allows us to extrapolate data from comminuted cell walls to the continuous wall matrix of plant tissues with increased confidence it also implies that these structures and possibly cell wall structures cannot accurately be described as gels. However, this last statement would depend to some extent on the degree of disruption since plant cell walls, when sheared, form large lumps some 50-100μm in diameter. Biopolymer gels can be sheared to much smaller entities.

As mentioned in the results section, mechanical spectra of comminuted cell walls produced in this laboratory have previously been interpreted as having weak-gel properties. Evidence is cited as the limited frequency independence of G' and G'' and the fact that the frequency-dependent dynamic viscosity cannot be superimposed on the shear rate dependence of rotational viscosity ie they do not appear to obey the Cox-Merz rule (Cox & Merz, 1958), which appears to be a general property of weak gels (Ross-Murphy, 1983). Comminuted cell walls are described as hairy particles (M. Gidley, Unilever Research, pers. comm.) explaining why sequentially extracted material, intuitively weaker due to selective polymer removal, can have a higher overall modulus. The consistent and reproducible upturn in G'' at higher frequencies is purportedly due to loose polymer ends which contribute to a liquid-like response at higher frequencies. This has been observed for comminuted gellan gels (M.Gothard, Unilever Research, pers. comm.).

Results obtained for continuous and comminuted cellulose and cellulose composites suggest that this explanation for the upturn in G'' may not be adequate. Continuous cellulose pellicles comprise highly persistent, extremely long (many μms in length) fibres in an apparently random orientation (Chapter 5). Individual fibres are unlikely to form permanent cross-linkages due to their stiffness and length, particularly at these low concentrations. Although there would be little entropic disadvantage in association, the stiffness of fibres would cause orientation problems. However, it is possible that with the imposition of force such as shear, fibres would orient to form structures of a liquid crystal-like nature. Due to the unlikelihood of inter-fibre association, application of the 'weak-gel' system as used for cell walls seems intuitively incorrect. Furthermore, the observation of a similar modulus being obtained (adjusted for concentration differences) when an intact pellicle is homogenised is again inconsistent with a gel system. This suggests that the cellulose fibres are interacting both in continuous pellicles and in comminuted material in a manner which does not involve stable cross-linkages.

It was stated earlier in the discussion that the random entanglements seen in cellulose pellicles may exist for long enough to appear permanent over the time scale of the experiment. These may exceed the number of truely permanent junctions in a cross-linked structure such as the xyloglucan-modified composite and could explain why the apparently more ordered system can have the least 'gel-like' response. The following discussion looks at the concept of entanglement for explaining the rheological behaviour of cellulose. It should be noted however that caution should be applied in invoking the same explanation for apparently similar mechanical spectra in different systems. Cell walls are revealed as highly organised network structures (McCann *et al*, 1990; McCann & Roberts, 1991) and polymers within cell walls form stable interactions as revealed by sequential extraction techniques (eg Redgwell & Selvendran, 1986). It is therefore obviously not correct to use the entanglement theory, which may well be true for cellulose, as a complete explanation for cell wall behaviour. Note however, that in comminuted cell walls, there is entanglement at particle surfaces, which may increase with sequential extraction protocols due to increasing particle hairiness (see earlier discussion).

As mentioned in the introduction, time scale is an extemely important variable in rheological testing. The range of frequencies available experimentally is limited and effectively represents a snap-shot in time, part of a theoretical continuum occurring over a wide frequency range (Figure 10.17). Figure 10.18 shows the concentration dependence of zero-shear specific viscosity. The point at which the slope changes to a much higher value is called the 'critical concentration' and represents the point at which coil overlap occurs, obviously this is critically dependent on hydrodynamic voloume (Morris, 1983). For a polymer (such as cellulose) which does not self-associate, at a certain concentration coil overlap, and therefore molecular entanglement occurs. The frequency-dependent behaviour shown in Figure 10.17 reflects the time scale of molecular entanglement. For linear polymers of high molecular weight (eg cellulose), the characteristic viscoelastic property is the presence of two sets of relaxation times (Ferry, 1970). At high frequencies, in the transition zone, chains cannot disentangle within the time-scale of the oscillation period, and relaxation time relates to configurational rearrangements between entanglements, at lower frequencies, chains have time to disentangle and flow, in this terminal zone relaxation times relate to rearrangements beyond entanglements (Ferry, 1970; Morris, 1983).

For solutions of guar, a polymer which does not self associate, the transition from liquid-like behaviour with G''>G' to a more solid-like response where G'>G'' using a suitable frequency range has been demonstrated (Richardson & Ross-Murphy, 1987a). This behaviour is typical for an entanglement system in the region between the terminal and plateau zones of frequency response. Xanthan polymers, which are also stiff, linear polymers have different rheological properties and are believed to have a degree interchain coupling (Richardson & Ross-Murphy, 1987b).

Conventionally, it is believed that it is not possible to obtain hydrocolloid solutions of entangled polymers sufficiently concentrated to show rheological behaviour towards the glass transition zone ie upturn in G' and G''. In the light of the apparently randomly oriented fibres in the cellulose network, coupled with the barriers to self-association of these fibres, we believe that the upturn in G' at high frequencies in mechanical spectra may in fact represent the region between the plateau and transition

Figure 10.17 Theoretical Range of Frequency Response for Molecular Entanglement

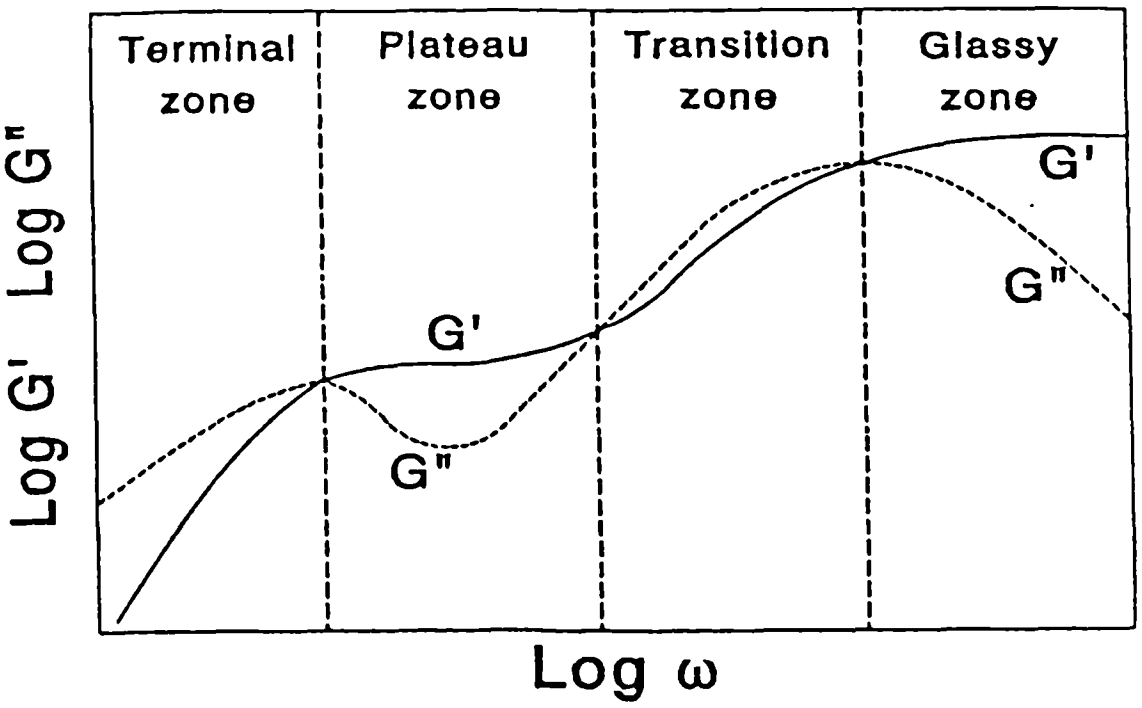

Reproduced from Groot and Agterof, Macromolecules, 1995

Figure 10.18: Concentration-Dependence of Zero-Shear Specific Viscosity

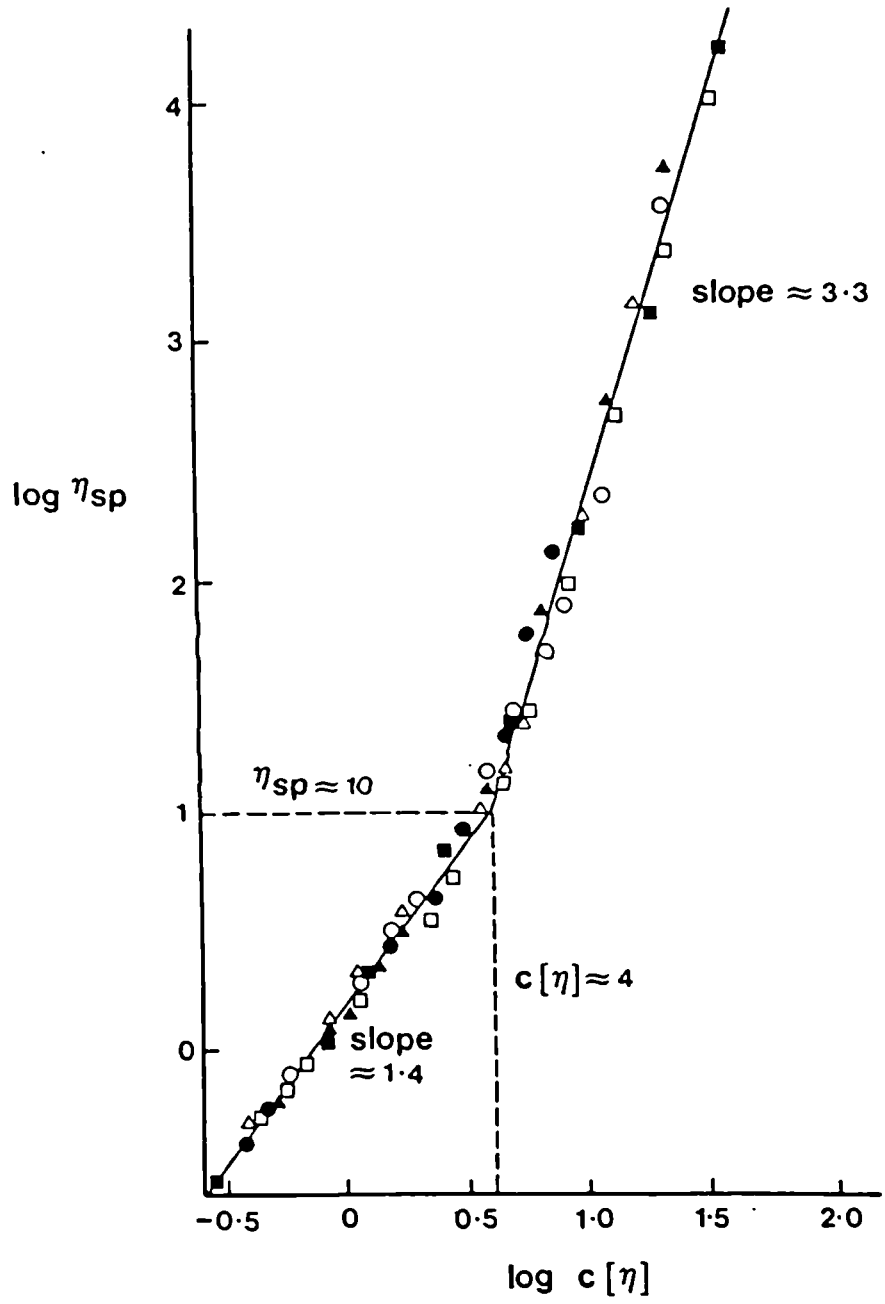

Concentration dependence of 'zero shear' specific viscosity (η_{sp}) for dextran (○), carboxymethylamylose (●), 'high mannuronate' alginate (△), 'high guluronate' alginate (▲), λ-carrageenan (□), and hyaluronate (■).

Reproduced from Morris *et al* (1981)

undergo a glass transition. Recently in our laboratory very concentrated solutions of guar (ca. 15%) have been shown to have rheological behaviour similar to that of cellulose (M. Gothard, Unilever Research, pers.comm.). The fact that cellulose can exhibit this behaviour at such low concentrations may be a reflection of the extreme length and persistence of fibres relative to guar galactomannan molecules. Further evidence for an entangled system could be gained by determining the variation in rotational viscosity with shear rate, for a true entangled system, the curve of η^* (ω) should be essentially coincident with $\eta(\gamma)$ ie it obeys the Cox-Merz rule (Cox & Merz 1958) indicating no short range interaction which influences small deformation measurements, but are destroyed under steady shear.

There is, therefore, some evidence to suggest that the rheological behaviour of cellulose is due to it being an entangled system. Relevant experiments are currently being carried out to determine if this is indeed the case. It is unlikely however that the same explanation can be invoked for cellulose/hemicellulose composites or, as cautioned earlier, for comminuted cell walls. There is overwhelming evidence from electron microscopy that the presence of hemicelluloses radically alters network architecture, and there is chemical and molecular evidence that the polymers are tightly associated (Chapters 6 & 7). In the light of large deformation results, which show a significant alteration in mechanical behaviour in modified structures, it is apparent that small deformation rheology is limited in detecting changes at the molecular level in these systems probably because of the dominant effect of cellulose. The consistency of mechanical spectra for all the systems studied here cannot be adequately explained with the data currently available, and we await further experimentation.

Large deformation rheolgy, using tensile testing, has revealed dramatic differences between modified and unmodified structures. Man-made composite structures such as reinforced concrete derive their mechanical strength from the reinforcing rods (steel) embedded in a matrix (concrete), It might have been predicted that the cellulose/hemicelluose composites, with a matrix of one polymer type

containing reinforcing cellulose rods, should in fact be the stronger material. Evidence from the video footage suggests that, for the composites, deformation is not elastic, and the small increase in force with a large increase in deformation is probably due to slippage. It will be of particular interest for the xyloglucan-modified composites, which show local ordering of structure, to use birefringence to detect any large scale ordering of the structure under deformation. These experiments are in progress. We tentatively propose that, in creating a more pliable structure, xyloglucan interacts with cellulose to form a wall well suited for processes such as cell expansion. This will be discussed in greater detail in Chapter 11. However, the result for glucomannan is less easy to rationalise. From electon microscopy data showing a dense, compact structure (Chapter 7) and the fact that it is a major polymer in secondary walls, generally more rigid structures laid down after cell expansion has ceased, we had predicted a stronger, more brittle material. In fact, it was even weaker and more pliable than the xyloglucan-modified composite. In Chapter 7 it was observed that regions of the cellulose-glucomannan composites were much less compact; possibly these are dominating the rheology although the EM data suggested that this was not the predominant effect.

It should be emphasised that the tensile tests were not standardised and were very much preliminary experiments to form the basis of further work. We therefore apply caution in the interpretation, but believe that mechanical differences are large enough to be of significance.

Chapter 11: Discussion

The cellulose/xyloglucan network is generally perceived to bear the majority of tensional stresses generated in the highly dynamic primary cell wall surrounding a cell undergoing the turgor-driven process of expansion (Fry, 1989; Passioura & Fry, 1992). As such, the nature of the interaction between the two polymers is of considerable interest not only to plant physiologists, but also to food technologists, in that plant cell wall components imparting physical strength to plant tissues are also likely to contribute to the textural attributes of those tissues. The development of the *Acetobacter aceti* ssp. *xylinum* (ATCC 53524) fermentation system described in this thesis, based on earlier work by Atalla *et al* (1993), Hackney *et al* (1994) and Haigler *et al* (1982) represents, we believe, a significant advance in understanding the molecular basis of the cellulose/xyloglucan interaction. Moreover, the nature of the material produced ie a large, continuous pellicle, is particularly appropriate for bulk mechanical testing under both large and small deformation conditions. This enables direct correlation of mechanical properties with molecular and ultrastructural features. The fermentation system has been extended to include a range of polysaccharide additives, derived from both plant cell walls and other sources, enabling characterisation of the interaction with cellulose at the molecular, ultrastructural and, in the future, mechanical level. Equally however, it has become clear that much more experimental work is required to refine the system for some of the polymers, in particular xylans and pectins.

When work on this thesis started, the specific nature of the interaction between xyloglucan and cellulose remained unclear. Chemical (Chambat *et al*, 1984; Edelmann & Fry, 1992a), NMR (MacKay *et al*, 1988) and microscopic (Baba *et al*, 1994b; Hayashi *et al*, 1987; McCann *et al*, 1990) indicated a tightly associated, highly ordered network in which xyloglucan was localised within, on the surface of and cross-linking adjacent cellulose microfibrlis. This network structure was incorporated into models of the primary type I cell wall, in which it was envisaged as embedded embedded in an independent

but co-extensive matrix of highly complex and heterogeneous pectic polymers (Carpita & Gibeaut, 1993; McCann *et al,* 1990; McCann & Roberts, 1991; Talbott & Ray, 1992a).

In fact, this proposed structure for the cellulse/xyloglucan framework posed almost as many questions as it answered. For an intramicrofibril association to occur, it is envisaged that xyloglucan must be present at or very close to the point of cellulose synthesis, which occurs in terminal complexes located on the surface of the plasma membrane. This would facilitate co-crystallisation of the cellulose/xyloglucan crystal lattice (Hayashi, 1989). The precise mechanism by which the two polymers are co-localised at the correct time is unknown. Furthermore, what structural features, if any, determine the localisation of individual xyloglucan molecules within the complex? How are the intermicrofibril cross-linkages, which show conservation in length (McCann *et al,* 1992b), generated? What are the precise functions of enzymes such as XET (Nishitani & Tominaga, 1991; Smith & Fry, 1991), which has been shown to be associated with xyloglucan elongation *in muro* (Thompson & Fry, 1995), in modifying the complex? At least some of these questions have been answered using the *Acetobacter* fermentation system (Chapter 6, this thesis; Whitney *et al,* 1995), and the composite structures formed are promising materials for looking at other features such as enzyme action (see below).

The idea of using *Acetobacter xylinum* as a model for studying at cellulose/xyloglucan interactions was first proposed by Haigler *et al* (1982), but it was the discovery of the agitation tolerant strain ATCC 53524 (Atalla *et al,* 1993) and the observations of altered molecular organisation of the cellulose component to become more like cellulose derived from higher plants (Hackney *et al,* 1994; Uhlin *et al,* 1995; Yamamoto & Horii, 1994) that really focused attention on the system. Work in this thesis significantly expanded the work of these authors to examine both ultrastructural and mechanical aspects of these structures, and it was evidence such as this which confirmed the validity of this system as a model for primary cell walls (Whitney *et al,* 1995).

In a fermentation system containing *A.aceti* ssp. *xylinum* (ATCC 53524) and a dilute xyloglucan solution, tightly associated, organised networks are formed with ultrastructural and molecular features akin to similar networks derived from primary cell walls (Chapter 6, this thesis). Formation of cross-linkages between adjacent cellulose fibres, imparting lateral order, was shown to require no specific structural feature of the xyloglucan molecule, contrary to molecular modelling predictions (Finkenstadt *et al*, 1995; Levy *et al*, 1991). Cross-linking could be explained purely by physico-chemical factors, in terms of entropy requirements. Cross-bridge lengths, highly conserved in both composites and the cell wall, was demonstrated to be a function of characteristic ratio (Gidley *et al,* 1991a), which defines hydrodynamic behaviour in terms of persistence length (Burton & Brant, 1983). Bridge lengths of the order of the persistence length are required to confer significant entropic mobility. As the characteristic ratio is a function of side-chain substitution (Gidley *et al*, 1991a), it can be inferred that most cell wall xyloglucans, with the possible exception of xyloglucan derived from Graminaceous monocotyledons, which typically has a much lower level of backbone substitution (Hayashi, 1989), will have a similar persistence length. This explanation for conservation of cross-bridge lengths can therefore be extrapolated, with some confidence, to the situation in the cell wall.

Structures formed in the presence of lower mwt xyloglucan had different ultrastructural features to those formed using xyloglucan of higher mwt, although molecular features were essentially identical (Chapter 6, this thesis). In the fermentation system, it was suggested, the driving force for enthalpic association predominates, possibly because entropy requirements for the system are more fully realised in a population of smaller molecules. Cross-linking events were proposed to involve longer xyloglucan molecules. Work in Chapter 9 however, indicated that cell wall derived xyloglucan is of a much lower mwt than even the low mwt tamarind xyloglucan used in this study. The work in Chapter 6 shows that, in the fermentation system, with high mwt xyloglucan, cross-linked structures can be generated purely as a result of the physical properties of the polymers involved. This does not preclude the involvement of other physical and biological factors in generation of similar structures within the cell wall, where local environment and molecular characteristics of the polymer may be different.

The altered molecular organisation of the cellulose component of the composite, coupled with the requirement for concentrated alkali to effect complete dissociation, provides compelling evidence for an intimate, intrafibre interaction. However, it remains difficult to reconcile this evidence with the conservation of fibre dimensions between both control and modified celluloses. Indeed, of all the polysaccharide additives incorporated into the system, only CMC, in accordance with previously published results (Haigler *et al*, 1982) effected a reduction in fibre widths. This result is at variance with all previous reports on the effect of xyloglucan on *Acetobacter* cellulose (Hayashi *et al,* 1987; Uhlin *et al,* 1995; Yamamoto & Horii, 1994), which all used the strain ATCC 23769. Until we are able to induce cellulose synthesis *in situ* using strain 53524 attached to EM grids, such as was employed by Haigler *et al* (1982) but which proved very difficult in practice (Chapter 5, this thesis), to allow measurement of fibre widths immediately after synthesis, we remain unable to identify the reasons for this apparent discrepancy.

Apart from a single, unsuccessful attempt to introduce pea xyloglucan into the system, all work carried out thus far has used tamarind xyloglucan, which has advantages in being both full characterised (Gidley *et al*, 1991a; Lang *et al,* 1992; York *et al*, 1993) and readily available in large quantities. However, this storage polysaccharide is unrepresentative of most primary cell wall xyloglucans in that it is of very high mwt and also lacks either the fucosyl residues that characterise most wall xyloglucans from dicotyledons and non-graminaceous monocotyledons or the arabinosyl residues found in xyloglucans derived from the primary walls of Solanaceous species. It is a major aim of future work to incorporate xyloglucan derived from primary cell walls into the fermentation system. However, whilst tomato fruit will provide an abundant source of arabinoxyloglucan, it has become clear that extraction of pea stems generates very little xyloglucan for a great deal of effort (Chapter 9, this thesis). It is hoped that a proposed collaboration with the CCRC will make available high mwt fucosylated xyloglucan from suspension cultured *Phaseolus aureus* cells. By *in vitro* association studies, it has recently been proposed that fucosylated xyloglucan binds cellulose at a faster rate than xyloglucan lacking the fucose residue, in agreement with molecular modelling predictions (Levy, 1995), and we

hope to use the fermentation system, which is, we believe, more representative of cell wall processes, to provide further evidence for this.

Collaborative research by the Unilever laboratory and Stirling University has isolated and characterised a range of plant-derived enzymes which modify xyloglucan specifically. Although the chemical basis of modification is established, the precise function of these enzymes in the cell wall and the subsequent effects on cellulose/xyloglucan interactions has yet to be elucidated. Xyloglucans specifically tailored by the action of these enzyme will be incorporated into the *Acetobacter* system, and molecular, ultrastructural and mechanical effects characterised. It is important to insert a word of caution however. Although the results obtained thus far using xyloglucan have been extremely encouraging, in that structures formed mimic those seen in the wall, more background work needs to be performed to refine the fermentation system. Results are highly reproducible for fermentations using the same bacterial culture, however considerable variation in the rate of cellulose synthesis between cultures of different ages and source have been observed qualitatively. It is essential that we standardise this technique before meaningful conclusions on the effect of different xyloglucans can be made.

The continuous cellulose/xyloglucan pellicles formed in this system provide unique possibilities for mechanical testing. The small deformation rheology experimentation formed on these composites provided valuable insights into interpretation of results obtained with comminuted cell wall material (Chapter 10, this thesis). Most significant is the dominance of the cellulose component in determining the mechanical behaviour under these conditions. Most interesting however was the dramatic alteration in mechanical behaviour under conditions of large deformation imparted by the presence of modifying polymers. It should be stressed that these were very preliminary results, however it did appear that xyloglucan caused the structure to become more pliable, such that it could be stretched to a much greater extent than the controls and, when the material failed, it appeared to be a plastic failure. This behaviour is of particular interest to the Unilever Laboratory. A more pliable structure can be reconciled with the functional requirements of cellulose/xyloglucan structures around expanding cells,

however, the molecular basis for this difference in behaviour needs to be established. The cross-linked ordered structure seen using deep-etch freeze-fracture TEM defines structures at the μm distance scale, and caution must be applied in invoking explanations of mechanical behaviour, measured at the mm distance scale with such architectures. This is particularly true in that individual pellicles displayed heterogeneity of structure, and the orientation of fibres was not maintained even at the μm distance scale (see Figure 6.1a). Consequently, other techniques, capable of assessing fibre orientation at a larger distance scale, require investigation. In particular, a combination of WAXS and SAXS techniques, performed in real time on a sample undergoing large deformation, could be explored. Observation of plastic failure suggests that the effects of tension on the structure will be preserved, and these structures should be examined at both the mm and μm distance scale.

The ability to monitor the behaviour of these composites under tension, also implies that the relaxation of the structure after tension has been applied can be investigated ie creep tests can be performed. The elegant work of Simon McQueen Mason and Dan Cosgrove has led to the characterisation of 'expansins' small molecules with no hydrolytic or endo-transglycosylase activity (McQueen-Mason *et al*, 1992,1993) which induce *in vitro* wall extension in isolated cucumber hypocotyls. These proteins apparently disrupt hydrogen bonding between cell wall polymers, but interestingly, the presence of xyloglucan, which might have been anticitated to be the primary target for expansin action, actually decreases the affinity of expansins for cellulose (McQueen-Mason & Cosgrove, 1994). It will be extremely interesting to perform creep test experiments on the cellulose/xyloglucan composites in the presence of expansins, since the composites represent a much simpler system than excised hypocotyls and a collaborative venture with Simon McQueen-Mason is currently being established.

Incorporation of polysaccharides other than xyloglucan into the *Acetobacter* system met with variable success. Composites formed in the presence of glucomannan produced densely packed structures, which were less hydrated either than controls or xyloglucan-modified structures. Although, unlike the results obtained with xyloglucan, these structures were not similar to those found in the secondary wall

where glucomannans predominate, in that there was no apparent 'bundling' of cellulose fibres, this compact structure could be reconciled with secondary wall strucutural requirements, at least to an extent (Chapter 7, this thesis). Only one glucomannan was studied however, and factors such as degree of acetylation and Man:Gal ratio may be significant (contrast Man:Gal ratio for tomato glucomannan (Chapter 9) with that for konjac glucomannan (Chapter 7). Association of cellulose fibres, such as is seen in secondary cell walls was seen in the presence of galactomannans however (Chapter 8, this thesis). For both mannans, conformational alteration of the mannosyl residues in the presence of a cellulose template, into the 'extended-cellulosic' mannan I structure (Chanzy *et al*, 1982) was observed. The effect of altering Man:Gal ratios could be studied using enzymically modified guar of different fractions of LBG.

For the other major polymer of interest, namely xylans, no ultrastructural effects were observed, and the molecular organisation of the cellulose component remained essentially unaltered. Alignment of xylans with cellulose was inferred by NMR, but there was no conformational alteration of the xylan, in contrast with previous results (Mitikka *et al*, 1995). Previous authors had reported a reduction of fibre width in the presence of xylan and a similar perturbation of cellulose organisation as was seen with xyloglucan (Uhlin *et al*, 1995). As xylan carries a negative charge, which is proposed to be important in driving helicoidal ordering in cellulose/glucuronoxylan assembleys (Reis *et al*, 1994), it might have been anticipated that xylan would act in a similar way to CMC in which, upon association with cellulose, the negative charge is presumed to prevent further association by electrostatic repulsion (Haigler *et al*, 1982). For ultrastructural and molecular effects to be observed in this system, there appears to be a real requirement for the modifying polymer to be of high mwt. That this is not attributable solely to a high viscosity medium alone was demonstrated by the lack of observable effect of guar galactomannan (Chapter 8, this thesis). Colonisation of cellulose fibres might be predicted to be more effective with shorter, rather than longer molecules (Vincken *et al*, 1995) and this is indicated by the massive incorporation of xylan into the composite. Why this extensive colonisation is not translated into effects at the ultrastructural and molecular level remains unclear, but as work on the system progresses it is hoped that this question can be answered. It is necessary therefore to obtain high

mwt glucuronoxylan and a collaboration with Chris Brett from the University of Glasgow should provide this.

Addition of high mwt mixed-linkage glucan conferred both ultrastructural and molecular differences on the composite. As this was just a preliminary experiment, much more work needs to be performed, but the initial results were encouraging. In contrast, the incorporation of pectin, designed to investigate the structural requirements for the observed strong association of a proportion of the pectic fraction of primary cell walls with the cellulosic component (Mitchell, J., Unilever Research, pers.comm., Redgwell & Selvendran, 1986) proved singularly ineffective. Bear in mind though the highly complex and heterogeneous character of cell wall pectins, and the proposal that pectin may be incorporated into the cell wall as an almost completely esterified polysdaccharide (Roberts, K., John Innes Institute, pers. comm.). Much more work, using a range of different pectins, will be performed in this area.

The *Acetobacter* fermentation system has been demonstrated to be extremely useful in investigating the molecular basis of the interaction of a number of polysaccharides with cellulose. Of these, the most extensively characterised has been xyloglucan, and composite structures thus formed have many properties similar to the primary cell walls in which xyloglucans comprise a major component. Extrapolation of the data thus obtained to the situation in the cell wall by using cell wall-derived xyloglucans and xyloglucans which have been chemically modified by cell wall enzymes is a priority for future work. Other cell wall polysaccharides have also been partially investigated, but for the system to be useful, there is apparently an absolute requirement for high mwt additives. Future work will concentrate on obtaining high mwt polysaccharides for incorporation into the fermentation system.

REFERENCES

Acebes, J.L., Lorences, E.P., Revilla, G., Zarra, I. (1993) Pine xyloglucan - Occurrence, localisation and interaction with cellulose. *Physiol. Plant.* **89**, 417-422

Akiyama, Y. and Kato, K. (1982) An arabinoxyloglucan from extracellular polysaccharides of suspension-cultured tobacco cells. *Phytochemistry*, **21**, 2112-2114

Albersheim, P., Nevins, D.J., English, P.D., Karr, A. (1967) A method for the analysis of sugars in plant cell wall polysaccharides by gas-liquid chromatography. *Carbohydr.Res.* **5**, 340-345

Aldington, S. and Fry, S.C. (1993) Oligosaccharins. *Adv.Bot.Res.*, 19, 1-101

Aloni, Y., Cohen, Y. and Benziman, M. (1983) Solubilisation of UDP-glucose:1,4-β-D-glucan 4-β-D-glucosyl transferase (cellulose synthase) from *Acetobacter xylinum. J.Biol.Chem.*, **258**, 4419-4423

Aloni, Y., Delmer, D.P. and Benziman, M. (1982) Achievement of high rates of in vitro synthesis of 1,4-β-D-glucan. Activation by cooperative interaction of the *Acetobacter xylinum* enzyme system with GTP, polyethylene glycol and a protein factor. *Proc.Natl Acad.Sci. USA*, **79**, 6448-6452

Amor, Y., Haigler, C.H., Johnson, S., Wainscott, M. and Delmer, D.P. (1995) A membrane-associated form of sucrose synthase and its potential role in synthesis of cellulose and callose in plants. *Proc.Natl.Acad.Sci. (USA)* **92**, 9353-9357

Arioli, T., Betzner, A., Peng, L., Baskin, T., Wittke, W., Herth, W., Cork, A., Birch, R., Rolfe, B., Redmond, J. and Williamson, R.E. (1995) Radial swelling mutants deficient in cellulose biosynthesis. In: *Proceedings of the Seventh Cell Wall Meeting, Santaigo de Compestela* (Zarra,I. and Revilla, G. eds.) University Press, Santiago de Compestela, pp182

Aspinall, G.O. (1980). Chemistry of polysaccharides. In: The Biochemistry of Plants, Vol.3., (Preiss, J. ed.), Academic Press, New York, pp 473-500

Atalla, R.H., Gast, J.C., Sindorf, D.W., Bartuska, V.J. and Maciel, G.E. (1980) ^{13}C NMR spectra of cellulose polymorphs. *J.Am.Chem.Soc.* **102**, 3249-3251

Atalla, R.H. and VanderHart, D.L. (1984) Native cellulose: a composite of two distinct crystalline forms. *Science (Wash. D.C.)* **223**, 283-284

Atalla, R.H., Hackney, J.M., Uhlin, I. and Thompson,, N.S. (1993). Hemicelluloses as structure regulators in the aggregation of native cellulose. *Int.J.Biol.Macromol.* **15**, 109-112

Augur, C., Benhamou, N., Darvill, A.G. and Albersheim, P. (1993) Purification, characterization and cell wall localisation of an α-fucosidase that inactivates a xyloglucan oligosaccharin. *Plant J.*, **3**, 415-426

Avigad, G., Amaral, D., Asensio, C. and Horecker, B.L. (1962) The D-galactose oxidase of *Polyporus circinatus. J.Biol.Chem.* **237**, 2736-2743

Baba, K-i., Sone, Y., Misaki, A. and Hayashi, T. (1994a) Localisation of xyloglucan in the macromolecular complex composed of xyloglucan and cellulose in pea stems. *Plant Cell Physiol.* **35**, 439-444

Baba, K-i., Sone, Y., Kaku, H., Misaki, A., Shibuya, N. and Itoh, T. (1994b). Localization of the hemicelluloses in the cell walls of some woody plants using immuno-gold electron microscopy. *Holzforschung*, **48**, 297-300

Bacic, A., Harris, P.J. and Stone, B.A. (1988) Structure and function of plant cell walls. In *The Biochemistry of Plants*, Volume 14 (Priess, J. ed.). NY, Academic Press, 297-371

Baron-Epel, O., Gharyal, P.K. and Schindler, M. (1988) Pectins as mediators of wall porosity in soybean cells. *Planta*, **175**, 389-395

Barnes, A.H., Hutton, J.F. and Walters, K. (1993) Rheology Series 3: An Introduction to Rheology, Elsevier Science Publishers, Amsterdam, The Netherlands.

Baskin, T.I., Betzner, A.S., Hoggart, R., Cork, A. and Williamson, R.E. (1992) Root morphology mutants in *Arabidopsis thaliana. Aust.J.Plant Physiol.*, **19**, 427-437

Bauer, W.D., Talmadge, K.W., Keegstra, K. and Albersheim, P. (1973) The structure of plant cell walls. II. The hemicellulose of the walls of suspension-cultured sycamore cells. *Plant Physiol.*, **51**, 174-187

Ben-Hayim, G. and Ohad, I. (1965) Synthesis of cellulose by *Acetobacter xylinum*. VIII. On the formation and orientation of the bacterial cellulose fibrils in the presence of acidic polysaccharides. *J.Cell Biol.*, **25**, 191-207

Benziman, M., Haigler, C.H., Brown, R.M. Jr, White, A.R. and Cooper, K.M. (1980) Cellulose biogenesis: polymerisation and crystallization are coupled processes in *Acetobacter xylinum. Proc.Natl.Acad.Sci. (USA)* **77**, 6678-6682

Blakeney, A.B., Harris, P.J., Henry, R.J. and Stone, B.A. (1983) A simple and rapid preparation of alditol acetates for monosaccharide analysis. *Carbohydr.Res.*, **113**, 291-299

Blanton, R.L. and Haigler, C.H. (1995) Cellulose biosynthesis. In: *Membranes: Specialized Functions in Plants.* (Smallwood, M., Knox, P. and Bowles, D. eds.) JAI Press, Greenwich, CT, in press

Boyer, J.S. (1968) Relationship of water potential to growth of leaves. *Plant Physiol.*, **43**, 1056-1062

Braccini, I., Penhoat, C.H., Michon, V., Goldberg, R., Clochard, M., Jarvis, M.C., Huang, Z-H and Gage, D.A. (1995) Structural analysis of cyclamen seed xyloglucan oligosaccharides using cellulase digestion and spectroscopic methods. *Carbohydr.Res.*, **276**, 167-181

Bradbury, A.G.W. and Halliday, D.J. (1990). Chemical Structures of green coffee bean polysaccharides. *J.Agric.Food Chem.*, **38**, 389-392

Brett, C. and Waldron, K. (1991) In: *Topics in Plant Physiology 2. Physiology and Biochemistry of Plant Cell Walls.* (Black, M. and Chapman, J. eds). Unwin Hyman Ltd, London, UK

Brown, R.M. Jr, Li, L., Okuda, K., Kuga, S., Kudlicka, K., Drake, R., Santos, R. and Clement, S. (1994) *In vitro* cellulose synthesis in plants. *Plant Physiol.*, **105**, 1-2

Brown, R.M.Jr, Wilson, J.H.M. and Richardson, C.L. (1976) Cellulose biosynthesis in *Acetobacter xylinum*: Visualization of the site of synthesis and direct measurement of the in vivo process. *Proc.Natl Acad.Sci. (USA),* **73**, 4565-4569

Buckeridge, M.S., Rocha, D.C., Reid, J.S.G. and Dietrich, S.M.C. (1992) Xyloglucan structure and post-germinative metabolism in seeds of *Copaifera langsdorfii* from savanna and froest populations. *Physiol.Plant.*, **84**, 1-7

Buliga, G.S., Brandt, D.A. and Fincher, G.B. (1986) Sequence statistics and solution conformation of a barley (1→3, 1→4)β-D-glucan. *Carbohydr.Res.*, **157**, 139-156

Burton, B.A. and Brant, D.A. (1983). Comparative flexibility, extension and conformation of some simple polysaccharide chains. *Biopolymers*, **22**, 1769-1792

Cael, J.J., Kwoh, D.L.W., Bhattacharjee, S.S. and Patt, S.L. (1985) Cellulose crystallites: a perspective from solid-state ^{13}C-NMR *Macromolecules*, **18**, 819-821

Camirand, A., Brummell, D. and Maclachlan, G.J. (1987) Fucosylation of xyloglucan: localisation of the transferase in dictyosomes of pea stem cells. *Plant Physiol.*, **84**, 753-756

Capek, P., Toman, R., Kardosova, A. and Rosik, J. (1983) Polysaccharides from the roots of the marsh mallow (*Althaea officinalis* L.): structure of an arabinan. *Carbohydr.Res.*, **117**, 133-140

Carpita, N.C. (1983) Hemicellulosic polymers of cell walls of *Zea* coleoptiles. *Plant Physiol.*, **72**, 515-521

Carpita, N.C. (1987) The biochemistry of the 'growing' plant cell wall. In *Physiology of Cell Expansion During Plant Growth* (Cosgrove, D.J. and Knievel, D.P. eds) Rockville, MD Am.Soc.Plant Physiol., 28-45

Carpita, N.C. and Gibeaut, D.M. (1993) Structural models of primary cell walls in flowering plants: consistency of molecular structure with the physical properties of the walls during growth. *Plant J.*, **3**, 1-30

Carrington, C.M.S., Greve, L.C. and Labavitch, J.M. (1993). Cell wall metabolism in ripening fruit. VI. Effect of the antisense polygalacturonase gene on cell wall changes accompanying ripening in transgenic tomatoes. *Plant Physiol.*, **103**, 429-434

Chambat, G., Barnoud, F. and Joseleau, J-P. (1984) Structure of the primary cell walls of suspension-cultured *Rosa glauca* cells. I. Polysaccharides associated with cellulose. *Plant Physiol.* **74**, 687-693

Chanzy, H.D., Grosrenaud, A., Joseleau, J.-P., Dube, M. and Marchessault, R.H. (1982) Crystallisation behaviour of glucomannan. *Biopolymers*, **21**, 301-319

Chanzy, H., Perez, S., Miller, D.P., Paradossi, G. and Winter, W.T. (1987) An electron diffraction study of mannan I crystal and molecular structure. *Macromolecules*, **20**, 2407-2413

Clark, A.H., Richardson, R.K., Ross-Murphy, S.B. and Stubbs, J.M. (1983) Structural and mechanical properties of agar/gelatin co-gels. Small deformation studies. *Macromolecules,* **16**, 1367-1374

Cleland, R.E. (1981) Wall extensibility: hormones and wall extension. In *Plant Physiology*, New Series, Volume 13B (Tanner, W. and Loewus, F.A. eds). Berlin: Springer-Verlag, 255-273

Cosgrove, D.J. (1987) Linkage of wall extension with water and solute uptake. In: *Physiology of Cell Expansion during Plant Growth.* (Cosgrove, D.J. and Knievel, P.D. eds) The American Society of Plant Physiologists, Rockville, MD, USA pp88-100

Cosgrove, D.J. (1993a) How do plant walls extend? *Plant Physiol.*, **102**, 1-6

Cosgrove, D.J. (1993b) Tansley Review No 46. Wall extensibility: its nature, measurement and relationship to plant growth. *New Phytol.*, **124**, pp1-23

Cosgrove, D.J. and Li, Z.C. (1993) Role of expansin in cell enlargement of oat coleoptiles. Analysis of developmental gradients and photocontrol. *Plant Physiol.*, **103**, 1321-1328

Cousins, S.K. and Brown, R.M. Jr (1995) Cellulose I microfibril assembly: computational molecular mechanics energy analysis favours bonding by van der Waals forces as the initial step in crystallisation. *Polymer* **36**, 3885-3888

Cox, W.P. and Merz. E.H. (1958) Correlation of dynamic and steady viscosities. *J.Polym.Sci.*, **28**, 619-622

Darvill, A.G., Azadi, P., O'Neill, M.A., Gelineo, I., York, W.S., Zablackis, E., Pauly, M., Freshoui, G., Williams, M. and Albersheim, P. (1996). Structrure and Biochemistry of cell wall matrix polysaccharides. "The Extracellular Matrix of Plants: Molecular, Cellular and Developmental Biology", Tamarron, Colorado, USA, March 15-21, 1996

Darvill, A.G., Auger, C., Bergmann, C., Carlson, R.W., Cheong, J.-J., Eberhard, S., Hahn, M.G., Lo, V.-M., Marfa, V., Meyer, B., *et al* (1992) Oligosaccharins - oligosaccharides that regulate growth and defense response in plants. *Glycobiology*, **2**, 181-198

Darvill, A.G., McNeill, M., Albersheim, P.and Delmer, P. (1980) The primary cell walls of flowering plants. In *The Plant Cell* (Talbott, N.E. ed.), NY, Academic Press, 91-162

Dea, I.C.M. and Morrison, A. (1975) Chemistry and interactions of seed galactomannans. *Adv.Carbohydr.Chem.Biochem.*, **31**, 241-312

Dea, I.C.M., Clark, A.H. and McCleary, B.V. (1986) Effect of galactose substitution patterns on the interaction properties of galactomannans. *Carbohydr.Res.*, **147**, 275-294

Debzi, E.M., Chanzy, H., Sugiyama, J., Tekely, P. and Excoffier, G. (1991) The Iα→Iβ transformation of highly crystalline cellulose by annealing in various mediums. *Macromolecules* **24**, 6816-22

Delmer, D.P. (1987) Cellulose biosynthesis. *Annu.Rev.Plant Physiol.*, **38**, 259-290

Delmer, D.P. and Amor, Y. (1995) Cellulose Biosynthesis. *Plant Cell*, **7**, 987-1000

Delmer, D.P., Amor, Y., Johnson, S., Wainscott, M. and Haigler, C.H. (1995) Discovery of a membrane-associated form of sucrose synthase and its potential role in β-glucan synthesis in plants. In:

Proceedings of the Seventh Cell Wall Meeting, Santaigo de Compestela (Zarra,I. and Revilla, G. eds.) University Press, Santiago de Compestela. pp185

Delmer, D.P., Ohana, P., Gonen, L. and Benziman, M. (1993) *In vitro* synthesis of cellulose in plants. Still a long way to go! *Plant Physiol.*, **103**, 307-308

Dentini, M. and Crescenzi, V. (1986) On a polycarboxylate derived from guar. *Carbohydr.Polym.* **6**, 493-498

de Silva, J., Chengappa, S., Arrowsmith, D., Jarman, C. and Smith, C. (1992) Molecular characterisation of a xyloglucan-specific endo-1,4-β-D-glucanase (xyolglucan endo-transglycosylase) from nasturtium seeds. *Plant J.*, **3**, 701-710

Dubois, M., Gilles, K.A., Hamilton, J.K., Rebers, P.A. and Smith, F. (1956) Colorimetric method for determination of sugars and related substances. *Anal.Chem.*, **28**, 350-356

Duckert., L, Byers, E. and Thompson, N.S. (1988) The structure of a xylan from kenaf (*Hibiscus cannabinus*) *Cellulose Chem. Technol.* **22**, 29-37

Durran, D.M., Howlin, B.J., Webb, G.A. and Gidley, M.J. (1995). *Ab initio* nuclear shielding calculations of a model α-(1→4) glucan. *Carbohydr.Res.*, **271**, C1-C5

Earl, W.L and VanderHart, D.L. (1981) Observations by high-resolution carbon-13 nuclear magnetic resonance of cellulose I related to morphology and crystal structure. *Macromolecules*, **14**, 570-574

Eda, S. and Kato, K. (1978) An arabinoxyloglucan isolated from the midrib of the leaves of *Nicotiana tabacum. Agric.Biol.Chem.*, **42**, 351-357

Eda, S., Kodama, H., Akiyama, Y., Mori, M., Kato, K. et al (1983). An arabinoxyloglucan isolated from the cell walls of suspension-cultured tobacco cells. *Agric.Biol.Chem.*, **47**, 1791-1797

Edelmann, H.G. (1995) Characterization of hydration-dependent wall-extensible properties of rye coleoptiles: evidence for auxin-induced changes of hydrogen bonding. *J.Plant Physiol.*, **145**, 491-497

Edelmann, H.G. and Fry, S.C. (1992a) Factors that affect the extraction of xyloglucan from the primary cell walls of suspension-cultured rose cells. *Carbohydr.Res.* **228**, 423-431

Edelmann, H.G. and Fry, S.C. (1992b) Kinetics of integration of xyloglucan into the walls of suspension-cultured rose cells. *J.Exp.Bot.* **43**, 463-470

Edelmann, H.G. and Fry, S.C. (1992c) Effect of cellulose synthesis inhibition on growth and integration of xyloglucan into pea internode cell walls. *Plant Physiol.*, **100**, 993-997

Edelmann, H.G. and Kohler, K. (1995) Auxin increases elastic wall-properties in rye coleoptiles: implications for the mechanism of wall loosening. *Physiol.Plant.*, **93**, 85-92

Edwards, M., Bowman, Y.J.L., Dea, I.C.M. and Reid, J.S.G. (1988) A β-D-galactosidase from nasturtium (*Tropaeolum majus* L.) cotyledons. Purification, properties and demonstration that xyloglucan is the natural substrate. *J.Biol.Chem.*, **263**, 4333-4337

Edwards, M., Dea, I.C.M., Bulpin, P.V. and Reid, J.S.G (1985) Xyloglucan (amyloid) mobilisation in the cotyledons of *Tropaeolum majus* L. seeds following germination. *Planta* **163**, 133-140

Emons, A.M.C. (1985) Plasma membrane rosettes in root hairs of *Equisetum hyemale. Planta*, **163**, 350-359

Emons, A.M.C. (1991) Role of particle rosettes and terminal globules in cellulose synthesis. In: *Biosynthesis and Degradation of Cellulose* (Haigler, C.H. & Weimer, P.J. eds.) Marcel Dekker, NY, 71-98

Emmerling, M. and Seitz, N.V. (1990) Influence of a specifc xyloglucan-nonasaccharide derived from cell walls of suspension-cultured cells of *Daucus carota* L. on regenerating carrot protoplasts. *Planta*, **182**, 174-180

Englyst, H.N. and Cummings, J.H. (1984) Simplified method for the measurement of total non-starch polysaccharides by gas-liquid chromatography of constituent sugars as alditol acetates. *Analyst*, **109**, 937-942

Fanutti, C., Gidley, M.J. and Reid, J.S.G. (1991) A xyloglucan-oligosaccharide-specific α-D-xylosidase or exo-oligoxyloglucan-α-xylohydrolase from germinated nasturtium (*Tropaeolum majus* L.) seeds. Purification, properties and its interaction with a xyloglucan-specific endo-(1→4)-β-D-glucanase and other hydrolases during storage-xyloglucan metabolism. *Planta*, **184**, 137-147

Fanutti, C., Gidley, M.J. and Reid, J.S.G. Transglycosylation action of a xyloglucan-specific endo-(1→4)-β-glucanase from germinated nasturtium seeds.

Farkas, V. and Maclachlan, G. (1988a) Stimulation of pea 1,4-β-glucanase activity by oligosaccharides derived from xyloglucan. *Carbohydr.Res.* **184**, 213-220

Farkas, V. and Maclachlan, G. (1988b) Fucosylation of exogenous xyloglucans by pea microsomal membranes. *Arch.Biochem.Biophys.*, **264**, 48-53

Farkas, V., Sulova, Z., Stratilova, E., Hanna, R. and Maclachlan, G. (1992) Cleavage of xyloglucan by nasturtium seed xyloglucanase and transglycosylation to xyloglucan subunit oligosaccharides. *Arch.Biochem.Biophys.*, **298**, 365-370

Feingold, D.S. (1982) Aldo (and keto) hexoses and uronic acids. in: *The Encyclopaedia of Plant Physiology. New Series.* (Loewus, F.A. and Tanner, W. eds.) Springer-Verlag, Berlin. Volume 13A, pp 3-76

Fernandes, P.B., Concalves, M.P. and Doublier, J.L. (1991). A rheological characterisation of *kappa*-carrageenan/galactomannan mixed gels: a comparison of locust bean gum samples. *Carbohydr. Polym.*, **16**, 253-274

Ferry, J.D. (1970) Viscoelastic Properties of Polymers. (2nd ed), John Wiley & Sons Inc., New Yprk

Finkenstadt, V.L., Hendrixson, T.L. and Millane, R.P. (1995) Models of xyloglucan binding to cellulose microfibrils. *J.Carbohydr.Chem.* **14**, 601-611

Foster, T.J., Ablett, S., McCann, M.C. and Gidley, M.J. (1996) Mobility-resolved ^{13}C NMR spectroscopy of primary plant cell walls. *Biopolymers. In press*

Frei, E. and Preston, R.D. (1968). Non-cellulosisc structural polysaccharides in algal cell walls. III. Mannan in siphoneous green algae. *Proc.R.Soc.London Ser.B*, **169**, 124-145

Fry, S.C. (1988) *The Growing Plant Cell wall: Chemical and Metabolic Analysis.* Longman, London

Fry, S.C. (1989) The structure and functions of xyloglucan. *J.Exp.Bot.* **40**, 1-11

Fry, S.C., Smith, R.C., Renwick, K.F., Martin, D.J., Hodge, S.K. and Matthews, K.J. (1991) Xyloglucan endotransglycosylase, a new wall-loosening enzyme activity from plants. *Biochem.J.*, **282**, 821-828

Fry, S.C., Smith, R.C., Renwick, K.F., Martin, D.J., Hodge, S.K. and Matthews, K.J. (1992) Xyloglucan endotransglycosylase, a new wall loosening enzyme activity from plants. *Biochem.J.*, **282**, 821-828

Fry, S.C., York, W.S., Albersheim, P., Darvill, A., Hayashi, T., Joseleau, J.-P., Kato, Y., Lorences, E.P., Maclachlan, G.A., McNeill, M., Mort, A.J., Reid, J.S.G., Seitz, H.U., Selvendran, R.R., Voragen, A.G.J. and White, A.R. (1993) An unambiguos nomenclature for xyloglucan-derived oligosaccharides. *Physiol.Plant.*, **89**, 1-3

Fyfe, C.A., Dudley, R.L., Stephenson, P.J., Deslandes, Y., Hamer, G.K. and Marchessault, R.H. (1983) Application of high-resolution solid-state NMR with cross-polarisation/magic-angle spinning (CP/MAS) techniques to cellulose chemistry. *JMS-Rev.Macromol.Chem.Phys.* **C23**, 187-216

Gardner, K.H. and Blackwell, J. (1974) The structure of native cellulose. *Biopolymers*, **13**, 1975-2001

Garbow, J.R., Ferrantello, L.M. and Stark, R.E. (1989) ^{13}C Nuclear magnetic resonance study of suberised potato cell wall. *Plant Physiol.*, **90**, 783-787

Gibeaut, D.M. and Carpita, N.C. (1991) Tracing cell wall biogenesis in intact cells and plants. Selective turnover and alteration of soluble and cell wall polsaccharides in grasses. *Plant Physiol.*, **97**, 551-561

Gibeaut, D.M. and Carpita, N.C. (1994) Biosynthesis of plant cell wall polysaccharides. *FASEB J.*, **8**, 904-915

Giddings, T.H., Browner, D.L. and Staehlin, L.A. (1980) Visualization of particle complexes in the plasma membrane of *Micrasterias denticulata* associated with the formation of cellulose fibrils in primary and secondary cell walls. *J.Cell Biol.*, 84, 327-229

Gidley, M.J. (1989) Molecular mechanisms underlying amylose aggregation and gelation. *Macromolecules*, 22, 351-358

Gidley, M.J. (1992) High resolution solid-state NMR of food materials. *Trends in Food Science and Technology*, **3**, 231-236

Gidley, M.J. and Bulpin, P.V. (1989) Aggregation of amylose in aqueous systems: the effect of chain length on phase behaviour and aggregation kinetics. *Macromolecules*, **22**, 341-346

Gidley, M.J., Lillford, P.J., Rowlands, D.W., Lang, P., Dentini, M., Crescenzi, V., Edwards, M., Fanutti, C. and Reid, J.S.G. (1991a) Structure and solution properties of tamarind seed polysaccharide. *Carbohydr.Res.* **214**, 299-314

Gidley, M.J., McArthur, A.J. and Underwood, D.R. (1991b) ^{13}C NMR characterization of molecular structures in powders, hydrates and gels of galactomannans and glucomannans. *Food Hydrocoll.*, **5**, 129-140

Gidley, M.J., Morris, E.R., Murray, E.J., Powell, D.A. and Rees, D.A. (1980) Evidence for two mechanisms of interchain association in calcium pectate gels. *Int.J.Biol.Macromol.*, **2**, 323-334

Glabe, C.G., Harty, P.K. and Rosen, S.D. (1983) Preparation and properties of fluorescent polsaccharides. *Anal.Biochem.* **130**, 287-294

Goycoolea, F.M., Richardson, R.K., Morris, E.R. and Gidley, M.J. (1995). Effect of locust bean gum and konjac glucomannan on the conformation and rheology of agarose and *k*-carrageenan. *Biopolymers*, **36**, 643-658

Goodenough, U. and Heuser, J. (1985) The *Chlamydomonas* cell wall and its consistent glycoproteins analysed by the quick-freeze, deep-etch technique. *J.Cell Biol.*, **101**, 1550-1568

Goodenough, U. and Heuser, J. (1988) Molecular organization of cell wall crystals from *Chlamydomonas reinhardtii* and *Volvox Carteri. J.Cell Sci.*, **90**, 717-733

Gunning, B.E.S. and Hardham, A.R. (1982) Microtubules. *Annu.Rev.Plant Physiol.* **33**, 651-698

Hackney, J.M., Atalla, R.H. and VanderHart, D.L. (1994) Modification of crystallinity and crystalline structure of *Acetobacter xylinum* cellulose in the presence of water-soluble β-1,4-linked polysaccharides. ^{13}C NMR evidence. *Int.J.Biol.Macromol.*, **16**, 215-218

Haigler, C.H. (1985) The functions and biogenesis of native cellulose. In: *Cellulose Chemistry and its Applications*. Horwood, Chichester, UK pp30-83

Haigler, C.H. and Benziman, M. (1982) Biogenesis of cellulose I microfibrils occurs by cell-directed self-assembly in Acetobacter xylinum. In: Cellulose and Other Natural Polymer Systems: Biogenesis, Structure and Degradation. (Brown, R.M. Jr, ed), Plenum Publishing Corp., New York, pp273-297

Haigler, C.H. and Brown, R.M. Jr (1981). Probing the relationship of polymerisation and crystallisation in the biogenesis of cellulose I. In *The Eckman Days 1981, International Symposium on Wood and Pulping Chemistry, Volume 5*. Stockholm: Swedish Association of Pulp and Paper Engineers, pp 14-16

Haigler, C.H., Brown, R.M. Jr and Benziman, M. (1980). Calcofluor white alters the *in vivo* assembly of cellulose microfibrils. *Science*, **210**, 903-906

Haigler, C.H., White, A.R., Brown, R.M. Jr and Cooper, K.M. (1982). Alteration of *in vivo* ribbon assembly by carboxymethylcellulose and other cellulose derivatives. *J.Cell Biol.*, **94**, 64-69

Hall, L.D. and Yalpani, M. (1980) A high yielding, specific method for the chemical derivatization of D-galactose-containing polysaccharides: oxidation with D-galactose oxidase, followed by reductive amination. *Carbohydr.Res.* **80**, C10-C12

Hamilton, G.A., Adolf, P.K., deJersey, J., DuBois, G.C., Dyrkacz, G.R. and Libby, R.D. (1978) Trivalent copper superoxide and galactose oxidase. *J.Am.Chem.Soc.* **100**, 1899-1912

Hayashi, T. (1989) Xyloglucans in the primary cell wall. *Annu.Rev.Plant Physiol.Mol.Biol.*, **40**, 139-168

Hayashi, T., Baba, K'i. and Ogawa, K. (1994a) Macromolecular complexes of xyloglucan and cellulose obtained by annealing. *Plant Cell Physiol.* **35**, 219-223

Hayashi, T. and Maclachlan, G. (1984) Pea xyloglucan and cellulose. I. Macromolecular organization. *Plant Physiol.* **75**, 596-604

Hayashi, T., Marsden, M.P.F. and Delmer, D.P. (1987) Pea xyloglucan and cellulose. V. Xyloglucan-cellulose interactions *in vitro* and *in vivo*. *Plant Physiol.* **83**, 384-389

Hayashi, T. and Matsuda, K. (1981) Biosynthesis of xyloglucan in suspension-cultured soybean cells: occurrence and some properties of xyloglucan 4-β-D-glucosyltransferase and 6-α-D-xylosyltransferase. *J.Biol.Chem.*, **21**, 11117-11122

Hayashi, T. and Ohsumi, C. *Endo-1,4-β-glucanase in the cell walls of stems of auxin-treated pea* seedlings. *Plant Cell Physiol.*, **35**, 419-424

Hayashi, T. and Takeda, T. (1994) Compositional analysis of the oligosaccharide units of xyloglucans from suspension-cultured poplar cells. *Biosci.Biotech.Biochem.*, **58**, 1707-1708

Hayashi, T., Takeda, T., Ogawa, K. and Mitsuisi, Y. (1994b) Effects of the degree of polymerisation on the binding of xyloglucans to cellulose. *Plant Cell Physiol.* **35**, 893-899

Hayashi, T., Wong, Y-S., and Maclachlan, G. (1984) Pea xyloglucan and cellulose. II. Hydrolysis by pea endo-1,4-β-glucanases. *Plant Physiol.*, **75**, 605-610

Hermans, J.R. (1965) Investigations of the elastic properties of the particle network in gelled solutions of hydrocolloids. I. Carboxymethylcellulose. *J.Polym.Sci.*, **A3**, 1859-1868

Herth, W. (1985) Plasma membrane rosettes involved in localised wall thickening during xylem vessel formation of *Lepidium sativum*. *Planta*, **164**, 12-21

Herth, W. and Weber, G. (1984) Occurrence of the putative cellulose-synthesising "rosettes" in the plasma membrane of *Glycine max* suspension culture cells. *Naturwissenschaften*, **71**, 153-154

Hestrin, S., Aschner, M. and Mager, J. (1947) Synthesis of cellulose by resting cells of *Acetobacter xylinum. Nature*, **159**, 64-65

Hestrin, S. and Schramm, M. (1954) Synthesis of cellulose by *Acetobacter xylinum. Biochem.J.*, 58, 345-352

Heuser, J. (1981). Preparing biological samples for steromicroscopy by the quick-freeze, deep-etch, rotary-replication technique. *Meth.Cell Biol.*, **22**, 97-122

Hisamatsu, M., Impallomeni, G., York, W.S., Albersheim, P. and Darvill, A.G. (1991) A new undecasaccharide subunit of xyloglucans with two α-L-fucosyl residues. *Carbohydr.Res.*, **211**, 117-129

Hisamatsu, M., York, W.S., Darvill, A.G. and Albersheim, P. (1992) Characterization of seven xyloglucan oligosaccharides containing from seventeen to twenty glycosyl residues. *Carbohydr.Res.*, **227**, 45-71

Horii, F., Hirai, A. and Kitamuru, R. (1984) CP/MAS and carbon-13 NMR study of spin-relaxation phenomena of cellulose containing crystalline and non-crystalline components. *J.Carbohydr.Res.* **3**, 641-662

Horii, F., Hirai, A. and Kitamaru, R. (1984) Cross-polarization/magic angle spinning 13C-NMR study: molecular chain conformations of native and regenerated cellulose. *In Polymers for Fibers and Elastomers, ACS Symposium Series 260*, (Arthur, J.C. Jr ed.), American Chemical Society, Washington, DC, USA pp 27-42

Horii, F., Hirai, A. and Kitamura, R. (1987a) CP/MAS ^{13}C NMR spectra of the crystalline components of native celluloses *Macromolecules*, **20**, 2117-2120

Horii, F., Yamamoto, H., Kitamaru, R., Tanahashi, M. and Higuchi, T. (1987b) Transformation of native cellulose crystals by saturated steam at high temperatures. *Macromolecules*, **20**, 2946-2949

Hoson, T. and Masuda, Y. (1991) Effect of xyloglucan nonasaccharide on cell elongation induced by 2,4-dichlorophenoxyacetic acid and indole-3-acetic acid. *Plant Cell Physiol.*, **32**, 777-782

Huber, D.J. and Nevins, D.J. (1981) Parrtial purification of endo- and exo-β-D-glucanase enzymes from *Zea mays* seedlings and their involvement in cell wall autohydrolysis. *Planta*, **151**, 206-214

Hulleman, H.D., van Hazendonk, J.M. and van Dam, J.E.G. (1994) Determination of crystallinity in native cellulose from higher plants with diffuse reflectance Fourier transform infrared spectroscopy. *Carbohydr.Res.*, **261**, 163-172

Iraki, N.M., Bressan, R.A., Hasegawa, P.M. and Carpita, N.C. (1989a) Alteration of the physical and chemical structure of the primary cell wall of growth-limited plant cells adapted to osmotic stress. *Plant Physiol.*, **91**, 39-47

Iraki, N.M., Singh, N.K., Bressan, R.A. and Carpita, N.C. (1989b) Cell walls of tobacco cells and changes in composition associated with reduced growth upon adaptation to water and saline stress. *Plant Physiol.*, **91**, 47-53

Iraki, N.M., Bressan, R.A. and Carpita, N.C. (1989c) Extracellular polysaccharides and proteins of tobacco cell cultures and changes in composition with growth-limiting adaptation to water and saline stress. *Plant Physiol.*, **91**, 54-61

Ishizu, A. (1983) Hemicelluloses. In: *Mokuzaikagaku* (Nakano, J., Sumimoto, M., Higuchi, T. and Ishuzu, A. eds), Uni Shuppan, Tokyo, Japan, pp 91-144

Itoh, T. and Brown, R.M. Jr (1984) Assembly of cellulose microfibrils in *Valonia macrophysa* Kutz. *Planta*, **160**, 372-381

Itoh, T. and Brown, R.M. Jr (1988) Development of cellulose synthesising complexes in *Boergesenia* and *Valonia. Protoplasma*, **144**, 160-169

Jarvis, M.C. (1992) Self-assembly of plant cell walls. *Plant, Cell, Environ.*, **15**, 1-5

Jarvis, M.C. and Apperly, D.C. (1990) Direct observation of cell wall strcuture in living plant tissues by solid-state ^{13}C NMR spectroscopy. Plant Physiol., **92**, 61-65

Joseleau, J.-P., Chambat, G., Cortelazzo, A., Faik, A. and Ruel, K. (1994) Putative biological action of oligosaccharides on enzymes involved in cell-wall development. *Biochem.Soc.Trans.*, **22**, 403-407

Kai, A., Xu, P., Horii, F. and Hu, S. (1994) C.p./m.a.s. ^{13}C n.m.r. study on microbial cellulose-fluorescent brightener complexes. *Polymer*, 35, 75-79

Kato, Y. and Matsuda, K. (1976) Presence of a xyloglucan in the cell wall of *Phaseolous aureus* hypocotyls. *Plant Cell Physiol.*, **17**, 1185-1198

Kato, Y. and Matsuda, K. (1980a) Structure of oligosaccharides obtained by controlled degradation of mung bean xyloglucan with acid and *Aspergillus oryzae* enzyme preparation. *Agric.Biol.Chem.*, **44**, 1751-1758

Kato, Y. and Matsuda, K. (1980b) Structure of oligosaccharides obtained by hydrolysis of mung bean xyloglucan with *Trichoderma viride* cellulase. *Agric.Biol.Chem.*, **44**, 1759-1766

Kato, Y. and Nevins, D.J. (1986) Fine structure of (1→3),(1→4)β-D-glucan from *Zea* shoot cell walls. *Carbohydr.Res.*, **147**, 69-85

Kato, Y. and Watanabe, T. (1993) Isolation and characterisation of a xyloglucan from Gobo (*Arctium lappa* L.). *Biosci.Biotech.Biochem.*, **57**, 1591-1592

Katsaros, C., Reiss, H.D. and Schnepf, E. (1996) Freeze-fracture studies in brown algae: putative cellulose-synthesising complexes on the plasma membrane. *Eur.J.Phycol.*, **31**, 41-48

Kawagoe, Y. and Delmer, D.P. (1995) Cotton sucrose synthase interacts in vitro with calnexin: A possible mechanism for β-glucan synthase complex assembly. In: *Proceedings of the Seventh Cell Wall Meeting, Santaigo de Compestela* (Zarra,I. and Revilla, G. eds.) University Press, Santiago de Compestela. pp 188

Keegstra, K., Talmadge, K.W., Bauer, W.D. and Albersheim, P. (1973) The structure of plant cell walls. III. A model of the walls of suspension-cultured sycamore cells based on the interconnections of the macromolecular components. *Plant Physiol.*, **51**, 188-198

Kiefer, L.L., York, W.S., Albersheim, P. and Darvill, A.G. (1990). Structural characterization of an arabinose-containing heptadecasaccharide enzymically isolated from sycamore extracellular xyloglucan.*Carbohydr.Res.*, **197**, 139-158

Kim, T.S. and Newman, R.H. (1995) Solid state ^{13}C-NMR study of wood degraded by the brown rot fungus *Gloeophyllum trabeum. Holzforschung*, **49**, 109-114

Knox, J.P., Linstead, P.J., King, J., Cooper, C. and Roberts, K. (1990) Pectin esterification is spatially regulated both within cell walls and between developing tissues of root apices. *Planta*, **181**, 512-521

Kooiman, P. (1960a) On the occurrence of amyloids in plant seeds. *Acta Bot.Neerl.* **9**, 208-219

Kooiman, P. (1960b) A method for the determination of amyloid in plant seeds. *Recl.Trav.Chi.Pays-Bas*, 79, 675-678

Kroon-Batenberg, L.M.J., Kroon, J., Leeflang, B.R. and Vliegenthart, J.F.G. (1993). Conformational analysis of methyl β-cellobioside by ROESY NMR spectroscopy and MD simulations in combination with the CROSREL method. *Carbohydr.Res.*, **245**, 21-42

Kudlicka, , K., Brown, R.M., Jr, Li, L., Shen, H. and Kuga, S. (1995) β-Glucan synthesis in the cotton fiber. IV. *In vitro* assembly of the cellulose I allomorph

Kuga, S. and Brown, R.M. Jr (1989) Correlation between structure and the biogenic mechanisms of cellulose: new insights based on recent electron microscopic findings. In *Cellulose and Wood - Cemistry and Technology.* (Schuerch, C. ed.), Wiley, NY, 677-688

Kuga, S., Takagi, S. and Brown, R.M. Jr (1993) Native folded-chain cellulose II. *Polymer*, **34**, 3293-3297

Kvernheim, A.L. (1987) Methylation analysis of polysaccharides with butyllithium in dimethylsulfoxide. *Acta Chem.Scand.*, **B41**, 150-152

Labavitch, J.M. and Ray, P.M. (1974) Relationship between promotion of xyloglucan metabolism and induction of elongation by indoleacetic acid. *Plant Physiol.*, **54**, 499-502

Lamport, D.T.A. (1965). The protein component of primary cell walls. In *Advances in Botanical Research,* Volume 2 (Preston, R.D. ed.), John Wiley, NY

Lamport, D.T.A. (1986) The primary cell wall : a new model. In *Cellulose: Structure, Modification and Hydrolysis* (ed. Young, R.A. and Rowell, R.M.). John Wiley & Sons Inc., NY

Lamport, D.T.A. and Northcote, D.H. (1960). Hydroxyproline in the cell walls of higher plants. *Nature,* **188**, 665-666

Lang, P., Masci, G., Dentini, M., Crescenzi, V., Cooke, D., Gidley, M.J., Fanutti, C. and Reid, J.S.G. (1992) Tamarind seed polysaccharide: preparation, characterisation and solution properties of carboxylated, sulphated and alkylaminated derivatives. *Carbohydr.Polym.* **17**, 185-198

Lee, J.H., Brown, R.M. Jr, Kuga, S., Shoda, S-i and Kobayashi, S (1994) Assembly of synthetic cellulose I. *Proc.Natl.Acad.Sci. (USA),* 91, 7425-7429

Lennholm, H., Larsson, T. and Iversen, T (1994) Determination of cellulose Iα and Iβ in lignocellulosic materials. *Carbohydr.Res.* **261**, 119-131

Lever, M. (1972) A new reaction for the colorimetric determination of carbohydrates. *Anal.Biochem.*, **47**, 273-279

Levy, S. (1995) Investigating xyloglucan-cellulose interactions by computer simulation and in vitro binding assays. In: *Proceedings of the Seventh Cell Wall Meeting, Santaigo de Compestela* (Zarra,I. and Revilla, G. eds.) University Press, Santiago de Compestela. pp 31

Levy, S., York, W.S., Stuike-Prill, R., Meyer, B. and Staehlin, L.A. (1991) Simulations of the static and dynamic molecular conformations of xyloglucan. The role of the fucosylated sidechain in surface-specific sidechain folding. *Plant J.* **1**, 195-215

Li, L. and Brown, R.M. Jr (1993) β-Glucan synthesis in the cotton fiber. II. Regulation and kinetic properties of β-glucan synthases. *Plant Physiol.*, **101**, 1143-1148

Li, L., Drake, R.R. Jr., Clement, S. and Brown, R.M. Jr (1993) β-Glucan synthesis in the cotton fibre. III. Identification of UDP-glucose binding subunits of β-glucan synthases by photoaffinity labelling with [β-^{32}P]5'N_3-UDP-glucose. *Plant Physiol.*, **101**, 1149-1156

Lockhart, J.A. (1865) An analysis of irrevesible plant cell elongation. *J.Theor.Biol.*, **8**, 264-275

Lorences, E.P. and Fry, S.C. (1993) Xyloglucan oligosaccharides with at least two α-D-xylose residues act as acceptor substrates for xyloglucan endotransglycosylase and promote the depolymerisation of xyloglucan. *Physiol.Plant.*, **88**, 105-112

Lorences, E.P., Suarez, L. and Zarra, I. (1987) Hypocotyl growth of *Pinus pinaster* seedlings. Changes in the molecular weight distribution of hemicellulosic polysaccharides. *Physiol.Plant.*, **69**, 466-471`

Marchessault, R.H., Taylor, M.G. and Winter, W.T. (1990) 13C CP/MAS NMR spectra of poly-β-D(1→4) mannose: mannan. *Can.J.Chem.*, **68**, 1192-1195

Markwell, M.A.K. (1982) A new solid-state reagent to iodinate proteins. I. Conditions for the efficient labelling of antiserum. *Anal.Biochem.* **125**, 427-432

Matthyse, A.G. (1983). Role of bacterial cellulose fibrils in *Agrobacterium tumefaciens* infection. *J.Bacteriol.*, **154**, 906-915

Matthyse, A.G., Holmes, K.V. and Gurlitz, R.H.G. (1981) Elaboration of cellulose fibrils by *Agrobacterium tumefaciens* during attachment to carrot cells. *J.Bacteriol.*, **145**, 583-595

Matthysse, A.G., Thomas, D.L. and White, A.R. (1995a) Mechanism of cellulose synthesis in *Agrobacterium tumefaciens. J.Bact.*, **177**, 1076-1081

Matthysse, A.G., White, S. and Lightfoot, R. (1995b) Genes required for cellulose synthesis in *Agrobacterium tumefaciens. J.Bact.*, **177**, 1069-1075

McCann, M.C., Hammouri, M., Wilson, R., Belton, P. and Roberts, K. (1992a) Fourier transform infra-red microspecroscopy: a new way to look at plant cell walls. *Plant Physiol.*, **100**, 1940-1947

McCann, M.C. and Roberts, K. (1991) Architecture of the primary cell wall. In *The Cytoskeletal Basis of Plant Growth and Form* (Lloyd, C.W., ed.). London: Academic Press, pp109-129

McCann, M.C., Shi, J., Roberts, K. and Carpita, N.C. (1994) Changes in pectin structure and localisation during the growth of unadapted and NaCl-adapted tobacco cells. Plant J., 5, 773-785

McCann, M.C., Stacey, N.J., Wilson, R. and Roberts, K. (1993) Orientation of macromolecules in the walls of elongating carrot cells. *J.Cell Sci.*, **106**, 1347-1356

McCann, M.C., Wells, B. and Roberts, K. (1990) Direct visualisation of cross-links in the primary plant cell wall. *J.Cell Sci.* **96**, 323-334

McCann, M.C., Roberts, K., Wilson, R.H., Gidley, M.J., Gibeaut, D.M., Kim, J-B., and Carpita, N.C. (1995). Old and new ways to probe plant architecture. *Can.J.Bot.*, **73**, S103-S113

McCann, M.C., Wells, B. and Roberts, K. (1992b) Complexity in the spatial localisation and length distribution of plant cell wall matrix polysaccharides. *J.Microsc.*, **166**, 123-136

McDougall G.J. and Fry, S.C. (1988) Inhibition of auxin-stimulated growth of pea stem segments by a specific nonasaccharide of xyloglucan. *Planta*, **175**, 412-416

McDougall, G.J. and Fry, S.C. (1989a) Anti-auxin activity of xyloglucan oligosaccharides: the role of groups other than the terminal α-L-fucose residue. *J.Exp.Bot.*, **40**, 233-239

McDougall, G.J. and Fry, S.C. (1989b) Structure-activity relationships for xyloglucan oligosaccharides with antiauxin activity. *Plant Physiol.*, **89**, 883-887

McDougall, G.J. and Fry, S.C. (1990) Xyloglucan oligosaccharides promote growth and activate cellulase: Evidence for a role of cellulase in cell expansion. *Plant Physiol*, **93**, 1042-1048

McDougall, G.J. and Fry, S.C. (1991) Xyloglucan nonasaccharide, a naturally occurring oligosaccharin, arises *in vivo* by polysaccharide breakdown. *J.Plant Physiol.* **137**, 332-336

McNeill, M., Darvill, A.G., Fry, S.C. and Albersheim, P. (1984) Structure and function of the primary cell walls of plants. *Annu.Rev.Biochem.*, **53**, 625-663

McQueen-Mason, S.J. and Cosgrove, D.J. (1994) Disruption of hydrogen bonding between plant cell wall polymers by proteins that induce wall extension. *Proc.Natl.Acad.Sci. (USA)*, **91**, 6574-6578

McQueen-Mason, S.J., Durachko, D.M. and Cosgrove, D.J. (1992) Two endogenous proteins that induce cell wall extension in plants. *Plant Cell*, **4**, 1425-1433

McQueen-Mason, S.J., Fry, S.C., Durachko, D.M. and Cosgrove, D.J. (1993) The relationship between xyloglucan endotransglycosylase and *in vitro* cell wall extension in cucumber hypocotyls. *Planta*, **190**, 327-331

Meier, H. (1958) On the structure of cell walls and cell wall mannans from ivory nuts and from dates. *Biochem.Biophys.Acta*, **28**, 229-240

Meier, H. and Reid, J.S.G. (1982) Reserve polysaccharides other than starch in higher plants. In: Encyclopedia of Plant Physiology, N.S., Vol. 13A: Plant Carbohydrates, pp 418-471. Loewus, F.A., Tanner, W., eds. Springer. Berlin-Heidelberg New York

Mitikka, M., Teeaar, R., Tenkanen, M., Laine, J. and Vuorinen, T. (1995) Sorption of xylans on cellulose fibers. In: *Proceedings of the 8th International Symposium on Wood and Pulping Chemistry, June 6-9, 1995, Helsinki, Finland, Volume III*, pp231-236

Mizuta, S. and Brown, R.M. Jr (1992) Effects of 2,6-dichlorobenzonitrile and Tinopal LPW on the structure of the cellulose synthesing complexes of *Vaucheria hamata. Protoplasma*, **166**, 200-207

Monro, J.A., Penny, D. and Bailey, R.W. (1976) The organization and growth of primary cell walls of lupin hypocotyl. *Phytochemistry*, **15**, 1193-1198

Mori, M., Eda, S. and Kato, K. (1979) Two xyloglucan oligosaccharides obtained by cellulase-degradation of tobacco arabinoxyloglucan. *Agric.Biol.Chem.*, **43**, 145-149

Morgan, C.F., Schleich, T., Caines, G.H. and Farnsworth, P.N. (1989) Elucidation of intermediate (mobile) and slow (solid like) protein motions in bovine lens homogenates by Carbon-13 NMR spectroscopy. *Biochemistry*, **28**, 5065-5074

Morris, E.R. (1983) Rheology of hydrocolloids. In: *Gums and Stabilisers for the Food Industry 2.* (Phillips, G.O., Wedlock, D.J. and Williams, P.A. eds), Pergamon Press, UK. pp57-78

Morris, E.R., Gidley, M.J., Murray, E.J., Powell, D.A. and Rees, D.A. (1980) Characterization of pectin gelation under conditions of low water activity by circular dichroism, competitive inhibition and mechanical properties. *Int.J.Biol.Macromol.*, **2**, 327-330

Mort, A.J., Moerschbacher, B.M., Pierce, M.L. and Maness, N.O. (1991) Problems encountered during the extraction, purification and chromatography of pectic fragments and some solutions to them. *Carbohydr.Res.*, **215**, 219-227

Mueller, S.C. and Brown, R.M. Jr (1980) Evidence for an intramembrane compnoent associated with a cellulose-synthesising complex in higher plants. *J.Cell Biol.*, **84**, 315-326

Murayama, A., Ichikawa, Y. and Kawabata, A. (1995a). Rheological properties of mixed gels of *k*-carrageenan with galactomannan. *Biosci.Biotech.Biochem.*, **59**, 5-10

Murayama, A., Ichikawa, Y. and Kawabata, A. (1995b). Sensory and rheological properties of *k*-carrageenan gels mixed with locust bean gum, tara gum and guar gum. *J.Texture Stud.*, **26**, 239-254

Nari, J., Noat, G., Diamantidis, G. and Ricard, J. (1986) Electrostatic effects and the dynamics of enzymic reactions at the surface of plant cells. 3. Interplay between limited cell-wall autolysis, pectin methylesterase activity and electrostatic effects in soybean cell walls. *Eur.J.Biochem.*, 155, 199-202

Newman, R.H. and Hemmingson, J.A. (1994) Carbon-13 NMR distinction between categories of molecular order and disorder in cellulose. *Cellulose*, **2**, 95-110

Newman, R.H., Ha, M-A. and Melton, L.D. (1994) Solid-state ^{13}C NMR investigation of molecular ordering in the cellulose of apple cell walls. *J.Agric.Food Chem.* **42**, 1402-1406

Nishitani, K. and Masuda, Y. (1981) Auxin-induced changes in the cell wall structure: changes in sugar composition, intrinsic viscosity and molecular weight distribution of matrix polysaccharides of the epicotyl cell wall of *Vigna angularis. Physiol.Plant.*, **52**, 482-494

Nishitani, K. and Masuda, Y. (1982) Acid-induced structural changes in cell wall xyloglucans in *Vigna angularis* epicotyl segments. *Plant Sci.Lett.*, **28**, 87-94

Nishitani, K and Masuda, Y. (1983) Auxin-induced changes in the cell wall xyloglucans: effects of auxin on the two different subfractions of xyloglucan in the epicotyl cell wall of *Vigna angularis. Plant Cell Physiol.*, **24**, 345-356

Nishitani, K. and Tominaga, R. (1992) Endo-xyloglucan transferase, a novel class of glycosyltransferase that catalyzes transfer of a segment of xyloglucan molecule to another xyloglucan molecule. *J.Biol.Chem.*, **267**, 21058-21064

Northnagel, E.A., McNeill, M., Albersheim, P. and Dell, A. (1983) Host-pathogen interactions. XXII. A galacturonic acid oligosaccharide from plant cell walls eklicits phytoalexins. *Plant Physiol.*, **71**, 916-926

Ogawa, K., Hayashi, T. and Okamura, K. (1990) Conformational analysis of xyloglucans. *Int.J.Biol.Macromol.*, **42**, 1402-1406

Ohsumi, C. and Hayashi, T. (1994) The oligosaccharide units of the xyloglucans in the cell walls of bulbs of onion, garlic and their hybrid. *Plant Cell Physiol.*, **35**, 963-967

Okuda, K., Li, L., Kudlicka, K., Kuga, S., and Brown, R.M. Jr (1993) β-Glucan synthesis in the cotton fibre. I. Identification of β-1,4 and β-1,3-glucans synthesised *in vitro*. *Plant Physiol.*, **101**, 1131-1142

Okuda, K., Tsekos, I. and Brown, R.M. Jr (1994) Cellulose microfibril assembly in Erythrocladia subintegra Rosenv.: an ideal system for understanding the relationship between synthesising complexes (TCs) and microfibril crystallisation. *Protoplasma*, **180**, 49-58

O'Neill, R.A., Albersheim, P. and Darvill, A.G. (1989) Purification and characterization of a xyloglucan oligosaccharide specific xylosidase from pea seedlings. *J.Biol.Chem.*, **264**, 20430-20437

Passioura, J.B. and Fry, S.C. Turgor and cell expansion: Beyond the Lockhart equation. *Aust.J.Plant Physiol.*, **19**, 565-576

Pasto, D.J. and Lepeska, B. (1976) The measurement and interpretation of hydrogen-tritium kinetic isotope effects in borane and borohydride reductions of ketones. Implications on steric approach control vs. product development control. *J.Am.Chem.Soc.* **98**, 1091-1095

Pauly, M., York, W.S., Albersheim, P. and Darvill, A.G. (1995) Xyloglucan oligosaccharide profile of pea epicotyls. . In: *Proceedings of the Seventh Cell Wall Meeting, Santaigo de Compestela* (Zarra,I. and Revilla, G. eds.) University Press, Santiago de Compestela. pp34

Potikha, T. and Delmer, D.P. (1995) A mutant of *Arabidopsis thaliana* displaying altered patterns of cellulose deposition. *Plant J.*, **7**, 453-460

Powell, D.A., Morris, E.R., Gidley, M.J. and Rees, D.A. (1982) Conformations and interactions of pectins. II. Influence of residue sequence on chain association in calcium-pectate gels. *J.Mol.Biol.*, **155**, 517-531

Pressey, R. and Himmelsbach, D.S. (1984) ^{13}C-N.m.r. spectrum of a D-galactose-rich polysaccharide from tomato fruit. *Carbohydr.Res.*, **127**, 356-359

Qi, X., Behrens, B.X., West, P.R. and Mort, A.J. (1995) Solubilization and partial characterization of extensin fragments from cell walls of cotton suspension cultures. Evidence for a covalent cross-link between extensin and pectin. *Plant Physiol.*, **108**, 1691-1701

Quadar, H. (1991) Role of linear terminal complexes in cellulose synthesis. In: *Biosynthesis and Degradation of Cellulose*. (Haigler, C.H. & Weimer, P.J. eds.) Marcel Dekker, NY, 51-69

Quemener, B. and Thibault, J-F. (1990). Assessment of methanolysis for the determination of sugars in pectins. *Carbohydr.Res.*, **206**, 277-287

Ranby, B.G. (1952) The mercerisation of cellulose I. A thermodynamic study. *Acta Chem.Scand.*, **6**, 101-115

Ray, P.M. (1980) Cooperative action of β-glucan synthetase and UDP-xylose xylosyl transferase of Golgi membranes in the synthesis of xyloglucan-like polysaccharide. *Biochem.Biophys.Acta.* **629**, 431-444

Ray, P.M., Green, P.B. and Cleland, R.E. (1972) Role of turgor in plant cell growth. *Nature*, **239**, 163-164

Redgwell, R.J. and Selvendran, R.R. (1986) Structural features of cell wall polysaccharides of onion *Allium cepa. Carbohydr.Res.* **157**, 183-199

Rees, D.A. (1977) *Polysaccharide Shapes*. Chapman and Hall, London

Renard, C.M.G.C., Lomax, J.A. and Boon, J.J. (1992) Apple fruit xyloglucans: a comparative study of enzyme digests of whole cell walls and of alkali-extracted xyloglucans. *Carbohydr.Res.*, **232**, 303-320

Reis, D., Vian, B., Chanzy, H. and Roland, J.C. (1991) Liquid-crystal type assembly of native cellulose-glucuronoxylans extracted from plant cell walls. *Biol.Cell*, **73**, 173-178

Reis, D., Roland, J.C., Mosiniak, M., Darzens, D. and Vian, B. (1992). The sustained and warped pattern of a xylan-cellulose composite: The stony endocarp model. *Protoplasma*, **166**, 21-34

Reis, D., Vian, B. and Roland, J.C. (1994) Cellulose-glucuronoxylans and plant cell wall structure. *Micron*, **25**, 171-187

Reiter, W.-F., Chapple, C.C.S., Somerville, C.R. (1993) Altered growth and cell walls in a fucose-deficient mutant of *Arabidopsis. Science*, **261**, 1032-1035

Richardson, R.K. and Ross-Murphy, S.B. (1987a) Non-linear viscoelasticity of polysaccharide solutions. I. Guar galactomannan solutions. *Int.J.Biol.Macromol.*, **9**, 250-256

Richardson, R.K. and Ross-Murphy, S.B. (1987b) Non-linear viscoelasticity of polysaccharide solutions. 2. Xanthan polysaccharide solutions. *Int.J.Biol.Macromol.*, **9**, 257-264

Ring, G.J.F. (1982) A study of the polymerization kinetics of bacterial cellulose through gel permeation chromatography. In: *Cellulose and Other Natural Polymer Systems* (Brown, R.M. Jr ed.), Plenum Publishing Corp., NY pp299-325

Ring, S.G. and Selvendran, R.R. (1981) An arabinogalactoxyloglucan from the cell wall of *Solanum tuberosum. Phytochemistry*, **20**, 2511-2519

Roberts, E.M., Saxena, I.M. and Brown, R.M. Jr (1989). Biosynthesis of cellulose II in *Acetobacter xylinum.* In*: Cellulose and Wood- Chemistry and Technology* (Schuerch, C. ed.) Wiley, New York. pp 689-704

Roberts, K. (1989) The plant extracellular matrix. *Curr.Op.Cell Biol.*, **1**, 1020-1027

Robinson, G., Ross-Murphy, S.B. and Morris, E.R. (1992). Viscosity-molecular weight relationships, intrinsic chain flexibility, and dynamic solution properties of guar galactomannan. *Carbohydr.Res.*, **107**, 17-32

Robinson, D.G. and Quadar, H. (1981) Structure, synthesis and orientation of microfibrils. IX. A freeze-fracture investigation of the *Oocystis* plasma membrane after inhibitor treatments. *Eur.J.Cell Biol.*, **25**, 278-288

Rogers, J.K. and Thompson, N.S. (1968) The oxidation of D-galactopyranosyl residues of polysaccharides to D-galactopyranosyluronic acid residues. *Carbohydr.Res.* 7, 66-75

Ross, P., Weinhouse, H., Aloni, Y., Michaeli, D., Ohana, P., Mayer, R., Braun, S., deVroom, E., van der Marel, G.A., van Boom, J.H. and Benziman, M. (1987) Regulation of cellulose synthesis in *Acetobacter xylinum* by cyclic diguanylic acid. *Nature*, **325**, 279-281

Ross, P., Mayer, R. and Benziman, M. (1991) Cellulose biosynthesis and function in bacteria. *Microbiol. Rev.*, **55**, 35-58

Ross-Murphy, S.B. (1983) Rheological methods. In: *Biophysical Methods in Food Research*, Critical Reports on Applied Chemistry, (Chan, H.W.-S. ed.), SCI, London, pp138-199

Ruel, K., Cortelazzo, A.L., Chambat, G., Marais, M.F. and Joseleau, J-P (1995) Auxin and oligosaccharides affect the ultrastructural wall organization of growing cells. *Proceedings of the Seventh Cell Wall Meeting, Santaigo de Compestela* (Zarra,I. and Revilla, G. eds.) University Press, Santiago de Compestela. pp 63

Ruel, K. and Joseleau, J-P (1993) Influence of xyloglucan oligosaccharides on the micromorphology of the walls of suspension-cultured *Rubus fruticosus* cells. *Acta Bot. Neerl.*, **42**, 363-378

Sakurai, N. and Nevins, D.J. (1993) Changes in physical properties and cell wall polysaccharides of tomato (*Lycopersicon esculentum*) pericarp tissues. *Physiol.Plant.*, **89**, 681-686

Sakurai, N. and Nevins, D.J. (1995) Degradation of xyloglucans during ripening of tomato and avocado fruit. Abstract presented at *7th Cell Wall Meeting, Santiago de Compestela, Spain, 26-29 September, 1995*

Sarko, A. and Muggli, R. (1974) Packing analysis of carbohydrates and polysaccharides. III. *Valonia* cellulose and cellulose II. *Macromolecules*, 7 486-

Satiat-Jeunemaitre, B. (1989) Microtubules, microfibrilles parietales et morphogenese vegetale: cas des cellules en extension. *Bull.Soc.Bot.Fr 136 Actual*, **2**, 87-98

Satiat-Jeunemaitre, B., Martin, B. and Hawes, C. (1992) Plant cell wall architecture is revealed by rapid-freezing and deep-etching. *Protoplasma*, **167**, 33-42

Saxena, I.M. and Brown, R.M. Jr (1995) Identification of a second cellulose synthase gene (*acsAII*) in *Acetobacter xylinum. J.Bact.*, **177**, 5276-5283

Saxena, I.M., Lin, F.C. and Brown, R.M. Jr (1990) Cloning and sequencing of the cellulose synthase catalytic subunit gene of *Acetobacter xylinum. Plant Mol.Biol.*, **15**, 673-683

Saxena, I.M., Lin, F.C. and Brown, R.M. Jr (1991) Identification of a new gene in an operon for cellulose biosynthesis in *Acetobacter xylinum. Plant Mol.Biol.*, **16**, 947-954

Saxena, I.M., Kudlicka, K., Okuda, K. and Brown, R.M. Jr (1994) Characterization of genes in the cellulose-synthesising operon (acs operon) of *Acetobacter xylinum*: Implication for cellulose crystallization. *J.Bact.*, **176**, 5735-5752

Selvendran, R.R. (1983). The chemistry of plant cell walls. In: *Dietary Fibre* (Birch, G.G. and Parker, K.J. eds) London: Applied Science Publishers, pp 95-147

Seymour, G.B., Colquhoun, I.J., DuPont, M.S., Parsley, K.R. and Selvendran, R.R. (1990) Composition and structural features of cell wall polysaccharides from tomato fruits. *Phytochemistry*, **29**, 725-731

Shea, E.M., Gibeaut, D.M. and Carpita, N.C. (1989) Structural analysis of the cell walls regenerated by carrot protoplasts. *Planta*, **179**, 293-308

Shedletzky, E., Shmuel, M., Delmer, D.P. and Lamport, D.T.A. (1990) Adaptation and growth of tomato cells on the herbicide 2,6-dichlorobenzonitrile (DCB) leads to production of unique cell walls virtually lacking a cellulose-xyloglucan network. *Plant Physiol.*, **94**, 980-987

Shedletzky, E., Shmuel, M., Trainin, T., Kalman, S. and Delmer, D.P. (1992) Cell wall structure in cells adapted to growth on the cellulose synthesis inhibitor 2,6-dichlorobenzonitrile. A comparison between two dicotyledonous plants and a graminaceous monocot. *Plant Physiol.*, **100**, 120-130

Shomer, I., Lindner, P. and Vasiliver, R. (1984) Mechanism which enables the cell wall to retain the homogenous appearance of tomato juice. *J.Food Sci.*, **49**, 628-633

Sims, I.M. and Bacic, A. (1995) Extracellular polysaccharides from suspension cultures of *Nicotiana plumbaginifolia. Phytochemistry*, **38**, 1397-1405

Sjostrom, E. (1971). *Wood Chemistry, Fundamentals and Applications.* New York, Academic Press.

Smith, R.C. and Fry, S.C. (1991) Endotransglycosylation of xyloglucans in plant cell suspension cultures. *Biochem.J.* **279**, 529-535

Stading, M. and Hermansson, A.-M. (1993). Rheological behaviour of mixed gels of *k*-carrageenan-locust bean gum. *Carbohydr.Polym.*, **22**, 49-56

Staehlin, L.A. and Giddings, T.H. (1982) Membrane mediated control of microfibrillar order. In: *Developmental Order: Its Origin and Regulation* (Subtelny, S. and Green, P.B. eds.) AR liss, NY, 133-147

Staudte, R.G., Woodward, J.R., Fincher, G.B. and Stone, B.A. (1983) Water-soluble (1→3),(1→4)β-D-glucans from barley (*Hordeum vulgare*) endosperm. III. Distribution of cellotriosyl and cellotetraosyl residues. *Carbohydr.Polym.*, **3**, 299-312

Stevenson, T.T. and Furneaux, H. (1991) Chemical methods for the analysis of sulphated galactans from red algae.*Carbohydr.Res.*, **210**, 277-298

Stipanovich, A.J. and Sarko, A. (1976) Packing analysis of carbohydrates and polysaccharides 6. Molecular and crystal structure of regenerated cellulose II. *Macromolecules*, **9**, 851-857

Stone, B.A. (1984) Non-cellulose β-glucans in cell walls. In: *Structure, Function and Biosynthesis of Plant Cell Walls* (Dugger, W.M. and Bartnicki-Garcia, S., eds), Am.Soc.Plant Physiol., MD, USA., pp52-74

Stone, J.E. and Scallan, A.M. (1968) A structural model for the cell wall of water-swollen wood pulp fibers based on their accessibility to macromolevules. *Cellulose Chem.Technol.*, **2**, 343-358

Sugiyama, J., Chanzy, H. and Revol, J.F. (1994) On the polarity of cellulose in the cell wall of *Valonia. Planta*, **193**, 260-265

Sugiyama, J., Okano, T., Yamamoto, H. and Horii, F. (1990) Transformation of *Valonia* cellulose crystals by an alkaline hydrothermal treatment. *Macromolecules*, **23**, 3196-3198

Sugiyama, J., Persson, J. and Chanzy, H. (1991a) Combined infrared and electron diffraction study of the polymorphism of native celluloses. *Macromolecules*, **24**, 2461-2466

Sugiyama, J., Vuong, R. and Chanzy, H. (1991b) Electron diffraction study on the two crystalline phases occurring in native cellulose from an algal cell wall. *Macromolecules*, **24**, 4168-4175

Sutherland, J.W.H., Egan, W., Schechter, A.N. and Torchia, D.A. (1979). Carbon-13-proton nuclear magnetic resonance study of deoxyhemoglobin S gelation. *Biochemistry*, **18**, 1797-1803

Taiz, L. (1984) Plant cell expansion: regulation of cell wall mechanical properties. *Ann.Rev.Plant Physiol.*, **35**, 585-657

Taiz, L. (1994) Expansins: Proteins that promote cell wall loosening in plants. *Proc.Natl Acad.Sci. (USA)*, **91**, 7387-7389

Talbott, L.D. and Pickard, B.G. (1994) Differential changes in size distribution of xyloglucan in the cell walls of gravitropically responding *Pisum sativum* epicotyls. *Plant Physiol.*, **106**, 755-761

Talbott, L.D. and Ray, P.M. (1992a) Molecular size and separability featutes of pea cell wall polysaccharides. Implications for models of primary wall structure. *Plant Physiol.*, **98**, 357-368

Talbott, L.D and Ray, P.M. (1992b) Changes in molecular size of previously deposited and newly synthesised pea cell wall matrix polysaccharides. Effects of auxin and turgor. *Plant Physiol.*, **98**, 369-379

Tanaka, T., Fillmore, D., Sun, S.-T., Nishio, I., Swislow, G. and Shah, A. (1980) Phase transitions in ionic gels. *Phys.Rev.Lett.*, **45**, 1636-1639

Tanaka, T., Nishio, I., Sun, S.-T. and Ueno-Nishio, S. (1982) Collapse of gels in an electric field. *Science*, **218**, 467-469

Taylor, and Conrad (1972) Stoichiometric depolymerisation of polyuronides and glycosaminoglycuronans to monosaccharides following reduction of their carbodiimide-activated carboxyl groups. *Biochemistry*, **11**, 1383-1388

Taylor, I.P. and Atkins, E.D.T. (1985) X-ray diffraction studies on the xyloglucan from tamarind (*Tamarindus indica*) seed. *FEBS Lett.*, **181**, 300-302

Taylor, J.G. and Haigler, C.H. (1993) Patterned secondary cell wall assembly in tracheary elements occurs in a self-perpetuating cascade. *Acta.Bot.Neer.*, **42**, 153-163

Taylor, J.G., Owen, T.P. Jr, Koonce, L.T. and Haigler, C.H. (1992) Dispersed lignin in tracheary elements treated with cellulose synthesis inhibitors provides evidence that molecules of the secondary cell wall mediate wall patterning. *Plant J.*, **2**, 959-970

Thompson, J.E. and Fry, S.C. (1995) Application of a density labelling technique to detect transglycosylation between xyloglucans in muro. In: *Proceedings of the Seventh Cell Wall Meeting, Santaigo de Compestela* (Zarra,I. and Revilla, G. eds.) University Press, Santiago de Compestela. pp143

Toyosaki, H., Naritomi, T., Seto, A., Matsuoka, M., Tsuchida, T. and Yoshinaga, F. (1995) Screening on bacterial cellulose-producing *Acetobacter* strains suitable for agitated culture. *Biosci.Biotech.Biochem.*, **59**, 1498-1502

Uhlin, K.I., Atall, R.H. and Thompson, N.S. (1995) Influence of hemicelluloses on the aggregation patterns of bacterial cellulose. *Cellulose*, **2**, 129-144

Valent, B.S. and Albersheim, P. (1974) The structure of plant cell walls. V. On the binding of xyloglucan to cellulose fibers. *Plant Physiol.* **54**, 105-108

Valla, S. and Kjosbakken, J. (1982) Cellulose-negative mutants of *Acetobacter xylinum*. *J.Gen.Microbiol.*, **128**, 1401-1408

VanderHart, D.L. and Atalla, R.H. (1984) Studies of microstructure in native cellulose using solid-state NMR. *Macromolecules* **17**, 1465-1472

Vian, B., Reis, D., Darzens, D. and Roland, J.C. (1994) Cholesteric-like crystal analogs in glucuronxylan-rich cell wall composites: experimental approach of acellular re-assembly from native cellulosic suspension. *Protoplasma*, **180**, 70-81

Vian, B., Roland, J.C., reis, D. and Mosiniak, M. (1992) Distribution and possible morphogenetic role of the sylans within the secondary vessel wall of linden wood. *IAWA Bull.*, **13**, 269-282

Viebke, C. (1995). A light-scattering study of carrageenan/galactomannan interactions. *Carbohydr.Polym.*, **28**, 101-105

Vincken, J.P., Beldman, G. and Voragen, A.G.J. (1994). The effect of xyloglucans on the degradation of cell-wall-embedded cellulose by the combined action of cellobiohydrolase and endoglucanases from *Trichoderma viride. Plant Physiol.*, **104**, 99-107

Vincken, J-P., de Keizer, A., Beldman, G., Voragen, A.G.J. (1995a) Fractionation of xyloglucan fragments and their interaction with cellulose.

Vincken, J-P., Wijsman, A.J.M., Beldman, G.,Niessen, W.M.A. and Voragen, A.G.J. (1996) Different action patterns of endoglucanases on xyloglucan from potato. *Plant Physiol., submitted for publication*

Warneck, H. and Seitz, H.U. (1993) Inhibition of gibberellic acid-induced elongation-growth of pea epicotyls by xyloglucan oligosaccharides. *J.Exp.Bot.*, **44**, 1105-1109

Wasserman, B.P., Qi, X. and Barone, L.M. (1995) Plasma membrane intrinsic proteins: Channels for translocation of elongating β-glucan polymers across membrane bilayers. In:. In: *Proceedings of the Seventh Cell Wall Meeting, Santaigo de Compestela* (Zarra,I. and Revilla, G. eds.) University Press, Santiago de Compestela pp 186

Wells, B., McCann, M.C., Shedletzky, E., Delmer, D.P. and Roberts, K. (1994) Structural features of cell walls from tomato cells adapted to grow on the herbicide 2,6-dichlorobenzonitrile. *J.Microsc.*, **173**, 155-164

Williamson, R.E., Baskin, T.I., Cork, A. and Birch, R. (1992) Genetic analysis of the microtubule and microfibril-dependent mechanism that determines cell and root shape in Arabidopsis thaliana. In: Proceedings of the Sixth Cell Wall Meeting, Nijmegen (Sasson, M.M.A., Derksen, A.M.C. and Emons, A.M.C.) University Press, Nijmegen, pp128

Wong, H.C., Fear, A.L., Calhoon, R.D., Eichinger, G.H., Mayer, R., Amikam, D., Benziman, M., Gelfand, D.H., Meade, J.H., Emerick, A.W., Bruner, R., Ben-Basat, B.A. and Tal, R. (1990) Genetic organization of the cellulose synthase operon in *Acetobacter xylinum. Proc.Natl.Acad.Sci. (USA),* **87**, 8130-8134

Woodward, J.R., Fincher, G.B. and Stone, B.A. (1983) Water-soluble (1→3),(1→4)β-D-glucans from barley (*Hordeum vulgare*) endosperm. II. Fine structure. *Carbohydr.Polym.*, **3**, 207-225

Yamamoto, H. and Horii, F. (1993) CP/MAS ^{13}C NMR analysis of the crystal transformation induced for *Valonia* cellulose by annealing at high temperatures. *Macromolecules* **26**, 1313-1317

Yamamoto, H. and Horii, F. (1994) *In situ* crystallisation of bacterial cellulose I. Influences of polymeric additives, stirring and temperature on the formation of celluloses Iα and Iβ as revealed by cross-polarisation/magic angle spinning (CP/MAS) ^{13}C NMR spectroscopy. *Cellulose*, **1**, 57-66

Yamamoto, H., Horii, F. and Odani, H. (1989) Structural changes of native cellulose crystals induced by annealing in aqueous alkaline and acidic solutions at high temperatures. *Macromolecules*, 22, 4130-4132

York, W.S., Darvill, A.G. and Albersheim, P. (1984). Inhibition of 2,4-dichlorophenoxyacetic acid-stimulated elongation of pea stem segments by a xyloglucan oligosaccharide. *Plant Physiol.*, **72**, 295-297

York, W.S., Darvill, A.G., McNeill, M., Stevenson, T.T. and Albersheim, P. (1985) Isolation and characterization of plant cell walls and cell wall components. *Meth.Enzym.*, **118**, 3-41

York, W.S., Oates, J.E., van Halbeek, H., Darvill, A.G., Albersheim, P., Tiller, P.R. and Dell, A. (1988) Location of *O*-acetyl substituents on a nonasaccharide repeating unit of sycamore extracellular xyloglucan. *Carbohydr.Res.*, **173**, 113-132

York, W.S., Harvey, W.S., Guillen, R., Albersheim, P. and Darvill, A.G. (1993) Structural analysis of tamarind seed xyloglucan oligosaccharides using β-galactosidase digestion and spectroscopic methods. *Carbohydr,Res.*, **248**, 285-301

York, W.S., Pauly, M., Zablackis, E., Hantos, S., Valafar, F., Albersheim, P. and Darvill, A.G. (1996) Structural analysis of xyloglucans by NMR spectroscopy. "The Extracellular Matrix of Plants: Molecular, Cellular and Developmental Biology", Tamarron, Colorado, USA, March 15-21, 1996

York, W.S., Impallomeni, G., Hisamatsu, M., Albersheim, P. and Darvill, A.G. (1995) Eleven newly characterised xyloglucan oligoglycosyl alditols: the specific effects of sidechain structure and location on ^{1}H-NMR chemical shifts. *Carbohydr.Res.*, **267**, 79-104

York, W.S., van Halbeek, H., Darvill, A.G. and Albersheim, P. (1990) Structural analysis of xyloglucan oligosaccharides by ^{1}H-n.m.r. spectroscopy and fast atom bombardment mass spectrometry. *Carbohydr.Res.*, **200**, 9-31

Zaar, K. (1979) Visualization of pores (export sites) correlated with cellulose production in the envelope of the Gram negative bacterium *Acetobacter xylinum*. *J.Cell Biol.*, **80**, 773-777